

DYNAMIC RESPONSE OF SPRING MOUNTED
FLEXIBLE PLATFORMS CARRYING ROTATING MACHINERY

by

WAGDY BAKR SADIK OSMAN B.Sc. , M.Sc.

A Thesis Submitted in Fulfilment of the
Requirement for the degree of
Doctor of Philosophy
Faculty of Engineering
The University of Aston in Birmingham

AWARDED THE DEGREE OF M.Phil.

JUNE 1979

29 JAN 1960

247552

621.811 OSM

DEDICATED TO THE MEMORY
OF MY PARENTS

Summary

A study was performed as an investigation to determine the dynamic response, natural frequencies and modal shapes of a spring-supported flexible platform.

Both theoretical and experimental approaches have been used in the investigation. Finite Element Methods were used in the theoretical analysis.

The purpose of the study was to ascertain the vibration characteristics and dynamic responses of the platform in order to elucidate the conditions which favoured the build-up of excessive vibration, especially when the rig was excited by more than one force, i.e. with different speed ratios.

The structure consisted of a platform belt-driven unit of the frame type, carrying two machines, one with a rigid base and the other with a more flexible base. It was necessary to establish the different speed ratios of the motor and alternator in order to excite the structure at these ratios.

The Finite Element Method was used in the numerical analysis. This method is preferred to classical methods for determining natural frequencies since reliability is improved by taking into consideration the flexibility of the platform. The natural frequencies and related mode shapes were measured and the experimental results were correlated with results obtained by a computer in the cases of the three rigid body modes and the plate mode. A high degree of correlation was found between these results.

The experimental work included an investigation of the non-linearity of the springs, the stiffness coefficient of the structure, and the behaviour of the structure as shown by the response curves.

Prediction based on the matrices of physical mass, stiffness and damping, defined a model whose responses matched the response data for the selected locations. The response analysis provided an estimate for the level of vibration that could be expected from the rotating machinery.

Some interesting resonances resulting from the non-linearity of the springs were observed.

An attempt was made at a quantitative comparison of amplitudes, but this was very difficult because the relative magnitude of various mode peaks kept going up and down.

It is concluded that a well-constructed spring supported platform is physically and economically better than the classical construction.

BOUNDARY: Dynamic Response of Spring Mounted Flexible
 Platforms Carrying Rotating Machinery

ACKNOWLEDGEMENTS

I wish to thank PROFESSOR K. FOSTER, M.A., Ph.D., C.Eng., M.I.Mech.E., Head of the Department of Mechanical Engineering, The University of Aston in Birmingham, for his encouragement throughout the last two years. Also my Supervisor, PROFESSOR E. DOWNHAM, B.Sc.(Eng.), Ph.D., C.Eng., A.M.R.Ae.S., for his ready and willing help, valuable advice, encouragement, suggestions and contribution throughout the course of this work.

My thanks are also extended to DR. J.E.T. PENNY, Senior Lecturer in the Mechanical Engineering Department, and to DR. L.J. HAZLEWOOD in the Computer Centre, The University of Aston.

I wish to thank also the technical staff of the Department of Mechanical Engineering, in particular MR. B. MUDDYMAN for his help in the experimental work.

I acknowledge the financial support given to me for this project by the Ministry of Higher Education, Egypt, A.R.

I acknowledge also the help of the office of the Cultural Counsellor and Egyptian Education Bureau in London.

I wish to thank MRS. M. BELLAMY for her co-operation and typing of this thesis, without whose help it would not have been finished in time.

Sincere thanks are also due to those closely associated with me during the course of this work.

<u>CONTENTS</u>		<u>Page</u>
	Summary	i
	Acknowledgements	ii
	List of Figures and Tables	iv
	List of Symbols	xii
<u>CHAPTER 1</u>	Introduction	1
1.1	General Introduction	1
1.2	Object of the Study	4
1.3	Survey of Literature	9
<u>CHAPTER 2</u>	Theoretical Consideration of the Dynamic Structure	22
2.1	Introduction	22
2.1.1.	Methods of Analysis of Structure	26
2.2	Consistent Mass and Stiffness Matrices of Beam Elements	30
2.2.1	Axial Vibration in the X_e -Axis	32
2.2.2	Twisting about the X_e -axis	35
2.2.3	Shearing and Bending in the $X_e Y_e$ Plane	37
2.2.4	Shearing and Bending in the $X_e Z_e$ Plane	40
2.2.5	Beam Matrices in assembled form	44
2.3	Beam Properties in Frame Co-ordinate System	47
2.3.1	Plane Axis Transformation	48
2.3.2	Overall Transformation Matrix	50
2.4	Assembly of Structure Mass and Stiffness Matrices	54
2.4.1	Beam Elements of Transverse Vibration Only	55

		<u>Page</u>
<u>CHAPTER 3</u>	Two-dimensional Elements and Numerical Solution	59
3.1	Two-dimensional elements	59
3.2	The Interaction between Beams and Plates	68
3.3	Folded Plate Members	70
3.4	Numerical Solutions	78
3.4.1	Introduction	78
3.5	Determination of Natural Frequencies	85
3.6	Determination of the Higher Modes	89
3.7	Reliability and Accuracy of Solutions	92
3.8	Computer Programme	93
3.8.1	Elimination of Rotational Displacement	100
3.9	Discussion of the Results	103
3.10	Conventional Methods and Mathematical Model	111
 <u>CHAPTER 4</u>	 Some Considerations of Linear and Non-Linear Restoring Forces	 116
4.1	Non-linearity in General	116
4.2	Ultraharmonics and Subharmonics in Forced Non-linear Oscillations	119
4.3	Solution of Non-linear Vibration by Taylor's Series	126
4.4	Response of the Linear System	130
	A. The Single Forcing Case	130
	B. The Double Forcing Case	131
4.5	General Note on Duffings Equations	132

	<u>Page</u>
<u>CHAPTER 5</u>	138
Experimental Technique and Measurements	
5.1	138
5.2	140
5.3	144
5.4	146
5.5	149
5.5.1	151
5.5.2	153
5.5.3	154
5.6	159
5.7	162
5.8	164
5.9	166
 <u>CHAPTER 6</u>	 169
Conclusion and Suggestions for Further Work	
6.1	169
6.2	181
References	
 <u>Appendices</u>	
A.	Response of Discrete Systems by Modal Analysis
B.	Response Curves
C.	Why steel Springs Act Admirably as Isolators
D.	The Effect of an Antivibration Mounting on the Machinery
E.	Why the Change from Traditional Massive Concrete to more Flexible Steel Structure is Desirable
F.	Computer programmes
G.	Conversion Table

LIST OF FIGURES AND TABLES

(Each group of Figures or Tables will be found at the end of the appropriate chapter)

- Fig. 1.1 Main details of the rig.
- Fig. A. Photograph shows a general view of the rig and measuring instruments.
- Fig. 2.1 Typical beam element and typical node
- " 2.2 Beam element
- " 2.3 Axial vibration in X_e axis
- " 2.4 Torsional vibration in X_e axis
- 2.5 Shearing and bending in $X_e Y_e$ plane
- " 2.6 Shearing and bending in $X_e Z_e$ plane
- " 2.7 Typical beam element in three dimensional space
- " 2.8 A Beam element connecting two joints M and N with finite element discretization
- " 2.9 Rotation about the Z axis
- " 2.10 Rotation about the X_2 axis
- " 2.11 Beam element considering only transverse vibration
- " 3.1 Rectangular plate element
- " 3.2 A rectangular plate with two opposite edges simply supported and with the two edges connected to the other structure
- " 3.3 Theoretical idealisation
- " 3.4 Exploded view of idealized structure showing all the elements
- " 4.1 Typical amplitude/frequency response curve
- " 4.2 Response curve indicating that three possible solutions of the amplitude exist
- " 4.3 Response curve for a subharmonic oscillation
- " 4.4 x,t diagram showing that the motion x does not vary significantly from the sinusoidal curve
- " 4.5 The single and double forcing cases

Fig. 5.1 Spectral dynamics SD 1001-2A System

- " 5.2 Spectral dynamics SD 101-A Tracking filter facilities
- " 5.3 Vibration meter model D.V.A.
- " 5.4 Concept of operation for general purpose Tachometer
- " 5.5 Fiberoptic Tachometer system
- " 5.6 Block diagram of setup spectroscope/oscilloscope/plotter
- " 5.7 Simplified block diagram Spectroscope II
- " 5.8 Data classification
- " B Photograph shows a view of the rig excited by vibrator
- " 5.9 1st Rigid Body Mode experimentally measured and the result of computer programme
- " 5.10 2nd Rigid Body Mode experimentally measured and the result of computer programme
- " 5.11 3rd Rigid Body Mode experimentally measured and the result of computer programme
- " 5.12 The plate mode experimentally measured and the result of computer programme
- " 5.13 Indicates the measured value for the four mode shapes
- " 5.14 Pictorial representation for the surface covered by bases of motor and alternator 1st plate mode
- " 5.15 Pictorial representation for the surface covered by bases of motor and alternator 2nd plate mode
- " 5.16 Response curve for the structure excited by vibrator

Response curves for Case 1 speed ratio 7:5

- Fig. 5.17 Fixed filter frequency = 4.3 Hz
- " 5.18 Fixed filter frequency = 8.2 Hz
- " 5.19 Fixed filter frequency = 9.1 Hz
- " 5.20 Fixed filter frequency = 37.4 Hz

Response curves for Case 2 speed ratio 5:3

- Fig. 5.21 Fixed filter frequency = 4.3 Hz
 " 5.22 Fixed filter frequency = 8.2 Hz
 " 5.23 Fixed filter frequency = 9.1 Hz
 " 5.24 Fixed filter frequency = 37.4 Hz

Response curves for Case 3 speed ratio 3:1

- " 5.25 Fixed filter frequency = 4.3 Hz
 " 5.26 Fixed filter frequency = 8.2 Hz
 " 5.27 Fixed filter frequency = 9.1 Hz
 " 5.28 Fixed filter frequency = 37.4 Hz

Response curves for Case 4 speed ratio 5:2

- " 5.29 Fixed filter frequency = 4.3 Hz
 " 5.30 Fixed filter frequency = 8.2 Hz
 " 5.31 Fixed filter frequency = 9.1 Hz
 " 5.32 Fixed filter frequency = 37.4 Hz

Response curves for Case 5 just the motor
running without the alternator

- " 5.33 Fixed filter frequency = 4.3 Hz
 " 5.34 Fixed filter frequency = 8.2 Hz
 " 5.35 Fixed filter frequency = 9.1 Hz
 " 5.36 Fixed filter frequency = 37.4 Hz

Response curves drawn by computer

Case 1.1.1

- " 5.37 Response curve and the wave form
 Speed setting 7:5, motor started to maximum speed,
 pick-up signal at point 1

Case 1.2.1

- " 5.38 Response curve and the wave form
 Speed setting 7:5, shut down the unit, pick up
 signal at point 1

Case 1.3.1

Fig. 5.39 Response curve and the wave form

Speed setting 7:5, motor at 50 Hz, pick up
signal at point 1

Case 1.4.1

" 5.40 Response curve and wave form

Speed setting 7:5, motor at 35 Hz, pick up
signal at point 1

Case 1.5.1

" 5.41 Response curve and wave form

Speed setting 7:5, motor at 25 Hz, pick up
signal at point 1

Case 2.4.4

" 5.42 Response curve and wave form

Speed setting 5:3, motor at 35 Hz, pick up
signal at point 4.

Case 4.4.2

" 5.43 Response curve and wave form

Speed setting 5:2 motor 35 Hz, pick up
signal, from point 2

The following photographs show the use of the
real time analyzer.

" 5.44 Photographs Case 1 speed ratio 7:5

A Pick up signal position 1

B Pick up signal position 2

C Pick up signal position 3

D Pick up signal position 4

- Fig. 5.45 Photographs Case 2 speed ratio 5:3
- A Pick up signal position 1
 - B Pick up signal position 2
 - C Pick up signal position 3
 - D Pick up signal position 4
- " 5.46 Photographs Case 3 speed ratio 3:1
- A Pick up signal position 1
 - B Pick up signal position 2
 - C Pick up signal position 3
 - D Pick up signal position 4
- " 5.47 Photographs Case 4 speed ratio 5:2
- A Pick up signal position 1
 - B Pick up signal position 2
 - C Pick up signal position 3
 - D Pick up signal position 4
- " 5.48 Photographs Case 5 Just the motor running at maximum speed
- A Pick up signal position 1
 - B Pick up signal position 2
 - C Pick up signal position 3
 - D Pick up signal position 4
- " 5.49 Stiffness coefficient
- " 5.50 Load deflection curve for the structure supported by four knife edges
- " 5.51 Load deflection curve for the spring behaviour (Vertical stiffness)
- " 5.52 Load deflection curve for the spring supporting the structure (longitudinal stiffness)

- Fig. C Photograph of the rig with equipment to measure the sideways stiffness
- " 5.53 Load deflection curve and deflection for 1st and 2nd coils
- " 5.54 Load deflection curve and deflection for 1st and 2nd coils

Tables

Table 5.1	Relation between the modes from Fig.	5.44
" 5.2	" " " " " "	5.45
" 5.3	" " " " " "	5.46
" 5.4	" " " " " "	5.47
" 5.5	" " " " " "	5.48
" 5.6	Type of expected resonance para.	5.6
" 5.7	The Vibration pattern shape para.	5.7
" 5.8	Load and deflection relation para.	5.8
" 5.9	Load and deflection-load increased and Load decreased para.	5.8
" 5.10	Applied load and effected deflection para.	5.9
" 5.11	" " " " " para.	5.9
" 5.12	" " " " " para.	5.9
" 5.13	" " " " " para.	5.9

LIST OF SYMBOLS

A	Acceleration
A	Cross-sectional area of the beam
[m]	Mass matrix
[K]	Stiffness matrix
C	Linear damping coefficient
[C]	Matrix elastic moduli
C	Elastic constants are independent of state of stress and strain
D	Diameter of the coil
D	$Eh^3/12(1-\nu^2)$ = Flexural rigidity of the plate
[D]	Dynamic stiffness matrix in harmonic vibration
d	Diameter of the coil
D.E.	Dissipation energy
E	Youngs modulus of elasticity
EI	Flexural rigidity
f	Coefficient of Coulomb damping
f_f	Coulomb damping force
F	Force
f (t)	Function of time
F_b	Elastic force
F_d	Damping force
F_N	Normal force
g	Gravitational
G	Shear modulus of elasticity
GJ	Torsional rigidity
h_1	Height
h	Plate thickness

I_{xx}, I_{yy}, I_{zz}	Moment of inertia
I_{xy}, I_{yz}, I_{zy}	Product of inertia
J	Mass moment of inertia
$K=P/\delta$	Linear spring stiffness
K_x, K_y, K_z	Linear spring stiffness in x, y, z direction
K.E. = T =	Kinetic energy
L	Lagrangian = function of generalised co-ordinates
L	T - U = Lagrangian
$[m_o]$	Consistent mass matrix
M_y	Bending moment of the plate
Nx	Axial compressive force
M_y	Bending moment
n	Number of active coils in spring
N_s	Axial compression force
P.E. = V_1	Potential energy
P_i	Natural frequency
P (x, y)	Downward distributed load density
Q_1	Shear force
Q	Generalised force
{q}	Co-ordinate vector
q_1, q_2, q_3	Generalised co-ordinate
$\dot{q}_1, \dot{q}_2, \dot{q}_3$	Differentiation with respect to time
t	Thickness
{r}	Positive vector
TR	Transmissibility
T	Torsional moment of inertia
Q	Resonance amplification factor
Q_y	Kirchoff's shear coefficient

$\{u\}$	Displacement response vector
$U_0 (u_i)$	Strain energy density
U	Strain energy of an elastic body
$\{u\}$	Displacement of body at any instant
V	Volume
V	Distributed transverse load per unit length along the beam
Vol	Total volume of the body
w	Load density
w	Weight
w_0	Uncoupled vertical frequency
$w_1 = \Omega_1$	First eigen value
$w_2 = \Omega_2$	Second eigen value
$w_3 = \Omega_3$	Third eigen value
$\lambda = \omega^2 / \omega_0^2$	Dimensional frequency ratio
$\{\delta u\}$	Compatible virtual displacement vector
x	Rectilinear displacement
$\bar{x}, \bar{y}, \bar{z}$	Co-ordinates in x, y, z direction
C.F.	Complementary solution
P.I.	Particular solution
\dot{x}	Rectilinear velocity
\ddot{x}	Rectilinear acceleration
χ	Normal function
$\{\chi\}$	Body force vector
$\{\delta u\}$	Compatible virtual
$\{\Phi\}$	Surface vector
$\{y\}$	Vector
α, β	Parameter determining the restoring force character

α_{ij}	Influence coefficient
γ	Specific weight
$\{\epsilon\}$	Strain vector
ϵ_{ij}	Component of strain
ζ	Damping factor
μ	Coefficient of friction
ν	Poissons ratio
$\{\rho\}$	Scalar mass density in linear motion OR an inertia tensor in angular motion
ρ	Mass per unit length
σ_{ij}	Component of the stress
ω_d	Damped natural angular frequency
λ_i	Langranges multiplier
∇^4	Biharmonic operator in (x,y) co-ordinate

CHAPTER 1

Introduction

1.1 General Introduction

The continuous trend in engineering development towards high speed in all forms of machinery, together with the construction of lighter structures and foundations, has given rise to more noise and vibration.

Material failure in practice is more generally due to fatigue than to static overstressing. The cause of the fatigue failure is often unforeseen vibrations. The transmission of vibrations can be minimised by mounting the offending machine resiliently. Equipment can be protected from vibration by similar means. Many anti-vibration installations have proved their worth with many years of satisfactory service, although spurious modes of vibration do occur occasionally.

An essential feature in the design is the calculation of the natural frequencies of the resilient installations so as to ensure that no resonance will occur with any of the possible exciting forces.

The dynamic behaviour and response of structures continues to exercise a considerable and often decisive influence on the analysis or design of man-made and natural systems. The modes and periods of natural oscillations have to be determined to study the dynamic response of structures to periodic loading and shock.

The dynamics of structure will be considered first, since the prediction of this behaviour in complex structures represents a difficult problem, and the elementary theories are often incapable of providing accurate results.

Naturally, extensive efforts have been expended over the years in the development of techniques to provide results of acceptable accuracy. Although empirical formulae for the fundamental frequency of vibrations of buildings (for example) existed for many years, there were many structures for which precedents did not exist. The natural frequency had then to be determined by experiment or by calculation. Calculation was preferable, since it was a cheaper process than experiment. Calculations could be made analytically by various methods for configurations of relatively simple geometry. Alternatively, quite complex structures could be studied by limiting the infinite degree of freedom to a finite one. Finite elements were a method by which this could be achieved. A matrix method of structural analysis is defined as an algebraic approach formulated largely in terms of matrix operations capable of being programmed as a completely automatic sequence of computer operations, commencing with the basic problem data and concluding with the desired results.

Furthermore, a proviso is appended that the governing equations be based on an analytical model composed of discrete structural elements, e.g. bars, plate, segments.

Matrix methods of structure analysis have experienced their greatest advances in recent years. Developments

have taken place on a wide front and have involved the contributions of numerous, often isolated, investigations in many countries.

Hence, it is not surprising that individual developments have sometimes suffered from a narrowness of scope not befitting the potentialities of matrix methods. Also there has been a lack of unification of the multitude of seemingly different methods which actually have a common basis.

Among the organisations entrusted with the function of performing analyses in the field of structural mechanics, there has been a remarkable growth of computer programmes based on matrix methods for specific purposes. Nevertheless, very few organisations have undertaken the programming of any such method in a reasonable general form. General purpose formulations of matrix structural analysis are desirable from the standpoint of efficiency, however, and are even mandatory if investigations beyond the confines of linear elastic analysis are contemplated.

Interested groups are faced with a difficult choice. They are uncertain as to whether any one of the available published references can be depended upon to provide an optimum basis for a desired general purpose computational programme. If the choice of a suitable procedure can be made, there still remains uncertainty as to the method of obtaining maximum accuracy most efficiently.

If the numerical error is disregarded, the inexactitudes of the solution in comparison with the behaviour of the real

structure are dependent upon how well the idealised discrete element system represents the real structure.

The correlation of procedures for the determination of discrete element force displacement relationships leads to the conclusion that there are two levels of approximation in the development of such properties. First, in the "essential" behaviour of the element, and secondly in the definition of the lumped masses and node point displacements as required by the complete framework of analysis. The alternative types of elements and the numerous procedures for the derivation of the properties for a particular type of element require the analyst to exercise his engineering judgement.

1.2 Object of the study

There is a great need in heavy industrial, petrochemical and oil refining plants for a simple, new and economical approach to the design of mounting rotating machinery with confidence that the machinery mounted on a flexible platform supported by springs do not give any disturbance regarding the transmission of vibration to the surroundings.

There is also no need for any foundation design other than the ease of manufacture. According to the classical approach, about 22 tons of concrete cement are required as a foundation for small rotating machinery (the rig).

This method is more economical, efficient and is less time-consuming than the classical one. Such a design also seems to be favourable as far as bearings and damping

are concerned.

The springs supporting the structure must be as soft as the stability of the structure allows and designed in such a way as to give the first natural frequency of the structure in the range 4-5 Hz. By this means the first plate mode will also be in the range of between 4 and 4.2 times the third rigid body mode.

As stated, by designing the isolators very soft, the resonance speed will occur at a very low machine speed. In the case under consideration the three rigid body modes will occur at very low machine speeds (4.3, 8.2, 9.1 Hz). So it may be concluded that benefits obtained by using a spring-supported structure are very great, both physically and economically, and one of the main advantages of this approach is that it is very easy to determine the natural frequency at the design stage with very great accuracy.

There is no comparison between these two methods of predicting the vibration characteristics of the structure; the classical approach with a concrete foundation, and the new method which uses a flexible platform to carry the rotating machinery.

Another effect of mounting the machinery resiliently is to reduce its effective weight by detaching it from the ground, which would otherwise play an important part in adding to the machinery's inertia. A consequence of this is that the machinery which generates unbalanced forces

will tend to vibrate more when it is mounted resiliently than when it is attached firmly to the ground.

It is evident that a vibration isolation of 100 percent with no oscillation of the operating system is impossible. However, for a frequency ratio 5:1, and with zero damping, the amplitude of motion will be within 4 percent of the ideal machinery. And the vibration absorbing efficiency will be approximately 97 percent. This means that the motion of the structure would be virtually imperceptible.

A low frequency ratio with increased damping gives an increase of vibration transmission so for the low frequency ratio the phase angle is not 180° but 0° . The phase angle is less than 90° below the resonances. It increases rapidly and changes to practically 180° simultaneous with zero damping. The amplitude of motion is reduced quickly when a structure is supported on springs. The frame becomes an effective stabilising mass as the phase angle suddenly changes from 0° to 180° . The greater the damping factor the slower the change in phase angle that takes place. This is an added indication of the disadvantage of damping.

For the vertical vibratory motions, the deflection of the springs controls the natural frequency of the supported structure. Hence it is important that the calculation of such deflection in the isolator be made on a simple and reliable basis.

The calculation of steel springs, based on modern practice employing the "Wahl" coefficient for the determination of deflection and stress, is very simple indeed. The necessary deflection for maximum isolating efficiency is easily obtainable through the choice of the proper physical characteristics, especially with the coil spring, which has a higher loading capacity per pound of spring material than any other type of isolator usually used for this purpose.

Therefore, this type of spring would appear to be the best choice for this isolation problem.

Organic materials do not show the simplicity and the advantages of the steel spring which does not depend upon its material, but rather upon its wire diameter, outside diameter etc., which may be chosen at will, while the former are restricted in their use as their elasticity depends upon the material itself, and only to a minor degree upon its shape. This defect explains why organic materials cannot provide the necessary large deflections in the isolator for any reasonable thickness. So it may be said that steel springs act admirably as isolators because of their shape, form, and heat treatment possibilities.

One might ask why it is necessary to use fewer degrees of freedom for the dynamic analysis stage of a problem. The answer to this is that the cost per solution is excessive if the problem is too big to be contained in the core store of a computer and has to be programmed in terms of partitioned matrices.

Looking at the problem from another angle we need to investigate the vibration characteristics of a flexible spring mounted platform carrying machinery in order to cure a case of severe vibrations. The best way to tackle this problem is to make a theoretical model of the machinery and its frame structure and to develop this until it agrees with measurements taken on site. Having proved the theoretical model to be correct, it will then be necessary to try it out and make modifications to see if a solution can be found to avoid the severe vibrations.

The first stage of the work consists of taking site measurements of the machine's vibration pattern over the speed range of the machine. Recordings will have to be taken and analysed of the motion of various points of the structure in sufficient detail to demonstrate the validity of the theoretical model's predictions. From the theoretical model, Finite Element Techniques can be used to model the whole structure. Considerable detail is required in the idealisation before the predictions will finally agree with the site test results. When this agreement is obtained, any modifications may be put into the theoretical model.

Summarising:

1. Make comprehensive measurements of the machine's pattern of vibrational behaviour.
2. Convert the theory into a computer programme.

3. Set up an idealisation of the machine and its supporting frame structure and develop it until a version is formed which, when fed into the computer programme, would reproduce the results measured on site.
4. Having proved the basic theoretical model, insert into it representations of modifications to the machine until one is found which will reduce the vibration to an acceptable level.

Fig. (1.1) Main details of the rig

Fig. A. shows a general view of the rig and measuring instruments.

1.3 Survey of literature:

Vesselowski ⁽¹⁸⁾ carried out his investigation in an effort to eliminate the uncertainties which exist in the design of the foundations of turbogenerators, particularly where a steel substructure is used.

Hull's ⁽¹⁹⁾ work was an attempt to clarify the problem of determining the effects of elastic foundations under rotating machines on the resonant speeds of those machines.

Lürenbaum ⁽²⁰⁾ investigated the unexpected frequencies of machine foundation supported by springs with two levels of symmetry. He used calculations and graphs to arrive at a

solution for the equation of motion and the position of the rotating pole and the coupling effect. He discussed a machine with variable speeds and explained the reason for the coupling of odd frequencies.

Schäff⁽²¹⁾ looked at a 50 mw quiet turbogenerator. This became agitated suddenly when it was under inspection above the normal running speed. The cause was the coupling between the rotating shaft and the foundation.

Püst⁽²²⁾ used the model method for the determination of dynamic properties of framed foundation. He carried out theoretical and experimental analysis of forced vibration of a complex damped mechanical system with several degrees of freedom and showed that resonance peaks, measured at different points of the system correspond to various frequencies of exciting force.

Ramsden⁽²⁴⁾ represented a method for reducing the size of a vibration analysis by generating an inertia matrix referring to a limited set of master vibrational freedoms. The transformation from the full set of degrees of freedom to the master set makes extensive vibration calculations economically feasible giving solutions in terms of the amplitudes of the master freedoms.

Gupta⁽²⁵⁾ used a general digital computer method based on a Sturm sequence procedure, which is described for determining the natural frequencies and associated modes of undamped free vibration of frames and other structures whose stiffness and mass matrices are of band form.

Wilson ⁽²⁶⁾ considered the structure as an assemblage of beams, columns and plates. The finite element displacement method was used to determine matrices representing the mass and stiffness of the foundation.

Steel foundations have been used in Germany for many years for small and medium sized sets and a number of different methods of analysis have been applied to them. The first analytical models consisted of a simple mass-spring system with the parameters determined empirically. As a refinement another mass was used for the shaft joined to the first by a dashpot and a second spring to represent the bearing (Dietz ⁽²⁷⁾).

Analytical solutions of the resulting equations of motion were used to predict the behaviour of the foundation. By using the computer this type of analysis was extended to a model with seven interconnected masses (Kramer ⁽²⁸⁾). With a similar idealisation of the structure, an analysis was also carried out using the transfer matrix technique (Pestel and Leckie ⁽²⁹⁾ and Weber ⁽³⁰⁾).

More recently, two other methods have been used: Crook ⁽³¹⁾ combined a more detailed representation of the bearing with the structure. Prohl ⁽³²⁾ used a variation of Holzer's method.

Mykelstad ⁽³³⁾ used a structure still represented by a series of springs and masses.

In his work, Stoker ⁽³⁴⁾ derived expressions for the total potential and Kinetic energies of the shaft and

structure and the resulting Lagrange's equation was solved.

Continuing with structural analysis, Wiberg ⁽³⁵⁾ used mixed force and displacement variables as a key to a reliable solution for many physical problems, since the analysis of elastic structures with large rigid motion using the displacement method may fail due to ill-conditioning, but the use of mixed variables may work owing to the possibility of using relative displacements within substructures.

Ramsden ⁽³⁶⁾ used a method based on matrix algebra for the dynamic analysis of mixed rotating and non-rotating vibration systems.

Raney ⁽³⁷⁾ determined the set of governing different equations of motion of a complex structure. Numerical values for mass, stiffness and damping coefficients of the dynamic equations associated with a particular input response or transmission path were computed from data usually obtained in conventional vibration tests of a structure.

Thoren ⁽³⁸⁾ used a technique to describe the orthonormal modal vectors computed from dynamic test response data to derive mass, stiffness and damping matrices for a discrete model of the distributed elastic system.

Young and On ⁽³⁹⁾ represented a survey of activities to produce logically-based schemes to generate mathematical models by making use of experimentally derived information. Emphasis was given to the efforts of Goddard to the recent studies designed to verify the practical effectiveness of a

specific modelling scheme.

Andrews ⁽⁴⁰⁾ in his investigation derived the equation of motion for a rigid body supported by an arbitrary number of arbitrarily oriented and located resilient mounts with damping.

Bapat ⁽⁴²⁾ examined the possibility of applying two approximate methods for determining the salient features of the response of undamped non-linear spring mass systems subject to a step input.

Mercer ⁽⁴³⁾ used the concept of a variable friction force as a new form of shock isolator. This is adaptive in its action but is still composed of entirely passive elements.

Johnson ⁽⁴⁵⁾ used analytical and experimental investigations of helical springs subject to vibratory motion. He showed that an actual spring displays frequency response characteristics over most of the frequency spectrum that would render its function useless in many cases.

Vogt ⁽⁴⁶⁾ studied the effect of active coils in helical springs and explained the effect of inactive coils on each end of the springs.

Ancker ⁽⁴⁷⁾ used the thin-slice method to analyse the tension and torsion in helical springs with round cross section. Stresses, deflections, curvature changes, diametral contractions, and coupling effects were also studied.

Wood ⁽⁴⁸⁾ in his work explained the need for the correlation of data on mechanical springs and the formulation of

a standard code of design for helical springs.

Henry ⁽⁴⁹⁾ dealt with the stability of modes at rest in a free undamped non-linear two degrees of freedom system governed by equations of motion.

Dooren ⁽⁵⁰⁾ studied Duffing's coupled equations in non-linear mechanical systems with two degrees of freedom from the computational viewpoint.

Spinivasan ⁽⁵¹⁾ obtained an exact expression for the frequency of a non-linear cubic spring mass system.

Stern ⁽⁵²⁾ used a variational technique for the computation of the steady state response of a rigid jointed framestructure to harmonically varying load systems.

Rubinstein ⁽⁵³⁾ used the stiffness matrix method combined with an iteration technique to analyse frames in which the members are non-prismatic and have shapes which are complex to analyse, or cannot be expressed analytically.

Lund ⁽⁵⁴⁾ investigated the accuracy of the conventional method of field balance.

Ehrich ⁽⁵⁵⁾ looked at the case of sum and difference frequencies in vibration of high speed rotating machinery.

Allaway ⁽⁵⁶⁾ presented a simplified method for computing the amplitude of self-induced vibration for a machine which generates unbalances; unfortunately, his work was summarising some of the classical work of Wilson ⁽⁷⁰⁾ and Crede ⁽⁶⁸⁾.

Warburton ⁽⁵⁷⁾ made it clear that in order to determine the response of a structure to vibrations of a given type it is necessary to appreciate the factor controlling the transmission of vibration.

Waller ⁽⁵⁸⁾ summarised the factors influencing the decision to incorporate anti-vibration devices, in particular the effects of vibration on personnel, machines and structures. This was the only work found which examined the cost and various forms of anti-vibration mounting were compared and the cheapest springs for various degrees of isolation were indicated. It is unusual to find any work relating to the cost of vibration effects on machines or structures or personnel.

According to some researchers ⁽⁴¹⁾, the behaviour of an isolation vibration system possessing even small non-linearity is likely to be substantially different from that predicted by a linearised analysis. A significant feature of non-linear systems is the existence of steady state oscillations with values of the phase angle other than 0 or π , even in the undamped system. Such an effect can only arise when the degrees of freedom are subject to non-linear coupling and only then under suitable conditions.

Naturally, the resultant motion at the point of application of the exciting force must be either in-phase or anti-phase to the exciting force, otherwise energy transfer would occur. This does not, however, prevent each degree of freedom itself from vibrating out of phase with its own

generalised components of the exciting force. The first effect was first found by Tobias and Arnold in experimental work on disks.

Both exact and approximate solutions have been developed for the vibration isolation system with directly coupled coulomb damping.

Den Hartog ⁽⁷⁶⁾ developed an exact solution for the displacement amplification factor.

An approximate analytical method known as equivalent viscous damping, was developed by Jacobsen ⁽⁷⁷⁾ and applied to obtain an approximate for the displacement amplification factor. This method was later employed by Ruzicka ⁽⁷⁸⁾ and Painter ⁽⁷⁹⁾ to obtain an approximate solution for absolute and relative displacement transmissibility.

Following Den Hartog's approach, Van Bommel ⁽⁸⁰⁾ developed an exact solution for absolute relative displacement transmissibility.

Finally, Levitan ⁽⁸¹⁾ employed a Fourier series analysis to develop exact solutions for absolute and relative displacement transmissibility.

The case of a rigid body supported resiliently

All the steps of investigation in the case of a rigid body supported resiliently will be explained. Unfortunately, it has always been assumed that the body is rigid. And this assumption allows no flexibility in the structure. Another

point worth mentioning here is that all these analyses consider the centre of gravity and from there it is assumed that the structure is permitted to move in six degrees of freedom. These are the displacement of the centre of gravity along ox , oy and oz and the rotation of the body about ox , oy and oz ; in other words, vertical, longitudinal and transverse displacement and yawing, rolling and pitching.

Grootenhuis ⁽²³⁾ indicated that the general case of the motion of a rigid body supported resiliently has never been discussed in detail with allowance for the stiffness of each anti-vibration mounting in three directions and for the possibility of the centre of gravity (c.g.) not being at the geometric centre, thus introducing additional products of inertia terms. Consideration of an offset centre of gravity is of considerable practical importance as it is often inconvenient if not impossible to provide a truly symmetrical foundation or installation. Many items of machinery and equipment that have to be mounted resiliently do not have the centre of gravity positioned symmetrically with respect to the mountings. Several degrees of asymmetry may be considered. For a single degree of asymmetry, the centre of gravity would be situated along one of the axes of an orthogonal co-ordinate system with its origin at the geometric centre. With two degrees of asymmetry the centre of gravity would be situated in a plane containing two axes of this co-ordinate system. The general case has three degrees of asymmetry in which case the centre of gravity can be anywhere within the body.

He derived the equation of motion for a rigid body supported on four springs (this was the classical method). But he considered the general case of the centre of gravity being anywhere within the body and allowing for the sideways as well as the longitudinal stiffness of the springs. This constitutes a six degrees of freedom case with three degrees of asymmetry.

His work proved that coupling between motions in all directions occurs even when the centre of gravity is at the geometric centre with the exception of the vertical oscillations and rotation about the vertical axis. Any number of additional springs can be allowed for by adding terms to the expression for the potential energy stored in the springs. Allowance is made in the expression for kinetic energy for the products of inertia which arise with an offset centre of gravity.

Why is this considered to be the classical method? Because the real case is simulated for purposes of analysis by replacing the rigid body by a rectangular box with a light framework and all the mass concentrated at eight corners. The matrix solution is changed into dimensionless parameters and the effect of an offset centre of gravity upon the eigen value and eigen vector studied. Only the proportions of the box and the stiffness ratio between sideways and longitudinal stiffness of the springs remain as factors. He also concluded that small amounts of offset of the centre of gravity from the geometric centre do not alter the dynamic behaviour of the system much, but displacing the total mass

towards either a lower or an upper corner has marked effects. Some of the natural frequencies associated with motion in rotation when the system is symmetric become less than the frequencies connected with motion in translation for the centre of gravity being close to the corner connected to a spring. A large region free from any natural frequency arises when the centre of gravity is moved towards one of the corners farthest away from the plane containing the springs. The asymptotic conditions for the position of the centre of gravity had also been considered. It is well known that an offset centre of gravity can lead to coupled oscillations at frequencies differing from those for the uncoupled modes.

It is rather astonishing therefore to find that a hand-book on vibration isolation ⁽⁶⁷⁾ has been restricted to symmetrical installations without paying any regard to coupling due to the sideways stiffness of the springs.

The more complete analyses are by Crede ⁽⁶⁸⁾ and more recently Crede and Ruzicka ⁽⁶⁹⁾ for one and two degrees of asymmetry but with the planes containing the centre of gravity restricted to those defined by the vertical and horizontal axes only.

An attempt at a solution of the general case of a body supported on any spring system has been made by Ker Wilson ⁽⁷⁰⁾ but the product-of-inertia terms were unfortunately omitted. Some one and two degrees of asymmetry cases are analysed in detail.

Many of the observations on practical anti-vibration installations made by Ker Wilson are of great value, but some of the equations of motion are not exact, however, owing to the neglect of the product of inertia terms.

Some interesting experiments with a box mounted on four springs have been described by Lürenbaum ⁽²⁰⁾. The motions of specific points on the box have been shown in photographs and the strong coupling was easily seen for this single degree of asymmetry. The necessity to include the product-of-inertia terms has been realised by Sethna ⁽⁷¹⁾, who has derived the equations of motion for the sprung mass of a four-wheeled vehicle but has not solved them.

A detailed analysis of a spring-supported body, symmetric in shape and with the centre of gravity always at the geometric centre has been made by MacDuff ⁽⁷²⁾. The natural frequencies for a large number of shapes of a body with bottom mounts were presented graphically and other configurations of springs were also considered. The complete equations of motion for a rigid body supported on four springs were derived and a method of solution was outlined. Linear springs were assumed (there is, however, always some non-linearity of springs), permitting the superposition of modes. Some dissipation of energy always occurs in practice, but has only a very slight effect upon the natural frequencies. Damping has therefore been neglected.

The first notable instance of using the steel helical springs in a flexible mounting for large oil engines was given by Hummell ⁽⁷⁵⁾, in which the flexible mounting of

the main propelling engines of the twin-screw passenger vessel "Hansestadt Köln" was described. Each engine, a Deutz six-cylinder four-stroke cycle type, with cylinders 270 mm bore 360 mm stroke, developing 375 b.h.p. at 500 r.p.m., rested upon 16 helical springs each 7.75 inches mean coil diameter, arranged in two rows, one at each side of the fabricated steel bed plates. Damping was provided by the frictional resistance of spring-loaded snubbers and the propeller shafts were flexibly connected to the engine crankshaft through "Frost type" flexible couplings. The total weight supported by the springs was about 8 tons.

SPRINGS MOUNTED THE RIG IN FOUR CORNERS
(ABCD)

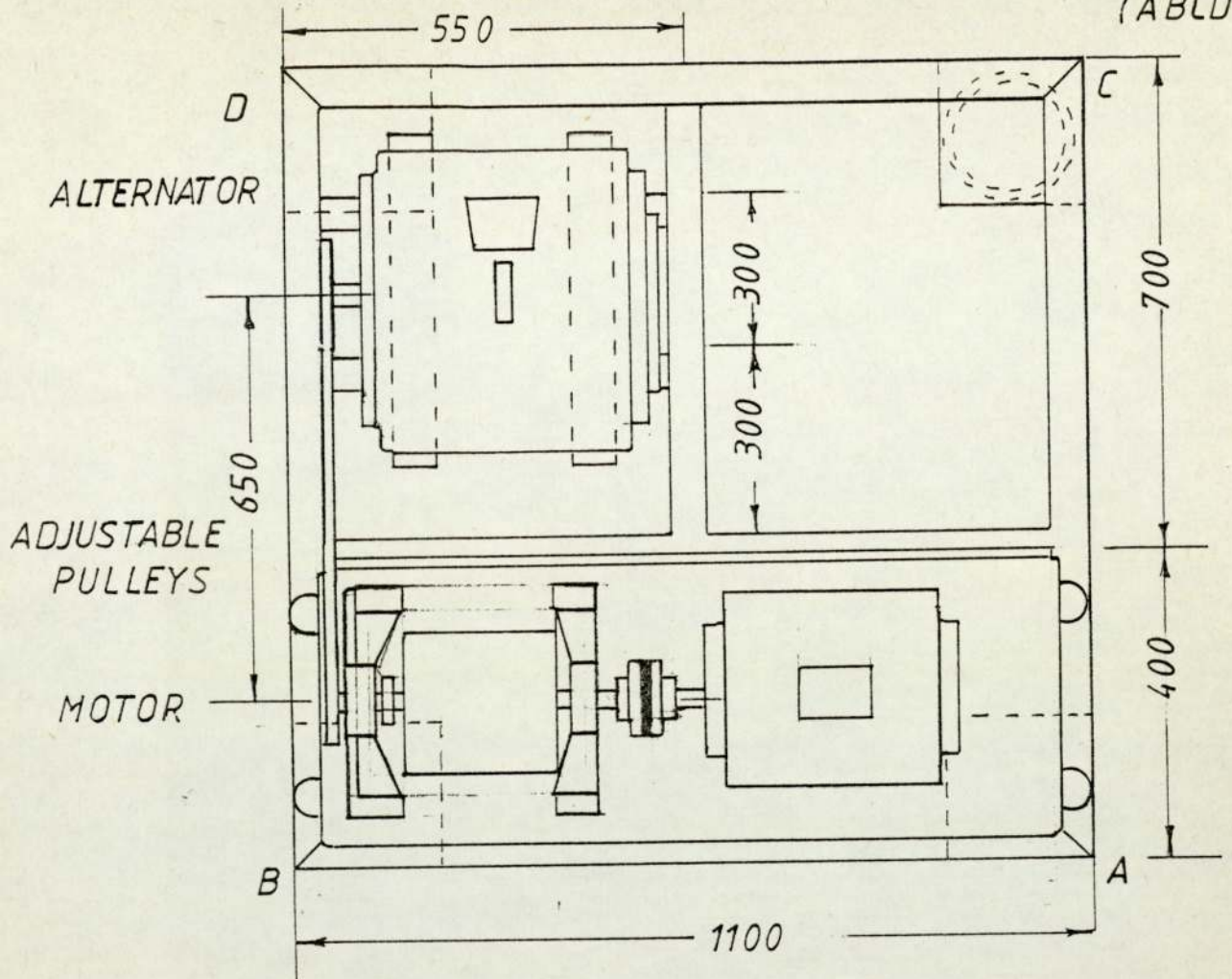
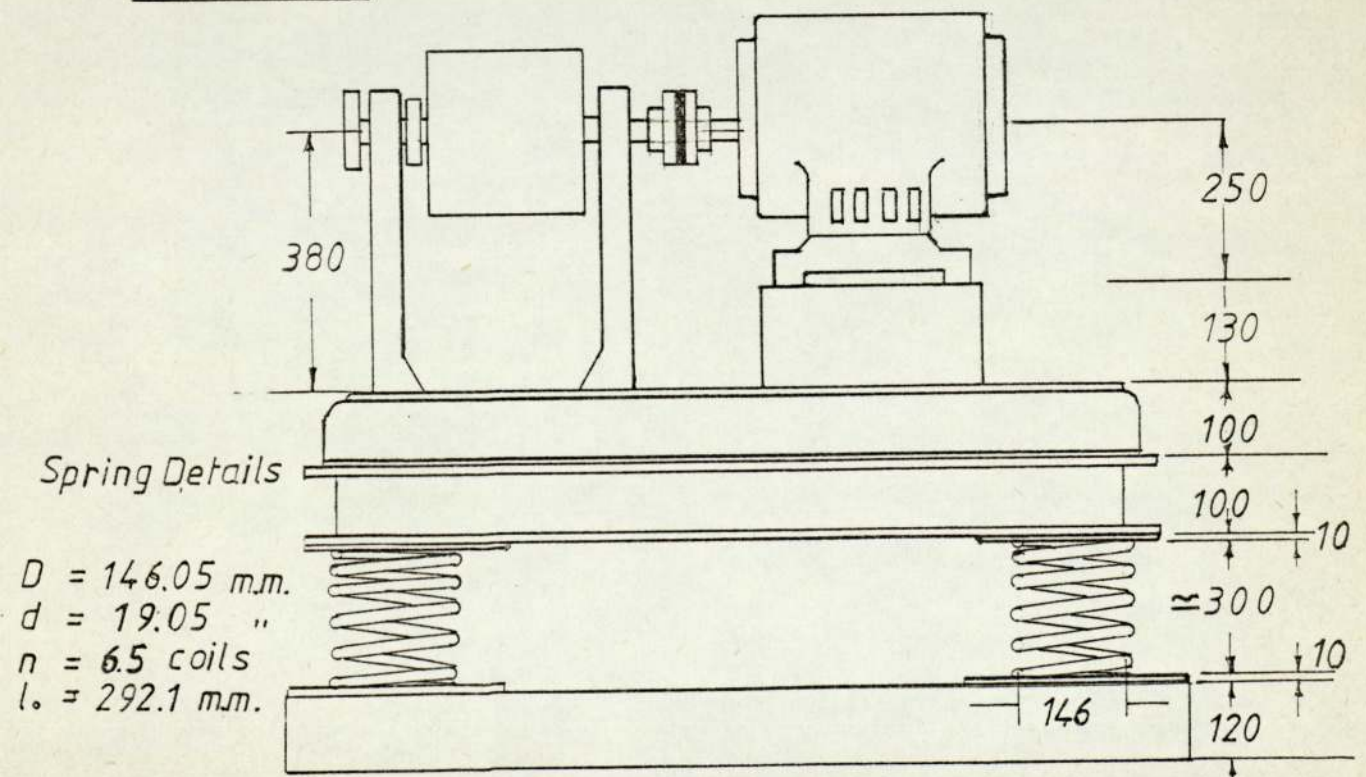


Fig. 1.1

MAIN DETAILS OF THE RIG

Dim. in m.m.



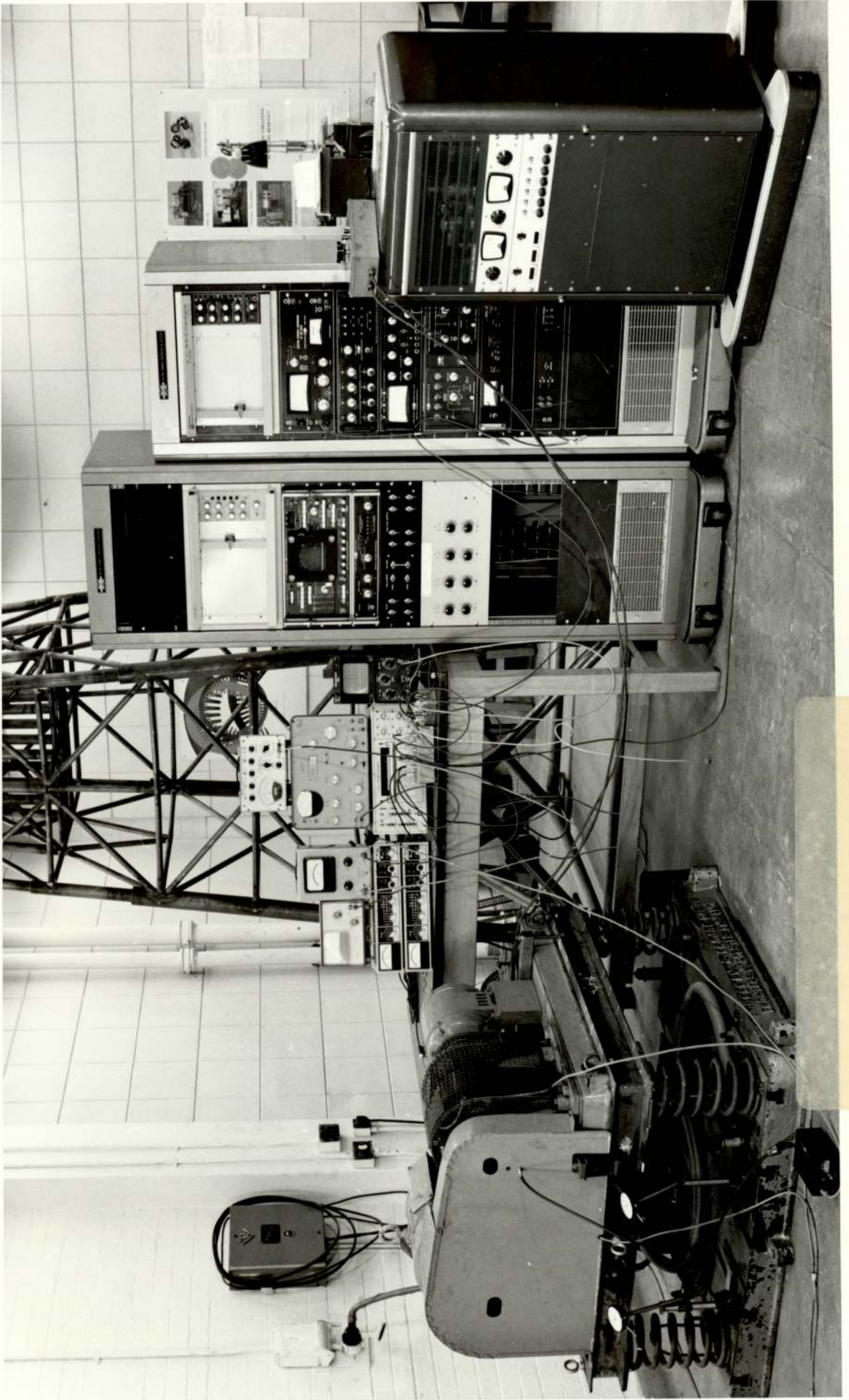


Fig A. General view of the rig and measuring instruments

CHAPTER 2

Theoretical consideration of the Dynamic of
structure

2.1 Introduction

Solutions to the problems of vibrations of elastic systems can be explained by the analysis of small harmonic oscillations of elastic systems having a finite number of degrees of freedom.

The harmonic oscillations may be induced in an elastic system by imposing properly selected initial displacements and then releasing these constraints, thereby causing the system to go into an oscillatory motion. This oscillatory motion is a characteristic property of the system, and it depends on the mass and stiffness distribution. In the absence of any damping forces, e.g. viscous forces proportional to velocities, the oscillatory motion will continue indefinitely, with the amplitudes of oscillations depending on the initially imposed displacement; however, if damping is present, the amplitudes will decay progressively, and if the amount of damping exceeds a certain critical value, the oscillatory character of motion will cease altogether. The oscillatory motion occurs at certain frequencies and it follows well-defined deformation patterns described as the "characteristic modes". The study of such free vibrations is an important prerequisite for all dynamic-response calculations for elastic systems.

Whatever the vibration analysis for both the stiffness and flexibility formulations, a comparison between the force and displacement methods is needed, because we are faced with the natural question as to which method is best for practical applications. To answer this question, we must consider a number of different factors. First, it should be emphasised that since the same element properties can be used for either the displacement or force methods, it is obvious that, theoretically, both methods lead to identical results. But the computational path leading to the calculation of stresses and displacements is different in each method. This means that because of the different rounding-off errors and possible ill-conditioning of equations, the actual numerical results may differ slightly. For some special applications, numerical solutions are obtained using both methods with different assumptions regarding the element stress or displacement distributions i.e. compatible but non-equilibrium stress states for the displacement method and statically equivalent (equilibrium) but non-compatible stress states for the force method. This leads to the so-called bracketing of the solution. Such solutions are particularly useful if the bracketing is small, since they provide meaningful information on the accuracy of the results.

To examine briefly the matrix operations involved in the two methods: The displacement method is based on the solution of a simple equation

$$P = K U \quad (2.1)$$

relating the external forces P to the displacement U at the node points of the idealised structure.

As will be shown later, the element stiffness matrices are assembled into the stiffness matrix K for the assembled structure. The procedure is indeed very simple, and does not require any complicated programming. Once the displacements U have been calculated, they are used to calculate stresses in individual elements. Some difficulties may occur due to ill-conditioning of Equation (2.1) when inverting the stiffness matrix K . Some conditioning problems have been discussed by Taig and Kerr ⁽¹⁾. However, constant improvements in computer technology result in increased accuracy, such as double-precision inversion programmes, and tend to eliminate ill-conditioning as a source of error.

In modern computer programmes for the matrix methods, human mistakes in the basic input data are probably the most frequent sources of error. So care and attention must be considered. These errors are the most difficult ones to detect automatically.

Special attention must be paid also to the design of input data in order to reduce the chances of erroneous entries. One noteworthy innovation in this respect is the method by Argyris ⁽²⁾ whereby intermediate node points are generated automatically by the computer. This means that some of the idealisation is performed by the computer, and therefore the amount of input data required from the analyst is greatly reduced.

In the force method of analysis the sequence of matrix operations required to obtain stresses and displacement is considerably more complicated than for the displacement method. By using the Jordanian elimination technique it is easy to demonstrate that the self-equilibrating force systems can be generated automatically from the equations of equilibrium. This technique allows us to use the same input information for the force method as for the displacement method. When the matrix force methods were first introduced, considerable difficulty was experienced in formulating the self-equilibrating force systems. The determination of the degree of redundancy and the distribution of the self-equilibrating force system was sometimes an intractable proposition for exceedingly complex structural systems. Special programmes have been written for specific structures, (3,4,5) force systems were orthogonalised to improve conditioning, (3) regularisation procedures were used for cutouts, (6) and so on. The development of the automatic selection of redundancies and generation of the self-equilibrating force systems completely changed the approach to the force method of analysis. Any arbitrary structural system, no matter how complex, can now be analysed by the force methods. Furthermore, the selection procedures based on the Jordanian elimination technique lead invariably to well-conditioned equations (7).

Since the input information is identical in the two methods, it would appear at first that the choice of one or the other is largely a matter of taste and the availability of suitable

computer programmes. There is, however, one important consideration that has not been discussed. That is the number of unknown displacements or forces and the number of structural elements. Computer programmes for the displacement method have built-in limitations on the number of displacements and elements, while those for the force method have limitations on the number of node points, redundancies and elements.

Since the number of unknowns in the two methods may be widely different for the same structure, this alone may be the deciding criterion for selecting the method of analysis. Mainly because of the simplicity of matrix operations there has been a tendency to use the displacement method for complex structural configurations. For some special structures, however, particularly if the selection of redundancies and generation of the self-equilibrating system can be pre-programmed, the matrix force method can be used very effectively, and should be simpler than the displacement method.

2.1.1 Methods of analysing structures:

Two methods exist for the analysis of structures: the analytical and numerical methods. The limitations and difficulties associated with analytical methods are well-known and cannot be over-emphasised. Generally, these methods cannot be applied to complex structures.

Numerical methods are the most practical for complex structure analysis. This fact has been re-inforced by the arrival of the digital computer. Numerical methods of

structural analysis can be divided into two types:

- 1) A numerical solution of the differential equations is based upon the mathematical approximation of these equations. The process is achieved either by direct numerical integration or by finite-difference techniques. Again, practical limitations exist in the application of this method. Hence, it is mainly restricted to the analysis of simple structures. The numerical solution to the differential equations usually has equations which can be cast into matrix notation. But this is still not classified as a matrix method since the original formulations do not entail matrix connotations.
- 2) In the matrix method of structural analysis, matrix algebra is used throughout all the stages of the development of the analysis. First, the structure is idealized into an assemblage of discrete structural elements (beams, plates, etc.) The assumed displacements are then combined into a matrix equation satisfying the boundary conditions at the junctions of these elements.

Matrix methods based on structural analysis are suitable for the automation and programming of digital computers. The analysis is based on very simple numerical steps. This method is therefore suitable for the analysis of complex structures given access to a suitably sized digital computer. The matrix method of analysis has been found to provide

a reliable solution to the problem under consideration.

The Finite Element Method of structural analysis falls into the category of matrix methods of numerical analysis. In the structural analysis of the flexible platform in particular, the Finite Element Method is preferable to other numerical methods because of its versatility and flexibility of usage.

The application of the Finite Element Method to plane frame vibration involves imagining the platform to be actually split into a number of beam elements and plates of 'finite' length. This concept has given rise to its name. The plane frame contains both one- and two-dimensional components (beam and plates). Generally, a structure would be imagined to be actually broken up into a number of "elements" of finite dimensions . The structure under consideration was subdivided into finite elements connected by nodes as shown in Fig.(2.1.) These finite elements may be of equal or unequal length. The versatility of the Finite Element Method means that variation in the element length can be easily taken into account.

The next step in this method of analysis is the determination of the "element stiffness and mass matrices" of the individual elements describing the structure. These are then assembled to form the "overall stiffness and mass matrices" for the entire "discretized" structure by requiring that the continuity of displacements and equilibrium of forces prevail

at all nodes in the finite element model.

The equation of vibrating motion can then be written in matrix form:

$$[M]\{\ddot{q}\} + [K]\{q\} = \{Q\} \quad (2.2)$$

where

- $\{Q\}$ = column matrix of exciting force
- $\{q\}$ = displacement column matrix
- $\{\ddot{q}\}$ = acceleration column matrix
- $[K]$ = overall stiffness matrix of the structure
- and $[M]$ = overall mass matrix of the structure

In free vibration $\{Q\} = 0$ and

$\{q\}$ is a harmonic function of time

Then

$$\begin{aligned} \{q\} &= \{U\} \sin(\omega t + \phi) \\ \{\ddot{q}\} &= -\{U\} \omega^2 \sin(\omega t + \phi) \end{aligned} \quad (2.3)$$

substituting equations 2.3 in equation 2.2 yields

$$[K]\{U\} = \omega^2 [M]\{U\} \quad (2.4)$$

Equation 2.4 represents an eigen value problem. The solution of this eigen value problem will yield the eigen values $\omega_1^2, \omega_2^2, \omega_3^2, \omega_4^2, \dots$ hence $\omega_1, \omega_2, \omega_3, \dots$ which correspond to the natural frequencies of vibration of the discretized structure whilst the corresponding $\{U\}_1, \{U\}_2, \{U\}_3, \{U\}_4, \dots$ are its eigen vectors of natural modes of vibration.

To summarize, therefore, the finite element solution to the free vibration of a given flexible platform requires

the execution of the following operations in this order:

- 1) Discretization or subdivision of the structure into a system of finite elements.
- 2) Derivation of the element stiffness and mass matrices for each individual element representing the platform structure.
- 3) Construction of the "Overall stiffness and mass matrices" of the structure.
- 4) Solving the eigen value problem (equation 2.4)
- 5) Plotting of the eigen vectors, when necessary, as is most often the case, to get the feel of the modal shape of free vibration of the structure.

2.2 Consistent mass and stiffness matrices of beam elements.

It has already been shown that the discretization of a platform structure should produce beam and plate finite elements. Hence the next step in its vibration analysis is the derivation of the consistent mass and stiffness matrices of the beam element and the plate element.

Consider a beam element shown in Fig. (2.1). Its extremities are identified by the letters M and N. These represent its points of connection to the nodes of the finite element discretization of the frame.

The beam element is considered first in three-dimensional space and its orthogonal axes x_e , y_e , z_e are chosen such that the x_e -axis lies on the beam neutral axis. If the beam element is subjected to a set of arbitrary external

forces, then it will give rise to six internal reactive forces at each extremity of the beam. These will have their associated displacements. Forces here denote both moment and forces, and displacements include linear and angular displacements.

As shown in Fig. (2.2) these forces include:

Axial forces	F_1 and F_7
Shearing "	F_2, F_3, F_8 and F_9
Twisting moments	F_4 and F_{10}
and Bending "	F_5, F_6, F_{11} and F_{12}

The corresponding displacements are:

- i) Axial displacements U_1 and U_7
- ii) Transverse displacements U_2, U_3, U_8 and U_9
- iii) Twisting angles U_4 and U_{10}
- iv) Bending angles U_5, U_6, U_{11} and U_{12}

The positive directions of these displacements correspond to the positive directions of the corresponding forces as shown in Fig. (2.2). The consistent mass and stiffness matrices of the beam element are of order 12×12 . In this case, since the element axes are chosen to coincide with the principal axes of the beam cross-section, it is now possible to construct the 12×12 matrices from sets of 2×2 and 4×4 submatrices. From the theories of beam bending and torsion, it is obvious that the axial forces F_1 and F_7 are functions of their corresponding displacements U_1 and U_7 only; the same is true also for the twisting moments (torques) F_4 and F_{10} in relation to their twisting angles U_4 and U_{10} .

For arbitrarily chosen bending planes, the bending moments and shearing forces in the $x_e y_e$ plane would depend on their corresponding displacements as well as on the displacements corresponding to the forces in the $x_e y_e$ plane. But in this case, the choice of axis has been such that the $x_e y_e$ and $x_e z_e$ planes coincide with the principal axes of the cross-section. Hence the bending and shearing in these planes can be considered to be independent of each other. All forces acting on the beam elements can then be separated into four groups and considered independently of each other. With a suitable choice of corresponding displacement patterns within these groups, expressions can be obtained for the kinetic energy (T_e) and strain energy (U_e) of the beam in terms of the displacement. The consistent mass and stiffness matrix terms will then be derived from these energy expressions.

2.2.1 Axial Vibration in x_e axis

Fig. (2.3) shows the beam element under consideration. The beam is undergoing very small axial deformation or vibration. Elementary mechanics of materials show that the state of strain varies linearly within the beam element. Here, vibration is involved, hence the displacement is a function of time (t) also.

Thus a suitable displacement function is of the form

$$U(x,t) = a_0 + a_1 x = \begin{bmatrix} 1 & x \end{bmatrix} \begin{Bmatrix} a_0 \\ a_1 \end{Bmatrix} \quad (2.5)$$

Applying the element boundary conditions of $U(0,t) = U_1$ and $U(\ell,t) = U_7$, we have

$$\begin{Bmatrix} U_1 \\ U_7 \end{Bmatrix} = \begin{bmatrix} 1 & 0 \\ 1 & \ell \end{bmatrix} \begin{Bmatrix} a_0 \\ a_1 \end{Bmatrix} \quad (2.6)$$

or

$$\{U\} = [S] \{a\}$$

Solving for $\{a\}$ in equation (2.5) we have

$$\begin{Bmatrix} a_0 \\ a_1 \end{Bmatrix} = \begin{bmatrix} 1 & 0 \\ 1 & \ell \end{bmatrix}^{-1} \begin{Bmatrix} U_1 \\ U_7 \end{Bmatrix} = \begin{bmatrix} 1 & 0 \\ -1/\ell & 1/\ell \end{bmatrix} \begin{Bmatrix} U_1 \\ U_7 \end{Bmatrix}$$

Substituting into equation (2.5)

$$U(x,t) = [1 \quad x] \begin{bmatrix} 1 & 0 \\ -1/\ell & 1/\ell \end{bmatrix} \begin{Bmatrix} U_1 \\ U_7 \end{Bmatrix} \quad (2.7)$$

$$\text{so that } U(x,t) = [(1 - x/\ell) \quad x/\ell] \begin{Bmatrix} U_1 \\ U_7 \end{Bmatrix} \quad (2.8)$$

$$\text{or } U(x,t) = [N_1(x) \quad N_2(x)] \begin{Bmatrix} U_1 \\ U_7 \end{Bmatrix} \quad (2.9)$$

Let A be the cross sectional area of the beam. Then the strain energy of the beam in axial direction is given by

$$U = \frac{1}{2} \int_0^{\ell} E A \left(\frac{\partial u(x,t)}{\partial x} \right)^2 dx \quad (2.10)$$

substituting equation (2.8) in (2.10) we have

$$U = \frac{1}{2} \int_0^l ([u_1 \quad u_7] \begin{Bmatrix} -1/l \\ -1/l \end{Bmatrix} EA \begin{bmatrix} -1/l & 1/l \end{bmatrix} \begin{Bmatrix} u_1 \\ u_7 \end{Bmatrix}) dx \quad (2.11)$$

on integrating this reduces to the form

$$U = \frac{1}{2} [u_1 \quad u_7] \begin{bmatrix} \frac{EA}{l} & -\frac{EA}{l} \\ -\frac{EA}{l} & \frac{EA}{l} \end{bmatrix} \begin{Bmatrix} u_1 \\ u_7 \end{Bmatrix} \quad (2.12)$$

This is of the form

$$U = \frac{1}{2} \{u\}^t [K] \{u\} \quad (2.13)$$

Thus comparison of equation (2.12) and (2.13) shows that

$$[K] = \begin{bmatrix} K_{1,1} & K_{1,7} \\ K_{7,1} & K_{7,7} \end{bmatrix} = \frac{EA}{l} \begin{bmatrix} 1 & -1 \\ -1 & 1 \end{bmatrix} \quad (2.14)$$

which is the axial stiffness matrix of the beam element.

Similarly, the kinetic energy of the beam in axial motion is given by

$$T = \frac{1}{2} \int_0^l \rho A \left(\frac{\partial u(x,t)}{\partial t} \right)^2 dx \quad (2.15)$$

where ρ is the mass density of the beam.

Substituting from equation (2.8) into (2.15) and noting that

$\{u_1 \quad u_7\}^t$ is in fact a function of time t , integrating and simplifying gives

$$T = \frac{1}{2} \begin{Bmatrix} \frac{\partial u_1}{\partial t} & \frac{\partial u_7}{\partial t} \end{Bmatrix} \begin{bmatrix} \frac{\rho A l}{3} & \frac{\rho A l}{6} \\ \frac{\rho A l}{6} & \frac{\rho A l}{3} \end{bmatrix} \begin{Bmatrix} \frac{\partial u_1}{\partial t} \\ \frac{\partial u_7}{\partial t} \end{Bmatrix} \quad (2.16)$$

This is again of the form

$$T = \frac{1}{2} \left\{ \frac{\partial u}{\partial t} \right\}^t [m] \left\{ \frac{\partial u}{\partial t} \right\} \quad (2.17)$$

Thus, from equation (2.16) and (2.17), the axial mass matrix of the beam element may be given by

$$[m] = \begin{bmatrix} m_{1,1} & m_{1,7} \\ m_{7,1} & m_{7,7} \end{bmatrix} = \rho A l \begin{bmatrix} \frac{1}{3} & \frac{1}{6} \\ \frac{1}{6} & \frac{1}{3} \end{bmatrix} \quad (2.18)$$

2.2.2 Twisting about the x_e -axis

The beam element under torsional vibration is as shown in Fig. (2.4)

As with the axial case, the angle of twist varies linearly along the beam in the form

$$\begin{aligned} \text{i.e.} \quad \theta(x,t) &= a_{10} + a_{11} x \\ \theta(x,t) &= \begin{bmatrix} 1 & x \end{bmatrix} \begin{Bmatrix} a_{10} \\ a_{11} \end{Bmatrix} \end{aligned} \quad (2.19)$$

The appropriate boundary conditions are

$$\theta(0,t) = u_4 \quad \text{and} \quad \theta(l,t) = u_{10}$$

Hence from equation (2.19) we have

$$\begin{Bmatrix} u_4 \\ u_{10} \end{Bmatrix} = \begin{bmatrix} 1 & 0 \\ 1 & l \end{bmatrix} \begin{Bmatrix} a_{10} \\ a_{11} \end{Bmatrix} \quad (2.20)$$

$$\text{or} \quad \{u\} = [S] \{a\} \quad (2.21)$$

From equation (2.20), we have

$$\begin{Bmatrix} a_{10} \\ a_{11} \end{Bmatrix} = \begin{bmatrix} 1 & 0 \\ 1 & l \end{bmatrix}^{-1} \begin{Bmatrix} u_4 \\ u_{10} \end{Bmatrix} = \begin{bmatrix} 1 & 0 \\ -1/l & 1/l \end{bmatrix} \begin{Bmatrix} u_4 \\ u_{10} \end{Bmatrix}$$

Substituting for {a} into equation (2.19) we have

$$\theta(x, t) = [1 \quad x] \begin{bmatrix} 1 & 0 \\ -1/l & -1/l \end{bmatrix} \begin{Bmatrix} u_4 \\ u_{10} \end{Bmatrix}$$

Thus

$$\theta(x, t) = \begin{bmatrix} (1 - \frac{x}{l}) & \frac{x}{l} \end{bmatrix} \begin{Bmatrix} u_4 \\ u_{10} \end{Bmatrix} \quad (2.22)$$

Let I_x be the polar second moment of area of the beam cross section about the x_e axis.

Then the torsional strain energy of the beam is given by

$$U = \frac{1}{2} \int_0^l GI_x \left(\frac{\partial \theta(x, t)}{\partial x} \right)^2 dx \quad (2.23)$$

Substituting equation (2.22) into (2.23), integrating and simplifying yields

$$U = \frac{1}{2} [u_4 \quad u_{10}] \begin{bmatrix} \frac{GI_x}{l} & -\frac{GI_x}{l} \\ -\frac{GI_x}{l} & \frac{GI_x}{l} \end{bmatrix} \begin{Bmatrix} u_4 \\ u_{10} \end{Bmatrix} \quad (2.24)$$

which is of the form

$$U = \frac{1}{2} \{u\}^t [K] \{u\} \quad (2.25)$$

Hence the torsional stiffness matrix of the beam element is given by

$$[K] = \begin{bmatrix} K_{4,4} & K_{4,10} \\ K_{10,4} & K_{10,10} \end{bmatrix} = \frac{GI_x}{\ell} \begin{bmatrix} 1 & -1 \\ -1 & 1 \end{bmatrix} \quad (2.26)$$

And the torsional kinetic energy of the beam element is given by

$$T = \frac{1}{2} \int_0^{\ell} \rho I_x \left(\frac{\partial \theta(x,t)}{\partial t} \right)^2 dx \quad (2.27)$$

Substituting equation (2.22) into (2.27); ,integrating and simplifying we have

$$T = \frac{1}{2} \begin{bmatrix} -\frac{\partial u_4}{\partial t} & \frac{\partial u_{10}}{\partial t} \end{bmatrix} \begin{bmatrix} \frac{\rho I_x \ell}{3} & \frac{\rho I_x \ell}{6} \\ \frac{\rho I_x \ell}{6} & \frac{\rho I_x \ell}{3} \end{bmatrix} \begin{Bmatrix} \frac{\partial u_4}{\partial t} \\ \frac{\partial u_{10}}{\partial t} \end{Bmatrix} \quad (2.28)$$

which is of the form

$$T = \frac{1}{2} \left\{ \frac{\partial u}{\partial t} \right\}^t [M] \left\{ \frac{\partial u}{\partial t} \right\} \quad (2.29)$$

Thus the torsional mass matrix of the beam element is given by

$$[M] = \begin{bmatrix} m_{4,4} & m_{4,10} \\ m_{10,4} & m_{10,10} \end{bmatrix} = \rho A \ell \begin{bmatrix} \frac{I_x}{3A} & \frac{I_x}{6A} \\ \frac{I_x}{6A} & \frac{I_x}{3A} \end{bmatrix} \quad (2.30)$$

2.2.3 Shearing and bending in $x_e y_e$ plane

The beam under consideration is shown in Fig.(2.5). Engineering theory of bar bending indicates that the deformation is characterised by the deflection curve taken up by the centre line of the bar. The element has four degrees of freedom. Hence a suitable displacement model

is of the form

$$u(x,t) = a_{20} + a_{21}x + a_{22}x^2 + a_{23}x^3$$

or

$$u(x,t) = \begin{bmatrix} 1 & x & x^2 & x^3 \end{bmatrix} \begin{pmatrix} a_{20} \\ a_{21} \\ a_{22} \\ a_{23} \end{pmatrix} \quad (2.31)$$

The boundary conditions are

$$u(0,t) = u_2, \quad \frac{\partial u}{\partial x}(0,t) = u_6$$

$$u(l,t) = u_8, \quad \text{and} \quad \frac{\partial u}{\partial x}(l,t) = u_{12}$$

Substituting the above boundary conditions into equation

(2.31) we have

$$\begin{pmatrix} u_2 \\ u_6 \\ u_8 \\ u_{12} \end{pmatrix} = \begin{bmatrix} 1 & 0 & 0 & 0 \\ 0 & 1 & 0 & 0 \\ 1 & l & l^2 & l^3 \\ 0 & 1 & 2l & 3l^2 \end{bmatrix} \begin{pmatrix} a_{20} \\ a_{21} \\ a_{22} \\ a_{23} \end{pmatrix} \quad (2.32)$$

$$\text{i.e. } \{u\} = [S] \{a\}$$

$$\text{and } \{a\} = [S]^{-1} \{u\} \quad (2.33)$$

Now

$$[S]^{-1} = \begin{bmatrix} 1 & 0 & 0 & 0 \\ 0 & 1 & 0 & 0 \\ 1 & l & l^2 & l^3 \\ 0 & 1 & 2l & 3l^2 \end{bmatrix}$$

i.e.

$$[S]^{-1} = \begin{bmatrix} 1 & 0 & \frac{3}{l^2} & \frac{2}{l^3} \\ 0 & 1 & \frac{1}{l^2} & \frac{1}{l^3} \\ 0 & 0 & \frac{3}{l^2} & \frac{2}{l^3} \\ 0 & 0 & \frac{1}{l} & \frac{1}{l^2} \end{bmatrix} \quad (2.34)$$

Substituting equations (2.33) and (2.24) into equation (2.31) we have

$$u(x_1 t) = \begin{bmatrix} 1 & x & x^2 & x^3 \end{bmatrix} \begin{bmatrix} 1 & 0 & -\frac{3}{l^2} & \frac{2}{l^3} \\ 0 & 1 & -\frac{2}{l} & \frac{1}{l^2} \\ 0 & 0 & \frac{3}{l^2} & \frac{2}{l^3} \\ 0 & 0 & -\frac{1}{l} & \frac{1}{l^2} \end{bmatrix} \begin{Bmatrix} u_2 \\ u_6 \\ u_8 \\ u_{12} \end{Bmatrix} \quad (2.35)$$

Let I_z be the second moment of area of the cross section about the z_e -axis. Then, neglecting the effects of shear deformation, the strain energy of the beam element under the action of the shearing forces and bending moments in the $x_e y_e$ plane is given by

$$U = \frac{1}{2} \int_0^l EI_z \left(\frac{\partial^2 u(x_1 t)}{\partial x^2} \right)^2 dx \quad (2.36)$$

Substituting equation (2.31) into equation (2.32) and simplifying we have

$$U = \frac{1}{2} \begin{Bmatrix} u_2 \\ u_6 \\ u_8 \\ u_{12} \end{Bmatrix} \begin{bmatrix} \frac{12 EI_z}{l^3} & & & \\ & \text{Symmetric} & & \\ \frac{6 EI_z}{l^2} & & \frac{4 EI_z}{l} & \\ -\frac{12 EI_z}{l^3} & -\frac{6 EI_z}{l^2} & -\frac{12 EI_z}{l^3} & \\ \frac{6 EI_z}{l^2} & \frac{2 EI_z}{l} & -\frac{6 EI_z}{l^2} & \frac{4 EI_z}{l} \end{bmatrix} \begin{Bmatrix} u_2 \\ u_6 \\ u_8 \\ u_{12} \end{Bmatrix} \quad (2.37)$$

Thus the beam stiffness matrix in flexure in the $x_e y_e$ plane is given by

$$[K] = \begin{bmatrix} K_{2,2} & & & & \text{Symmetric} \\ K_{2,6} & K_{6,6} & & & \\ K_{2,8} & K_{6,8} & K_{8,8} & & \\ K_{2,12} & K_{6,12} & K_{8,12} & K_{12,12} & \end{bmatrix} = \frac{EI_z}{l^3} \begin{bmatrix} 12 & 6l & -12 & 6l \\ 6l & 4l^2 & -6l & 2l^2 \\ -12 & -6l & 12 & -6l \\ 6l & 2l^2 & -6l & 4l^2 \\ \dots & \dots & \dots & \dots \end{bmatrix} \quad (2.38)$$

Also, the kinetic energy of the beam element in $x_e y_e$ plane due to shearing forces and bending moment is given by

$$T = \frac{1}{2} \int_0^l \rho A \left(\frac{\partial u(x,t)}{\partial t} \right)^2 dx \quad (2.39)$$

Substituting from equation (2.35) into equation (2.39) and simplifying we have

$$T = \begin{pmatrix} \frac{\partial u_2}{\partial t} \\ \frac{\partial u_6}{\partial t} \\ \frac{\partial u_8}{\partial t} \\ \frac{\partial u_{12}}{\partial t} \end{pmatrix}^T \begin{bmatrix} \frac{13\rho A l}{35} & & & & \text{Symmetric} \\ \frac{11\rho A l^2}{210} & \frac{\rho A l^3}{105} & & & \\ \frac{9\rho A l}{70} & \frac{13\rho A l^2}{420} & \frac{13\rho A l}{35} & & \\ -\frac{13\rho A l^2}{420} & -\frac{\rho A l^3}{140} & \frac{11\rho A l^2}{210} & \frac{\rho A l^3}{105} & \end{bmatrix} \begin{pmatrix} \frac{\partial u_2}{\partial t} \\ \frac{\partial u_6}{\partial t} \\ \frac{\partial u_8}{\partial t} \\ \frac{\partial u_{12}}{\partial t} \end{pmatrix}$$

Thus the beam mass matrix in flexure in the $x_e y_e$ plane (neglecting the effects of shear deformation) is given by

$$[m] = \begin{bmatrix} m_{2,2} & & & & \text{Symmetric} \\ m_{2,6} & m_{6,6} & & & \\ m_{2,8} & m_{6,8} & m_{8,8} & & \\ m_{2,12} & m_{6,12} & m_{8,12} & m_{12,12} & \end{bmatrix} = \rho A l \begin{bmatrix} \frac{13}{35} & & & & \text{symmetric} \\ \frac{11l}{210} & \frac{l^2}{105} & & & \\ \frac{9}{70} & \frac{13l}{420} & \frac{13}{35} & & \\ -\frac{13l}{420} & -\frac{l^2}{140} & -\frac{11l}{210} & \frac{l^2}{105} & \\ \dots & \dots & \dots & \dots & \end{bmatrix} \quad (2.40)$$

2.2.4 Shearing and bending in the $x_e z_e$ plane

Fig. (2.6) shows the beam under consideration

Positive directions of forces and displacement are as illustrated.

Four degrees of freedom are envisaged and a suitable displacement model is of the form

$$u(x,t) = a_{30} + a_{31}x + a_{32}x^2 + a_{33}x^3$$

$$\text{or } u(x,t) = [1 \quad x \quad x^2 \quad x^3] \begin{pmatrix} a_{30} \\ a_{31} \\ a_{32} \\ a_{33} \end{pmatrix} \quad (2.41)$$

The geometric boundary conditions as illustrated in Fig. (2.6) are as follows

$$\begin{aligned} u(0,t) &= u_3, \quad \frac{\partial u(0,t)}{\partial x} = -u_5 \\ u(l,t) &= u_9, \quad \frac{\partial u(l,t)}{\partial x} = -u_{11} \end{aligned} \quad (2.42)$$

Hence, equations (2.42) and (2.41) give

$$\begin{pmatrix} u_3 \\ -u_5 \\ u_9 \\ -u_{11} \end{pmatrix} = \begin{bmatrix} 1 & 0 & 0 & 0 \\ 0 & 1 & 0 & 0 \\ 1 & l & l^2 & l^3 \\ 0 & 1 & 2l & 3l^3 \end{bmatrix} \begin{pmatrix} a_{30} \\ a_{31} \\ a_{32} \\ a_{33} \end{pmatrix} \quad (2.43)$$

Thus from equation (2.43) we have

$$\begin{pmatrix} a_{30} \\ a_{31} \\ a_{32} \\ a_{33} \end{pmatrix} = \begin{bmatrix} 1 & 0 & 0 & 0 \\ 0 & 1 & 0 & 0 \\ 1 & l & l^2 & l^3 \\ 0 & 1 & 2l & 3l^3 \end{bmatrix}^{-1} \begin{pmatrix} u_3 \\ -u_5 \\ u_9 \\ -u_{11} \end{pmatrix}$$

and

$$\begin{Bmatrix} a_{30} \\ a_{31} \\ a_{32} \\ a_{33} \end{Bmatrix} = \begin{bmatrix} 1 & 0 & -\frac{3}{\ell^2} & \frac{2}{\ell^3} \\ 0 & 1 & -2/\ell & 1/\ell^2 \\ 0 & 0 & 3/\ell^2 & 2/\ell^3 \\ 0 & 0 & -1/\ell & 1/\ell^2 \end{bmatrix} \begin{Bmatrix} u_3 \\ -u_5 \\ u_9 \\ -u_{11} \end{Bmatrix} \quad (2.44)$$

Substituting equation (2.44) into equation (2.41) we have

$$u(x, t) = [1 \quad x \quad x^2 \quad x^3] \begin{bmatrix} 1 & 0 & -\frac{3}{\ell^2} & \frac{2}{\ell^3} \\ 0 & -1 & 2/\ell & -1/\ell^2 \\ 0 & 0 & 3/\ell^2 & 2/\ell^3 \\ 0 & 0 & 1/\ell & -1/\ell^2 \end{bmatrix} \begin{Bmatrix} u_3 \\ u_5 \\ u_9 \\ u_{11} \end{Bmatrix} \quad (2.45)$$

Let I_y be the second moment of area of the cross-section about the y_e axis. Then neglecting the effects of shear deformation and the strain energy of the beam element under the action of shearing forces and bending moments in the $x_e z_e$ plane is given by

$$U = \frac{1}{2} \int_0^\ell EI_y \left(\frac{\partial^2 u(x, t)}{\partial x^2} \right)^2 dx \quad (2.46)$$

Substituting equation (2.45) into equation (2.46) integrating and simplifying we have

$$U = \frac{1}{2} \begin{Bmatrix} u_3 \\ u_5 \\ u_9 \\ u_{11} \end{Bmatrix} \begin{bmatrix} \frac{12EI_y}{\ell} & & & & \text{Symmetric} \\ -\frac{6EI_y}{\ell^2} & \frac{4EI_y}{\ell} & & & \\ -\frac{12EI_y}{\ell^3} & \frac{6EI_y}{\ell} & \frac{12EI_y}{\ell} & & \\ -\frac{6EI_y}{\ell^2} & \frac{2EI_y}{\ell} & \frac{6EI_y}{\ell^2} & \frac{4EI_y}{\ell} & \end{bmatrix} \begin{Bmatrix} u_3 \\ u_5 \\ u_9 \\ u_{11} \end{Bmatrix} \quad (2.47)$$

From equation (2.47), the flexural beam stiffness matrix in the plane is given by

$$[K] = \begin{bmatrix} K_{3,3} & \text{Symmetric} & & \\ K_{3,5} & K_{5,5} & & \\ K_{3,9} & K_{5,9} & K_{9,9} & \\ K_{3,11} & K_{5,11} & K_{9,11} & K_{11,11} \end{bmatrix} = \begin{bmatrix} \frac{12EIy}{l} & \text{Symmetric} & & \\ -\frac{6EIy}{l^2} & \frac{4EIy}{l} & & \\ -\frac{12EIy}{l^3} & \frac{6EIy}{l^2} & \frac{12EIy}{l} & \\ -\frac{6EIy}{l^2} & \frac{2EIy}{l} & \frac{6EIy}{l^2} & \frac{4EIy}{l} \end{bmatrix} \dots\dots\dots (2.48)$$

Similarly, the expression for the kinetic energy of the beam is given by equation (2.39). Substitution of equation (2.45) into (2.29) gives

$$T = \begin{Bmatrix} \frac{\partial u_3}{\partial t} \\ \frac{\partial u_5}{\partial t} \\ \frac{\partial u_9}{\partial t} \\ \frac{\partial u_{11}}{\partial t} \end{Bmatrix}^t \begin{bmatrix} \frac{13\rho Al}{35} & \text{Symmetric} & & \\ -\frac{11\rho Al^2}{210} & \frac{\rho Al^3}{105} & & \\ \frac{9\rho Al}{70} & -\frac{13\rho Al^2}{420} & \frac{13\rho Al}{35} & \\ \frac{13\rho Al^2}{420} & -\frac{\rho Al^3}{140} & \frac{11\rho Al^2}{210} & \frac{\rho Al^3}{105} \end{bmatrix} \begin{Bmatrix} \frac{\partial u_3}{\partial t} \\ \frac{\partial u_5}{\partial t} \\ \frac{\partial u_9}{\partial t} \\ \frac{\partial u_{11}}{\partial t} \end{Bmatrix} \dots\dots\dots (2.49)$$

and from equation (2.49), the flexural beam mass matrix in the $x_e y_e$ plane is given by

$$[M] = \begin{bmatrix} m_{3,3} & \text{Symmetric} & & \\ m_{3,5} & m_{5,5} & & \\ m_{3,9} & m_{5,9} & m_{9,9} & \\ m_{3,11} & m_{5,11} & m_{9,11} & m_{11,11} \end{bmatrix}$$

$$[M] = \rho A \ell \begin{bmatrix} \frac{13}{35} & \text{Symmetrical} & & & \\ -\frac{11}{210} & \frac{\ell^2}{105} & & & \\ \frac{9}{70} & -\frac{13\ell}{420} & \frac{13}{35} & & \\ \frac{13\ell}{420} & -\frac{\ell^2}{140} & \frac{11\ell}{210} & \frac{\ell^2}{105} & \end{bmatrix} \quad (2.50)$$

2.2.5 Beam matrices in assembled form

From the above analysis and results, the 12 X 12 consistent mass and stiffness matrices of the beam element can be obtained.

Assembling equations (2.14), (2.26), (2.38) and (2.48) we have the complete stiffness matrix $[K_e]$ of the beam element given by equation (2.51).

Similarly, assembling equations (2.18), (2.30), (2.40) and (2.50) we have the complete mass matrix $[M_e]$ of the beam element given by equation (2.52).

$$[K_e] =$$

1	EA/ρ																		
2	0	$\frac{12EI}{\rho^3} z$																	
3	0	0	$\frac{12EI}{\rho^3} y$																
4	0	0	0	$\frac{GI}{\rho} x$															
5	0	0	$-\frac{6EI}{\rho^2} y$	0	$\frac{4EI}{\rho} y$														
6	0	$\frac{6EI}{\rho^2} z$	0	0	0	$\frac{4EI}{\rho} z$													
7	$-\frac{EA}{\rho}$	0	0	0	0	0	$\frac{EA}{\rho}$												
8	0	$-\frac{12EI}{\rho^3} z$	0	0	0	$-\frac{6EI}{\rho^2} z$	0	$\frac{12EI}{\rho^3} z$											
9	0	0	$-\frac{12EI}{\rho^3} y$	0	$\frac{6EI}{\rho^2} y$	0	0	$\frac{12EI}{\rho^3} y$											
10	0	0	0	$-\frac{GI}{\rho} x$	0	0	0	0	$\frac{GI}{\rho} x$										
11	0	0	$-\frac{6EI}{\rho^2} y$	0	$\frac{2EI}{\rho} y$	0	0	$\frac{6EI}{\rho^2} y$	0	$\frac{4EI}{\rho} y$									
12	0	$\frac{6EI}{\rho^2} z$	0	0	0	$\frac{2EI}{\rho} z$	0	$\frac{6EI}{\rho^2} z$	0	0	$\frac{4EI}{\rho} z$								

Symmetric

1	$\frac{1}{3}$											
2	0	$\frac{13}{35}$										
3	0	0	$\frac{13}{35}$									
4	0	0	0	$\frac{I_x}{3A}$								
5	0	0	$-\frac{11\ell}{210}$	0	$\frac{\ell^2}{105}$							
6	0	$\frac{11\ell}{210}$	0	0	0	$\frac{\ell^2}{105}$						
7	$\frac{1}{6}$	0	0	0	0	0	$\frac{1}{3}$					
8	0	$\frac{9}{70}$	0	0	0	$\frac{13\ell}{420}$	0	$\frac{13}{35}$				
9	0	0	$\frac{9}{70}$	0	$-\frac{13\ell}{420}$	0	0	0	$\frac{13}{35}$			
10	0	0	0	$\frac{I_x}{3A}$	0	0	0	0	0	$\frac{I_x}{3A}$		
11	0	0	$\frac{13\ell}{420}$	0	$-\frac{\ell^2}{140}$	0	0	0	$\frac{11\ell}{210}$	0	$\frac{\ell^2}{105}$	
12	0	$-\frac{13\ell}{420}$	0	0	0	$-\frac{\ell^2}{140}$	0	$-\frac{11\ell}{210}$	0	0	0	$\frac{\ell^2}{105}$

Symmetric

$[M_e] = \rho A \ell$

(2.52)

2.3 Beam properties in frame co-ordinate system

The mass and stiffness matrices obtained in section 2.2.5 consist of 12 X 12 dimensional arrays. These have been derived with respect to a convenient set of orthogonal axes x_e, y_e, z_e such that x_e lies on the beam natural axis while $x_e y_e$ and $x_e z_e$ plane coincides with the principal axis of the beam cross-section. The choice of this co-ordinate system has led to a simplified derivation and results in equations (2.51) and (2.52).

The set of axes x_e, y_e, z_e are therefore localised axis or beam element axes. The beam element considered is one of many beam elements in the finite element discretization of the plane frame in question. Each element will generally have a different set of axes such that these axes will not coincide with each other.

It is therefore necessary to define for the frame a global system or a set of co-ordinates to which each beam element's properties will have to be transformed. Fig.(2.7) shows a typical beam element in three-dimensional space. The x_e, y_e, z_e axes define the beam element co-ordinate system as explained in 2.2 while the X, Y, Z axes define the global or frame co-ordinate system. A transformation matrix should exist which relates the beam element properties (stiffness, mass, force, displacement, etc.) in the element co-ordinate system x_e, y_e, z_e to their frame co-ordinate counterparts.

2.3.1 Plane axes transformations

Looking at the transformation of the beam element properties from its local system to the frame system in a plane frame situation may be helpful, and easier to derive and understand.

Fig.(2.7) shows a beam element connecting two joints M and N in a plane finite element discretization. The x_e - and y_e - axes are the element co-ordinate axes, while the X and Y-axes are the frame co-ordinate axes. Angle α is the angle of rotation from X-axis to x_e -axis, the position direction being the anti-clockwise rotation shown in the figure.

The forces (forces and moments) acting at the two joints M and N are as shown in the figure in both the element co-ordinate system and the frame co-ordinate system.

The following are the equilibrium of forces equations at the two joints :

At joint M

$$FX_M + Fx_{eM} \cos\alpha - Fy_{eM} \sin\alpha = 0$$

$$FY_M + Fx_{eM} \sin\alpha - Fy_{eM} \cos\alpha = 0$$

$$M_M + M_{eM} = 0$$

At joint N

$$FX_N + Fx_{eN} \cos\alpha - Fy_{eN} \sin\alpha = 0$$

$$FY_N + Fx_{eN} \sin\alpha - Fy_{eN} \cos\alpha = 0$$

$$M_N + M_{eN} = 0$$

In matrix notation, we have

At joint M

$$\begin{Bmatrix} F_{X_M} \\ F_{Y_M} \\ M_M \end{Bmatrix} = \begin{bmatrix} -\cos \alpha & \sin \alpha & 0 \\ -\sin \alpha & -\cos \alpha & 0 \\ 0 & 0 & 1 \end{bmatrix} \begin{Bmatrix} F_{X_{eM}} \\ F_{Y_{eM}} \\ M_{eM} \end{Bmatrix} \quad (2.53)$$

At joint N

$$\begin{Bmatrix} F_{X_N} \\ F_{Y_N} \\ M_N \end{Bmatrix} = \begin{bmatrix} -\cos \alpha & \sin \alpha & 0 \\ -\sin \alpha & -\cos \alpha & 0 \\ 0 & 0 & -1 \end{bmatrix} \begin{Bmatrix} F_{X_{eN}} \\ F_{Y_{eN}} \\ M_{eN} \end{Bmatrix} \quad (2.54)$$

Thus the transformation for a plane beam element is of the form

$$\begin{Bmatrix} F_{X_M} \\ F_{Y_M} \\ M_M \\ F_{X_N} \\ F_{Y_N} \\ M_N \end{Bmatrix} = \begin{bmatrix} [TM] & & & & & \\ & 0 & 0 & 0 & & \\ & 0 & 0 & 0 & & \\ & 0 & 0 & 0 & & \\ & & & & [TM] & \\ & & & & & 0 & 0 & 0 \end{bmatrix} \begin{Bmatrix} F_{X_{eM}} \\ F_{Y_{eM}} \\ M_{eM} \\ F_{X_{eN}} \\ F_{Y_{eN}} \\ M_{eN} \end{Bmatrix} \quad (2.55)$$

The transformation matrix is, therefore, a 6 X 6 matrix.

The same matrix will transform the stiffness, mass, and

displacement. It should be noted that a plane beam element

as analysed above has six degrees of freedom. This in turn requires a 6 X 6 transformation matrix.

2.3.2 Overall transformation matrix

The three step rotation has a final effect of rotation of the frame co-ordinate system (X,Y,Z) into the beam element co-ordinate system (X_e, Y_e, Z_e) for the joint M as a general case in matrix form

$$\{F\} = [T M] \{F_e\} \quad (2.56)$$

or

$$\{F\} = [T \alpha] [TB] [T\gamma] \{F_e\} \quad (2.57)$$

or

$$[T M] = \begin{bmatrix} -\cos \alpha & \sin \alpha & 0 \\ -\sin \alpha & -\cos \alpha & 0 \\ 0 & 0 & -1 \end{bmatrix} \begin{bmatrix} -\cos \beta & 0 & -\sin \beta \\ 0 & -1 & 0 \\ \sin \beta & 0 & -\cos \beta \end{bmatrix} \begin{bmatrix} -1 & 0 & 0 \\ 0 & -\cos \alpha & \sin \alpha \\ 0 & -\sin \alpha & \cos \alpha \end{bmatrix} \quad \dots\dots (2.58)$$

Only sets of three orthogonal forces (excluding moments) have been considered. But generally with the beam element under investigation, there is the set of three orthogonal moments also acting on the beam element. These moments will act about the orthogonal axis. Considering that a positive moment is a clockwise moment when viewed along its axis, the operations described above for transformation of forces will also be applicable to moment transformations. Thus the equations (2.56) and (2.57) also hold true for moments.

Let Q₁, Q₂, Q₃, Q₄, Q₅, Q₆ be the forces (and moments) acting on the beam element at the joint M in the frame co-ordinate system. And Q₇, Q₈, Q₉, Q₁₀, Q₁₁, Q₁₂ be the

forces (and moments) acting on the beam element at the other point N in the frame co-ordinate system.

Also let $F_{e_1}, F_{e_2}, F_{e_3}$ ---- F_{e_6} and F_{e_7}, F_{e_8} --- $F_{e_{12}}$ be the other set of forces (and moments) acting on the beam element at the joints M and N respectively in the beam element co-ordinate system. Then the 12 equilibrium equations relating actions on the element in the frame co-ordinate system and the beam co-ordinate system can be seen to be similar to the results obtained above. In fact, the transformation in matrix terms is given by

$$\begin{Bmatrix} Q_1 \\ Q_2 \\ \\ Q_{12} \end{Bmatrix} = \begin{bmatrix} [TM] & [Z] & [Z] & [Z] \\ [Z] & [TM] & [Z] & [Z] \\ [Z] & [Z] & [TM] & [Z] \\ [Z] & [Z] & [Z] & [TM] \end{bmatrix} \begin{Bmatrix} F_{e_1} \\ F_{e_2} \\ F_{e_3} \\ \\ \\ F_{e_{12}} \end{Bmatrix} \quad (2.59)$$

$$\text{where } [Z] = \begin{bmatrix} 0 & 0 & 0 \\ 0 & 0 & 0 \\ 0 & 0 & 0 \end{bmatrix} \quad (2.60)$$

and from equation (2.58)

$$[TM] = \begin{bmatrix} -\cos\alpha \cdot \cos\beta & \sin\alpha \cdot \cos\gamma - \cos\alpha \cdot \sin\beta \cdot \sin\gamma & -\sin\alpha \cdot \sin\gamma - \cos\alpha \cdot \sin\beta \cdot \cos\gamma \\ -\sin\alpha \cdot \cos\beta & -\cos\alpha \cos\gamma - \sin\alpha \cdot \sin\beta \cdot \sin\gamma & \cos\alpha \cdot \sin\gamma - \sin\alpha \cdot \sin\beta \cdot \cos\gamma \\ \sin\beta & -\cos\beta \cdot \sin\gamma & -\cos\beta \cdot \cos\gamma \end{bmatrix} \quad (2.61)$$

Equation (2.59) is of the form

$$\{Q\} = [R] \{F_e\} \quad (2.62)$$

$$[R] = \begin{bmatrix} [TM] & [Z] & [Z] & [Z] \\ [Z] & [TM] & [Z] & [Z] \\ [Z] & [Z] & [TM] & [Z] \\ [Z] & [Z] & [Z] & [TM] \end{bmatrix} \quad (2.63)$$

All force transformations discussed so far also hold true for displacements. Thus, if the corresponding displacements of the beam element in the frame co-ordinate system are denoted by q_1, q_2, \dots, q_{12} , then equation (2.62) can be written for the displacement as follows

$$\{q\} = [R] \{u\} \quad (2.64)$$

where $\{u\}^t = [u_1, u_2, u_3, \dots, u_{12}]$, represents the displacement of the beam element in the beam element co-ordinate system.

Now, the strain energy of the beam element is given by

$$U = \{u\}^t [K_e] \{u\} \quad (2.65)$$

the transformation matrix $[R]$ is an orthogonal one. Thus, its inverse is equal to its transpose, hence from equation (2.64), we have

$$\begin{aligned} \{u\} &= [R]^{-1} \{q\} \\ &= [R]^t \{q\} \end{aligned} \quad (2.66)$$

And substituting equation (2.66) into equation (2.65), the strain energy of the beam element is given by

$$U = \{q\}^t [R] [K_e] [R]^t \{q\} \quad (2.67)$$

Equation (2.67) is of the form

$$U = \{q\}^t [K] \{q\} \quad (2.68)$$

which is an expression of strain energy of the beam element in terms of the displacement q_i ($i=1, \dots, 12$) in the frame co-ordinate system. The matrix $[K]$ is a 12 X 12 matrix and it is the stiffness matrix of the beam element in the frame co-ordinate system. From equations (2.67) and (2.68) it can be deduced that

$$[K] = [R] [K_e] [R]^t$$

where the matrix $[K_e]$ is given by equation (2.51).

Similarly, the kinetic energy of the beam element is given by

$$T = \left\{ \frac{\partial u}{\partial t} \right\}^t [m_e] \left\{ \frac{\partial u}{\partial t} \right\} \quad (2.69)$$

Substituting equation (2.66) into equation (2.69) we have the kinetic energy of the beam element which is given by

$$T = \left\{ \frac{\partial q}{\partial t} \right\}^t [R] [m_e] [R]^t \left\{ \frac{\partial q}{\partial t} \right\} \quad (2.70)$$

again, this is of the form

$$T = \left\{ \frac{\partial q}{\partial t} \right\}^t [m] \left\{ \frac{\partial q}{\partial t} \right\} \quad (2.71)$$

which is an expression of the kinetic energy of the beam element in terms of the displacements q_i ($i=1,2,3,\dots, 12$) in the force co-ordinate system. Comparing equations (2.70) and (2.71) we have

$$[m] = [R] [m_e] [R]^t \quad (2.72)$$

where the matrix $[m_e]$ is given by equation (2.52). The matrix $[m]$ is a 12 X 12 matrix which represents the mass matrix of the beam element in the frame co-ordinate system.

2.4 Assembly of system mass and stiffness matrices

The stiffness and mass matrices obtained after the co-ordinate transformation, express the beam element properties in terms of the global co-ordinate system. These need to be assembled into the overall matrices for the frame. Thus the contribution of the beam element in question to the frame stiffness and mass matrices is to be identified and added accordingly. The code number method is utilised here. The transformed beam element matrices are each 12 X 12 matrices. The first 6 rows or columns of these matrices are related to the frame co-ordinates at the end M of the beam, which the other 6 (7-12) rows or columns are related to frame co-ordinates at the other end N of the beam element. Thus, the matrices are such that the rows and columns 1, 2 and 3 relate to the translated displacement components in the X-, Y- and Z- directions

of the frame axis system at the end M. The rows and columns 4,5 and 6 relate to the rotational displacement components about the X-Y- and z-axes of the frame axis system at the end M.

Similarly, the rows and columns 7, 8 and 9 relate to the translational displacement components in the X- Y- and Z- directions of the frame axis system at the end N. And the rows and columns 10, 11 and 12 relate to rotational displacement components about the X-, Y- and Z- axes of the frame axis system at the end N. The idea of the code number method is to assign to each of these 12 beam element matrix rows and columns, a number which represents the corresponding frame co-ordinate points.

Each of the 12 beam element co-ordinates should have a corresponding co-ordinate in the frame co-ordinate system. Any element co-ordinate which does not contribute to the frame co-ordinate system is assigned a zero code number. All other element co-ordinates are given code numbers equal to the value of the co-ordinate in the frame co-ordinate system. Thus the code number at any point is a positive - including zero - integer not greater than the total number of degrees of freedom of the discretized frame structure. It is worth noting that the inclusion of the zero code number makes it possible to analyse 1 - dimensional and plane frame structures from the general 3 - dimensional beam finite element discretization model.

2.4.1 Beam Elements

Consider the transverse vibration only of a uniform beam element as shown in Fig. (2.11) where q_i and Q_i ,

$i=1,2,3,4$ are the displacements and end forces respectively. The quantities such as U, q, ϵ etc. are referred to their amplitudes of vibration.

A simple displacement pattern of the beam may be assumed to be:

$$U(x) = \alpha_0 + \alpha_1 x + \alpha_2 x^2 + \alpha_3 x^3 \quad (2.73)$$

where $\alpha_i, i = 0,1,2,3$ are constants to be determined. The displacement vector in this case consists of one component i.e. the transverse displacement, therefore we may drop the brackets for vector notation. Where the functions $x^i, i = 0,1,2,3$ were chosen as co-ordinate functions, α_i would have been taken as the generalised co-ordinates.

Now since α_i does not have direct physical interpretation, we prefer to transform it to q_i , so that the conditions of compatibility between elements can be applied directly to form the overall system equations.

The transformation may proceed as follows:

In order to determine the coefficients $\alpha_i, i = 0,1,2,3$ in equation (2.73) it is necessary to use the following boundary conditions:

$$U(0) = q_1, \quad U'(0) = q_2, \quad U(l) = q_3, \quad U'(l) = q_4 \\ \dots\dots (2.74)$$

substituting equation (2.73) into equation (2.74) we obtain a set of four equations for $\alpha_i, i = 0,1,2,3$.

After solving these equations for α_i in terms of $q_i, i = 1,2,3,4$ the equation (2.73) can be rewritten in the form:

$$U(x) = [a(x)] \{q\} \quad (2.75)$$

where $\{q\} = [q_1 \ q_2 \ q_3 \ q_4]^T$

and

$$[a(x)] = \left[1 - 3\left(\frac{x}{l}\right)^2 + 2\left(\frac{x}{l}\right)^3 \quad \left(\frac{x}{l} - 2\left(\frac{x}{l}\right)^2 + \left(\frac{x}{l}\right)^3\right) l \right. \\ \left. 3\left(\frac{x}{l}\right) - 2\left(\frac{x}{l}\right)^3 \quad \left(-\left(\frac{x}{l}\right)^2 + \left(\frac{x}{l}\right)^3\right) l \right] \quad (2.76)$$

The strain and displacement relationship for a beam is

$$\epsilon_x(x) = \frac{\partial v}{\partial x} = -y \frac{\partial^2 u}{\partial x^2} \quad (2.77)$$

where v is the longitudinal displacement and y is the co-ordinate normal to x and in the plane of vibration. From equations (2.77) and (2.75) we get the strain and generalised displacement relationship:

$$\epsilon_x(x) = [b(x)] \{q\} \quad (2.78)$$

where

$$[b(x)] = \frac{-y}{l^2} \left[-6 + 12\left(\frac{x}{l}\right) \quad (-4 + 6\left(\frac{x}{l}\right)) \quad 6 - 12\left(\frac{x}{l}\right) \quad (-2 + 6\left(\frac{x}{l}\right)) l \right] \quad (2.79)$$

The substitution of equations (2.79) and (2.76) in the following equations

$$[m] = \int_{vol} [a]^T [\rho] [a] \, dvol \quad (A)$$

$$[k] = \int_{vol} [b]^T [C] [b] \, dvol \quad (B)$$

gives the mass and stiffness matrices respectively.

$$[m] = \frac{\rho AL}{420} \begin{bmatrix} 156 & 22l & 54 & -13l \\ 22l & 4l^2 & 13l & -3l^2 \\ 54 & 13l & 156 & -22l \\ -13l & -3l^2 & -22l & 4l^2 \end{bmatrix} \quad (2.80)$$

and

$$[K] = \frac{EI}{l^3} \begin{bmatrix} 12 & 6l & -12 & 6l \\ 6l & 4l^2 & -6l & 2l^2 \\ -12 & -6l & 12 & -6l \\ 6l & 2l^2 & -6l & 4l^2 \end{bmatrix} \quad (2.81)$$

which is the same as in Equation (2.51) considering the rows 2, 6, 8, 12 to give the stiffness matrix $[K]$ as above, (2.81).

In the case of $[m]$ it is as in Equation (2.52), considering the same rows 2, 6, 8, 12 to give the previous mass matrix (2.80).

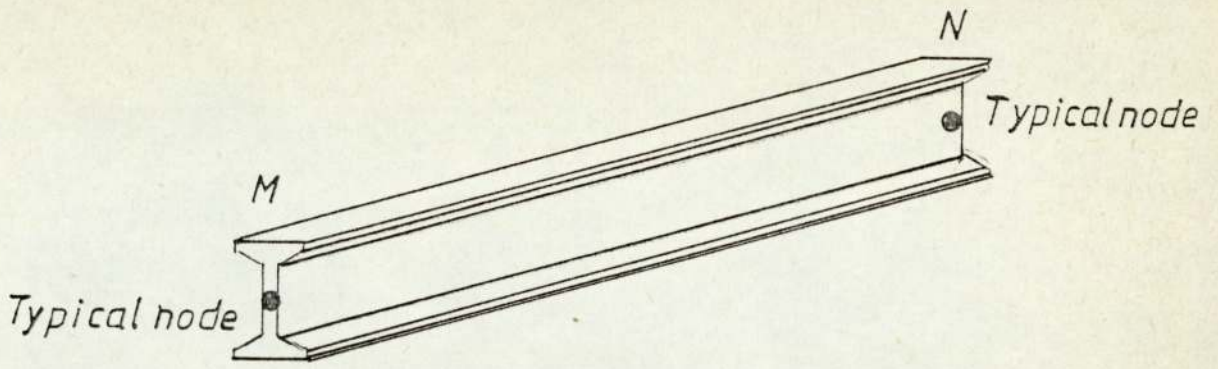


Fig. 2.1.

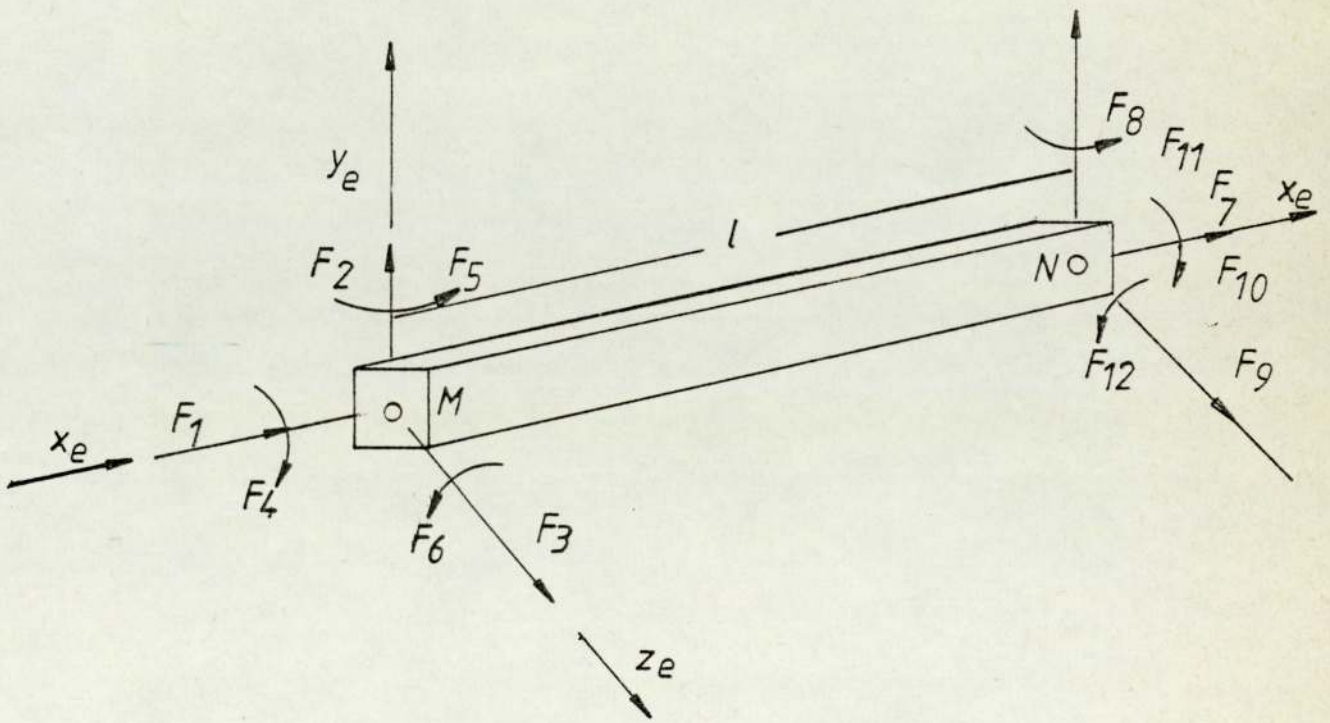


Fig. 2.2. Beam element.

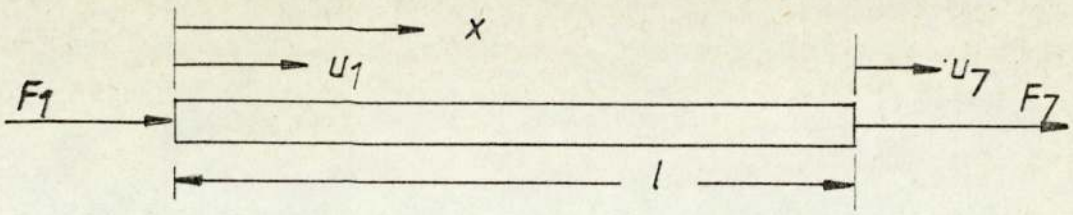


Fig. 2.3

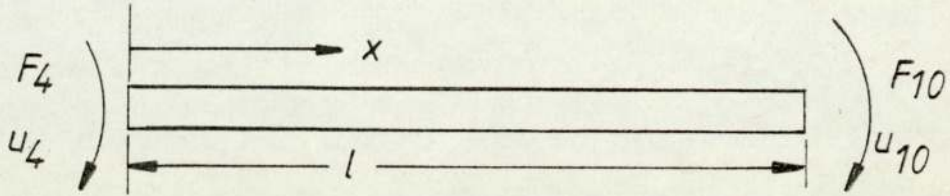


Fig. 2.4

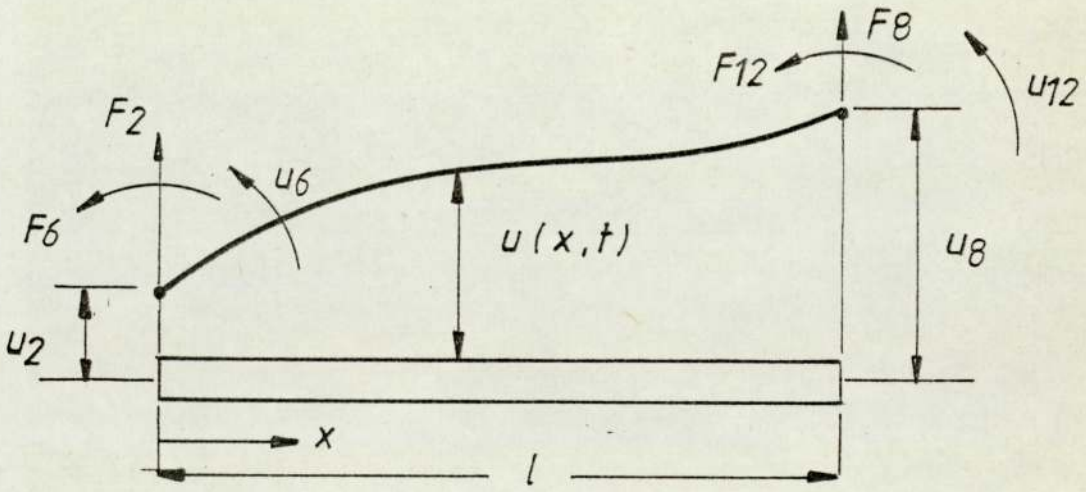


Fig. 2.5

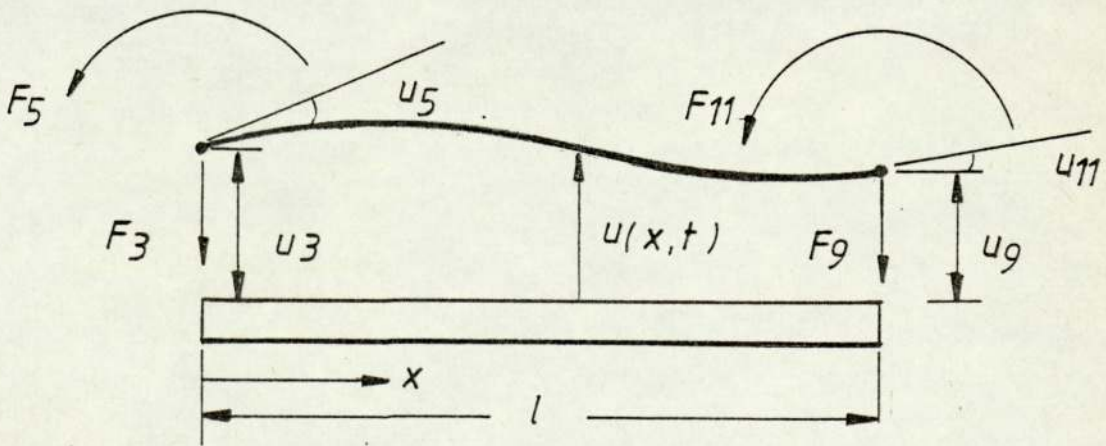


Fig. 2.6

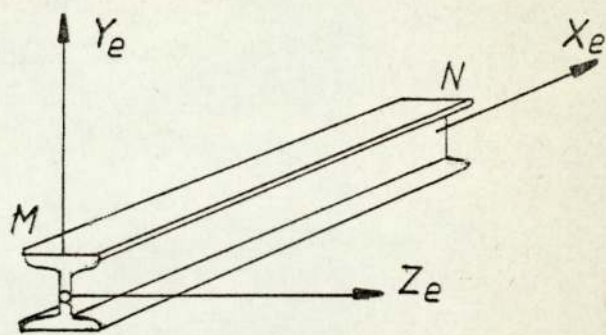
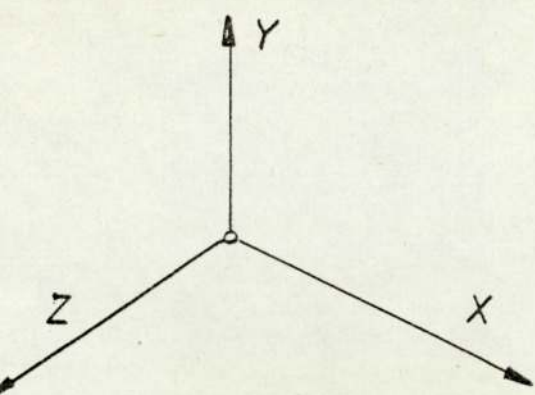


Fig. 2.7

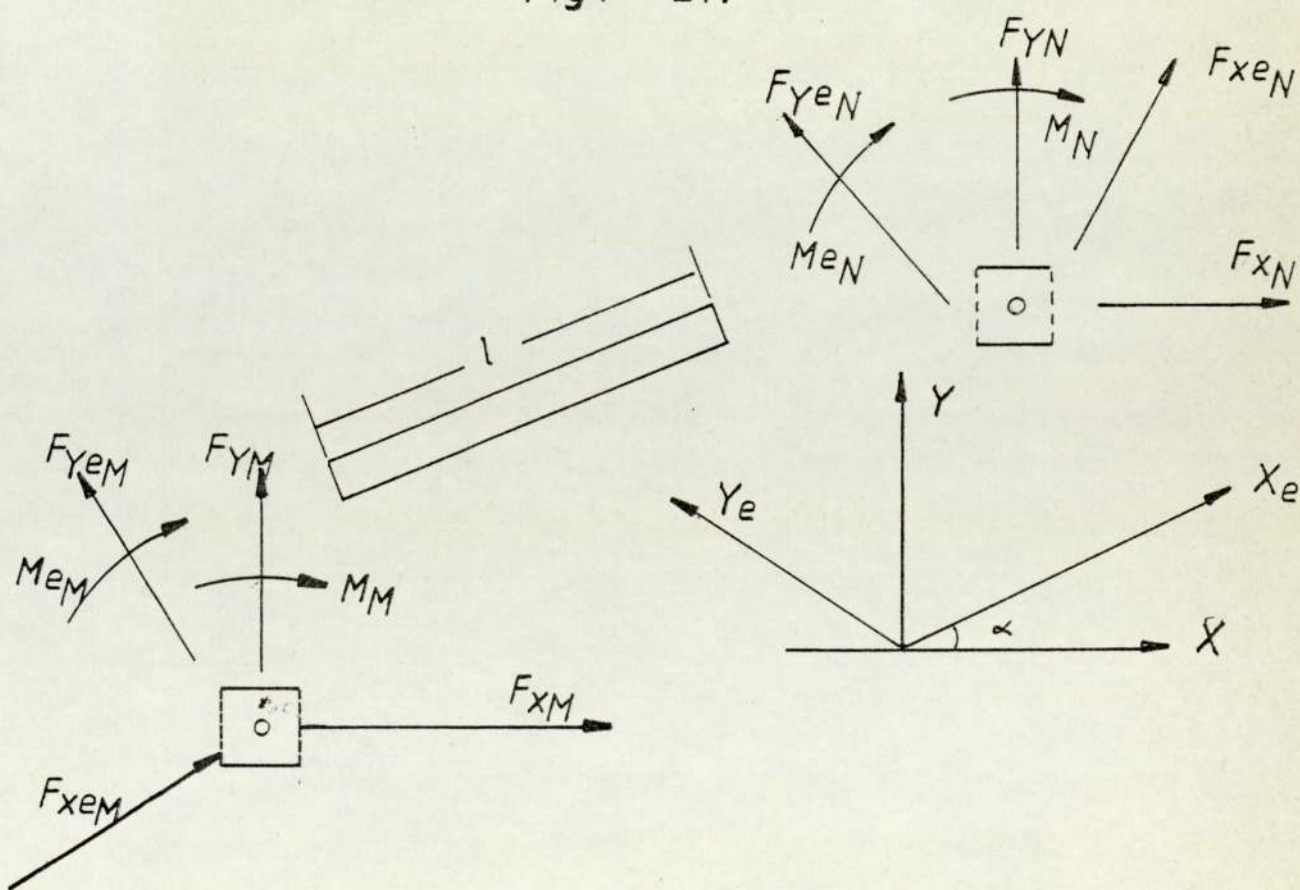


Fig. 2.8

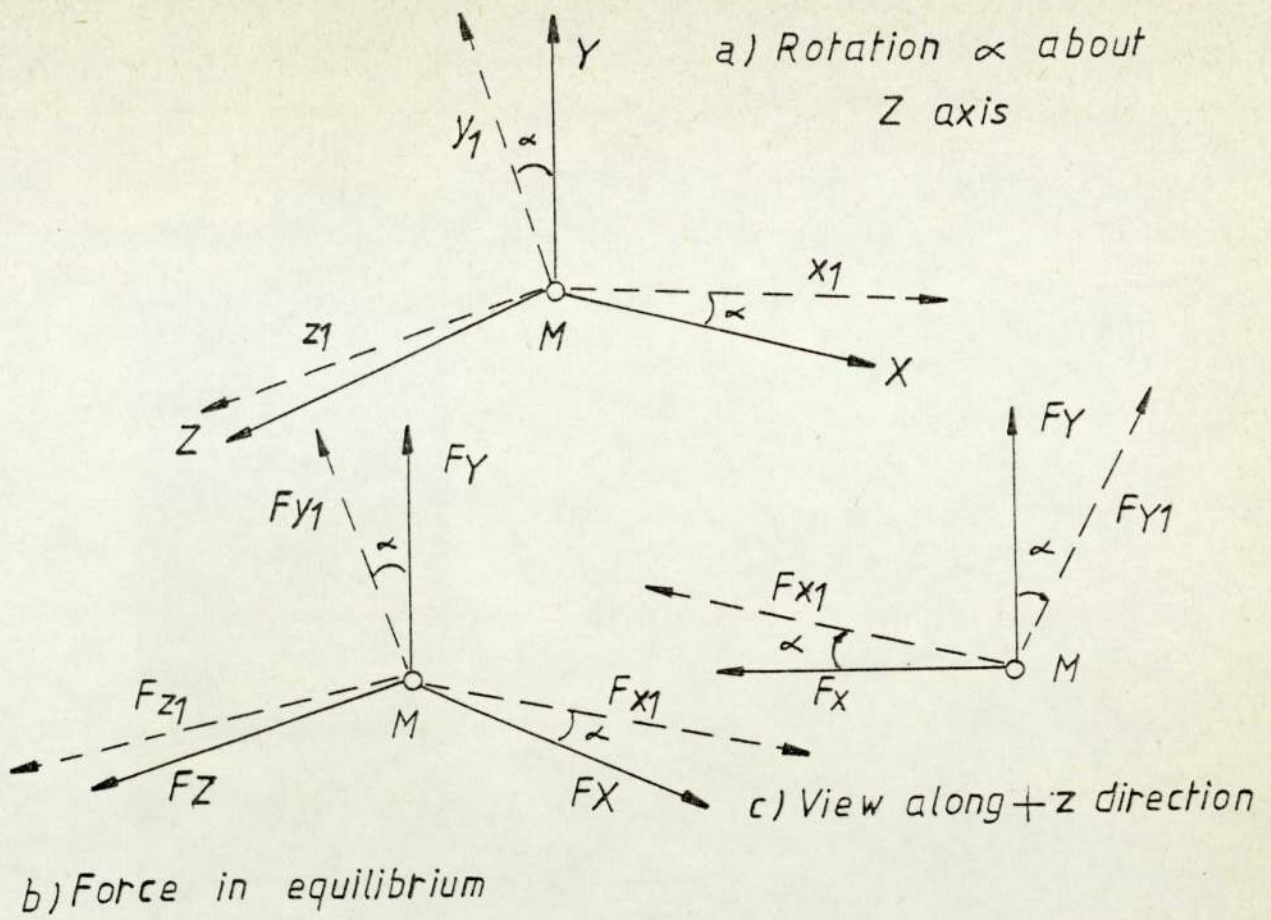


Fig. 2.9

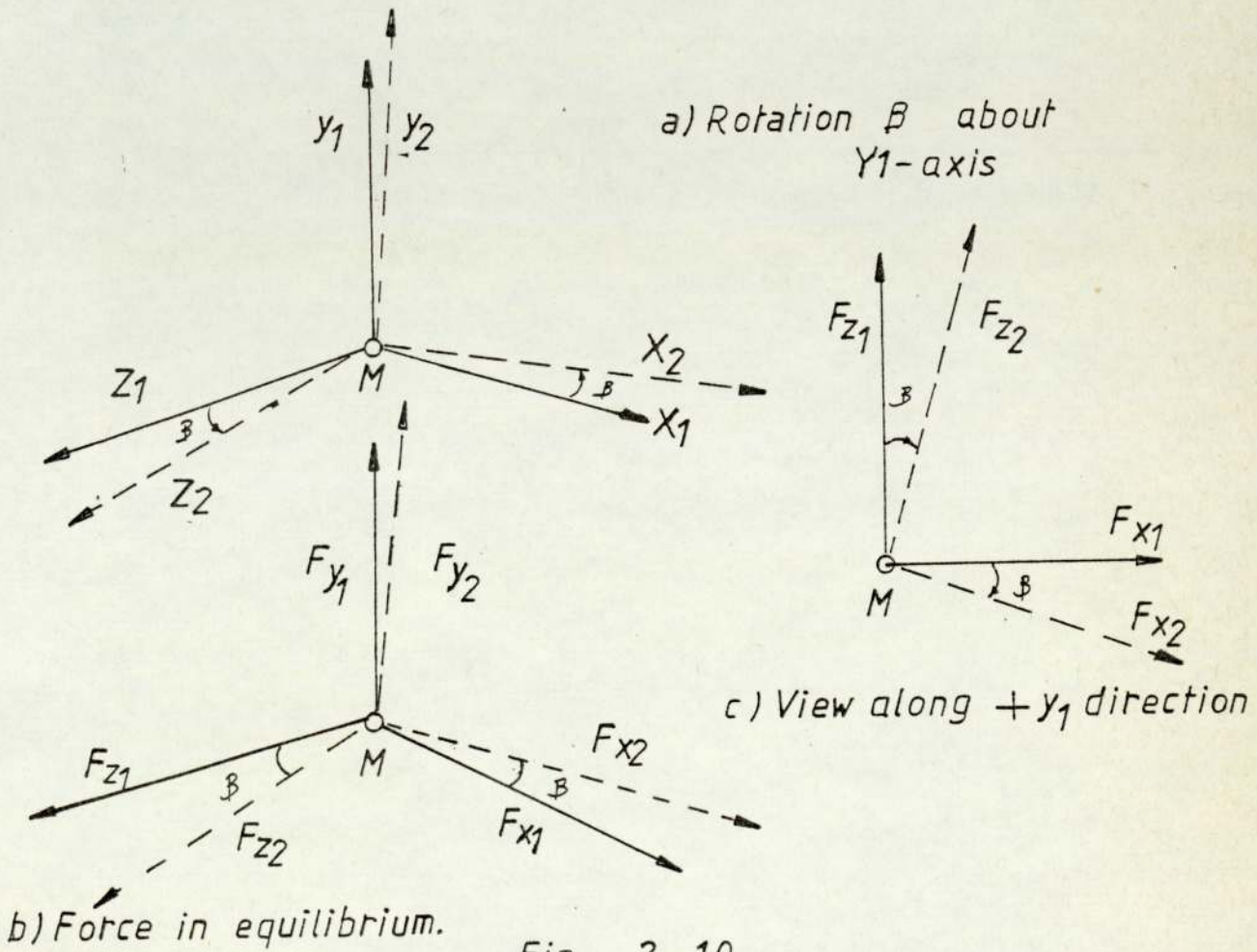


Fig. 2.10

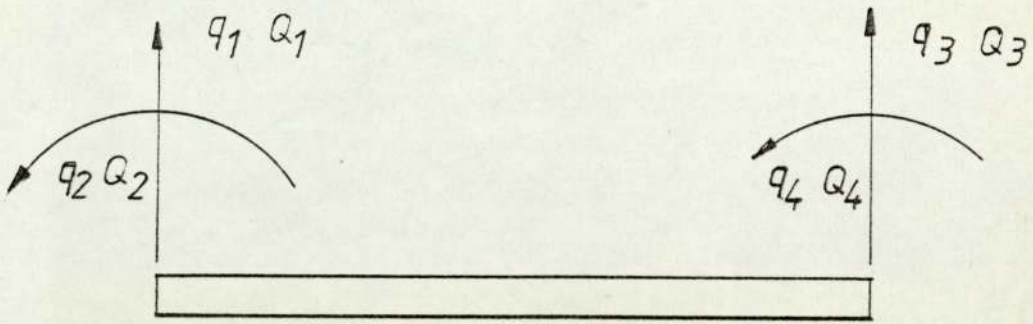


Fig. 2.11

CHAPTER 3

Two-dimensional Elements and Numerical

Solution

3.1 Two-Dimensional Elements

A two-dimensional element is one whose displacement at any point is described by two spatial parameters. The smallest geometric dimension, i.e. the thickness, of such an element is much smaller than the other two dimensions so that the configuration of its middle surface can be expressed. If this element is a flat one, then it is a plate element, otherwise it is a shell element.

A dynamic stiffness of a general two-dimensional element has not received very much attention in the literature because of its continuous contour of boundaries and the coupling effect between the two dimensions.

The only model which may be found is that of a plate element whose two opposite edges are simply supported⁽⁸⁸⁾. In this case, the governing equation of vibration is degenerated into that of a beam by choosing a set of distributed generalised co-ordinates on the two other edges which are not simply supported.

An approximation method of finite strip⁽⁸⁹⁾ was introduced by Cheung. Again, this method is limited to plate elements with the boundary condition of two opposite edges prescribed and therefore the treatment of the plate element is degenerated to that of one-dimensional elements.

Dill and Pister ⁽⁹⁰⁾ introduced a rectangular plate element where the displacements of the four edges are expressible by Fourier series. However, the coupling effects between the two spatial co-ordinates give rise to a large matrix, and the numerical convergency is very poor.

Section (3.2) discusses a rectangular plate element whose two opposite edges are simply supported.

In the following, a dynamic stiffness matrix will be derived for the plate where all the edges are subjected to prescribed boundary displacements.

Two sets of information are required about the vibrating plate element to form the dynamic stiffness matrices. One is the modal information when all the edges of the plate are clamped and the other is the static deflection patterns when the plate is subjected to unit boundary displacements.

To demonstrate the method by rectangular members as a clamped plate.

So far, the most popular method of calculating the natural frequencies and modes for an individual member is that of Rayleigh-Ritz. Although the polynomial co-ordinate functions have been used by many authors ⁽⁹¹⁾, Mikhlin has proved that the Ritz system for polynomial co-ordinate functions is numerically unstable ⁽²²⁾. To eliminate the effect, beam functions are used as co-ordinate functions.

The natural frequency will be denoted by ω_k and the corresponding mode by ϕ_k for the plate member

where

$$\begin{aligned}\zeta_1 &= (1+2\zeta)(1-\zeta)^2 & \eta_1 &= (1+2\eta)(1-\eta)^2 \\ \zeta_2 &= \zeta(1-\zeta)^2 & \eta_2 &= \eta(1-\eta)^2 \\ \zeta_3 &= (3-2\zeta)\zeta^2 & \eta_3 &= (3-2\eta)\eta^2 \\ \zeta_4 &= \zeta^2(1-\zeta) & \eta_4 &= \eta^2(1-\eta)\end{aligned}\tag{3.3}$$

substituting equation (3.2) into the following equation

$$[m] = \int_{\text{vol}} [a]^T [\rho] [a] \, d\text{vol}$$

we obtain the consistent mass matrix:

Consistent Mass Matrix

	1	2	3	4	5	6	7	8	9	10	11	12
1	24,336											
2	3,432b	624b ²										
3	-3,432a	-484ab	624a ²									
4	8,424	2,028b	-1,188a	24,336								
5	-2,028b	-468b ²	286ab	-3,432b	624b ²							
6	-1,188a	-286ab	216a ²	-3,432a	484ab	624a ²						
7	2,916	702b	-702a	8,424	-1,188b	-2,028a	24,336					
8	-702b	-162b ²	169ab	-1,188b	216b ²	285ab	-3,432b	624b ²				
9	702a	169ab	-162a ²	2,028a	-286ab	-468a ²	3,432a	-484ab	624a ²			
10	8,424	1,188b	-2,028a	2,916	-702b	-702a	8,424	-2,028b	1,188a	24,336		
11	1,188b	216b ²	-286ab	702b	-162b ²	-169ab	-2,028b	-468b ²	286ab	3,432b	624b ²	
12	2,028a	286ab	-468a ²	702a	-169ab	-162a ²	1,188a	-286ab	216a ²	3,432a	484ab	624a ²

symmetrical

$$[m] = \frac{\rho ab}{176,400}$$

(3.4)

For the stiffness matrix, if we denote

$$[D_0] = \frac{Eh^3}{12(1-\nu^2)ab} \begin{bmatrix} K_{11} & K_{21} \\ K_{21} & K_{22} \end{bmatrix}$$

and $B = b/a$, then

	1	2	3	4	5	6
1	$\frac{156}{35} (\beta^2 + \beta^{-2}) + \frac{72}{25}$					
2	$\left[\frac{22}{35} \beta^2 + \frac{78}{35} \beta^{-2} + \frac{6}{25} (1+\nu) \right] b$	$\left(\frac{4}{35} \beta^2 + \frac{52}{35} \beta^{-2} + \frac{8}{25} \right) b^2$				
3	$-\left[\frac{78}{35} \beta^2 + \frac{22}{35} \beta^{-2} + \frac{6}{25} (1+\nu) \right] a$	$-\left[\frac{11}{35} (\beta^2 + \beta^{-2}) + \frac{1}{50} (1+6\nu) \right] \times ab$	$\left(\frac{52}{35} \beta^2 + \frac{4}{35} \beta^2 + \frac{8}{25} \right) a^2$			
4	$\frac{54}{35} \beta^2 - \frac{156}{35} \beta^{-2} - \frac{72}{25}$	$\left(\frac{13}{35} \beta^2 - \frac{78}{35} \beta^{-2} - \frac{6}{25} \right) b$	$\left[-\frac{27}{35} \beta^2 + \frac{22}{35} \beta^{-2} + \frac{6}{25} (1+\nu) \right] a$	$\frac{156(\beta^2 + \beta^{-2})}{35} + \frac{72}{35}$		
5	$\left(-\frac{13}{35} \beta^2 + \frac{78}{35} \beta^{-2} + \frac{6}{25} \right) b$	$\left(\frac{3}{35} \beta^2 + \frac{26}{35} \beta^{-2} - \frac{2}{25} \right) b^2$	$\left[\frac{13}{70} \beta^2 - \frac{11}{35} \beta^{-2} - \frac{1}{50} (1+\nu) \right] ab$	$-\left[\frac{22}{35} \beta^2 + \frac{78}{35} \beta^{-2} + \frac{6}{25} (1+\nu) \right] b$	$\left(\frac{4}{35} \beta^2 + \frac{52}{35} \beta^{-2} + \frac{8}{25} \right) b^2$	
	$\left[-\frac{27}{35} \beta^2 + \frac{22}{35} \beta^{-2} + \frac{6}{25} (1+\nu) \right] a$	$\left[-\frac{13}{70} \beta^2 + \frac{11}{35} \beta^2 + \frac{1}{50} (1+\nu) \right] ab$	$\left(\frac{13}{35} \beta^2 - \frac{4}{35} \beta^{-2} - \frac{8}{25} \right) a^2$	$-\left[\frac{73}{25} \beta^2 + \frac{22}{35} \beta^{-2} + \frac{6}{25} (1+\nu) \right] a$	$\left[\frac{11}{35} (\beta^2 + \beta^{-2}) + \frac{1}{50} (1+6\nu) \right] ab$	$\left(\frac{52}{35} \beta^2 + \frac{4}{35} \beta^{-2} + \frac{8}{25} \right) a^2$

Symmetrical

(3.5)

7

8

9

10

11

12

7	$\frac{156}{35}(\beta^2 + \beta^{-2}) + \frac{72}{25}$					
8	$-\left[\frac{22}{35}\beta^2 + \frac{78}{35}\beta^{-2} + \frac{6}{25}\right]b$ $(1+5v)]b$	$\left(\frac{4}{35}\beta^2 + \frac{52}{35}\beta^{-2} + \frac{8}{25}\right)b^2$		Symmetrical		
9	$\left[\frac{78}{35}\beta^2 + \frac{22}{35}\beta^{-2} + \frac{6}{25}\right]a$ $(1+5v)]a$	$-\left[\frac{11}{35}(\beta^2 + \beta^{-2}) + \frac{1}{50}\right]x$ ab	$\left(\frac{52}{35}\beta^2 + \frac{4}{35}\beta^2 + \frac{8}{25}\right)a^2$			
10	$\frac{54}{35}\beta^2 - \frac{156}{35}\beta^{-2} - \frac{72}{25}$	$\left(-\frac{13}{25}\beta^2 + \frac{70}{35}\beta^{-2} + \frac{6}{25}\right)b$	$\left[\frac{27}{35}\beta^2 - \frac{22}{35}\beta^{-2} - \frac{6}{25}\right]a$ $(1+5v)]a$	$156(\beta^2 + \beta^{-2}) + \frac{72}{25}$		
$[K_{22}] =$						
11	$\left(\frac{13}{35}\beta^2 - \frac{78}{35}\beta^{-2} - \frac{6}{25}\right)b$	$\left(-\frac{3}{35}\beta^2 + \frac{26}{35}\beta^{-2} - \frac{2}{25}\right)b^2$	$\left[\frac{13}{70}\beta^2 - \frac{11}{35}\beta^{-2} - \frac{1}{50}\right]ab$ $(1+5v)]ab$	$\left[\frac{22}{25}\beta^2 + \frac{78}{35}\beta^{-2} + \frac{6}{25}\right]b$ $(1+5v)]b$	$\left(\frac{4}{35}\beta^2 + \frac{52}{35}\beta^{-2} + \frac{8}{25}\right)b^2$	
12	$\left[\frac{27}{35}\beta^2 - \frac{22}{35}\beta^{-2} - \frac{6}{25}\right]a$ $(1+5v)]a$	$\left[-\frac{13}{70}\beta^2 - \frac{11}{35}\beta^{-2} + \frac{1}{50}\right]ab$ $(1+5v)]ab$	$\left(\frac{18}{35}\beta^2 - \frac{4}{35}\beta^2 - \frac{8}{25}\right)a^2$ $(1+5v)]a$	$\left(\frac{78}{35}\beta^2 + \frac{22}{35}\beta^{-2} + \frac{6}{25}\right]a$ $(1+5v)]a$	$\left[\frac{11}{35}(\beta^2 + \beta^{-2}) + \frac{1}{50}\right]ab$ $(1+60v)]ab$	$\left(\frac{52}{35}\beta^2 + \frac{4}{35}\beta^2 + \frac{8}{35}\right)a^2$

The constants $G_{\ell k}$ can be found as

$$G_{\ell k} = \int_{\text{vol}} \{\phi_k\}^T [\rho] \{a_\ell\} \text{dvol}$$

from assuming that the eigen functions are normalised and the condition of orthogonality

$$a_i = \sum_{j=1}^{\infty} G_{ij} \{\phi_j\}$$

where

$$\begin{aligned} G_{ij} &= \int_{\text{vol}} \{\phi_i\}^T [\rho] \{a_j\} \text{dvol} \\ &= \rho h \sum_{i=1}^{n_i} \sum_{j=1}^{n_j} A_{ij}^k \int_0^b \int_0^a X_i(x) Y_j(y) \\ &\quad a_\ell(x,y) \text{d}x \text{d}y \end{aligned} \quad (3.6)$$

where ϕ_k and a_ℓ are scalars and a_ℓ is the ℓ th element of the matrix $[a_0]$ in equation (3.2).

In order to evaluate the integrals of equation (3.6) integrals must be calculated of the form:

$$\int \psi_i(\zeta) \zeta_m(\zeta) \text{d}\zeta \quad m = 1, 2, 3, 4 \quad (3.7)$$

where ψ_i represents either $X_i(x)$ or $Y_i(y)$ and $\zeta_m(\zeta)$ are polynomials of ζ as given by equation (3.3). Then the dynamic stiffness matrix of rectangular plate is given by the equation:

$$[D] = [D_0] - w^2 [m_0] - w^4 \sum_{k=1}^n \left[\frac{G_{ik} G_{jk}}{w^2 k - w^2} \right]$$

where n = number of terms taken.

It must be noted that since the expression (3.1) is not exact and the modal corrections are made in the interior of



the plate, to satisfy the differential equation, but not the boundaries; exact results cannot be expected for the dynamic matrices. The accuracy may be increased by increasing the number of generalised co-ordinates on the edges.

3.2 The Interaction between Beams and plates

It is common engineering practice to stiffen a plate system by beams. The effect of a stiffening beam is threefold; axial, flexural and torsional.

The flexural and torsional effects are considered separately in the following analysis.

The governing equation of a beam in flexural vibration is given by:

$$EI \frac{\partial^4 w}{\partial x^4} + \rho A \frac{\partial^2 w}{\partial t^2} + N_x \frac{\partial^2 w}{\partial x^2} = V \quad (3.8)$$

where N_x is the axial compressive force, and V the distributed transverse load per unit length along the beam.

For the harmonic excitation of a simply supported beam:

$$V = \sum_{m=1}^N V_m \sin \frac{m\pi x}{a} e^{i\omega t} \quad (3.9)$$

and

$$w = \sum_{m=1}^N w_m \sin \frac{m\pi x}{a} e^{i\omega t} \quad (3.10)$$

From equations (3.9), (3.10) and (3.8) we have:

$$\sum_{m=1}^N \sin \frac{m\pi x}{a} \left[EI \left(\frac{m\pi}{a} \right)^4 w_m - \rho A \omega^2 N_m - N_x \left(\frac{m\pi}{a} \right)^2 w_m - V_m \right] = 0 \quad (3.11)$$

Multiplying the equation by $\frac{n\pi x}{a}$ and integrating over $x = 0$ and $x=a$ we have:

$$V_m = \left[EI \left(\frac{m\pi}{a}\right)^4 - \rho A_0 w^2 - N_x \left(\frac{m\pi}{a}\right)^2 \right] w_m \quad (3.12)$$

which is the stiffness relation required.

The torsional effect is derived as follows:

The differential equation governing the torsional vibration of a beam, where the shear coincides with the mass centre of cross sectional area, is

$$GJ \frac{\partial^2 \theta}{\partial x^2} - \rho I_0 \frac{\partial^2 \theta}{\partial x^2} + T = 0 \quad (3.13)$$

where

GJ is the torsional rigidity

ρ is the mass density

I_0 is the polar moment of inertia

T is the torsional moment acting on the beams per unit length.

The harmonic oscillation of a simply supported beam is obtained by:

$$T = \sum_{m=1}^N T_m \sin \frac{m\pi x}{a} e^{i\omega t} \quad (3.14)$$

$$\theta = \sum_{m=1}^N \theta_m \sin \frac{m\pi x}{a} e^{i\omega t} \quad (3.15)$$

and equation (3.13) becomes

$$\sum_{m=1}^N \sin \frac{m\pi x}{a} \left[-GJ \left(\frac{m\pi}{a}\right)^2 \theta_m + \rho I_0 w^2 \theta_m + T_m \right] = 0$$

Multiplying the equation by $\sin \frac{n\pi x}{a}$ and integrating

over $x = 0$ and $x = a$ gives :

$$T_m = \left[GJ \left(\frac{m\pi}{a} \right)^2 - \rho I_o w^2 \right] \theta_m \quad (3.16)$$

which is the required stiffness relation.

When the beam member is on an edge of the folded plate, then the generalised displacements of the beam w_m and θ_m will correspond to the generalised displacements of the plate, either q_{m1} and q_{m2} or q_{m3} and q_{m4} , depending on which edge of the plate the beam is situated.

3.3 Folded Plate Members

A rectangular plate with two opposite edges simply supported and with the two edges connected to other structures by prescribed displacement patterns will be discussed. Distributed co-ordinates on the edges will be used in this example.

To satisfy the boundary conditions of two opposite edges being simply supported, the displacement pattern of the plate may be written as:

$$w(x,y) = \sum_{m=1}^N Y_m(y) \sin \frac{m\pi x}{a} \quad (3.17)$$

where N is the number of terms taken, a and b are the dimensions of the plate as shown in Fig.(3.2) and $Y_m(y)$ are the functions to be determined to satisfy the governing equation of vibration.

Fig.(3.2) shows the plate and its boundary conditions:

$x = 0$ and $x = a$, simply supported.

The generalised displacements q_{mi} , $m=1,2,\dots,N$ and $i=1,2,3,4$ are defined by:

$$\begin{aligned}
 w(x,0) &= \sum_{m=1}^N q_{m1} \sin \frac{m\pi x}{a} \\
 w(x,b) &= \sum_{m=1}^N q_{m2} \sin \frac{m\pi x}{a} \\
 \frac{\partial w(x,0)}{\partial y} &= -\sum_{m=1}^N q_{m3} \sin \frac{m\pi x}{a} \\
 \frac{\partial w(x,b)}{\partial y} &= \sum_{m=1}^N q_{m4} \sin \frac{m\pi x}{a}
 \end{aligned} \tag{3.18}$$

and the generalised forces Q_{mi} are defined by

$$\begin{aligned}
 Q_Y(x,0) &= \sum_{m=1}^N Q_{m1} \sin \frac{m\pi x}{a} \\
 -Q_Y(x,b) &= \sum_{m=1}^N Q_{m3} \sin \frac{m\pi x}{a} \\
 M_Y(x,0) &= \sum_{m=1}^N Q_{m2} \sin \frac{m\pi x}{a} \\
 -M_Y(x,b) &= \sum_{m=1}^N Q_{m4} \sin \frac{m\pi x}{a}
 \end{aligned} \tag{3.19}$$

where Q_Y and M_Y are Kirchoff's shear and the bending moment of the plate along $y = \text{constant}$ (9).

The generalised forces are related to the displacement through the conditions of equilibrium on the edges $y = 0$ and $y = b$,

$$Q_y(x,y) = -D \left[\frac{\partial^3 w}{\partial y^3} + (2-\nu) \frac{\partial^3 w}{\partial x^2 \partial y} \right]$$

$$M_y(x,y) = -D \left[\frac{\partial^2 w}{\partial y^2} + \nu \frac{\partial^2 w}{\partial x^2} \right] \quad (3.20)$$

where $D = Eh^3/12(1-\nu^2)$ is the flexural rigidity of the plate.

h = thickness and ν = the Poisson's ratio.

Before we can apply equation (3.18) to equation (3.20) in order to find the dynamic stiffness matrix, we must find out the functions $Y_m(y)$ in equation (3.17).

If the loadings are harmonic with time, the governing equation of vibration of the plate with frequency w is given by:

$$D \nabla^4 w - \rho h w^2 W + N_x \frac{\partial^2 w}{\partial x^2} + N_y \frac{\partial^2 w}{\partial y^2} = P(x,y) \quad (3.21)$$

where N_x and N_y are the compressive in plane loads in x and y directions respectively, ∇^4 is the biharmonic operator in (x,y) co-ordinate, $P(x,y)$ is the downward distributed load intensity and represented by:

$$P(x,y) = \sum_{m=1}^n P_m \sin \frac{m\pi x}{a} \text{ per unit area} \quad (3.22)$$

By substituting equation (3.17) into equation (3.19), we have:

$$\sum_{m=1}^N \sin \frac{m\pi x}{a} \left\{ \left(\frac{m\pi}{a}\right)^4 y_m - 2\left(\frac{m\pi}{a}\right)^2 y_m^2 + y_m^4 - \frac{\rho h w^2}{D} y_m \right.$$

$$\left. - \frac{N_x}{D} \left(\frac{m\pi}{a}\right)^2 y_m + \frac{N_y}{D} y_m^2 - \frac{P_m}{D} y_m \right\} = 0$$

Multiplying by $\sin \frac{n\pi x}{a}$ and integrating over $x = 0, a$ where n is a positive integer, and using the orthogonality of sine functions, we obtain:

$$y_m^4 - 2\left\{\frac{m\pi}{a}\right\}^2 - \left\{\frac{N_y}{2D}\right\} y_m^2 + \left\{\left(\frac{m\pi}{a}\right)^4 - \frac{\rho h w^2}{D} - \frac{N_x}{D} \left(\frac{m\pi}{a}\right)^2 - \frac{P_m}{D}\right\} y_m = 0 \quad m = 1, 2, \dots \quad (3.23)$$

The associated boundary conditions for these fourth order differential equations are obtained from equation (3.18)

$$\begin{aligned} Y_m(0) &= \alpha_{m4} & Y'_m(0) &= \alpha_{m2} \\ Y_m(b) &= \alpha_{m3} & Y'_m(b) &= \alpha_{m4} \end{aligned} \quad (3.24)$$

The auxiliary roots of equations (3.23) are obtained by letting $Y_m = e^{\sigma Y}$

$$\sigma^2 = \left[\left(\frac{m\pi}{a}\right)^2 - \frac{N_y}{2D} \right] \pm \left\{ \left[\left(\frac{m\pi}{a}\right)^2 - \frac{N_y}{D} \right]^2 - \left(\frac{m\pi}{a}\right)^4 + \frac{\rho h w^2}{D} + \frac{N_x}{D} \left(\frac{m\pi}{a}\right)^2 + \frac{P_m}{D} \right\}^{\frac{1}{2}} \quad (3.25)$$

Therefore $Y_m(y)$ will have four different forms of solution depending on whether σ^2 is positive, negative or complex.

We study these four cases as follows:

Case 1

When all four roots are real, which are $\pm\sigma_1, \pm\sigma_2$ then the general solution has the form:

$$Y_m(y) = A \cosh \frac{\sigma_2 y}{b} + B \sinh \frac{\sigma_2 y}{b} + C \cosh \frac{\sigma_1 y}{b} + D \sinh \frac{\sigma_1 y}{b} \dots (3.26)$$

where A,B,C,D are integration constants and are determined from the boundary conditions (3.24) as:

$$\begin{aligned} A &= \left(\frac{\sigma_1^2 - F_4}{\sigma_1^2 - \sigma_2^2} \right) q_{m1} + \left(\frac{-F_2}{\sigma_1^2 - \sigma_2^2} \right) b q_{m2} + \left(\frac{-F_3}{\sigma_1^2 - \sigma_2^2} \right) q_{m3} + \left(\frac{F_1}{\sigma_1^2 - \sigma_2^2} \right) b q_{m4} \\ B &= \left(\frac{F_6}{\sigma_2^2 - \sigma_1^2} \right) q_{m1} + \left(\frac{\sigma_2^2 - F_4}{\sigma_2^2 - \sigma_1^2} \right) b q_{m2} + \left(\frac{F_5}{\sigma_2^2 - \sigma_1^2} \right) q_{m3} + \left(\frac{F_3}{\sigma_2^2 - \sigma_1^2} \right) b q_{m4} \\ C &= q_{m1} - A, \quad D = \frac{b q_{m2}}{\sigma_1} - \frac{B \sigma_2}{\sigma_1} \end{aligned} \quad (3.27)$$

where $F_1 = -(\sigma_2 \sinh \sigma_1 - \sigma_1 \sinh \sigma_2) (\sigma_1^2 - \sigma_2^2) / \delta$

$F_2 = -(\sigma_1 \cosh \sigma_1 \sinh \sigma_2 - \sigma_2 \sinh \sigma_1 \cosh \sigma_2) (\sigma_1^2 - \sigma_2^2) / \delta$

$F_3 = -\sigma_1 \sigma_2 (\sigma_1^2 - \sigma_2^2) (\cosh \sigma_1 - \cosh \sigma_2) / \delta$

$F_4 = \sigma_1 \sigma_2 [(\sigma_1^2 + \sigma_2^2) (\cosh \sigma_1 \cosh \sigma_2 - 1) - 2\sigma_1 \sigma_2 \sinh \sigma_1 \sinh \sigma_2] / \delta$

$F_5 = \sigma_1 \sigma_2 (\sigma_1^2 - \sigma_2^2) (\sigma_1 \sinh \sigma_1 - \sigma_2 \sinh \sigma_2) / \delta$

$F_6 = -\sigma_1 \sigma_2 (\sigma_1^2 - \sigma_2^2) (-\sigma_2 \cosh \sigma_1 \sinh \sigma_2 + \sigma_1 \sinh \sigma_1 \cosh \sigma_2) / \delta$

$\delta = 2\sigma_1 \sigma_2 (\cosh \sigma_1 \cosh \sigma_2 - 1) - (\sigma_1^2 + \sigma_2^2) (\sinh \sigma_1 \sinh \sigma_2)$

..... (3.28)

Case 2

When there are two real and two imaginary roots which are $\pm \sigma_1, \pm i\sigma_2$ then the general solution has the form:

$$Y_m(y) = A \cos \frac{\sigma_2 Y}{b} + B \sin \frac{\sigma_2 Y}{b} + C \cosh \frac{\sigma_1 Y}{b} + D \sinh \frac{\sigma_1 Y}{b} \dots (3.29)$$

where A,B,C,D are integration constants depending on the boundary conditions (3.24) and they are found as:

$$A = \left(\frac{\sigma_2^2 - F_4}{\sigma_1^2 + \sigma_2^2} \right) a_{m1} + \left(\frac{F_2}{\sigma_1^2 + \sigma_2^2} \right) b a_{m2} + \left(\frac{-F_3}{\sigma_1^2 + \sigma_2^2} \right) a_{m3} + \left(\frac{F_1}{\sigma_1^2 + \sigma_2^2} \right) b a_{m4}$$

$$B = \left(\frac{-F_6}{\sigma_1^2 + \sigma_2^2} \right) \frac{a_{m1}}{\sigma_2} + \left(\frac{\sigma_2^2 + F_4}{\sigma_1^2 + \sigma_2^2} \right) \frac{b a_{m2}}{\sigma_2} + \left(\frac{-F_5}{\sigma_1^2 + \sigma_2^2} \right) \frac{a_{m3}}{\sigma_2} + \left(\frac{-F_3}{\sigma_1^2 + \sigma_2^2} \right) \frac{b a_{m4}}{\sigma_2}$$

$$C = a_{m1} - A \quad \text{and} \quad D = \frac{b a_{m2}}{\sigma_1} - \frac{\sigma_2}{\sigma_1} B \dots (3.30)$$

where the frequency functions are given by:

$$F_1 = -(\sigma_2 \sinh \sigma_1 - \sigma_1 \sin \sigma_2) (\sigma_1^2 + \sigma_2^2) / \delta$$

$$F_2 = -(\sigma_1 \cosh \sigma_1 \sin \sigma_2 - \sigma_2 \sinh \sigma_1 \sin \sigma_2) (\sigma_1^2 + \sigma_2^2) / \delta$$

$$F_3 = -\sigma_1 \sigma_2 (\sigma_1^2 - \sigma_2^2) (\cosh \sigma_1 - \cos \sigma_2) / \delta$$

$$F_4 = \sigma_1 \sigma_2 [+(\sigma_1^2 - \sigma_2^2) (\cosh \sigma_1 \cos \sigma_2 - 1) + 2\sigma_1 \sigma_2 \sinh \sigma_1 \sin \sigma_2] / \delta$$

$$F_5 = \sigma_1 \sigma_2 (\sigma_2^2 + \sigma_1^2) (\sigma_2 \sin \sigma_2 + \sigma_1 \sinh \sigma_1) / \delta$$

$$F_6 = -\sigma_1 \sigma_2 (\sigma_2^2 + \sigma_1^2) (\sigma_2 \cosh \sigma_1 \sin \sigma_2 + \sigma_1 \sinh \sigma_1 \cos \sigma_2) / \delta$$

$$\delta = 2\sigma_1 \sigma_2 (\cosh \sigma_1 \cos \sigma_2 - 1) + (\sigma_2^2 - \sigma_1^2) \sinh \sigma_1 \sin \sigma_2 \dots (3.31)$$

Case 3

When all four roots are imaginary, which are $\pm i\sigma_1$, $\pm i\sigma_2$ then the general solution has the form:

$$Y_m(y) = A \cos \frac{\sigma_2 y}{b} + B \sin \frac{\sigma_2 y}{b} + C \cos \frac{\sigma_1 y}{b} + D \sin \frac{\sigma_1 y}{b} \quad (3.32)$$

where

$$\begin{aligned} A &= \left(\frac{-\sigma_2^2 - F_4}{\sigma_2^2 - \sigma_1^2} \right) a_{m1} + \left(\frac{F_2}{\sigma_2^2 - \sigma_1^2} \right) b a_{m2} + \left(\frac{-F_3}{\sigma_2^2 - \sigma_1^2} \right) a_{m3} + \left(\frac{F_1}{\sigma_2^2 - \sigma_1^2} \right) b a_{m4} \\ B &= \left(\frac{-F_6}{\sigma_2^2 - \sigma_1^2} \right) \frac{a_{m1}}{\sigma_2} + \left(\frac{\sigma_2^2 + F_4}{\sigma_2^2 - \sigma_1^2} \right) \frac{b a_{m2}}{\sigma_2} + \left(\frac{-F_5}{\sigma_2^2 - \sigma_1^2} \right) \frac{a_{m3}}{\sigma_2} + \left(\frac{-F_3}{\sigma_2^2 - \sigma_1^2} \right) \frac{b a_{m4}}{\sigma_2} \\ C &= a_{m1} - A \quad \text{and} \quad D = \frac{b a_{m2}}{\sigma_1} - B \frac{\sigma_2}{\sigma_1} \end{aligned} \quad (3.33)$$

where the frequency functions are given by:

$$\begin{aligned} F_1 &= -(\sigma_2 \sin \sigma_1 - \sigma_1 \sin \sigma_2) (\sigma_2^2 - \sigma_1^2) / \delta \\ F_2 &= -(\sigma_1 \cos \sigma_1 \sin \sigma_2 - \sigma_2 \sin \sigma_1 \cos \sigma_2) (\sigma_2^2 - \sigma_1^2) / \delta \\ F_3 &= -\sigma_1 \sigma_2 (\sigma_2^2 - \sigma_1^2) (\cos \sigma_1 - \cos \sigma_2) / \delta \\ F_4 &= \sigma_1 \sigma_2 [-(\sigma_1^2 + \sigma_2^2) (\cos \sigma_1 \cos \sigma_2 - 1) - 2\sigma_1 \sigma_2 \sin \sigma_1 \sin \sigma_2] / \delta \\ F_5 &= \sigma_1 \sigma_2 (\sigma_2^2 - \sigma_1^2) (\sigma_2 \sin \sigma_2 - \sigma_1 \sin \sigma_1) / \delta \\ F_6 &= -\sigma_1 \sigma_2 (\sigma_2^2 - \sigma_1^2) (\sigma_2 \cos \sigma_1 \sin \sigma_2 - \sigma_1 \sin \sigma_1 \cos \sigma_2) / \delta \\ \delta &= 2\sigma_1 \sigma_2 (\cos \sigma_1 \cos \sigma_2 - 1) + (\sigma_1^2 + \sigma_2^2) \sin \sigma_1 \sin \sigma_2 \end{aligned} \quad \dots \dots \quad (3.34)$$

Case 4

When all four roots are complex and which are $\sigma_2 \pm i\sigma_1$, $-\sigma_2 \pm i\sigma_1$, then the general solution will have the form:

$$\begin{aligned} Y_m(x) &= A \cos \sigma_1 \frac{y}{b} \cosh \frac{\sigma_2 y}{b} + B \cos \frac{\sigma_1 y}{b} \sinh \frac{\sigma_2 y}{b} + \\ &C \sin \frac{\sigma_1 y}{b} \cosh \frac{\sigma_2 y}{b} + D \sin \frac{\sigma_1 y}{b} \sinh \frac{\sigma_2 y}{b} \end{aligned} \quad (3.35)$$

where the integration constants A,B,C,D are found from the boundary conditions (3.24) as:

$$\begin{aligned}
 A &= q_{m_1} \\
 B &= \{q_{m_1} (\sigma_1 \sigma_2 \sin \sigma_1 \cos \sigma_1 + \sigma_2^2 \sinh \sigma_2 \cosh \sigma_2) + \\
 &\quad bq_{m_2} (\sigma_2 \sin^2 \sigma_1) - q_{m_3} \sigma_1 (\sigma_1 \cos \sigma_1 \sinh \sigma_2 + \\
 &\quad \sigma_2 \sin \sigma_1 \cosh \sigma_2) + bq_{m_4} (\sigma_1 \sin \sigma_1 \sinh \sigma_2)\} / \delta \\
 C &= \{-q_{m_1} (\sigma_1 \sigma_2 \sinh \sigma_2 \cosh \sigma_2 + \sigma_2^2 \sin \sigma_1 \cos \sigma_1) - \\
 &\quad bq_{m_2} \sigma_1 \sinh^2 \sigma_2 + q_{m_3} \sigma_2 (\sigma_1 \cos \sigma_1 \sinh \sigma_2 \\
 &\quad + \sigma_2 \sin \sigma_1 \cosh \sigma_2) - bq_{m_4} (\sigma_2 \sin \sigma_1 \sinh \sigma_2)\} / \delta \\
 D &= \{q_{m_1} \sigma_1 \sigma_2 (\sin^2 \sigma_1 + \sinh^2 \sigma_2) + bq_{m_2} (\sigma_1 \sinh \sigma_2 \cosh \sigma_2 \\
 &\quad - \sigma_2 \sin \sigma_1 \cos \sigma_1) - q_{m_3} (\sigma_2^2 + \sigma_1^2) \sin \sigma_1 \sinh \sigma_2 + \\
 &\quad bq_{m_4} (\sigma_2 \sin \sigma_1 \cosh \sigma_2 - \sigma_1 \cos \sigma_1 \sinh \sigma_2)\} / \delta \\
 \delta &= \sigma_2^2 \sin^2 \sigma_1 - \sigma_1^2 \sinh^2 \sigma_2
 \end{aligned}
 \tag{3.36}$$

The frequency functions are given by

$$\begin{aligned}
 F_1 &= 2\sigma_1 \sigma_2 (\sigma_2 \sin \sigma_1 \cosh \sigma_2 - \sigma_1 \cos \sigma_1 \sinh \sigma_2) / \delta \\
 F_2 &= -2\sigma_1 \sigma_2 (\sigma_1 \sinh \sigma_2 \cosh \sigma_2 - \sigma_2 \sin \sigma_1 \cos \sigma_1) / \delta \\
 F_3 &= 2\sigma_1 \sigma_2 (\sigma_1^2 + \sigma_2^2) (\sin \sigma_1 \sinh \sigma_2) / \delta \\
 F_4 &= (x_2 \sigma_2 \sin^2 \sigma_1 + x_1 \sigma_1 \sinh^2 \sigma_2) / \delta \\
 F_5 &= 2\sigma_1 \sigma_2 (\sigma_1^2 + \sigma_2^2) (\sigma_1 \sinh \sigma_2 \cos \sigma_1 + \sigma_2 \sin \sigma_1 \cosh \sigma_2) / \delta \\
 F_6 &= -2\sigma_1 \sigma_2 (\sigma_1^2 + \sigma_2^2) (\sigma_1 \sinh \sigma_2 \cosh \sigma_2 + \sigma_2 \cos \sigma_1 \sin \sigma_1) / \delta \\
 \delta &= \sigma_2^2 \sin^2 \sigma_1 - \sigma_1^2 \sinh^2 \sigma_2 \\
 x_1 &= \sigma_1^3 - 3\sigma_1 \sigma_2^2 + (2-\nu) \sigma_1 \\
 x_2 &= \sigma_2^3 - 3\sigma_1^2 \sigma_2 - (2-\nu) \sigma_2
 \end{aligned}
 \tag{3.37}$$

The general solution of the differential equations (3.23) in these forms was not found in the literature.

However, we have not studied the physical implication of the various natures of the auxiliary roots and therefore,

these formulae are presented here merely for the completeness of the formulation.

Having determined the functions $Y_m(y)$ explicitly in terms of the generalised displacement q_{mi} , we can carry out the differentiation in equations (3.19) and make use of equation (3.18) and the orthogonality of sine functions to obtain the relationship between the generalised forces and generalised displacements.

After some simplification, the dynamic stiffness relations for all these four cases will have the form:

$$\begin{pmatrix} Q_{m_1} \\ Q_{m_2} \\ Q_{m_3} \\ Q_{m_4} \end{pmatrix} = \frac{D}{b^3} \begin{bmatrix} F_6 & -F_4b & F_5 & F_3b \\ -F_4b & F_2b^2 & -F_3b & F_1b^2 \\ F_5 & -F_3b & F_6 & F_4b \\ F_3b & F_1b^2 & F_4b & F_2b^2 \end{bmatrix} \begin{pmatrix} q_{m_1} \\ q_{m_2} \\ q_{m_3} \\ q_{m_4} \end{pmatrix}$$

$m = 1, 2 \dots N$ (3.38)

where the frequency function F_i has different forms for the four cases and should be calculated under the individual headings, i.e. from expressions (3.27) or (3.31) or (3.34) or (3.37) according to the nature of the auxiliary roots.

The vibration shape for every m is given by expressions (3.26) or (3.29) or (3.32) or (3.35) and the overall shape of vibration at frequency w is obtained from equation (3.17).

3.4 Numerical Solution

3.4.1 Introduction

Since the method of study is very close to the Finite Element Methods, a brief discussion of how these methods

apply to the elastic systems may be worth mentioning.

Finite Element Methods developed from torsional problems in 1943 ⁽¹³⁾. The term 'Finite Element Method' was not introduced until the middle of the fifties. At that time the electronic computers were rapidly entering the field of technical computations, and the matrix method of structural analysis was proved to be powerful. An extension of these methods for use in general structure was a natural progression. Pioneers in this development were Lagefors ⁽¹⁴⁾, Agris ⁽¹⁵⁾ and Clough ⁽¹⁶⁾ and this time the approach was based on simple engineering arguments. Continuous material was regarded as being split physically into finite elements. Each element was analyzed as being a separate piece of material making up the complete structure when joined to the other elements. For a thorough study of finite element methods, text books like the one by Zienkiewicz ⁽¹⁷⁾ are recommended.

Here, only a brief account of the theory may be included. Elastic problems are governed by three categories of field equations:

- stress-equilibrium equations
- stress-strain relations (constitutive material laws)
- strain-displacement relations (kinematic relations)

In addition, boundary conditions may be given as:

- specified boundary stress
- specified boundary displacements
- specified relations between boundary stress and boundary relations.

For a linear theory of elasticity, these equations are particularly simple. In terms of rectangular Cartesian co-ordinates, and by means of standard tensor notation, they may be written as follows:

1. stress equilibrium

$$\sigma_{ij,j} + F_i = 0 \quad i,j, = 1,2,3$$

where

σ_{ij} = stress tensor components

F_i = components of body forces

2. stress-strain relation

$$\sigma_{ij} = C_{ijkl} \epsilon_{kl} \quad i,j,k,l = 1,2,3$$

or inversely

$$\epsilon_{ij} = S_{ijkl} \sigma_{kl}$$

where the new notations are

ϵ_{ij} = component of strain tensor

C_{ijkl} = elastic stiffness coefficient

S_{ijkl} = elastic flexibility coefficient

3. strain-displacement relations for small displacements

$$\epsilon_{ij} = \frac{1}{2}(U_{i,j} + U_{j,i}) \quad i,j = 1,2,3$$

where U_i denotes displacement in the direction i .

For the formulation of stress boundary conditions, internal stresses must be related to surface tractions.

The surface traction \bar{T}_i in direction i at some part of the boundary S may be written as follows:

$$\bar{T}_i = \sigma_{i,j} n_j$$

where v_j is the direction cosine of the outward unit normal vector of the surface S .

All energy principles may be used as a basis for numerical analysis using the Finite Element Method.

The finite element separation implies a division of the total volume V into sub-volumes or sub-domains denoting finite elements.

The functions chosen to represent approximate displacement and stress field are specified within each element, and conditions imposed on certain parameters at inter-element boundaries provide the necessary continuity required by the field functions.

In the case of the standard displacement method, the displacement field is assumed to be:

$$\{ U(x,y,z) \} = [\phi(x,y,z)] \{ \alpha \}$$

where

$\{ \phi(x,y,z) \}$ is the vector of chosen nodes of displacement
 $\{ \alpha \}$ is a vector of constants to be determined by the nodal displacements

At any node i , the vector of displacement components is given by:

$$\{ q_i \} = \{ U(x_i, y_i, z_i) \} = [\phi(x_i, y_i, z_i)] \{ \alpha \}$$

where (x_i, y_i, z_i) are the co-ordinates of the node.

If all the displacement components of the nodes of the element are arranged in a vector $\{ q \}$ then:

$$\{q\} = [\Phi] \{\alpha\}$$

where the constant matrix $[\Phi]$ is given by:

$$[\Phi] = \begin{bmatrix} [\phi(x_1, y_1, z_1)] \\ [\phi(x_2, y_2, z_2)] \\ " \\ " \\ [\phi(x_n, y_n, z_n)] \end{bmatrix}$$

where n = number of nodes.

The displacement field is expressed in terms of nodal displacements:

$$\{U(x, y, z)\} = [\phi(x, y, z)] [\Phi]^{-1} \{q\} = [a(x, y, z)] \{q\} \quad (3.39)$$

where

$$[a(x, y, z)] = [\phi(x, y, z)] [\Phi]^{-1}$$

The strain field is obtained from the kinematic relation as

$$\{\epsilon(x, y, z)\} = [b(x, y, z)] \{q\} \quad (3.40)$$

For vibration analysis, if the external force can be expressed as the potential V , the most convenient energy principle is the Hamilton's Principle, which states:

"Among all admissible displacements which satisfy the prescribed geometrical constraints and the prescribed condition at the limits $t = t_1$ and $t = t_2$, the actual condition makes the functional stationary"

$$\int_{t_1}^{t_2} [T - U - \int_{vol} V \, dvol] \, dt \quad (3.41)$$

Now the Kinetic energy and the strain energy are given by

$$T = \frac{1}{2} \int_{vol} \{\dot{u}\}^T [\rho] \{\dot{u}\} dvol \quad (3.42)$$

and

$$U = \frac{1}{2} \int_{vol} \{\epsilon\}^T [C] \{\epsilon\} dvol$$

respectively.

We have

$$\delta \left(\frac{1}{2} \{\dot{q}\}^T [m] \{\dot{q}\} + \frac{1}{2} \{q\}^T [K] \{q\} - \{q\}^T \{Q\} \right) = 0 \quad (3.43)$$

where the mass matrix $[m]$, and the stiffness matrix $[k]$ are given by

$$[m] = [a]^T [\rho] [a] \quad (3.44)$$

and

$$[k] = [b]^T [C] [b]$$

respectively, and $\{Q\}$ is the load vector resulting from the volume integral of the expression.

The kinetic energy of the system is the summation of the kinetic energies associated with the individual elements, therefore:

$$T = \frac{1}{2} \sum_{\text{all elements}} \int_{\text{vol of element}} \{\dot{u}_e\}^T [\rho_e] \{\dot{u}_e\} dvol \quad (3.45a)$$

and so the potential energy is:

$$U = \frac{1}{2} \sum_{\text{all elements}} \int_{\text{vol of element}} \{\epsilon_e\}^T [C_e] \{\epsilon_e\} dvol \quad (3.45b)$$

where the subscript e denotes the quantities relating to the individual elements.

Applying the requirement of stationary energies and with reference to equations (3.39) and (3.40) this gives:

$$\delta \left(\sum_{\text{all elements}} \frac{1}{2} \{\dot{q}\}^T [m_e] \{\dot{q}_e\} + \sum_{\text{all elements}} \frac{1}{2} \{q_e\} [K_e] \{q_e\} - \sum_{\text{all elements}} \{q_e\} \{Q_e\} \right) = 0 \quad (3.46)$$

Now, if all the co-ordinate vectors $\{q_e\}$ are transferred to a common co-ordinate vector base $\{q\}$ by

$$\{q_e\} = [n_e] \{q\}$$

then we have

$$\delta \left[\frac{1}{2} \{\dot{q}\}^T \left(\sum_{\text{all elements}} [\bar{m}_e] \right) \{\dot{q}\} + \frac{1}{2} \{q\}^T \left(\sum_{\text{all elements}} [\bar{K}_e] \right) \{q\} - \{q\}^T \sum_{\text{all elements}} \{\bar{Q}_e\} \right] = 0 \quad (3.47)$$

where

$$\begin{aligned} [\bar{Q}_e] &= [n_e]^T [Q_e] \\ [\bar{K}_e] &= [n_e]^T [K_e] [n_e] \\ [\bar{m}_e] &= [n_e]^T [m_e] [n_e] \end{aligned} \quad (3.48)$$

Comparing the equations (3.47) and (3.48) we have, for the system

$$\begin{aligned} [Q] &= \sum_{\text{all elements}} [\bar{Q}_e] \\ [K] &= \sum_{\text{all elements}} [\bar{K}_e] \\ [m] &= \sum_{\text{all elements}} [\bar{m}_e] \end{aligned}$$

Equations (3.48) are used to assemble the system equations of motion.

If we perform the variation of equation (3.43) we have

$$[m] \{\ddot{q}\} + [K] \{q\} = \{Q\}$$

which is the governing equation of motion in the matrix form.

3.5 Determination of Natural Frequencies

For conservative systems the equation of motion in matrix form is

$$[M] \{\ddot{q}\} + [K] \{q\} = \{0\} \quad (3.49)$$

which can be reduced to either

$$[D] \{\ddot{q}\} + \{q\} = \{0\} \quad (3.50)$$

or

$$\{\ddot{q}\} + [D] \{q\} = \{0\} \quad (3.51)$$

where

$$\begin{aligned} [D] &= [K]^{-1} [M], \\ \text{and} \quad [D] &= [M]^{-1} [K] \end{aligned}$$

If an oscillatory solution of the form

$$\{q\} = \{\phi\} \sin (wt+\psi) \quad (3.52)$$

is assumed, substituting (3.52) into (3.50) leads to

$$((1/w^2) [I] - [D]) \{\phi\} = \{0\} \quad (3.53)$$

and substituting (3.52) into (3.51) yields

$$(w^2 [I] - [D]) \{\phi\} = \{0\} \quad (3.54)$$

Equations (3.53) and (3.54) define two separate eigen value problems, which can be written in the forms:

$$[D] \{\phi\}_i = \frac{1}{w_i^2} \{\phi\}_i \quad (3.55)$$

and

$$[D] \{\phi\}_i = w_i^2 \{\phi\}_i \quad i=1,2,\dots,n \quad (3.56)$$

respectively.

The iteration technique will be discussed with reference to equation (3.55), for reasons which will become clear in the ensuing derivation.

In starting the iteration, a trial column is selected which is premultiplied by the matrix $[D]$ to yield a new column matrix. Next the newly obtained column matrix is normalised by dividing all the elements, by the first for example, in order to reduce the first element to unity. This normalised matrix is then used as the second trial column to obtain a second column matrix to be normalised. This same process goes on until the new column matrix obtained differs very slightly from the last trial modal column. Then convergence has been effected. The last column matrix is the modal column corresponding to the lowest mode, and the factor used to normalise the column matrix is the lowest eigen value. If the equation (3.56) is used to set up the iteration process, the result will be the modal column appropriate to the highest mode and its frequency.

The basis of the iteration can be demonstrated in the following manner. Assuming that all the eigen values are distinct, we can express an arbitrary column vector in terms of the n orthogonal eigen vectors by linear combinations. Thus the first trial modal column can be expressed as

$$\{\phi_1\} = C_1 \{\phi\}_1 + C_2 \{\phi\}_2 + C_3 \{\phi\}_3 + \dots + C_n \{\phi\}_n \quad (3.57)$$

where C_1, C_2 etc are arbitrary constants and $\{\phi\}_1, \{\phi\}_2$ etc

are the eigen vectors of the matrix $[D]$. The trial modal column can be anything, but if it is reasonably close to the actual modal column, then the convergence will be hastened.

Premultiplying the trial column by $[D]$ we have

$$[D] \{\phi_1\} = C_1 [D] \{\phi\}_1 + C_2 [D] \{\phi\}_2 + \dots + C_n [D] \{\phi\}_n \quad (3.58)$$

By virtue of equation (3.55) the following relations are true:

$$\begin{aligned} [D] \{\phi\}_1 &= (1/w_1^2) \{\phi\}_1 \\ [D] \{\phi\}_2 &= (1/w_2^2) \{\phi\}_2 \\ \vdots & \\ [D] \{\phi\}_n &= (1/w_n^2) \{\phi\}_n \end{aligned} \quad (3.59)$$

where it is assumed that the eigen values are ordered such that

$$w_1 < w_2 < w_3 < \dots < w_n, \text{ since}$$

$$[D] \{\phi_1\} = \{\phi_2\} \quad (3.60)$$

where $\{\phi_2\}$ is the second trial modal column, it follows from equations (3.58) and (3.59) that

$$\{\phi_2\} = \frac{C_1}{w_1^2} \{\phi\}_1 + \frac{C_2}{w_2^2} \{\phi\}_2 + \dots + \frac{C_n}{w_n^2} \{\phi\}_n \quad (3.61)$$

The second iteration gives:

$$[D] \{\phi_2\} = \frac{C_1}{w_1^4} \{\phi\}_1 + \frac{C_2}{w_2^4} \{\phi\}_2 + \frac{C_n}{w_n^4} \{\phi\}_n \quad (3.62)$$

Here it is noted that in order to keep the algebra simple, the normalisation is purposely avoided. However, the validity of the process is not affected by the absence of the normalisation.

After (P - 1) iterations, we obtain

$$[\mathcal{D}] \{\phi_{p-1}\} = \{\phi_p\} = \frac{C_1}{w_1^{2P}} \{\phi\}_1 + \frac{C_2}{w_2^{2P}} \{\phi\}_2 + \dots$$

$$+ \frac{C_n}{w_n^{2P}} \{\phi\}_n$$

which can also be written as

$$\{\phi_p\} = \frac{1}{w_1^{2P}} [C_1 \{\phi\}_1 + C_2 \left(\frac{w_1}{w_2}\right)^{2P} \{\phi\}_2 + \dots$$

$$+ C_n \left(\frac{w_1}{w_n}\right)^{2P} \{\phi\}_n] \quad (3.63)$$

If no eigen values are very close to each other, after a few iterations, it will be valid to claim that

$$\{\phi_p\} \approx \frac{1}{w_1^{2P}} C_1 \{\phi\}_1 \quad (3.64)$$

One more iteration will yield

$$\{\phi_{p+1}\} = [\mathcal{D}] \{\phi_p\} = \frac{1}{w_1^{2P+1}} C_1 \{\phi\}_1 \quad (3.65)$$

Comparing (3.65) with (3.64) we obtain

$$\{\phi_{p+1}\} = \frac{1}{w_1^2} \{\phi_p\} \quad (3.66)$$

Equation (3.66) states that the iteration has proceeded to the point where convergence is evident. One more iteration will merely produce a multiple of the preceding column. The constant of multiplication is the value of $1/w_1^2$.

If the iteration is based on (3.57) it is easy to see that instead of (3.63) we shall have

$$\{\phi_p\} = w_n^{2P} [C_1 \left(\frac{w_1}{w_n}\right)^{2P} \{\phi\}_1 + C_2 \left(\frac{w_2}{w_n}\right)^{2P} \{\phi\}_2 + \dots$$

$$+ C_n \{\phi\}_n] \quad (3.67)$$

In this case it is evident that the largest eigen value is obtained by iteration.

3.6 Determination of the Higher Modes

The highest eigen value of the problem can be obtained by iteration using equation (3.56) instead of equation (3.55).

To obtain the intermediate eigen values is the central problem to be studied in the following section. A method is available for obtaining the successive eigen values in either ascending or descending order, depending on whether equation (3.55) or equation (3.56) is used as a basis for the iteration.

To make this method more clear, let us use equation (3.55) to start the iteration and assume that $\{\phi\}_1$ has now been obtained. To proceed to the second mode $\{\phi\}_2$ we shall again take an arbitrary column, but now it is necessary that this column should be orthogonal to the first modal column $\{\phi\}_1$. This constraint can be expressed in matrix form as

$$\{\phi\}_1^T [D] \{\phi\}_1 = 0 \quad (3.68)$$

Substituting equation (3.57) into equation (3.68), we obtain

$$C_1 \{\phi\}_1^T [D] \{\phi\}_1 + C_2 \{\phi\}_2^T [D] \{\phi\}_1 + \dots + C_n \{\phi\}_n^T [D] \{\phi\}_1 = 0 \quad (3.69)$$

By virtue of the orthogonality conditions existing between all modal columns, all the terms except the first one in equation (3.69) vanish. Hence we have

$$C_1 \{\phi\}_1^T [D] \{\phi\}_1 = 0 \quad (3.70)$$

which leads to the conclusion that $C_1 = 0$. Therefore, with

the constraints (3.68) and (3.57) become

$$\{\phi_1\} = C_2 \{\phi\}_2 + C_3 \{\phi\}_3 + \dots C_n \{\phi\}_n \quad (3.71)$$

The above equation shows that when a trial column is subjected to the condition in equation (3.71), then it can be expressed in a linear combination only of (n-1) modal columns with the first modal column deleted. Following the same reasoning, it is not hard to see that by using a trial column with constraints (3.71) to start the iteration, the second modal column $\{\phi\}_2$ will be obtained, when convergence is achieved. This same principle can be used in the selection of the trial columns in establishing other modes by iteration.

Let the elements of the trial column $\{\phi_1\}$ be ϕ_{1i} where the index i denotes the row:

$$\{\phi_1\} = \begin{pmatrix} \phi_{11} \\ \phi_{21} \\ \vdots \\ \phi_{n1} \end{pmatrix} \quad (3.72)$$

Expanding the triple matrix product in (3.68), we have

$$\phi_{11} \sum_j d_{1j} \phi_j^{(1)} + \phi_{21} \sum_j d_{2j} \phi_j^{(1)} + \dots + \phi_{n1} \sum_j d_{nj} \phi_j^{(1)} = 0 \quad (3.73)$$

where the superscripts inside each summation denote the first modal column. Thus $\phi_j^{(1)}$ is the first element of $\{\phi\}_1$, $\phi_j^{(2)}$ is the second, etc. Expressing the first element in the first trial column in terms of the rest of the elements of the column, we obtain:

$$\phi_{11} = - \frac{\sum d_{2j} \phi_j^{(1)}}{\sum d_{1j} \phi_j^{(1)}} \phi_{21} - \frac{\sum d_{3j} \phi_j^{(1)}}{\sum d_{1j} \phi_j^{(1)}} \phi_{31} - \dots - \frac{\sum d_{nj} \phi_j^{(1)}}{\sum d_{1j} \phi_j^{(1)}} \quad (3.74)$$

The trial column with the first element given by (3.74) and arbitrary elements for the rest of the array may be called the constrained trial column and is denoted by $\{\phi_1\}_c$. Then $\{\phi_1\}_c$ can be written as a product of two matrices:

$$\{\phi_1\}_c = \begin{pmatrix} \phi_{11} \\ \phi_{21} \\ \phi_{31} \\ \vdots \\ \phi_{n1} \end{pmatrix} = \begin{pmatrix} 0 & -\frac{\sum d_{2j} \phi_j^{(1)}}{\sum d_{1j} \phi_j^{(1)}} & -\frac{\sum d_{3j} \phi_j^{(1)}}{\sum d_{1j} \phi_j^{(1)}} & \dots & -\frac{\sum d_{nj} \phi_j^{(1)}}{\sum d_{1j} \phi_j^{(1)}} \\ 0 & 1 & 0 & \dots & 0 \\ 0 & 0 & 1 & \dots & 0 \\ \vdots & \vdots & \vdots & \vdots & \vdots \\ 0 & 0 & 0 & \dots & 1 \end{pmatrix} \begin{pmatrix} \phi_{11} \\ \phi_{21} \\ \phi_{31} \\ \vdots \\ \phi_{n1} \end{pmatrix} \quad (3.75)$$

for brevity, (3.75) may be written in the form:

$$\{\phi_1\}_c = [S]_1 \{\phi_1\} \quad (3.76)$$

where $[S]_1$ is called the sweeping matrix. Thus, the first iteration is expressed by

$$[D] \{\phi_1\}_c = [D] [S]_1 \{\phi_1\} = \{\phi_2\}$$

For the next iteration the newly obtained second trial column again has to be modified by the same constraint.

$$\{\phi_2\}_c = [S]_1 \{\phi_2\} \quad (3.77)$$

This process is repeated as many times as convergence requires.

Hence we have

$$\begin{aligned} [\mathbb{D}] \{\phi_2\}_c &= [\mathbb{D}] [S]_1 \{\phi_2\} = \{\phi_3\}, \\ &\vdots \\ [\mathbb{D}] \{\phi_p\}_c &= [\mathbb{D}] [S]_1 \{\phi_p\} = \{\phi_{p+1}\} \end{aligned} \quad (3.78)$$

Labour can be saved if the matrix $[\mathbb{D}]$ is postmultiplied by $[S]_1$ to get $[\mathbb{D}]_1$ which can be taken as the first modified dynamic matrix to be used over and over in the iteration to obtain the second eigen value. Thus, in terms of $[\mathbb{D}]_1$ we have:

$$\begin{aligned} [\mathbb{D}]_1 \{\phi_1\} &= \{\phi_2\} \\ [\mathbb{D}]_1 \{\phi_2\} &= \{\phi_3\} \\ &\text{etc} \end{aligned} \quad (3.79)$$

To obtain the third eigen value, two orthogonal relations must be used to constrain the trial column:

$$\begin{aligned} \{\phi\}_1^T [\mathbb{D}] \{\phi_1\} &= 0 \\ \text{and } \{\phi\}_2^T [\mathbb{D}] \{\phi_1\} &= 0 \end{aligned} \quad (3.80)$$

From equation (3.80) a second sweeping matrix $[S]_2$ can be constructed and the process of iteration can thus go on, guided by the routing just developed. The number of iterations required depends on the closeness of the assumption to the actual modal shape.

3.7 Reliability and Accuracy of Solutions

In dynamic analysis, the procedure involves four major steps:

- 1) The idealised description of the structural system by a mathematical model
- 2) The establishment of a system of governing equations of motion

- 3) The solution of this set of equations
- 4) The confirmation of the solution by experiments.

The reliability of a dynamic analysis procedure is determined by the 'completeness' of its results compared to the solutions of the original system and the accuracy is determined by their 'closeness'.

In other words, by reliability we mean that every solution obtained by such a procedure is a solution, exactly or approximately, of the original system, and there are no solutions of the original system which are missed out by the procedure within any domain of interest.

And by accuracy we mean the closeness of a solution by this procedure to the corresponding actual solution of the original system.

The requirements of 'how accurate' and 'how reliable' are the results within some economic limits of computation will determine the choice of procedure used for analysis.

3.8 Computer Programme

The numerical technique incorporated a programme developed for calculating the natural frequencies and the mode shapes.

Programmes for the solution of each parameter were developed initially and then combined into one programme. Using this programme it was possible to study the various vibration characteristics of the structure under consideration. Continuous structures have an infinite number of modes

of vibration, but generally only the lowest few of these are of importance in low frequency vibrations, so that in these cases it is necessary to consider these few modes.

The technique employed in this work was the Finite Element Method to find the solution to the structural vibration problem. The consistent stiffness and mass matrices of the structure elements were derived by discretization of the platform structure which consisted of beams and plates i.e. finite elements.

The programme read the following data:

A	= Area of cross section of the beam	mm ²
ρ	= Mass per unit length of beam	Kg/mm
E	= Young's Modulus of beam material	KN/mm ²
G	= Rigidity Modulus of beam material	KN/mm ²
I_x	= Polar second moment of area of beam cross section	mm ⁴
I_y	= Second moment of area of beam cross section about the y_e axis	mm ⁴
L	= Length of beam	mm
m_1	= mass	Kg
m_2	= mass	Kg
K	= spring constant	N/mm ²

It was possible to run the programme to change the iteration procedure from 100 to 500 times. Also worth mentioning here is that the number of iterations was significant in the accuracy but not for the speed of computation.

Due to the springs supporting the structure, the potential energy stored in the springs is:

$$2V = K_1 (q_4 - .55q_5 - .2q_6)^2 + K_2 (q_4 + .55q_5 - .2q_6)^2 \\ + K_3 q_7^2 + K_4 q_{13}^2 .$$

Then adding values in the consistent stiffness matrix for the spring's potential energy, (by modification of the main programme), the potential energy in the springs is as follows:

$$\begin{aligned} K_{4,4} &= (K_1 + K_2) \\ K_{5,5} &= .3025 (K_1 + K_2) \\ K_{6,6} &= .04 (K_1 + K_2) \\ K_{4,5} &= .55 (K_2 - K_1) \\ K_{5,6} &= .11 (K_1 - K_2) \\ K_{4,6} &= -.2 (K_1 + K_2) \\ K_{7,7} &= K_3 \\ K_{13,13} &= K_4 \end{aligned}$$

Fig.(3.3) shows the theoretical idealisation for the structure with 15 degrees of freedom. The method used offers considerable economic advantages in terms of computation, and can give insight into what is happening in the structure.

In any dynamic analysis a procedure involves four major steps. They are:

1. The idealised description of the structural system by a mathematical model
2. The establishment of a system of governing equations of motion
3. The solution of this set of equations.

4. The confirmation of the solutions by experiments.

Fig.(3.4) shows an exploded view of an idealised structure with all the elements.

It was assumed in the computer programme calculations that the spring stiffness was constant.

These findings indicate that the digital computer has become an indispensable tool to scientists in general and engineers in particular.

A proper use of the computer lies in one's ability to translate a problem into simple repeated steps of operations in a form which lends itself to the mode of working of the computer. In order to perform a particular job, the computer must be fed with the set of numbers to operate upon (data) and the set of operations required (programme).

The theories and processes for the solution of our problems have to be well represented in the form of computer programmes and data for the correct results to be obtained. In the previous sections the theories for obtaining the consistent stiffness and mass matrices of a beam element and plate element were developed.

The eventual goal of obtaining a computational dynamic analysis of a flexible platform structure can then be achieved through the sensible use of the digital computer.

The first programme was to produce the overall mass and stiffness matrices of the structure (properties) when

supplied with the suitable properties of the consistent beam and plate elements.

Secondly, the main programme solved the eigen value problem of the form given by equation (2.3) namely

$$[K] \{U\} = \omega^2 [M] \{U\}$$

The results from this programme include the natural frequencies (eigen-values) and normal modes (eigen-vectors) of the system under consideration. The eigen-vectors could be plotted to obtain a pictorial view of the modes of free vibration of the structure.

It must be said that the discretization of any structure into finite elements usually leads to large order overall mass and stiffness matrices. Most modern digital computers are capable of working with large order matrices. But even so, the largest computers available have limited capacities. Hence they have limits on the size of matrices that can input into them.

It is possible to use the useful property of the mass and stiffness matrices of a real structure which is symmetry. Thus, no data is lost by storing only the matrices as only upper or lower triangular matrices. But unfortunately, the modification in the main programme for the potential energy in the springs in the stiffness matrix made it impractical.

Another method is to store the consistent mass and stiffness matrices on a tape and call for them in the beginning of the main programme. A point to be mentioned here about the two plate element is that they were calculated

first then condensed to fit in the normal co-ordinate representing its parameters.

Using an intelligent numbering of the nodes (and nodal displacement co-ordinates) the overall mass and stiffness matrices of the structure can be made to become band matrices with as small a band width as possible, to use the computer most efficiently. But owing to the number of degrees of freedom taken into consideration it was preferable to use the complete consistent mass and stiffness matrices. In other words, the inevitable need for large core storage still exists. This in turn has placed a very high limitation on the number of degrees of freedom of structures which can be analysed on the available computer.

All computer programmes described here were written in Basic language, and run in the University of Aston-Mechanical Engineering Department model HP 901A.

The programme also incorporates the addition of concentrated mass and stiffness properties to any co-ordinate of the frame. Thus joint masses and other masses can be added to the appropriate elements of the mass matrix while the effect of spring stiffness can be added to the corresponding elements of the frame stiffness matrix. Again, the data which this programme required for processing included the number of degrees of freedom of the structure, maximum allowable error in the vector, the coefficient of consistent mass matrix, the coefficient of stiffness matrix, and any modifications before starting the iteration.

The printout included:

```
print  $1/\lambda = w_1^2, w_2^2, w_3^2$  natural frequency
print  $U = U_1, U_2, U_3 \dots U_{15}$  mode shapes
print Error in vector after the given number of iterations.
```

The programme included the number of finite elements of the discretized structure, the Young's and Rigidity moduluses of each component, the mass per unit length of beam, the second moments of area of the beam element cross-section about its x-y and z-axis and the area of cross-section of the beam elements.

Another computer programme was run with 41 elements. Finite element discretization of the flexible platform would yield a total of 20 elements for the two plates and 21 elements for the beams. From these 54 degrees of freedom would be due to translational displacement and 108 would be due to rotation.

The estimated computer core necessary to run this programme to solve the eigen value problem (NAG EIGNVAL) for a system with 162 degrees of freedom is about 175K. Unfortunately, the ICL 19045 computer currently available at the University of Aston Computer Centre only provides a maximum core size of 100K and under special arrangement can be run at 110 K which is about 0.62 of the size required for this programme.

The alternative computer at the Regional Computer Centre in Manchester provides a maximum core size of 200 K, which would be suitable for this work. However, bearing in mind the cost and time, it was decided not to make use of this

facility as very little productive outcome was expected from the results. In other words, the expected increase in productivity would not have justified the increased cost.

A practical way of avoiding the need for so much computer core is the reduction in the number of degrees of freedom of the system studied or alternatively, through some manipulation of the stiffness and mass matrices to obtain reduced matrices for the dynamic analysis. This usually involves distinguishing between the translational and rotational displacement of the structure.

3.8.1 Elimination of rotational displacement

Generally, in the dynamic analysis of structure, not all the static displacements are considered. The experimental modal shape measurements involved only the translational displacement components. For example, in the conventional dynamic of structure analysis of fighter wing structure only deflections normal to the wing midplane are held. By the same reasoning it is useful, in this work, to retain only the translational displacements and eliminate the rotational displacements. This will lead to condensed mass and stiffness matrices for the structure.

The first step in this elimination process is partitioning of the stiffness matrix $[K]$ and the displacement vector $\{q\}$ of the structure in the following form

$$[K] = \begin{bmatrix} [K]_{t,t} & [K]_{t,r} \\ [K]_{r,t} & [K]_{r,r} \end{bmatrix} \quad (3.81)$$

and

$$\{q\} = \begin{matrix} \{q\}_t \\ \{q\}_r \end{matrix} \quad (3.82)$$

The vector $\{q\}_r$ refers to all the rotational displacements which are to be eliminated for the dynamics of structure.

The vector $\{q\}_t$ refers to all the translational displacements which are to be retained as the degrees of freedom of the structure for the analysis. The stiffness matrix as partitioned in equation (3.81) is such that it is compatible with the partitioned displacement vector.

The static equilibrium is given by

$$[K] \{q\} = \{Q\} \quad (3.83)$$

and in its partitioned form, it is given by

$$\begin{bmatrix} [K]_{t,t} & [K]_{t,r} \\ [K]_{r,t} & [K]_{r,r} \end{bmatrix} \begin{matrix} \{q\}_t \\ \{q\}_r \end{matrix} = \begin{matrix} \{Q\}_t \\ \{Q\}_r \end{matrix} \quad (3.84)$$

Assuming that the external forces $\{Q\}_r$ corresponding to the rotational displacements are equal to zero, we have from equation (3.84)

$$q_r = -[K]_{r,r}^{-1} [K]_{r,t} \{q\}_t \quad (3.85)$$

provided $[K]_{r,r}$ is not singular

Substituting equation (3.85) into equation (3.84) we have

$$\{Q\}_t = ([K]_{t,t} - [K]_{t,r} [K]_{r,r}^{-1} [K]_{r,t}) \cdot \{q\}_t \quad (3.86)$$

or

$$\{Q\}_t = [K]_c \cdot \{q\}_t \quad (3.87)$$

where $[K]_c = [K]_{t,t} - [K]_{t,r} [K]_{r,r}^{-1} [K]_{r,t}$ (3.88)

$[K]_c$ represents the condensed stiffness mass matrix of the structure.

Let virtual displacement $\{\delta q\}$ be applied to the structure and $[M]_c$ be the corresponding condensed mass matrix of the structure.

It follows from the equivalence of the virtual work of the two equivalent mass representations of the continuous system that

$$\{\delta q\}_t^T [M]_c \{\ddot{q}\}_t = [\{\delta q\}_t^T \{\delta q\}_r^T] [M] \begin{matrix} \{\ddot{q}\}_t \\ \{\ddot{q}\}_r \end{matrix} \quad (3.89)$$

substituting equation (3.85) into equation (3.89) we have

$$\{\delta q\}_q^T [M]_c \{\ddot{q}\}_t = \{\delta q\}_t^T [A]_c^T [M] [A]_c \{\ddot{q}\}_t \quad \dots (3.90)$$

where

$$[A]_c = \begin{bmatrix} [I] \\ -[K]_{r,r}^{-1} [K]_{r,A} \end{bmatrix} \quad (3.91)$$

and $[I]$ is an identity matrix

Thus from equation (3.90), the condensed mass matrix of the structure is given by

$$[M]_c = [A]_c^T [M] [A]_c \quad (3.92)$$

Equations (3.92) and (3.88) give the condensed mass and stiffness matrices respectively for any structure.

However, large sized matrices are still to be manipulated

and still require more computer core. But there are ways to avoid the complete use of these large matrices during their manipulation.

Unfortunately, due to shortage of time, only the theoretical idealisation for the structure with 15 degrees of freedom was considered.

3.9 Discussion of Results

The computer programme was in good agreement with measurements within the limits allowed in the structural analysis. The results of the theoretical and experimental vibration analysis of the flexible platform are very satisfactory in relation to the natural frequency and the mode shapes.

The theoretical analysis used in this work has produced a very good agreement of the true modal shapes of vibration for the first three modes analysed (the rigid body mode) and the corresponding natural frequencies.

Also for the plate mode the modal shapes and the natural frequencies have been very close.

TABLE 3.1

MODE	Natural frequencies in Hz	
	computed	Experimental
1	4.55	4.3
2	7.141	8.2
3	8.656	9.1

Table 3.1 shows the first three computed and experimental natural frequencies of the flexible platform.

As for the platform itself, the following table 3.2 contains the three rigid body modes and the plate mode.

TABLE 3.2

MODE	Natural frequencies in Hz	
	computed	Experimental
1	4.55	4.3
2	7.14	8.2
3	8.656	9.1
4	42.34	37.4

The computed frequencies are on average about $\pm 5\%$ to 15% ; this is good enough in vibration analysis.

If it is necessary to trace the possible source(s) of error in the theoretical approach, the most likely sources of error are the derived stiffness and mass matrices, and the values of spring stiffness. The spring stiffness values used in the computer programme which were added to the structure stiffness coefficient were considered to be linear, but in actual fact the spring stiffness is not linear but has a minute amount of non-linearity, and has a stiff type spring character.

The following Table 3.3 shows the computed natural frequency for the platform with twice and three times the spring stiffness for the first 10 modes.

TABLE 3.3

MODE	Computed Natural frequency in Hz		
	Computer Calculation		
	1X spring stiff.	2X spring stiff.	3X spring
1	4.55	6.09	7.122
2	7.141	9.258	10.359
3	8.556	11.55	13.170
4	21.84	17.24	18.160
5	27.60	19.95	21.66
6	33.60	28.91	29.78
7	42.34	31.24	30.31
8	54.26	44.04	33.49
9	96.76	56.32	46.59
10	110.76	70.35	55.30

Errors of up to 15% higher than the computed natural frequencies would suggest a possible 37.5% over-estimation of the structure stiffness matrix or the same under-estimation of the structure mass matrix or some combination of these factors.

The computed frequencies, should, theoretically, tend to the lower limiting values equal to the actual natural frequencies. If a mass is placed at a nodal point, then it has negligible influence on the frequency, while if it is placed at anti-node, its influence on the frequency is a maximum. Changing the torsional rigidity at an anti node where the torque is zero, has negligible effect on the frequency, while changing it at a node has the maximum effect.

In other words, by adding a mass at an appropriate position, the frequency of a selected mode may be changed without affecting other modes and also changing the torsional rigidity at appropriate positions offers an alternative method of changing the frequency of a selected mode without affecting other modes.

Moreover, the good agreement in the corresponding modal shapes did not raise the suspicion of such percentage estimation. But this line of approach has proved reasonable upon investigation. Careful consideration and extensive checks on the programmes and data have not shown any trace of such errors.

Other sources of error may be the boundary conditions at the joints of the frame; most of the frame joints are of welded construction and it seems probable that the welded joint gives rise to some sort of increasing stiffness in these parts.

A factor of safety, which we may call a factor of ignorance, is usually applied to account for the difference in the theoretical and real deflections of the structure. It seems there is a need for obtaining more accurate assessment of the true joint conditions in the vibration analysis of structure. Unfortunately, this is not usually applied by the structural engineer at the design stage.

A true measurement of the joint boundary conditions would be preferred, because this is the main reason for the discrepancy between the experimental and theoretical results,

other than the nonlinearity of the spring supporting the structure.

Rockey (99) 1977 looked at various processes and fabrication procedures adopted which affect the residual and geometric imperfections occurring in the completed structure, e.g. roller-straightening, gaging (i.e. straightening at one point), flattening by local bending or pressing, stress relieving, normalising or hardening and tempering, flame-cutting, shot blasting, etc.

This gives rise to the need to look briefly at the model material used, hence some material properties, viz, stress-strain relationship, notch ductility, etc. are likely to have an important influence on the results of the test.

In a welded structure (for example) there will be very great rapid changes from compressive to tensile stress in the vicinity of the welds. In the stiffness, particularly those having local thick parts, there may be very significant local stress gradients and these are unpredictable, to the extent that stress of either sign, i.e. compressive or tensile, may occur.

Of course, the more practical parameter to be checked in this structure was the stiffness matrix. This was done by considering the static of the plane frame. Load deflection experiments were performed. Also, the corresponding deflection of the structure was calculated for a given load from the stiffness matrix and static equation

$$[K] \{q\} = \{Q\}$$

Experimental displacements at the same points were measured to obtain the average deflections of the frame structure for a fixed point load.

Finally, with an adequate size of computer the data were obtained for the real mass and stiffness matrices of the structure. These were used to obtain the true mass and stiffness matrices representing the true structure. This in turn should yield the true vibration characteristics of the flexible platform.

Rig Description:

The rig consisted of a plain frame with the dimensions (mm) $a, b, h = 1100, 1100, 100$ respectively. As shown in Fig.(1.1) the steel frame had I-shape cross section of $h = 100$ mm. and $I_{xx} = 198 \times 10^4$ mm⁴, $I_{yy} = 17.9 \times 10^4$. In every corner of the frame there was a piece of square plate with the dimensions $200 \times 200 \times 10$ mm. These pieces of plate were used as a rest base for the springs.

The motor was mounted on the big base. The alternator was mounted parallel to the motor on another base. The alternator was used just as an open circuit machine driven by the motor. The unit which here is called the motor, was in fact a Heenan-Dynamatic variable speed drives and couplings which drove a rotor. The Heenan-Dynamatic Air cooled variable speed coupling consisted basically of two revolving members, one of which had poles or teeth and carried one or more coils which were excited by D.C. current. This induced eddy currents in the adjacent iron face of the other, or armature member thus effecting a transfer of power from driving to

driven member by its insertion between a prime mover and the driven equipment. The outer member was carried by rotating bells so that it was concentric with the inner member, both being suitably supported in ball or roller bearings. The slip rings carrying the D.C. current to the coil were mounted on the output shaft which also drove the governor generator when fitted.

This coupling, as with all forms of slip coupling, was not a torque converter, and the output torque could not exceed that available from the prime mover. The power lost due to a reduction in output speed had to be dissipated as heat by the coupling which needed to have adequate ventilation.

Cooling was effected by means of the fan action of the outer member which drew air through the end bells and directed it across the inner surface of the armature member in which the heat from the induced eddy current was generated. The heated air was discharged into the surrounding atmosphere and a suitable air exit had to be provided in any protecting enclosures. Current to the coupling field coil was obtained from an excitation unit normally designed to operate from a 200/250 volts single phase 50 cycles A.C. supply. (This may consist of a metal rectifier with a transformer or a thyatron unit depending on the application).

The two more usual characteristics provided are:

Natural : where a fall in speed against an increase in load is desirable

Constant speed: where despite changes in load the speed is to be maintained at an adjustable pre-set value.

Heenan-Dynamic Governor Generator

The governor generator was of the A.C. type employing Alnico permanent magnets for field excitation. These magnets maintain their magnetic energy over a period of years, resulting in a constant output voltage for a given speed. No commutators were used in the design of this generator, therefore, no brush replacement is required, and with the exception of the bearing, in some cases, no maintenance is needed.

The output voltage rating of the coupling shaft mounted generator was usually in the vicinity of 25 volts at 1500 r.p.m. speed rating where the Alnico generator was of the separately mounted belt driven type and the output voltage was approximately 45 volts at 3000 r.p.m. In both cases, the output of the generator was substantially linear, and thus the voltage was proportional to the speed. The electronic control used in conjunction with this generator compensated and standardised this voltage at predetermined levels.

The wires connecting the generator to the electronic control had to be shielded or run in separate conduits. The voltage from the generator was not affected by the direction of rotation; this generator will operate in either direction.

The bearing was the separately mounted self-contained generators which are packed with grease before despatch and should not require attention for approximately 5,000 hours of operation in normal ambient conditions.

3.10 Conventional method and mathematical model

Conventional methods of structural dynamic analysis involve the mathematical representation of a physical system in the form of its equations of motion. For systems having many degrees of freedom, it is convenient to cast the equations in matrix form.

This has given rise to extensive use of matrix algebra in the formulation of dynamic response analyses. The process of reducing a physical system to a mathematical representation is a prevalent task mutual to all fields of analysis.

Typically, this reduction of a physical process to mathematical equations has resulted from exercising a blend of skill, insight, experience, and good judgement. At least, in the mechanical/structural field, this has been the past history. It is possible to generate mathematical models by making use of experimentally derived information. The point to be made here is that they all belong to the analyst's bag of tools and it is his task to best match the particular job.

The- derivation of mass, stiffness and damping matrices that correctly represent the physical system is often a formidable task involving engineering judgement on the part of the analyst.

The analytical process is usually accompanied by dynamic testing either to verify the mathematical model or to point the way to required modifications of the analysis.

Sometimes the system of equations, or mathematical models will be modified on a simple trial and error basis to make the model respond in some predetermined fashion or react so as to match behavioural data obtained from the actual physical system.

In the transient case, problems arise because the relative phase is not generally $\pm 90^\circ$ at resonance as it is in the steady-state case, although the phase varies around the structure because of "model overlap" (that is contributions from neighbouring modes) and "statistical variance error".

The mode shape at a given frequency corresponds to that which would be obtained when the structure is excited with a sine wave input at the same frequency.

The modal patterns at resonances do not represent the normal modes of the structure since they contain small contributions from the flanks of neighbouring modes.

It is often assumed in dynamic test analysis that the responses are purely modal. This is a reasonable approximation in cases where systems damping is low and test forcing points have been carefully selected. In point of fact, no test responses are purely modal. In a typical dynamic test the structure is forced at a single point in several of its modal frequencies. Its response is really a combination of the responses of all its modes.

Completed modal information

First consider the situation where mode shape and modal mass information for 'N' number of modes has been obtained

from experimental data prior to any formulation of a physical model.

If the physical model is to have the same number of degrees of freedom 'N' as known modes, theoretically the physical model can be completely identified. This identification is based simply on assuming orthogonality to exist between modes with respect to physical mass, stiffness and damping terms.

The matrix description of the physical model can be expressed as

$$[M] = [\phi]^{-T} [m] [\phi]^{-1} \quad \text{"Physical Mass"} \quad (A)$$

$$[K] = [\phi]^{-T} [\omega^2 m] [\phi]^{-1} \quad \text{"Physical stiffness"} \quad (B)$$

$$[C] = [\phi]^{-T} [2z\omega m] [\phi]^{-1} \quad \text{"Physical Damping"} \quad (C)$$

with the $[\phi]$, $[m]$ ω_j, z_j terms being the known modal information. In general this scheme is admittedly quite idealistic since in practice only a limited number of modes can be experimentally measured.

It is assumed that a "good" estimate of the physical mass model with 'P' degrees of freedom can be made initially.

Usually the conceptual physical model will possess a larger number of degrees of freedom 'P' than normal modes 'N' obtained from test data. What results from this scheme is an "Incomplete model" that retains 'P' dynamic co-ordinates but has only 'N' modes. This incomplete model is derived so as to have the properties of producing the true response in all 'P' degrees of freedom over the

frequency range of the valid test data and having a physical mass matrix which deviates least from the original estimate. In addition, the orthogonality relationship is forced to exist between the measured modes and derived mass matrix.

The stiffness matrix $[K]_{incomp}$ for the incomplete model is developed briefly as follows

$$\begin{aligned}
 [\tilde{m}] &= [\phi]^T [M] [\phi] \\
 [\phi]^{-T} [\tilde{m}] &= [M] [\phi] \\
 [K] &= [\phi]^{-T} [\omega^2 \tilde{m}] [\phi]^{-1} \\
 &= [M] [\phi] [\omega^2] [\tilde{m}]^{-1} [\phi]^T [M] \\
 &= \sum_{i=1}^P \frac{\omega_i^2}{m_i} [M] \{\phi_i\} \{\phi_i\}^T [M]
 \end{aligned}$$

When $N = P$, there exists a complete model as defined previously.

If $N < P$, an incomplete model stiffness matrix exists being expressed as

$$[K]_{incom.} = \sum_{i=1}^N \frac{\omega_i^2}{m_i} [M] \{\phi_i\} \{\phi_i\}^T [M]$$

Such a model can predict changes in the normal modes due to mass changes. Test data are required at each significant resonance of the system. In addition, the particular measurement locations to be used must be selected with care. Experience and common sense have indicated the desirability of selecting the locations so as to ensure that reasonable idea of the nature of the mode could be inferred from the test measurement. In practice, this means selecting locations on each side of the modal boundaries (neutral points) in the highest mode.

There is, in general, a choice of selections. This in turn means that unique solutions to Equations (A) through (C) do not exist, whichever test measurement locations are selected, however, the set of three matrices will define a model whose responses match resonance data for the selected locations. We are forcing the system to match a known output.

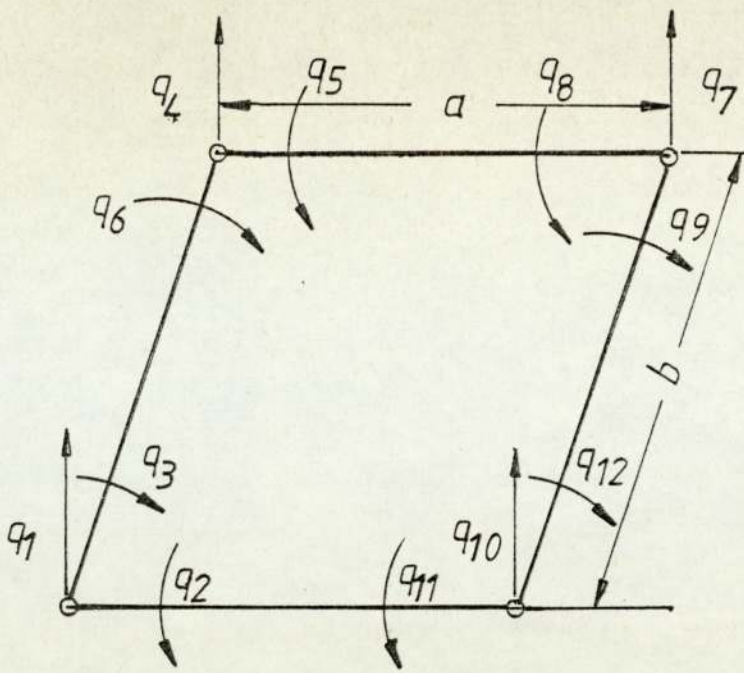


Fig. 3.1. Rectangular plate element.

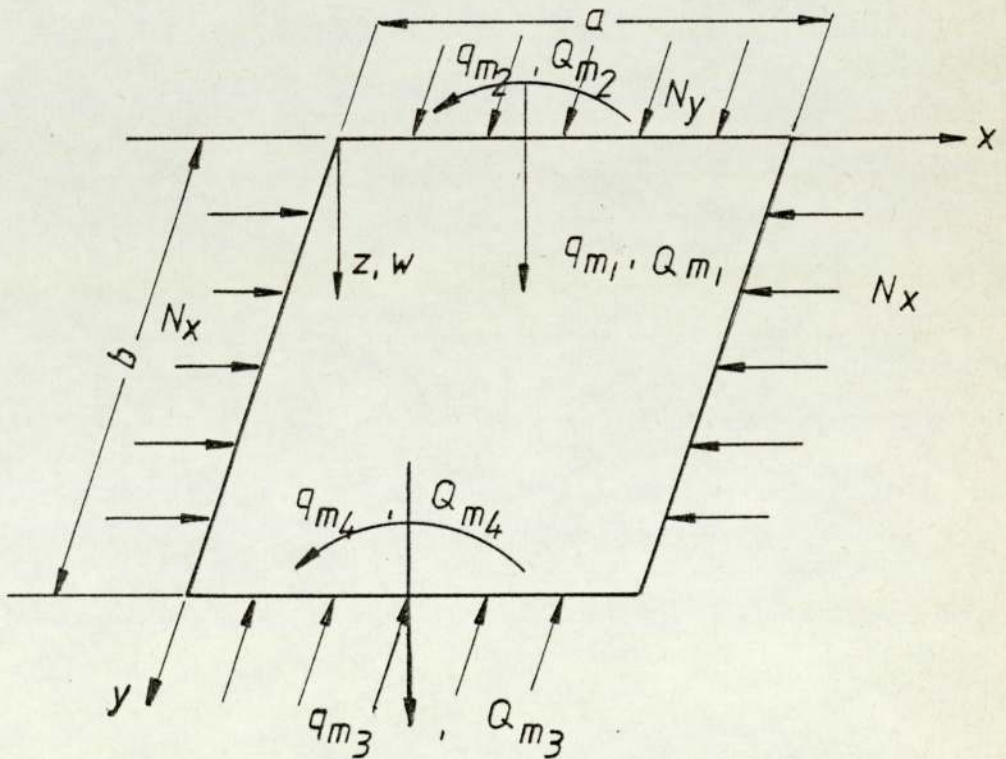


Fig. 3.2. A rectangular plate with two opposite edges simply supported and with the two edges connected to other structures.

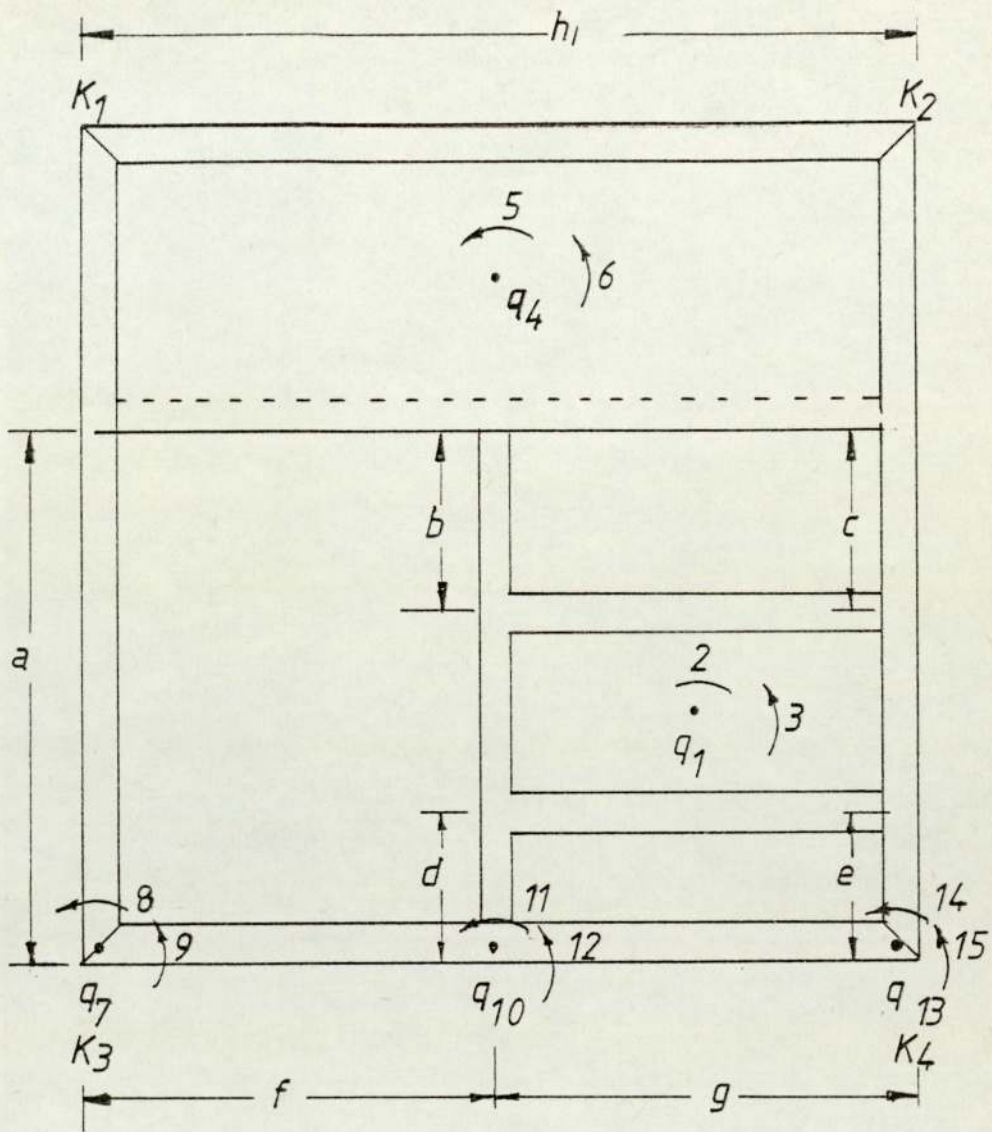


Fig. 3.3. THEORETICAL IDEALISATION

Dim. in m.m.

a	$=$	700
b	$=$	300
c	$=$	300
d	$=$	100
e	$=$	100
f	$=$	550
g	$=$	550
h_1	$=$	1100

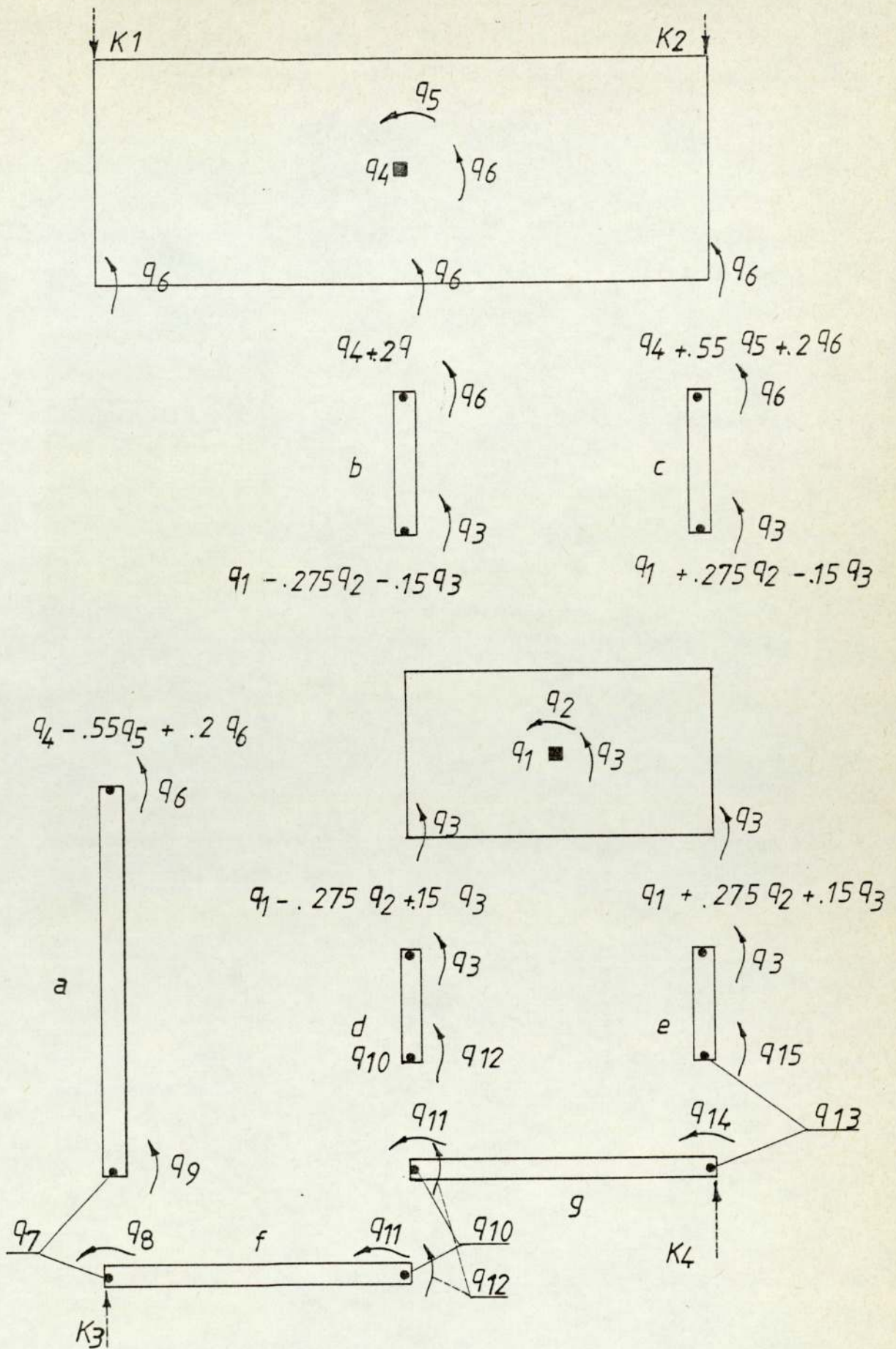


Fig. 3.4. EXPLODED VIEW OF IDEALIZED STRUCTURE
SHOWING ALL ELEMENTS

CHAPTER 4

Some Considerations of Linear and Non-Linear
Restoring Forces

It is essential to consider the factors of non-linearity in order to explain the unexpected behaviour in the modes of the response curves. This non-linearity can influence greatly the unforeseen resonances in the structure.

The stiffnesses of the supports were found experimentally to be almost linear within the normal working range.

In practice, however, elastic supports may possess some non-linear characteristics in the working range, giving rise to new phenomena which may be completely different from the linear case.

4.1 Non-linearity in General

In practice, non-linear problems may occur in all types of engineering works, such as in fluid dynamics the building up of a discontinuous shock wave from a smooth wave; in solid mechanics the presence of plasticity and non-linear elasticity; in mechanics the non-linear vibrations of machine components. Non-linear problems in mechanical vibration may occur in several ways:

- (i) non-linearity of restoring forces in the vibrational system i.e. the effect of a softening or hardening spring
- (ii) non-linearity in the nature of the damping, for example, coulomb damping, time-dependent

damping coefficients, etc.

- (iii) non-linearity inherent in the system parts, such as material damping, hysteresis, etc.
- (iv) periodical variation of vibrating mass, such as in the case of a reciprocating engine
- (v) oscillations in self-sustained systems. These always occur when a periodic motion is maintained through absorption of energy from a constant flow of energy, such as electrical systems containing vacuum tubes in which the energy for the oscillation is supplied by a direct current source, and
- (vi) oscillations due to time and amplitude dependent excitation forces.

In most cases linearisations as an approximating device may give valuable and sufficient solutions. These approximations occur mostly when the amplitudes of the vibrations are small. However, if the amplitudes are large, the accuracy can be improved by carrying out further approximations. New phenomena may be found in such non-linear systems which cannot in principle occur in linear systems.

In non-linear vibrations the occurrence of subharmonics and ultraharmonics, jump phenomena and combination tones will be formulated mathematically.

Various methods such as the Ritz averaging method iteration are illustrated.

The above methods are valid only if the non-linearity is small, i.e. if the oscillation is in the neighbourhood of the linear oscillation. However, the cases in which the departure from linearity is large will require the use of more sophisticated mathematics. Even so, in some cases such as the presence of small divisors in the problem of combination tones, mathematical results fail to describe the actual phenomena.

The effect of non-linear elastic restoring forces on the flexible platform will be discussed. That is, the restoring force which is obtained by either a softening or a hardening spring.

Thus to start with, the solution of Duffing's equation is assumed.

Damping is assumed to be linear in all cases. However, this is not applicable especially if the system has marked non-linearity. For systems of more than one degree-of-freedom, it is difficult to obtain an equivalent value of the damping coefficient for each mode.

The effect of beating in a non-linear system is quite significant, especially if the system has more than one degree-of-freedom. In these systems one instability occurs, that is the amplitude of vibration at each mode varies periodically.

4.2 Ultraharmonics and Sub-harmonics in Forced Non-linear Oscillations

Consider the equation

$$\ddot{x} + 2vp\dot{x} + p^2x + \mu x^3 = H \cos (\Omega t + \delta) \quad (4.1)$$

Since the forcing function is periodic, equation (4.1) can be solved by Fourier Series, i.e.

$$x = A_0 + \sum_{n=1}^{\infty} A_n \cos n \Omega t + \sum_{m=1}^{\infty} B_m \sin m \Omega t$$

In practice, it can be shown that ultrasonic oscillations predominate if $p = n \Omega$, where n is a positive integer other than 1. If $p = 3 \Omega$, then we can try a solution of the form:

$$x = A \cos \Omega t + U \cos (3\Omega t + \gamma) \quad \delta \neq 0$$

Substituting into equation (4.1) and equating separately to zero the coefficients of $\cos \Omega t$, $\sin \Omega t$, $\cos (3\Omega t + \gamma)$ gives:

$$6 \Omega \dot{U} + 6 vp \Omega U = \mu \frac{A^3}{4} \sin \gamma \quad (4.2)$$

$$6 \Omega U \dot{\gamma} = (p^2 - 9w^2) U + \mu \left(\frac{3}{2} A^2 U + \frac{3}{4} U^3 + \frac{A^3}{4} \cos \gamma \right) \quad (4.3)$$

$$(p^2 - \Omega^2) A + \mu \left(\frac{3}{4} A^3 + \frac{3}{4} A^2 U \cos \gamma + \frac{3}{2} AU^2 \right) = H \cos \delta \quad (4.4)$$

$$2v p \Omega A + \mu \frac{3}{4} A^2 U \sin \gamma = H \sin \delta \quad (4.5)$$

By squaring equations (4.4) and (4.5), and adding them together:

$$H^2 = A^2 \left\{ \left[(p^2 - \Omega^2) + \mu \frac{3}{4} (A^2 + AU \cos \gamma + 2U^2) \right]^2 + \right. \\ \left. (2vp\Omega + \mu \frac{3}{4} A U \sin \gamma)^2 \right\} \quad (4.6)$$

If μ is a very small quantity compared with p , and if v is of the same order as μ , then from equation (4.6):

$$H^2 = A^2 [(p^2 - \Omega^2) + O(\mu)]^2$$

If H is of order μ then:

$$A = \frac{H}{(p^2 - \Omega^2)} + O(\mu^2)$$

$$A = \frac{H}{(p^2 - \Omega^2)}$$

Steady State Solutions

$$\dot{U} = \dot{\gamma} = 0$$

From equations (4.2) and (4.3):

$$6vp\Omega U_0 = \mu \frac{A_0^3}{4} \sin \gamma_0 \quad (4.7)$$

and

$$U_0 (p^2 - 9\Omega^2) + \mu \left(\frac{3}{2} A_0^2 U_0 + \frac{3}{4} U_0^3 \right) = -\mu \frac{A_0^3}{4} \cos \gamma_0$$

..... (4.8)

By squaring equations (4.7) and (4.8) and adding them together we get:

$$\begin{aligned} \left(\frac{\mu A_0^3}{4} \right)^2 &= (6vp\Omega)^2 U_0^2 + \left[(p^2 - 9\Omega^2) U_0 \right. \\ &\quad \left. + \mu \left(\frac{3}{2} A_0^2 U_0 + \frac{3}{4} U_0^3 \right) \right]^2 \end{aligned} \quad (4.9)$$

From equation (4.2) we get:

$$\sin \gamma_0 = \frac{\pm 6vp\Omega}{\sqrt{\{(6vp\Omega)^2 + [p^2 - 9\Omega^2 + \mu \left(\frac{3}{2} A_0^2 + \frac{3}{4} U_0^2 \right)]^2\}}} \quad (4.10)$$

From equation (4.9) the loci of vertical tangency of U_0 is

$$(6vp\Omega)^2 + [p^2 - 9\Omega^2 + \mu(\frac{3}{2} A_0^2 + \frac{3}{4} U_0^2)] \times$$

$$[p^2 - 9\Omega^2 + \mu(\frac{3}{2} A_0^2 + \frac{9}{4} U_0^2)] = 0 \quad (4.11)$$

Approximations of the loci are given by:

$$p^2 - 9\Omega^2 + \mu(\frac{3}{2} A_0^2 + \frac{3}{4} U_0^2) = 0$$

$$p^2 - 9\Omega^2 + \mu(\frac{3}{2} A_0^2 + \frac{9}{4} U_0^2) = 0 \quad (4.11a)$$

Stability at steady state

Let $U = U_0 + \xi$

$\gamma = \gamma_0 + \eta$

Substituting into equations (4.2) and (4.3) :

$$6\Omega\dot{\xi} + 6vp\Omega\xi = \mu \frac{U_0^3}{4} \cos \gamma_0 \eta$$

and

$$6\Omega U_0 \dot{\eta} = [p^2 - 9\Omega^2 + \mu(\frac{3}{2} A_0^2 + \frac{9}{4} U_0^2)] \xi - \mu \frac{A_0^3}{4} \sin \gamma_0 \eta$$

Assuming solutions of the form $e^{\lambda t}$, and substituting into equations (4.7) and (4.8) for $\cos \gamma_0$ and $\sin \gamma_0$;

$$(6\Omega\lambda + 6vp\Omega)\zeta = [(9\Omega^2 - p^2) U_0 - \mu U_0(\frac{3}{2} A_0^2 + \frac{3}{4} U_0^2)] \eta$$

$$[(p^2 - 9\Omega^2) + \mu(\frac{3}{2} A_0^2 + \frac{9}{4} U_0^2)] \zeta = U_0 (6\Omega\lambda + 6vp\Omega) \eta \quad (4.12)$$

From equation (4.12), the characteristic solution is:

$$(6\Omega\lambda)^2 + (18vp\Omega^2)\lambda + \{(6vp\Omega)^2 + [p^2 - 9\Omega^2 + \mu(\frac{3}{2} A_0^2 + \frac{9}{4} U_0^2)]$$

$$\times [p^2 - 9\Omega^2 + \mu(\frac{3}{2} A_0^2 + \frac{3}{4} U_0^2)]\} = 0$$

For stability $\lambda \leq 0$, hence

$$2 p v \geq 0,$$

$$(6 v p \Omega)^2 + [6 p^2 - 9 \Omega^2] + \mu \left(\frac{3}{2} A_0^2 + \frac{9}{4} U_0^2 \right)$$

$$\times [(p^2 - 9 \Omega^2) + \mu \left(\frac{3}{2} A_0^2 + \frac{3}{4} U_0^2 \right)] \geq 0$$

The first condition implies that v must be positive. The second condition requires U_0 to be lying outside the region enclosed by the loci of vertical tangency. If the damping ratio is small, from equation (4.11a) the system cannot have vertical tangents unless

$$\Omega^2 \geq \frac{1}{9} (p^2 + \mu \frac{3}{2} A_0^2)$$

This shows that marked ultraharmonic behaviour cannot occur unless the frequency of the exciting force is slightly above 1/3 of the natural frequency of the system. Fig. (4.1) shows a typical amplitude/frequency response curve for an ultraharmonic of order 3. In the region close to 1/3 of the linear natural frequency the amplitude becomes triple-valued, two being stable and one unstable. In this region ultraharmonics predominate. Jump phenomena occur at the points P and Q.

Subharmonic motion

Under suitable conditions subharmonic motion may predominate in a non-linear system. In the case of cubic non-linearity, marked subharmonic behaviour of order 3 has been observed experimentally, if the frequency of the forcing function is about 3 times the natural frequency of the system.

The solution may be assumed to be of the form:

$$x = A \cos \Omega t + S \cos\left(\frac{\Omega}{3}t + \gamma\right)$$

Proceeding in the same way as in the ultraharmonic solution, we get:

$$\begin{aligned} \{A^2 [p^2 - \Omega^2 + \frac{\mu}{4} (3A^2 + 6S^2)]^2 + \mu \frac{A}{2} S^3 \cos 3\gamma [p^2 - \Omega^2 \\ + \frac{\mu}{4} (3A^2 + 6S^2)] + (2\nu p \Omega A)^2 + \mu \nu p \Omega A S^3 \sin 3\gamma\} = \\ = H^2 - \left(\frac{\mu S^3}{4}\right)^2 \end{aligned} \quad (4.13)$$

and the equation of the steady state solution is:

$$\begin{aligned} \left(\frac{3}{4} \mu S_0^2 A_0\right)^2 = \left[\left(p^2 + \frac{3}{2} \mu A_0^2 - \frac{\Omega^2}{9}\right) S_0 \right. \\ \left. + \mu \frac{3}{4} S_0^3 \right]^2 + \left(\frac{2}{3} \nu p \Omega S_0\right)^2 \end{aligned} \quad (4.14)$$

The locus of vertical tangency of S_0 is :

$$\begin{aligned} S_0 \left\{ \left[p^2 + \frac{3}{2} \mu A_0^2 - \frac{\Omega^2}{9} + \mu \frac{3}{4} S_0^2\right] \times \left[p^2 + \frac{3}{2} \mu A_0^2 - \frac{\Omega^2}{9} + \mu \right. \right. \\ \left. \left. \frac{9}{4} S_0^2\right] + \left[\frac{2}{3} \nu p \Omega\right]^2 - 2\left(\frac{3}{4} \mu S_0 A_0^2\right) \right\} = 0 \end{aligned} \quad (4.15)$$

Using equations (4.14) and (4.15), then either

$$S_0 = 0$$

$$\begin{aligned} \text{or } \left(\frac{2}{3} \nu p \Omega\right)^2 + \left(p^2 + \frac{3}{2} \mu A_0^2 - \frac{\Omega^2}{9}\right)^2 - \left(\mu \frac{3}{4} S_0^2\right)^2 = 0 \\ \dots \end{aligned} \quad (4.16)$$

If the damping ratio is small, the second locus is approximated by:

$$\mu \frac{3}{4} S_0^2 = \left(\frac{\Omega^2}{9} - p^2 - \frac{3}{2} \mu A_0^2\right)$$

Stability of steady-state solutions

For stability $\nu \geq 0$

$$\left(\frac{3}{4} \nu S_0^2\right)^2 - \left(p^2 - \frac{\Omega^2}{9} + \frac{3}{2} \mu A_0^2\right)^2 - \left(\frac{2}{3} \nu p \Omega\right)^2 \geq 0$$

This condition requires S_0 to be lying outside the region enclosed by the locus of vertical tangency as defined by equation (4.16).

From equation (4.14), if $S_0 \neq 0$, and taking A_0 as constant:

$$\begin{aligned} \frac{3}{4} \mu S_0^2 &= \left(\frac{\Omega^2}{9} - p^2 - \frac{9}{8} \mu A_0^2\right) \\ &\pm \sqrt{\left\{\frac{3}{4} \mu A_0^2 \left(\frac{\Omega^2}{9} - p^2 - \frac{21}{16} \mu A_0^2\right) - \left(\frac{2}{3} \nu p \Omega\right)^2\right\}} \\ &\dots \quad (4.17) \end{aligned}$$

If S_0 is real, equation (4.17) requires that:

$$\frac{\Omega^2}{9} \geq \frac{p^2 + \mu \frac{21}{16} A_0^2}{1 - \frac{16}{3\mu} \cdot \frac{\nu^2 p^2}{A_0^2}} \quad (4.18)$$

If the damping ratio is small, the lower boundary is:

$$\Omega^2 \geq 9\left(p^2 + \mu \frac{21}{16} A_0^2\right) \quad (4.18a)$$

As the frequency increases beyond the value given by (4.18a) the denominator of the equation (4.18) decreases due to the reduction of A_0 arising both from the increase in S_0 and from the rise of frequency, until a point is reached at which the equation cannot be satisfied. At this point S_0 enters the unstable region and a vertical jump downward occurs. From Fig. (4.2), for frequencies between points A and B, three solutions of the amplitude exist;

one equal to zero, the other (point N) is stable, and the remaining (point M) is unstable. Jump phenomena occur at the points A and B, both being downward.

If the frequency is outside the region $p''p'$, subharmonic motion cannot exist. Inside this region, subharmonic motion may exist at point N, if the initial conditions are favourable. If the initial conditions are unfavourable, subharmonic motion may not exist, as shown by point L.

Harmonic motions

In the case of predominantly harmonic motion, we may assume a solution of :

$$x = A \cos (\Omega t + \gamma) \quad \delta = 0$$

The steady state solution is found by the same procedure to be the same as the solution obtained by the iteration method:

$$(2\nu p \Omega)^2 A_0^2 + [(p^2 - \Omega^2) A_0 + \frac{3}{4} \mu A_0^3]^2 = H^2$$

$$\sin \gamma_0 = \frac{\pm 2\nu p \Omega A_0}{\sqrt{(2\nu p \Omega)^2 A_0^2 + [(p^2 - \Omega^2) A_0 + \frac{3}{4} \mu A_0^3]^2}}$$

.... (4.19)

The loci of vertical tangency are:

$$(2\nu p \Omega)^2 + (p^2 - \Omega^2 + \frac{3}{4} \mu A_0^2) (p^2 - \Omega^2 + \frac{9}{4} \mu A_0^2) = 0 \quad (4.20)$$

Stability of steady state solutions requires $\nu > 0$

$$(2\nu p \Omega)^2 + [(p^2 - \Omega^2) + \frac{3}{4} \mu A_0^2] [(p^2 - \Omega^2) + \frac{9}{4} \mu A_0^2] \geq 0$$

This condition requires A_0 to be lying outside the region enclosed by the loci of vertical tangency as defined by equation (4.20). Jump phenomena occur at points of vertical tangency in the same way as ultraharmonic motions.

From the above we can conclude that:

- 1) By simple approximate solutions new phenomena occur in non-linear systems.
- 2) For cubic non-linearity considered above the following conclusions can be made;
 - (a) close to linear natural frequency harmonic motion predominates
 - (b) slightly above $1/3$ of the linear natural frequency ultraharmonics of order 3 will predominate
 - (c) under suitable conditions at frequencies slightly greater than 3 times the natural frequency, subharmonics of order $1/3$ may exist.

4.3 Solution of Non-linear Vibration by Taylor's Series

Consider the equation of motion:

$$m \ddot{x} + c \dot{x} + \mu x^3 = H \cos \Omega t$$

If

$$c/m = c', \quad \mu/m = B, \quad H/m = F$$

then

$$\ddot{x} + c' \dot{x} + B x^3 = F \cos \Omega t \quad (4.21)$$

Let

$$x = a_0 + a_1 t + a_2 t^2 + \dots \quad a_n t^n$$

when

$$\begin{aligned}
 t &= 0, & x &= a_0, & \dot{x} &= a_1 \\
 x &= 2a_2 + 6a_3t + \dots & & + (n+2)(n+1)a_{n+2}t^n \dots \\
 \dot{x} &= a_1 + 2a_2t + \dots & & + (n+1)a_{n+1}t^n \dots \\
 x^3 &= a_0^3 + 3a_1a_0^2t + 3(a_0^2a_2 + a_1^2a_0)t^2 + \dots \\
 &+ 3\left\{ \sum_{j=0}^k a_j \sum_{i=j}^{n-2i-1} a_i a_{n-j-i} \right\} t^n + \dots
 \end{aligned}$$

$$\frac{n}{3} - 1 < K < \frac{n}{3} \qquad n > 3,$$

If $n = 3K$ then the coefficient of t^n is:

$$= \left\{ 3 \sum_{i=0}^{k-1} a_j \sum_{i=j}^{n-2j-1} a_i a_{n-j-i} + a^{3k} \right\},$$

k, n being both positive integers.

Substituting into equation (4.21):

$$\begin{aligned}
 &(n + 2)(n+1) a_{n+2} + C'(n+1) a_{n+1} + B(\text{coff of } t^n) \\
 &= \frac{F(-1)^{n/2} \Omega^n}{n!}, \text{ if } n \text{ is even} \\
 &0, \text{ if } n \text{ is odd.}
 \end{aligned}$$

If $n = 0$, then :

$$\begin{aligned}
 2a_2 + C'a_1 + B a_0^3 &= F \\
 a_2 &= \frac{F - C'a_1 - B a_0^3}{2}
 \end{aligned}$$

If $n = 1$, we get a_3 and so on. Therefore all the coefficients may be found in terms of F, c', B, a , and a_0 . For steady state solutions, a_1 and a_0 may be found by the equations

$$x(t) = x \left(t + \frac{2\pi}{\Omega} \right) \qquad (4.22)$$

$$\dot{x}(t) = \dot{x} \left(t + \frac{2\pi}{\Omega} \right) \qquad (4.23)$$

If the series diverges fairly quickly, numerical solutions may be possible by substituting F, c' and B. By taking sufficient terms of the series a_0 and a_1 may be found from equations (4.22) and (4.23).

Solution of Free Oscillation

If $c' = 0$ and $F = 0$, the equation becomes

$$\ddot{x} + \mu x^3 = 0$$

The period T is

$$4 \sqrt{\frac{2}{\mu a_0^2}} \int_0^1 \frac{dx}{\sqrt{1-x^4}} = 7.34 \sqrt{\frac{2}{\mu a_0^2}}$$

Frequency = $0.86 a_0 \sqrt{\mu}$

By Taylor's series

$$\begin{aligned} x_f &= a_0 \left[1 - \frac{1}{2} (a_0 t)^2 \mu + \frac{1}{8} (a_0 t)^4 \mu^2 \right. \\ &\quad - \frac{1}{80} (a_0 t)^6 \mu^3 + \frac{9}{1120} (a_0 t)^8 \mu^4 \\ &\quad \left. - \frac{1}{2688} (a_0 t)^{10} \mu^5 + \dots \right] \end{aligned}$$

if $x = a_0, \dot{x} = 0$ when $t = 0$

$$x_f = a_0 \bar{X} [(a_0 t)^2 \mu]$$

Solution of Forced Vibration (Free Oscillatory Motion)

If the forcing function is :

$$E(t) = F \bar{X}^3 [(\Omega a_0 t)^2 \mu]$$

the equation of motion becomes :

$$\ddot{x} + \mu x^3 = F \bar{X}^3 \tag{4.24}$$

then

$$x = a_0 \bar{X} [(\Omega a_0 t)^2 \mu]$$

Substituting into equation (4.24) gives:

$$(1-\Omega^2) a_o^3 \mu \bar{X}_3 = F\bar{X}^3$$

$$a_o^3 = \frac{F}{\mu(1-\Omega^2)}$$

If $\Omega < 1$, then

$$a_o = \sqrt[3]{\frac{F}{\mu(1-\Omega^2)}} \quad \text{or} \quad \Omega = \sqrt{1 - \frac{F}{\mu a_o^3}} \quad (4.25)$$

If $\Omega > 1$, then

$$a_o = \sqrt[3]{\frac{F}{\mu(\Omega^2-1)}} \quad \text{or} \quad \Omega = \sqrt{1 + \frac{F}{\mu a_o^3}} \quad (4.26)$$

Forcing frequency $\Omega_f = \Omega \times \Omega_o$

where $\Omega_o =$ natural frequency

$$\begin{aligned} \Omega_f &= 0.86 a_o \Omega \sqrt{\mu} \\ &= 0.86 a_o \sqrt{\mu \left(1 + \frac{F}{\mu a_o^3}\right)} \end{aligned}$$

In order to find the point T, from equation (4.26) we get another equation by differentiating Ω_f with respect to a_o and equating to zero:

$$2a_o = \frac{F}{\mu a_o^2} \quad \text{i.e.} \quad a_o = \sqrt[3]{\frac{F}{2\mu}}$$

$$\Omega_{FT} = 0.86 a_o \sqrt{3\mu} = 1.18 (\mu F^2)^{1/6}$$

The slope of the curve when $a_o \rightarrow \infty$ is found as

$$\begin{aligned} \left| \frac{d\Omega_f}{da_o} \right|_{a_o \rightarrow \infty} &= 0.86 \sqrt{\mu} \\ \left| \frac{da_o}{d\Omega_f} \right| &= 1.16 / \sqrt{\mu} \end{aligned}$$

The free vibration is excited if the forcing function is chosen appropriately. In this case, from the diagram the motion looks like that of the Duffings equation. Jumping occurs at the point T.

From Fig. (4.4) the x, t diagram, we find that the motion x does not vary significantly from the sinusoidal curve.

If the forcing function is not the one given above, we may calculate the amplitude approximately by considering the energy E_n of the forcing function produced during one quarter of a cycle. If that energy is equal to the energy produced by $F \bar{x}^3$ then the amplitude produced will be the same in both cases if their frequencies are equal.

$$\text{The energy produced by } F \bar{x}^3 = \int_0^1 F a_0 \bar{x}^3 d\bar{x} = \frac{F a_0}{4}$$

If the arbitrary forcing function is sinusoidal, assuming x to be sinusoidal, we find that the energy produced is:

$$\int_0^1 H a_0 \cos \Omega t d(\cos \Omega t) = \frac{H a_0}{2}$$

Equating the two energies we get $F = 2H$

4.4 Response of the Linear System

A. The Single Forcing Case

Ω_n = natural frequency

i.e. $\Omega_n^2 = K/m$

$$\text{Equation of motion: } \ddot{x} + \Omega_n^2 x = \frac{P}{m} \sin \Omega t \quad (4.27)$$

In the normal way, the general solution for all Ω except $\Omega = \Omega_n$ is as follows:

$$x = A \underbrace{\sin \Omega_n t}_{(C.F.)} + B \underbrace{\cos \Omega_n t}_{(P.I.)} + C \sin \Omega t \quad (4.28)$$

The complementary function (C.F.) included in the solution equation (4.28) describes the natural vibrations of the system and this function is important because when the force coincides with the natural frequency (i.e. $\Omega = \Omega_n$) a resonance is produced.

In considering forced vibrations, a steady-state solution is usually sought which ignores the natural vibrations. In any real system, these die away due to inherent damping and so only the Particular Integral (P.I.) part of the solution is considered.

The Particular Integral gives a response whose frequency is the same as the forcing frequency, and whose magnitude is independent of the initial conditions.

B. The Double Forcing Case

Equation of motion:

$$\ddot{x} + \Omega_n^2 x = \frac{p_1}{m} \cos \Omega_1 t + \frac{p_2}{m} \cos \Omega_2 t \quad (4.29)$$

In the normal way, we obtain the steady-state solution for all Ω except $\Omega_1 = \Omega_n$ and $\Omega_2 = \Omega_n$,

$$\text{i.e. } x = A \cos \Omega_1 t + B \cos \Omega_2 t \quad (4.30)$$

It may be seen that the solution, again, is independent of the initial conditions, and that it has components at both the forcing frequencies. Since the system is linear, the same result could be obtained by considering the system excited in turn by the two forcing functions and then adding the response obtained, using the "Super-Position Principle".

By the same Principle, a resonance will occur whenever the frequency of either of the forcing functions coincides with the natural frequency, that is when $\Omega_1 = \Omega_n$, or $\Omega_2 = \Omega_n$. This occurs in the single forcing case.

4.5 General Note on Duffings Equations

The equation of motion is :

$$\ddot{x} + \Omega_n^2 x + hx^3 = P \cos \Omega t \quad (4.31)$$

This equation is a particular case of the non-linear vibration system so far discussed. It is a standard case in the non-linear 'literature' and as such it has been studied extensively.

Solutions to the equation show that as well as having harmonics in its solution (as in the above case), it is possible to have subharmonics, (Magnus ⁽⁴⁴⁾).

The response to forcing at the resonant condition shows the well known 'jump phenomenon', Fig. (4.3).

Double Forcing

The equation of motion is

$$\ddot{x} + \Omega_n^2 x + \mu(h_1 x^2 + h_2 x^3 + \text{etc}) = P_1 \cos \Omega_1 t + P_2 \cos \Omega_2 t$$

..... (4.32)

It will again be assumed that μ is a small numerical parameter and the 'Perturbation Method' will be used, neglecting powers of x above x^3 .

Following this method:

$$\begin{aligned} x &= x_0(t) + x_1(t) \\ \Omega^2 &= \Omega_n^2 \end{aligned} \quad (4.33)$$

and substituting these into equation (4.32), while retaining terms leading to a first order approximation produces:

$$\begin{aligned} \ddot{x}_0 + \mu \ddot{x}_1 + x_0 \Omega^2 + \mu \Omega^2 x_1 + \mu (h_1 x_0^2 + h_2 x_0^3) \\ = P_1 \cos \Omega_1 t + P_2 \cos \Omega_2 t \end{aligned} \quad (4.34)$$

Generating a solution (equating powers of μ^0) gives:

$$\mu^0 :-) \quad \ddot{x} + x_0 \Omega^2 = P_1 \cos \Omega_1 t + P_2 \cos \Omega_2 t \quad (4.35)$$

and neglecting transients, produces:

$$x_0 = \frac{P_1}{(\Omega^2 - \Omega_1^2)} \cos \Omega_1 t + \frac{P_2}{(\Omega^2 - \Omega_2^2)} \cos \Omega_2 t$$

$$\therefore x_0 = Q_1 \cos \Omega_1 t + Q_2 \cos \Omega_2 t \quad (4.36)$$

First order correction (equating powers of μ^1) gives:

$\mu^1 :-)$

$$\begin{aligned} \ddot{x}_1 + \Omega^2 x_1 + h_1 x_0^2 + h_2 x_0^3 = 0 \\ \ddot{x}_1 + \Omega^2 x_1 = -h_1 x_0^2 - h_2 x_0^3 \end{aligned} \quad (4.37)$$

and substituting a generating solution produces:

$$\begin{aligned} \ddot{x}_1 + \Omega^2 x_1 = -h_1 (Q_1 \cos \Omega_1 t + Q_2 \cos \Omega_2 t)^2 \\ - h_2 (Q_1 \cos \Omega_1 t + Q_2 \cos \Omega_2 t)^3 \end{aligned} \quad (4.38)$$

Expanding the brackets and using trigonometric identities (only considering the first bracket) produces:

$$\ddot{x}_1 + \Omega^2 x_1 = \left(\frac{h_1 Q_1^2}{2} + \frac{h_2 Q_2^2}{2} \right) + \frac{h_1 Q_1^2}{2} \cos 2\Omega_1 t + \frac{h_2 Q_2^2}{2} \cos 2\Omega_2 t - h_1 Q_1 Q_2 \cos(\Omega_1 + \Omega_2)t - h_1 Q_1 Q_2 \cos(\Omega_1 - \Omega_2)t$$

+ the extra terms from the second bracket. (4.39)

And neglecting the transients produces:

$$x_1 = \frac{1}{\Omega^2} \left(\frac{h_1 Q_1^2}{2} + \frac{h_2 Q_2^2}{2} \right) + \frac{h_1 Q_1^2}{2(\Omega^2 - 4\Omega_1^2)} \cos 2\Omega_1 t + \frac{h_2 Q_2^2}{2(\Omega^2 - 4\Omega_2^2)} \cos 2\Omega_2 t - \frac{h_1 Q_1 Q_2}{(\Omega^2 - (\Omega_1 + \Omega_2)^2)} \cos(\Omega_1 + \Omega_2)t - \frac{h_1 Q_1 Q_2}{(\Omega^2 - (\Omega_1 - \Omega_2)^2)} \cos(\Omega_1 - \Omega_2)t + \text{extra terms} \quad (4.40)$$

The total solution is found by adding equations (4.36) and (4.40) i.e.

$$x = x_0 + x_1 \\ x = Q_1 \cos \Omega_1 t + Q_2 \cos \Omega_2 t + K_1 + K_2 \cos 2\Omega_1 t + K_3 \cos 2\Omega_2 t + K_4 \cos(\Omega_1 + \Omega_2)t + K_5 \cos(\Omega_1 - \Omega_2)t + \text{Extra terms} \quad (4.41)$$

The extra terms mentioned would contain $\cos 3\Omega_1 t$, $3\Omega_2$, $(\Omega_1 + 2\Omega_2)$, $(\Omega_2 - 2\Omega_1)$ etc., and in general if all the non-linear powers of x are considered, the frequencies $n\Omega_1, m\Omega_2, n\Omega_1 \pm m\Omega_2$ would be obtained where m and n are whole numbers. This fact is shown using a different analysis (recursion

equation) ⁽⁴⁴⁾).

This analysis shows that in a non-linear system under double forcing, 'combination frequencies' arise quite naturally ⁽⁵⁵⁾. It does not, however, show what the relative magnitudes of the various components of the response will be. Neither does it show what the effect would be if one of the combination frequencies happened to coincide with the natural frequency of the system or its harmonics.

Nevertheless, the difference between this analysis and the one performed for the linear case of double forcing is quite marked.

It may be concluded that if the system is excited by a single oscillator the discrepancy between the experimental and theoretical results may be due to miscalculations of all the input data.

For linear systems the damping force may not be linear, but it is practical to ignore the damping coefficient, as it is small compared with the stiffness of the spring. However, the assumption still holds that harmonic solutions can be found.

If the system is excited by two forces (i.e. the motor and an alternator) the results agree in general with the experimental observations. If the system is excited by more than one force, then both experimental and theoretical

solutions will be difficult to obtain. The difficulty in obtaining the experimental results is due to the fact that the system is unstable and varying in amplitude with time.

The effect of beating is marked if it coincides with the natural frequency of the system. If the beating frequency is a multiple of the natural frequency it can be found that the components have the same frequency as the natural frequency, even if the output has greater value. This may be explained by the fact that the natural frequency is excited by beating.

If the system has a marked non-linearity this jumping occurs when it is excited by a single vibrator and the beating effect is more significant. The structure studied had many subharmonics, ultra-harmonics, and combination frequencies, especially when it was excited by two forces.

Finally, it seems that resonance systems containing non-linear stiffness show a bend in their resonance curves. This bend is, of course, only theoretical as the vibrating system cannot "force" the frequency of the driving force.

In actual physical systems the bend therefore produces a region of instability. When the frequency response curve of such a system is measured by slowly sweeping the frequency of the driving force past resonance, certain jumps in the response amplitude occur, the frequency location of the jump being dependent both upon the magnitude of the driving force and upon the direction of the frequency sweep.

A main property of non-linear systems is that they distort the wave shape of the response signal, i.e. even if the force driving the system is purely sinusoidal, the wave-shape of the response will not be sinusoidal. Normally the response wave-shape will contain a number of frequency components harmonically related to the frequency of the driving force. This can be confirmed mathematically for instance, by approximating the solution to the non-linear differential equation by means of a series expansion, and experimentally by analyzing the response wave shape by means of an analogue frequency analyser.

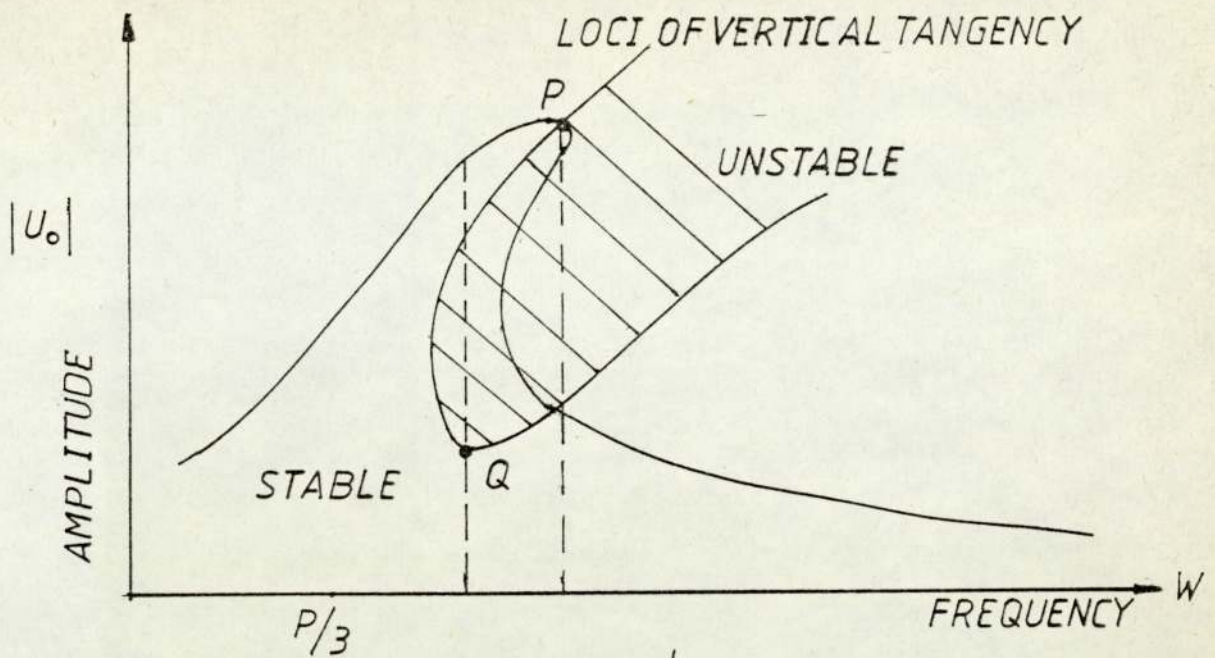


Fig. 4.1. TYPICAL AMPLITUDE / FREQUENCY RESPONSE CURVE FOR AN ULTRAHARMONIC OF ORDER 3 .

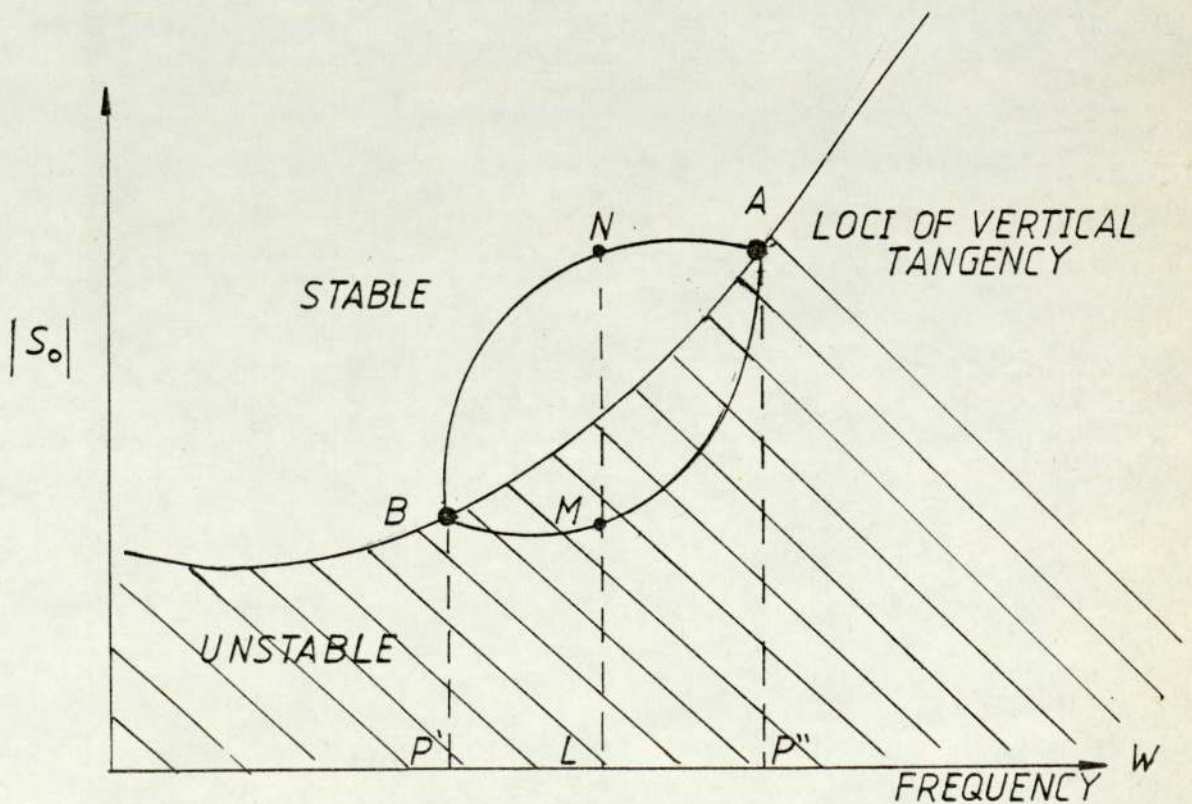


Fig. 4.2. RESPONSE CURVE INDICATING THAT THREE POSSIBLE SOLUTIONS OF THE AMPLITUDE EXIST.

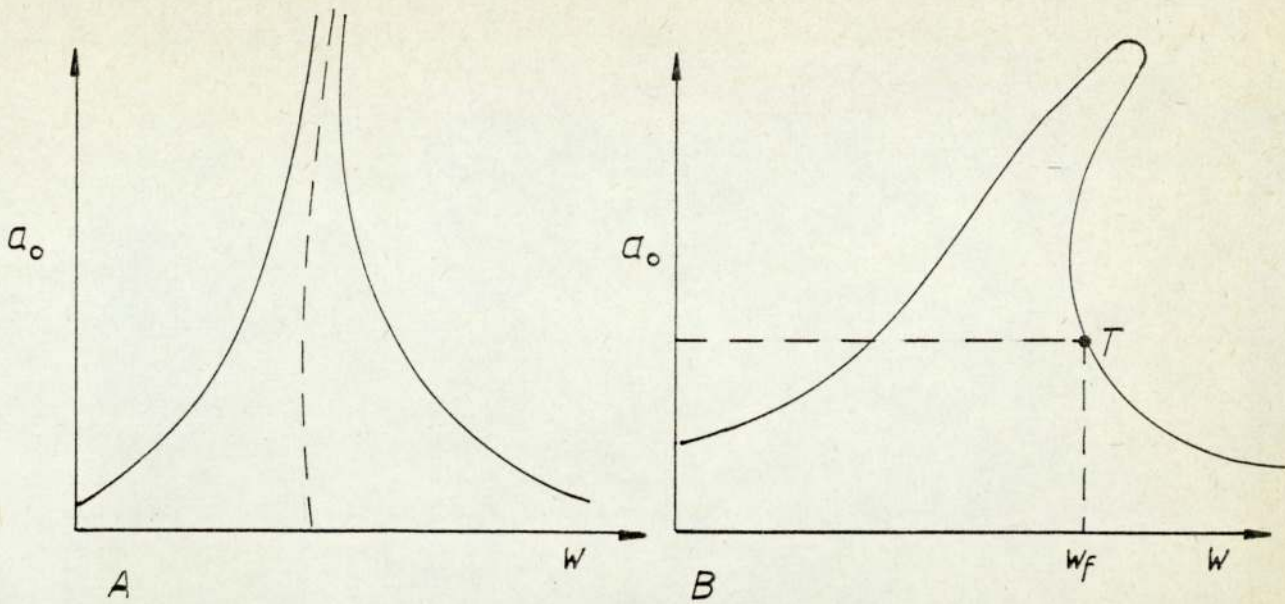


Fig. 4.3. RESPONSE CURVES FOR A SUBHARMONIC OSCILLATION.

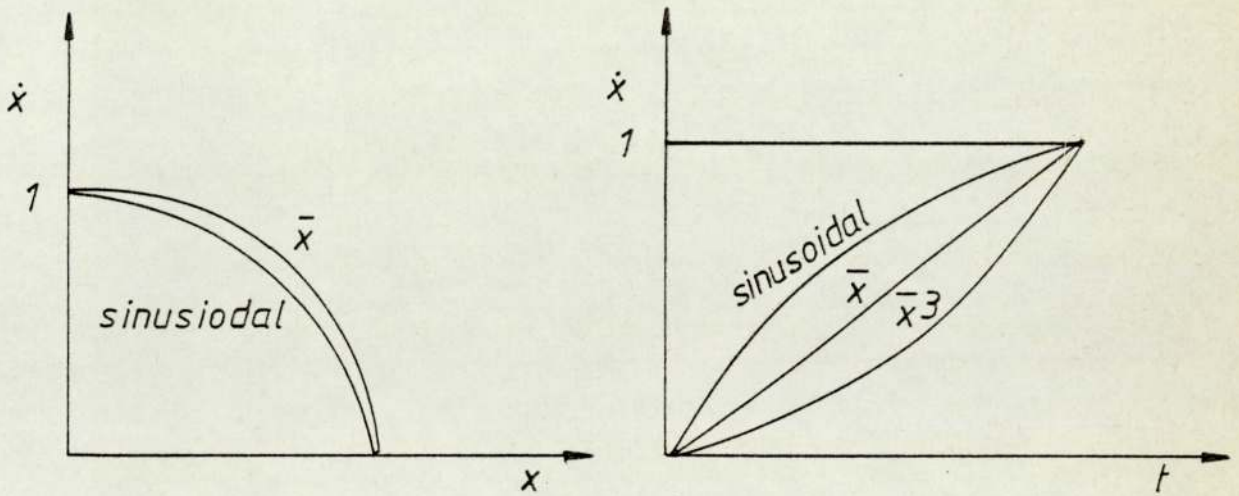


Fig. 4.4. FROM THE x, t DIAGRAM THE MOTION x DOES NOT VARY SIGNIFICANTLY FROM THE SINUSOIDAL CURVE.

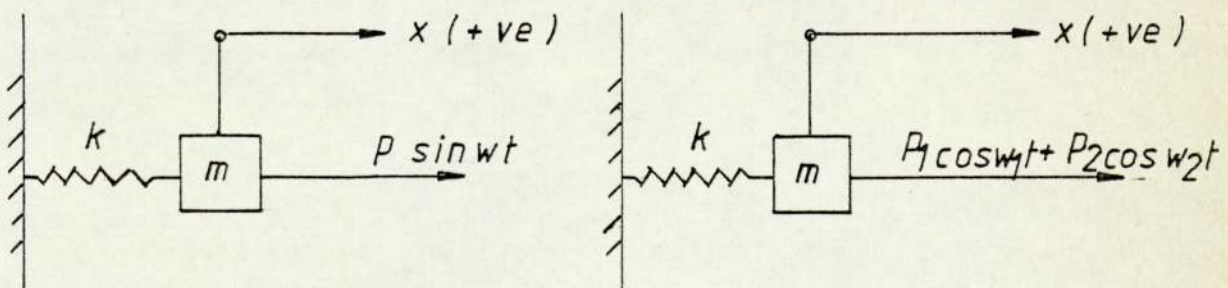


Fig. 4.5. THE SINGLE AND DOUBLE FORCING CASE

CHAPTER 5

Experimental Technique

5.1 Introduction

Both static and dynamic experimentations were involved in this work. But the main one was the dynamic experimentation where the vibration characteristics were measured when the structure was excited by either a single force (the vibrator excitation) or two exciting forces, that is, when the unit was running at different speed ratios.

The relevant static experiments were concerned with measuring the spring behaviour, also the measurement and verification of the structure stiffness matrix used in the analytical work. The static experiments were restricted to simple measurements in force displacement experiments. The requirement included a suitable arrangement for applying the load at a point of the structure and some dial gauges for measuring the corresponding displacement at various points of the structure. Average values of the force per unit displacement at the various points could then be calculated together with the equivalent stiffness coefficient.

The dynamic experimentation was more involved. Basically, what was required was the means of setting the structure under forced vibration and measuring the response at various points. When the forcing frequency coincided with the natural frequency of vibration of the structure resonance occurred when the forcing frequency was a single force. In the case of double forcing, the occurrence of a beat

frequency was predominant. Such periodic pulsation in vibration amplitude is generally due to simultaneous generation of two base frequency excitations. These give an apparent vibration signal in the mean frequency and a pulsation amplitude at the difference frequency.

By passing the measuring transducer round the various points of the structure, the pick resonances at these points can be obtained to produce the modal shape of vibration of the structure at that natural frequency.

For a complicated structure the measurement of the resonant frequencies and the corresponding modal shapes is not an easy task. An arbitrary choice of the point of excitation could lead to difficulties in producing the resonance at certain natural frequencies of the structure. For example, exciting the structure at a nodal point, (i.e. a point of zero amplitude of vibration) of a certain natural frequency would result in missing out the resonance at that natural frequency. In particular, it is very useful to excite the structure at the point of maximum amplitude of vibration of a given modal natural frequency. Hence, it is customary to change the point of excitation of a structure to obtain the different modes of vibration.

Each beam member of a frame structure is actually a continuum. As such, measurement of its amplitudes of vibration have to be made at many closed points in order to produce a true form of the modal shape. In the theoretical analysis, both linear and angular displacements can be

calculated. But experimental measurements are restricted to linear displacement only. This was an added difficulty in the experimentation.

5.2 Vibration Instrumentation

Modern vibration data analysis equipment was used in order to investigate the rig and its vibration characteristics. An extensive investigation was carried out into instrumentation, the techniques of frequency analysis, and method of excitation position.

The Equipment

The equipment used was:

- | | |
|------------------------------------|---------------------------------------|
| 1. Accelerometer | Brüel and Kjaer
Type No. 4333 |
| 2. Vibration meter | Model D.V.A. |
| 3. Voltmeters | B & K Random Noise
Voltmeter VM 78 |
| 4. Oscilloscope | Télémechanique D33R |
| 5. Vibrator | Detriton VP5 |
| 6. Dynamic Analyser | S.D. 101-A |
| 7. Sweep Oscillator | S.D. 104-1 |
| 8. Tracking Filter | Spectral Dynamics Corporation |
| 9. Fiberoptic Tachometer
System | Model SD43 GPT |
| 10. Spectroscope R.T.A. | S.D. 335 |
| 11. Frequency Counter | Advance Type Tc 2A |
| 12. Tunable Band Pass Filter | Type B & K 1621 |

The following block diagrams show the instruments used:

1. Spectral Dynamic S.D. 1001-2A system (Fig.5.1)
2. Spectral Dynamic Tracking Filter Facilities (Fig.5.2)
3. Vibration meter model D.V.A. (Fig.5.3)
4. Concept of operation for Tachometer (Fig.5.4)
5. Fiberoptic T.M. System (Fig.5.5)
6. Set up for Spectrascope/oscilloscope/plotter (Fig.5.6)
7. Simplified block diagram spectrascope II (Fig.5.7)
8. Data classification (Fig.5.8)

Block diagrams of the vibration instrumentation used in this work are shown in Figs. (5.1) to (5.8).

The accelerometer picked up the various response points on the structure. It should be noted that the accelerometer was an acceleration measuring transducer, not a displacement transducer as the vibration response was supposed to be measured. However, it was known that the amplitude of vibration is proportional to the pick value of the corresponding acceleration at that point, and acceleration transducers are more convenient than displacement transducers. Moreover, the modal shape of vibration required represents the relative shape of oscillation of the structure and not the absolute magnitude of its amplitude of vibration. Thus the use of the accelerometer met all the requirements to give the results expected from the experiment. By passing the signal through an integrator and by double integration in

the D.V.A., the output gave the displacement.

The sweep oscillator was the basic input instrument, while the accelerometer was the basic output instrument. The sweep oscillator is basically a wave signal generator. For the purpose of this work on vibration analysis, (as vibration excitation by one force only) the sweep oscillator was used to generate sine wave signals at any required frequency.

The frequency was either set at a fixed value or varied (swept) automatically or manually between any set frequency limits.

The signal from the signal generator was a weak one, and the power amplifier amplified it to a reasonable level as required by the vibrator. The vibrator then applied the amplified signal to the structure in the form of an oscillatory force to set the structure vibrating at a reasonable level.

Again, the response signal picked up by the accelerometer was amplified by the charge amplifier (D.V.A.) and double integrated. Owing to some degree of non-linearity in the structure and/or other external interference, the response signal obtained could be anything except a pure sine wave. The dynamic analyser received this impure sine signal and essentially acted as an inherently frequency-tuned bandpass filter.

The impure sine signal represented the signal input to the analyzer while the original signal from the sweep oscillator was fed in as the tuning frequency input. Output from the analyzer was represented by the filtered output signal which was a pure sine signal at the tuning frequency.

The valve voltmeter measured the R.M.S. value of the signal whose values for various points on the structure provided the modal shape of vibration of the structure at a particular frequency. The X-Y recorder could also be used to plot a graph of the response over a frequency range in the form of response (on the Y-axis) vs frequency (on the X-axis). The sweep oscillator provided the frequency input to the plotter on a D.C. scale proportional to log frequency or linear frequency. Points of relatively high response on the plot constituted possible resonance (or natural) frequencies of vibration of the structure.

The C.R.O. (Cathode Ray Oscilloscope) gave a more immediate view of the response. In addition, a comparison of the response signal and the original signal from the oscillator gave an instant relative phase shift of the response signals on the C.R.O. In fact, the in-phase and out-of-phase positions of the two signals have been used to designate positive and negative signs respectively to the response of the structure at any particular point.

A phase meter could have been used for the above purpose but this was considered to be too sophisticated and

unnecessary for this simple case of in and out phase measurement.

A frequency counter is usually connected to the instrumentation to give a more reliable reading of the frequency of the signal generated by the oscillator. The frequency counter was also used to check the actual frequency of the output signal from the analyzer. Both frequencies should have read the same.

5.3 Experimental Frequencies and Modes

In the experimental vibration work on the flexible platform, the basic node system used in the theoretical finite element analysis was followed.

The structure was vibrated at a convenient point and the response was measured at different points in the platform.

The experimentally measured natural frequencies and corresponding nodal responses for the first three modes are shown in Figs. (5.9), (5.10) and (5.11). The rotational displacements are not considered in the model measurement. A direct comparison may be made between the listed values of the responses Fig. (5.13).

The responses may be compared with each other from various points on the same mode. This is because the absolute value of these responses depends on the magnitude and the point of application of the exciting force. To obtain the

best results, a structure should be excited at a point of maximum possible vibration response.

In the first place, the magnitude of the exciting force was kept constant during the response measurement only for individual mode experimentations. The point of excitation was fixed for all the mode measurements. Plots of the theoretical modes of vibration and the corresponding plots of the experimental modes are shown in Figs.(5.9) to (5.12). Fig.(5.13) indicates the measured values for the four mode shapes. In all these cases, the theoretical and experimental modal shapes are similar.

Generally, the correlation between computed and experimental natural frequencies is very good. Figs.(5.14) and (5.15) show pictorial representation of patches of displaced surface covered by motor and Alternator bases for plates modes.

Fig. B shows a view of the rig excited by the vibrator.

The frequency of oscillation of the rig was increased until it reached the first mode, then the vibrator was held at this frequency whilst the 'mode shape' was monitored using the two accelerometers. One accelerometer was kept in its 'reference' position on the frame while the other was moved around the frame registering positive or negative readings (phase or anti-phase) with respect to the reference, initially moving the accelerometer 200 mm at a time. Then the procedure was repeated to obtain more accurate results

by only moving 100 mm at a time. This gave a number of point readings on the frame which could be translated into a picture of the modal shape. This same procedure was then carried out for the second and third modes.

For the plate modes, or to find the 'flexural', special arrangements were made. The frame with the motor and alternator in position was suspended by 'elastics' which were flexible enough to ensure that the 'rigid body' frequencies were far enough away from the 'plate' frequencies to have little effect. The vibrator was used to force the system, and the two accelerometers were used to measure the response. Higher modes were not tested because they were found to be well outside the frequency range of the motor's maximum speed, and hence would not show up in the response tests. It is worth noting here that the vibrator was then set in a different position (which had the smallest stiffness) to check if this altered the results. It made very little difference.

5.4 Response Analysis

Free vibration analysis can be used to give an estimate of the distribution of peaks in the displacement as the frequency of excitation is varied. However, it is generally very difficult to predict the relative importance of the different natural frequencies. A better estimate of this can be found by using a method which calculates the response of the structure. Since the main excitation of the rig arises from shaft eccentricity and from other forces which

vary as the shaft rotates, the special case of sinusoidal excitation may be considered.

If the structure is subjected to a set of sinusoidal forces $p e^{i\omega t}$ varying at a frequency ω , then we have

$$M\ddot{u} + C\dot{u} + Ku = p e^{i\omega t} \quad (5.1)$$

where M , C and K are the mass, damping and stiffness matrices and u , \dot{u} and \ddot{u} give respectively the displacements, velocities and accelerations at the nodes. The mass and stiffness matrices are the same as used in the forced vibration case. Since the structure is of steel, the structural damping may be expected to be very low. However, in the present analysis, it may be represented by a damping matrix proportional to the stiffness matrix.

For the steady state response of the structure

$$u = u^* e^{i\omega t} \quad (5.2)$$

where

u^* gives the amplitude and phase of the displacements.

Substituting equation (5.2) into equation (5.1), we have

$$(-\omega^2 M + i\omega C + K) u^* = p \quad (5.3)$$

This set of complex simultaneous equations may be solved to give the complex vector u^* , the components of which represent in amplitude and phase, the steady state displacement at the node. The forcing function chosen, P , may be determined by shaft eccentricity, and, thus, it will vary as the square of the shaft frequency. It may also be expected to vary with different operating conditions, which may also change appreciably during the lifetime of a machine.

In order that the response to a large number of sets of forces can be obtained, equation (5.3) may be solved with p as a unit force, applied in turn to each of the m nodes at which excitation is expected. By using Gaussian elimination, and replacing p by P in equation (5.3) where

$$P = (p_1, p_2, p_3 \dots p_m) \quad (5.4)$$

with p_i the i^{th} unit vector, the response U^* is obtained

$$U^* = (u_1^*, u_2^*, u_3^* \dots u_m^*) \quad (5.5)$$

where u_i^* is the response to p_i .

Any set of forces can be expressed as

$$P = \sum_{i=1}^m \alpha_i P_i$$

where the coefficients α_i are complex constants, each respectively giving the magnitude and relative phase of the i^{th} component. Thus the response u is given by

$$u = \sum_{i=1}^m \alpha_i U_i^*$$

Coefficients for the damping and stiffness of the bearings can be estimated and these additional terms can be added to the overall matrices.

In the idealisation used for the response analysis, the complete structure must be considered if the response has contributions from both symmetric and anti-symmetric modes.

Fig.(5.16) shows measured amplitude vibrations at point 1 as the frequency of excitation increases from 0 to 50 Hz.

The amount of out-of-balance that may be used is as suggested in German standard DIN 4042. The damping and

eccentricity are assumed not to vary with frequency and the structural damping is presented by having the damping matrix C proportional to the stiffness matrix K with a constant of proportionality 0.0002; for these results, the stiffness and damping of the bearings have been neglected.

At the higher frequencies, there will be contributions to the response from excitation of 50 Hz caused by auxiliary equipment, the characteristics of the structure and its springs. The analysis can clearly be extended to include the effect of these additional forces but no allowance has been made for this in the results presented here.

From the results outlined above, a method was presented for checking designs of flexible platforms by means of free vibration and response analysis programmes.

If a particular mode of vibration gives unacceptable amplitudes, the free vibration analysis can be used to estimate the effect of a structural modification of the resonance. In this way, any proposed alteration can be checked.

The response analysis provides, at the design stage, an estimate of the level of vibration that can be expected from the rotating machinery (for a given shaft eccentricity, and known out of balance).

5.5 Response Curves:

To measure the response curves it was important to have

a narrow band width filter. The filter used was a tunable pass frequency with frequency range 0.2 Hz to 20 Hz in 5 sub-ranges and the selected band with 3% (1/3 oct.)

The vibration meter was calibrated as was all the equipment used and adjusted to measure the displacement.

The signal from the vibration meter was fed to the Spectral Dynamic input. It was possible to use the output from the spectral Dynamic as values to draw the response curves. The output was also connected to the voltmeter for check.

The vibration frequency of the structure was increased from 1 to 50 Hz in steps of 1 Hz.

The above procedure was used for the response curves when the structure was excited by the vibrator.

In the case of response curves with the units running at different speed ratios, (such as with two exciting forces), it was necessary to know the exact motor speed ratio. This was estimated by using the Fiberoptic Tachometer system and the vibration counter. The Fiberoptic Tachometer system was used to detect the reflected light from the motor pulley which was divided radially into ten equal sections, with a piece of 5mm x 5mm reflective tape attached to the circumference of each section. This was arranged in such a way that the sensor could not detect more than one piece of the tape at any one time. A case of one of the response curves for the structure excited by the vibrator is shown in Fig. (5.16).

The response curves at different speeds are shown in Figs. (5.17) to (5.36) for the response curve drawn with Bruel & Kjaer narrow band width filter.

These speed ratios are Case 1 7:5
Case 2 5:3
Case 3 3:1
Case 4 5:2

Case 5 just the motor running without the alternator.

The fibre optic tachometer system was verified by the frequency counter.

5.5.1 Response curve in the case of vibrator excitation

The most important modes in this curve are the three rigid body modes and the plate mode, although there are many other modes. The modes may be classified as the classical approach, Longitudinal, Transverse, Vertical, Yawing, Pitching, Rolling, the first plate mode and other unexpected modes. The main reason for these modes may be the secondary effect and the non-linearity in the spring which gives rise to the coupling between the modes.

Another reason may be the effect of the non-linearity in the damping coefficient.

In the system used, the instability of one degree of freedom at rest is due to periodic fluctuations in the spring rate resulting from the oscillation of another degree of freedom; this almost happened in the case of the vibration isolation system with directly coupled coulomb damping ⁽⁴¹⁾.

The parallel combination of coulomb damper and a spring, which is known as Coulomb-Hook model, was used to represent the non-linear dynamic elasticity of vibrating mechanical systems with dry friction damping.

The damping force in these mechanisms, which is of constant magnitude, acts in phase with the relative velocity across the damping element but is independent of its magnitude. For certain magnitudes of the coulomb damping force it is possible for infinite resonance to exist. However, Den Hartog ⁽⁷⁶⁾ places the emphasis on the values of the damping force that results in finite responses at resonance.

Also it may be easy to conclude that the coulomb damping which was used was a non-linear-damping phenomenon, since discontinuities existed in the damping force time history when changes in direction of relative velocity occurred. This resulted in a non-linear equation of motion. The coulomb damping force F_f is of constant magnitude and is independent of the displacement.

In a physical sense, coulomb damping is obtainable from the relative motion of two surfaces arranged to slide against each other with a constant normal force F_N , such that $F_f = \mu F_N$ where the coefficient of friction between the two surfaces μ is a function primarily of the nature of the surfaces sliding on each other. The energy D_o dissipated per cycle by a coulomb damper experiencing a harmonic relative displacement $z = z \sin \Omega t$, is independent of the frequency of vibration, but depends on the vibration amplitude. The hysteresis loop is rectangular

having major and minor semi axes of F_f and z_o .

In very low damping conditions (under certain circumstances) the phenomenon of non-linear resonance systems occurs. This is the phenomenon of 'subharmonics'. A subharmonic is a response vibration occurring at $1/2$, $1/3$, $1/4$, $1/5$ etc. of the frequency of the driving force. The physical explanation for the occurrence of subharmonics which may be given is that the driving force supplies energy to one of the harmonics of the non-linear system and when energy is supplied it will start to oscillate. The higher harmonic then pulls all the other harmonics with it, as the specifically excited harmonic is an integral part of the whole motion. There are instances where a non-linear spring element in a multi-degree of freedom system produces a third harmonic of the order 1%.

If the frequency of this harmonic by chance coincides with the resonant frequency of another resonance in the system which happens to have a resonance amplification factor $Q = 100$, this specific resonance will respond with the same amplitude as the actually excited resonance, even though its frequency did not exist in the wave-shape of the driving force ⁽¹⁰⁰⁾.

5.5.2 Response curve with Fixed Frequency filter.

For every speed ratio the filter was fixed at one of the main frequencies, 4.3, 8.2, 9.1, 37.4 Hz in total there are 20 curves. These are shown in Figs. (5.17) to (5.36).

By fixing the frequency filter at 4.3 Hz, which is the first natural frequency, it is possible to find the main frequency and the higher components of it. In fact every mode in this curve is a 4.3 mode even though the motor speed is different. (In other words, frequency component harmonically related).

In such a system, because of its low damping condition, it is possible that the phenomenon of a non-linear resonance system may occur.

It is also possible that the rigid body modes can be excited by the motor speed or by $\frac{1}{2}$ the motor speed, or the 2nd Rigid body mode can be excited by twice the beat frequency.

The 1st Rigid body mode can also be excited by the beat frequency.

Finally, the response wave-shape will contain a number of frequency components harmonically related to the frequency of the driving force.

5.5.3 Response curves by computer

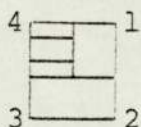
The modern high speed computer should be taken into account when investigating this point. The response curves are in the following order. Four speed ratio settings were measured. They are

- | | | |
|------------|---|-----|
| Case 1 | : | 7:5 |
| Case 2 | : | 5:3 |
| Case 3 | : | 3:1 |
| and Case 4 | : | 5:2 |

Every speed setting follows the same pattern.

1 - Starting the motor to maximum speed	(1,0,0,0)
2 - Shutting down the motor to zero speed	(1,0,0,0)
3 - Motor at maximum speed 50 Hz	(1,2,3,4)
4 - " " 35 Hz	(1,2,3,4)
5 - " " 25 Hz	(1,2,3,4)
6 - " " 15 Hz	(1,2,3,4)
7 - " " 8.2 Hz	(1,2,3,4)

(1,2,3,4) means the position of the measuring points from the corners. The pick-up signal was considered as in the drawing.



For example (1;3;3) denotes

1. Speed setting 7:5
3. Motor speed at maximum speed 50 Hz.
3. pick-up signal position 3

the following cases 1;1;1; & 1;2;1; & 1;3;1 & 1.4.1
1,5,1 & 2,4,4 and 2;4;2

are shown in figs. (5.37) to (5.43).

From the above procedure, for every pick-up position, a response curve and a wave form were drawn by the computer.

This made for each speed setting a total of 44 curves, and a number of these curves will be in the Appendix.

The high speed computer makes it possible not only to reduce the processing time, but also to increase the accuracy of the processing. From this mass of data and curves, it may be concluded that in the general case where there is a single degree of freedom system with non-linear spring characteristics and excited by two harmonic forces only, the equation of motion is given by

$$\ddot{x} + f(x) = P_1 \cos(\Omega_1 t + \alpha_1) + P_2 \cos(\Omega_2 t + \alpha_2)$$

where $f(x)$ represents the spring force and may be written in the form of a Taylor series thus:

$$f(x) = a_1 x + a_2 x^2 + a_3 x^3 + \dots$$

The constant term a_0 is eliminated by a suitable choice of origin.

Magnus ⁽⁴⁴⁾ (1965) ~~discussed~~ discussed the solution of this equation and shows that in the general case the solution will contain the frequencies $n\Omega_1$, $m\Omega_2$, $n\Omega_1 \pm m\Omega_2$ (where n and m are whole numbers). He also showed that an oscillator with a cubic restoring force and harmonic excitation will, under certain circumstances, perform harmonic oscillations whose frequency is one third of the exciting frequency.

So it may be concluded that a relatively small non-linear effect can result in vibrations not directly related frequency-wise to primary exciting forces. This may be one reason why the vibration characteristics of the flexible

platform show displacement responses at practically all the harmonics of rotational speed up to 2 or 3 or 4 times the passage frequency. This often occurs with significantly high, 2nd, 3rd and 4th, harmonics of rotational speed.

It seems that, using the accelerometer to pick up the signals, the effects due to acoustical excitation were unavoidable.

The accelerometer's main application was general vibration measurements and it was found that the response was obscured by 'noise' (probably from the motor and alternator bearings in such electrical machines).

This signal was put through an integrator to cut this down, double integration (in the D.V.A.) was used, which means that the output from the integrator is the displacement after being amplified, and then taken to the computer to give the response curve.

Unfortunately, the vibration meter (D.V.A.) was a high quality measuring instrument, and used 17 linear integrated circuits to ensure reliability and accuracy. But for the low frequencies, unexpected peaks came into view with some amplification factors. The accelerometers were connected to the frame by permanent magnets to allow for the possibility of removing them when necessary. The accelerometer cable was firmly clamped to the frame in order to avoid any micro-phonetic noise. This had a disturbing effect at the lower frequencies, due to local capacity and charge changes, owing to dynamic bending, or compression and tension of the cable when not clamped.

The physical model can be expressed as

$$\begin{aligned}
 [M] &= [\phi]^{-T} [m] [\phi]^{-1} && \text{"Physical Mass" (A)} \\
 [K] &= [\phi]^{-T} [\Omega^2 m] [\phi]^{-1} && \text{"Physical stiffness" (B)} \\
 [C] &= [\phi]^{-T} [2\zeta \Omega m] [\phi]^{-1} && \text{"Physical Damping" . (C)}
 \end{aligned}$$

with $[\phi]$ $[m]$ Ω_j and z_j terms being the known modal information. Experience and commonsense have indicated the desirability of selecting the location that ensures that a reasonable idea of the nature of the response curves could have been inferred from the test measurement. In practice, this meant selecting locations on each side of the modal boundaries.

There is, in general, a choice of selections. This in turn means that unique solutions to equations (A) through (C) do not exist, whichever test measurement locations are selected. The set of the three matrices will define a model whose responses match resonance data from the selected location.

It may be that this last statement looks too simple, but in point of fact it is not at all. The reason for this is the non-linearity of the damping coefficient, and the stiffness coefficient of the springs which play an important part in the vibration characteristics of any structure and give rise to many new phenomena in the non-linear resonance system.

In a linear multi-degree of freedom system, the classical vibration theory would indicate that the response may be

defined exactly for vibration characteristics (resonant and non-resonant excitation) in terms of its mass, damping and spring characteristics.

When more than one force is applied to the system the resultant vibration can be obtained by applying the principle of superposition - which means that the resultant is the sum of the individual vibrations excited by each force acting alone.

Unfortunately, complications arise when non-linearities occur in the dynamic system. When a number of exciting forces act at different frequencies on a non-linear system, the system vibrates at frequencies equal to the exciting frequencies as in the linear case, but also at frequencies which may be multiples or submultiples of the frequencies or the difference between any two (101) .

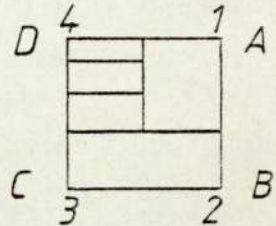
5.6 The Use of the Spectroscope (Real Time Analyser)

By using the spectroscope real time analyser, after calibration and using a harmonic cursor, we can locate the specific spectral components. When it comes to spectral description, a periodic signal may well be described in terms of the R.M.S. values of its various frequency components (its frequency spectrum), while random vibration signals are best described in terms of mean square spectral density functions. This is due to the fact that random signals produce continuous frequency spectra and R.M.S. values are measured within a certain frequency band width, and will therefore depend upon the width of the band. A calibrated signal comes from the vibration meter connected to the input

of the calibrated spectroscope (R.T.A.). And this picture has been taken for the spectrum information after it has been stored in the memory.

5 different cases were studied, each having 4 Polaroid pictures taken, making a total of 20 pictures.

A shows position 1 on the rig
B shows position 2 on the rig
C shows position 3 on the rig
D shows position 4 on the rig.



Case 1 as shown in Fig.(5.44) A,B,C, and D.

Speed ratio = 7:5. The relationship between the modes and their spectral components are presented in Table (5.1).

Case 2 as shown in Fig.(5.45) A,B, C and D.

Speed ratio = 5:3. See Table (5.2)

Case 3 as shown in Fig.(5.46) A,B,C and D.

Speed ratio = 3:1. See Table (5.3)

Case 4 as shown in Fig.(5.47) A,B,C and D.

Speed ration = 5:2. See Table (5.4)

Case 5 as shown in Fig.(5.48) A,B,C and D.

Just the motor running at maximum speed. See Table (5.5).

In all these cases the motor was running at its maximum speed, approximately 50 Hz.

A quantitative comparison was however very difficult because the relative magnitude of various frequency peaks went up and down.

This feature was masked, especially when the Real Time Analyser (spectroscope), and the spectrum information from all 500 filter locations were used.

The way to make this comparison was simply to keep the sampled spectrum information for all 500 filter locations after being converted into digital form. This digital information was processed for averaging or peak hold, and stored into averaging memory. By using the 'peak' hold button and storing this information, it could be recalled to make a comparison between the peaks in the spectrum information, by using the harmonic cursor for locating the specific spectral components.

From Table (5.6), it is clear that the modes of vibration of the structure have a variety of variables. This may look slightly ambiguous. It seems that the non-linearity in the springs supporting the structure gave rise to many resonances subharmonic, ultraharmonic, subultraharmonic, internal or even non-periodic combination resonance. There were also combination resonances as well as the main resonance.

In the case of structural dynamic analysis, the main factor governing these analyses is the assumption of the orthogonality of the modes with respect to the mass, stiffness and damping terms and the form of the exciting forces.

Table (5.6) classifies the types of resonance which can be expected in such a structure.

The internal resonance, non-periodic combination resonance and periodic combination resonance, are just the

resonances which distinguish systems with several degrees of freedom from those having a single degree of freedom.

Internal resonance represents a special case, where the main resonance coincides with the subharmonic, ultraharmonic or subultraharmonic resonance. The periodic combination resonance is again a special case, where the combination resonance coincides with the aforesaid resonances (Yamamoto⁽⁹⁵⁾, Hayashi⁽⁹⁶⁾, Benz⁽⁹⁷⁾).

5.7 Beat frequency in rotating machinery

It is fairly straightforward to explain the occasional occurrence of a "beat frequency" vibration signal from rotating machinery⁽⁵⁵⁾. Such a periodic pulsation in vibration amplitude is generally due to the simultaneous generation of two base frequency excitations (Ω_1) and (Ω_2). These give an apparent vibration signal in the mean frequency $(\Omega_1 + \Omega_2)/2$, and a pulsation in amplitude at the difference frequency $(\Omega_2 - \Omega_1)$.

One of the base frequencies is usually synchronous with rotor speed (i.e. attributable to rotor unbalance) and the second might be associated with one of a number of other vibration sources - unbalance of another shaft rotating at a different speed; rotor whipping, or journal bearing instability, or hysteretic whirl ... etc.

K. Magnus⁽⁴⁴⁾ was the first to indicate theoretically that where two frequencies are generated, the sum and difference frequencies are also possible.

Downham (101) indicated that when a number of exciting forces act at different frequencies on a non-linear system the system vibrates at frequency equal to the exciting frequencies as in the lineal case, but also at frequencies which may be multiples or submultiples of the frequencies or the difference between any two.

A spectral analysis of the wave form from the running unit showed that a synchronous vibration signal was indeed present and also a synchronous component associated with vibration due to unbalance.

But there are also large, unexpected components of a low frequency at a frequency equal to the difference between the two base frequencies.

It seems reasonable to conclude that the source of sum and difference frequency components was truncation of the "BEAT FREQUENCY" wave-form. It is clear from the response curve that it contains not only the two base excitation frequencies but also a component at the difference frequency.

In other words, the frequency components in truncated beat frequency wave form. The principal of centre frequencies and harmonic zone number and side band frequencies left and side band frequency right.

The vibration displayed the tendencies shown in Table (5.7).

Fourier analysis of the excitation wave form indicates that components at difference frequencies are indeed generated

The measurements for the rig were carried out. The frame was supported by four knife edges, one in each corner.

Five dial gauges were used and were zero adjusted before the reading. The applied load was varied between 40.028 and 336.41 Kp.

Fig. (5.49) shows one case in which the applied load was 218.499 Kp. applied at point 1. This case was for decreasing the load from maximum to minimum.

The graph Fig. (5.50) indicates the load deflection relation for the frame structure. The dial gauges were positioned as in Fig. (5.49) under the rig. Then the load was applied at point 1 and readings were taken for the five dial gauges. Table (5.9) shows the data when the load was increased and decreased.

In actual fact it was found that the frame deflected slightly under the load. This means that the readings on the five gauges differed considerably.

The load was applied in the downward direction while the spring balance was in the opposite direction. Also the load had to be increased fairly quickly. In this sense the term 'static reflection' is misleading, but it was used in order to distinguish the stiffness obtained from the 'dynamic stiffness' used in vibration work.

It should be noted that the graph would form a continuous loop known as an 'hysteresis loop', if the loading had itself been continuous.

5.9 Measuring the spring stiffness

It was possible to measure (K) the spring stiffness by adding weights to the machine and measuring the corresponding deflection, particularly if the springs were concentrated between the machine and the floor which was the case in the unit under consideration. Since the object of installing flexible mounting units was to place all significant resonance below the operating speed range, it was desirable that the mounting arrangement should be soft for the modes of vibration which were likely to be strongly excited, and the limitation of this procedure was only the stability of the structure as a whole which had to be carefully considered. By making the isolator very soft, resonance speed will occur at a very low motor speed, and could therefore be passed through so quickly that the small increase in movement due to resonance was hardly noticeable. The benefits obtainable with a spring supported structure were so great, both physically and economically, that slight oscillation, hardly exceeding a few hundredths of an inch, was immaterial. These operating amplitudes were negligible and the amplitudes varied from the time the machinery started, passed through resonance, and attained operating speed.

This measurement was attempted; however, owing to the unexpected behaviour of the readings of the dial gauges corresponding to the spring deflection, it was not easy to carry out the experiment. Thus it was decided to measure the behaviour of one spring only. So one of the springs was removed from beneath the rig and the following measurements were carried out.

Four tests were carried out to estimate the load deflection curves. Case 1 Vertical stiffness, Case 2 Longitudinal stiffness, Case 3 Measuring the total deflection between the first and second coil 180° from the end of the coil, Case 4 as Case 3 except decreasing the load.

Case 1. Measuring the Vertical stiffness

In order to determine the static deflection applied loads were varied from 22.4 to 448 lbf. Table (5.10) shows the applied load and the affected deflection. Dial gauges were used to measure the displacement. The results are shown in Fig. (5.51).

Case 2. Measuring the Longitudinal stiffness

Special arrangements were necessary to measure this stiffness. The four springs were in their position carrying the structure. The load was applied by pulling the frame in the load direction and two dial gauges were used at 200 mm either side of the pulling point. The pulling point had a hook which was connected to steel wire across a small pulley which lay horizontally and the wire was then connected to another hook. The load was applied vertically on a base connected by a lever to this second hook. The two dial gauges were adjusted to zero. The load was applied, varying between 30 and 140 lbf. Fig. (5.52) shows the load deflection relation and Table (5.11) shows the applied load and deflection.

Case 3. Measuring the total deflection - Increasing load

Measurement of the total deflection between the first and

second coils was taken 180° from the end of the coil as shown by distance A in Fig. (5.53). The total deflection equals distance δ . The applied load was varied between 28.92 and 254.3 lbf. Table (5.12) shows the applied load and deflection.

Case 4 Measuring the total deflection - decreasing load

This test was the same as the previous one except that the load varied from 254.48 to 28.92 lbf. Fig. (5.54) shows the load deflection curve, and also the load deflection from the first and second coils, distance A, 180° from the end of the coil. Table (5.13) shows the applied load and deflection. Fig. C. shows a view of the rig with the equipment to measure the sideways stiffness of the spring.

DC \propto FREQ for filter switching

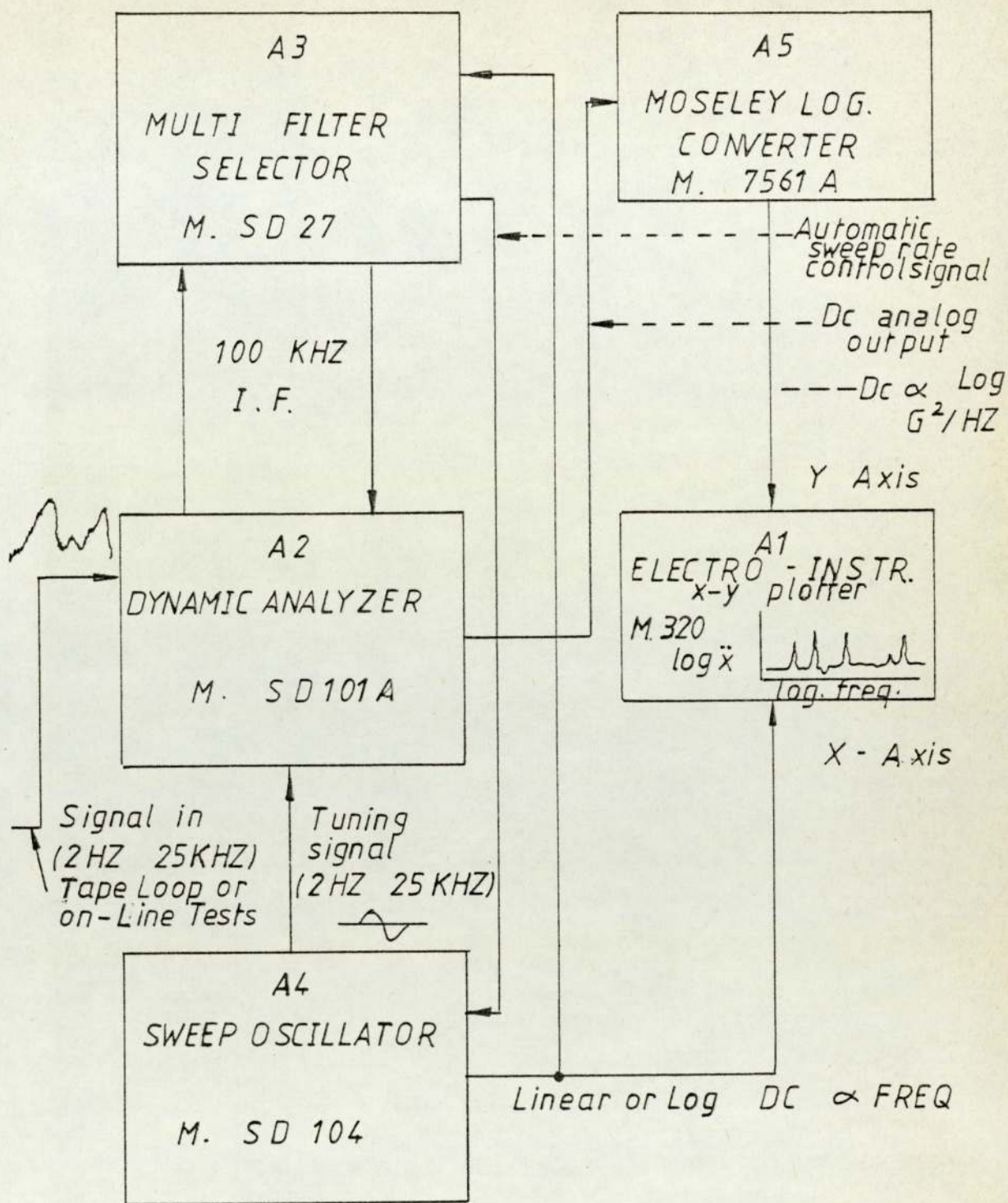


FIG. 5.1. SPECTRAL DYNAMICS SD 1001 - 2 A SYSTEM

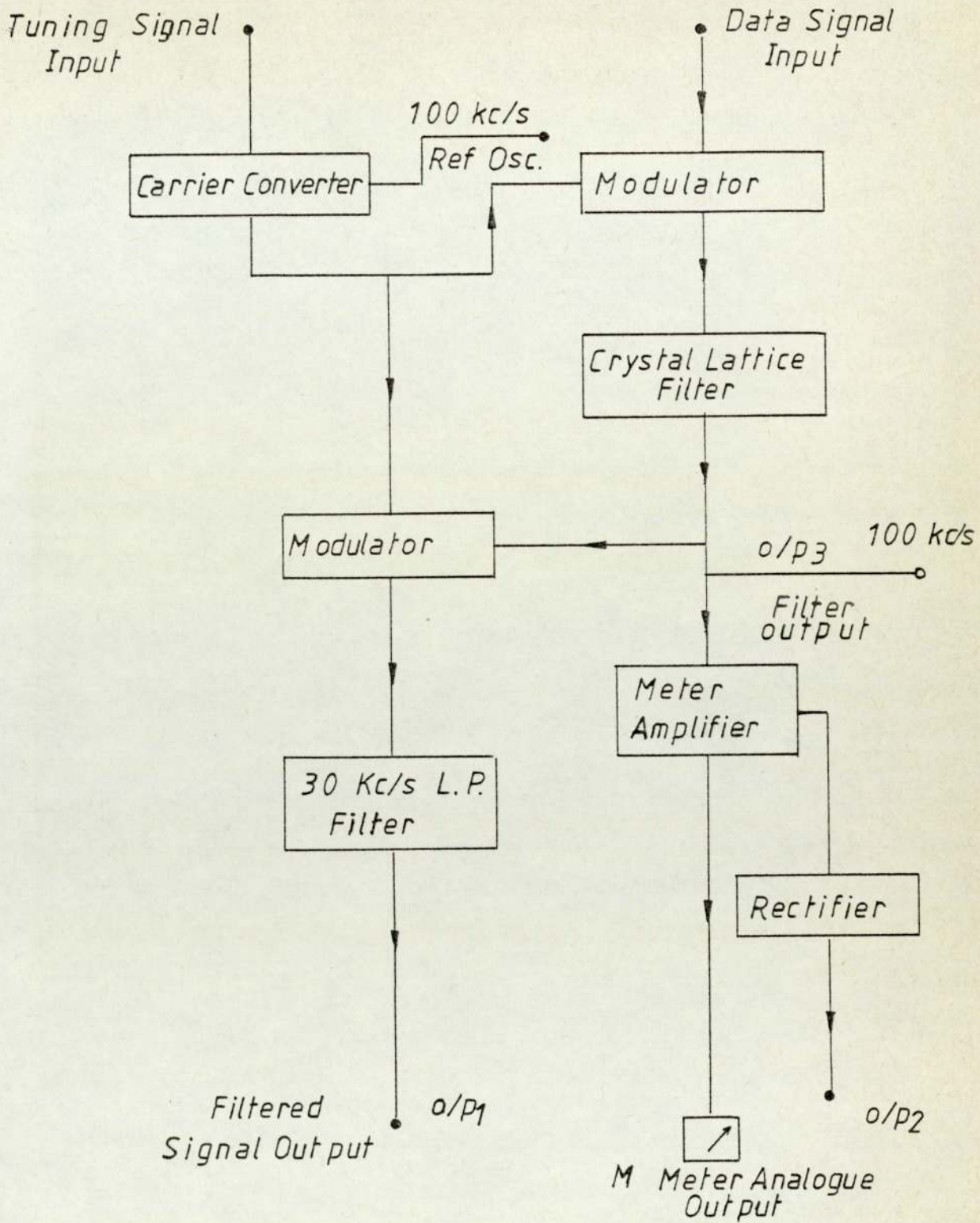


FIG. 5.2. SPECTRAL DYNAMICS SD 101 A
TRACKING FILTER FACILITIES

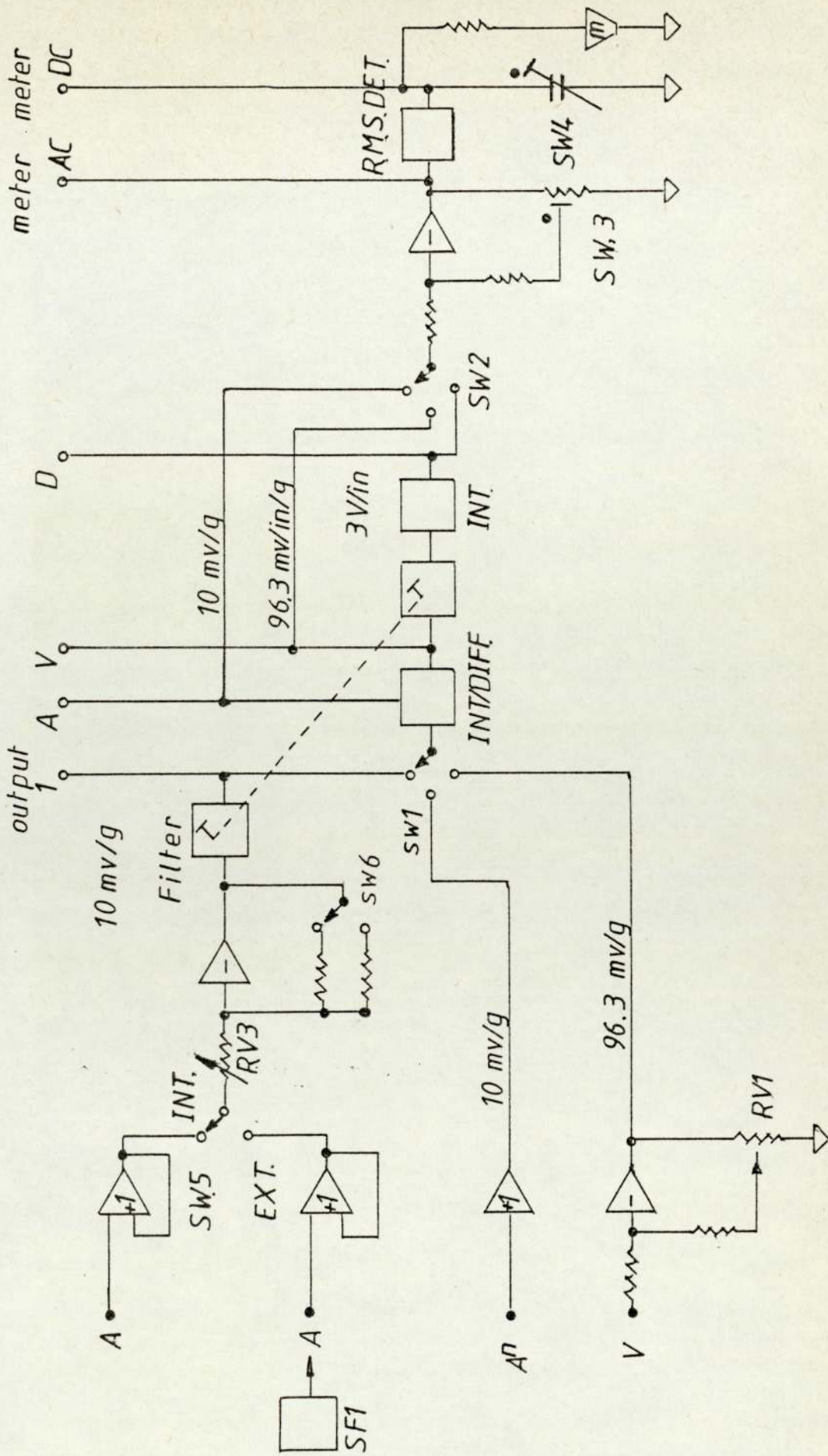


FIG. 5.3. BLOCK DIAGRAM VIBRATION METER MODEL DVA

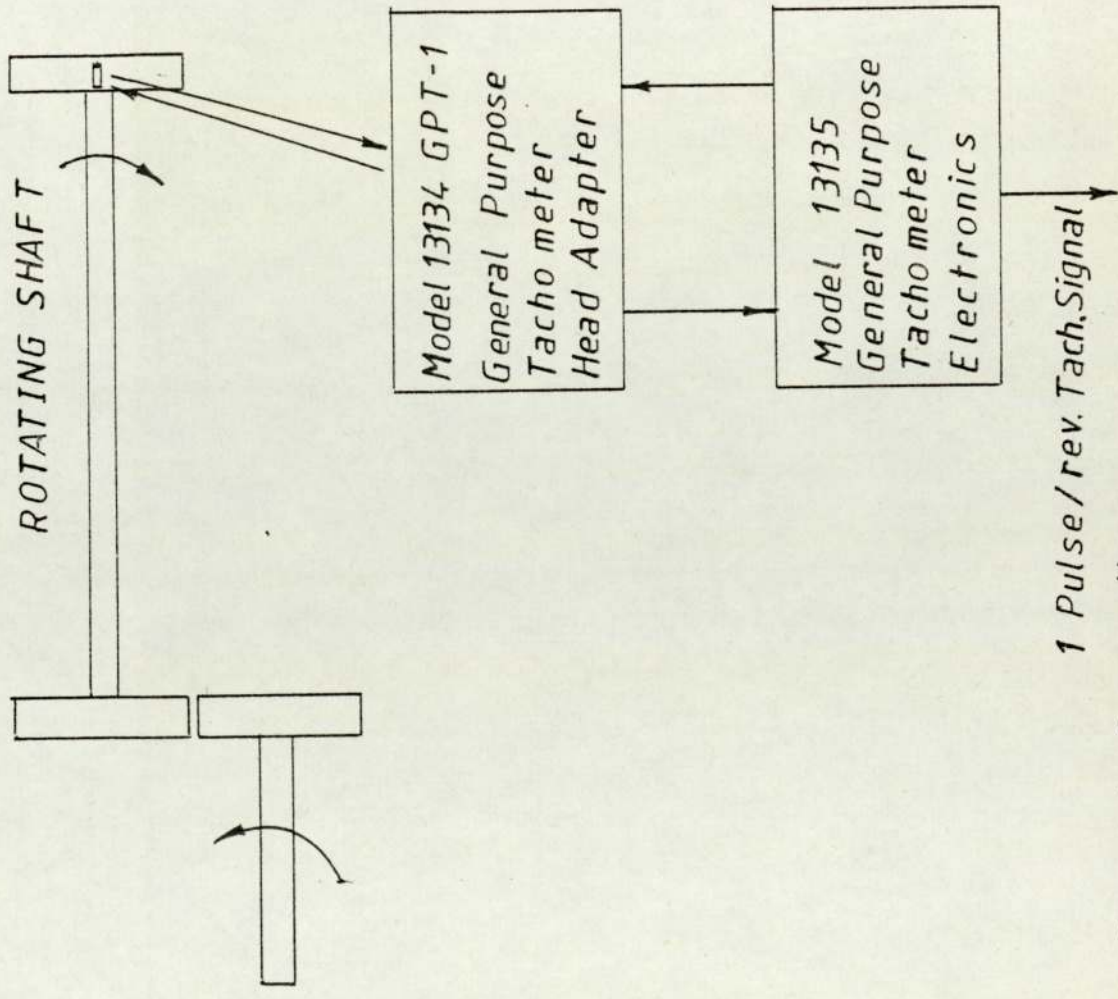


FIG. 5.4. Concept of operation

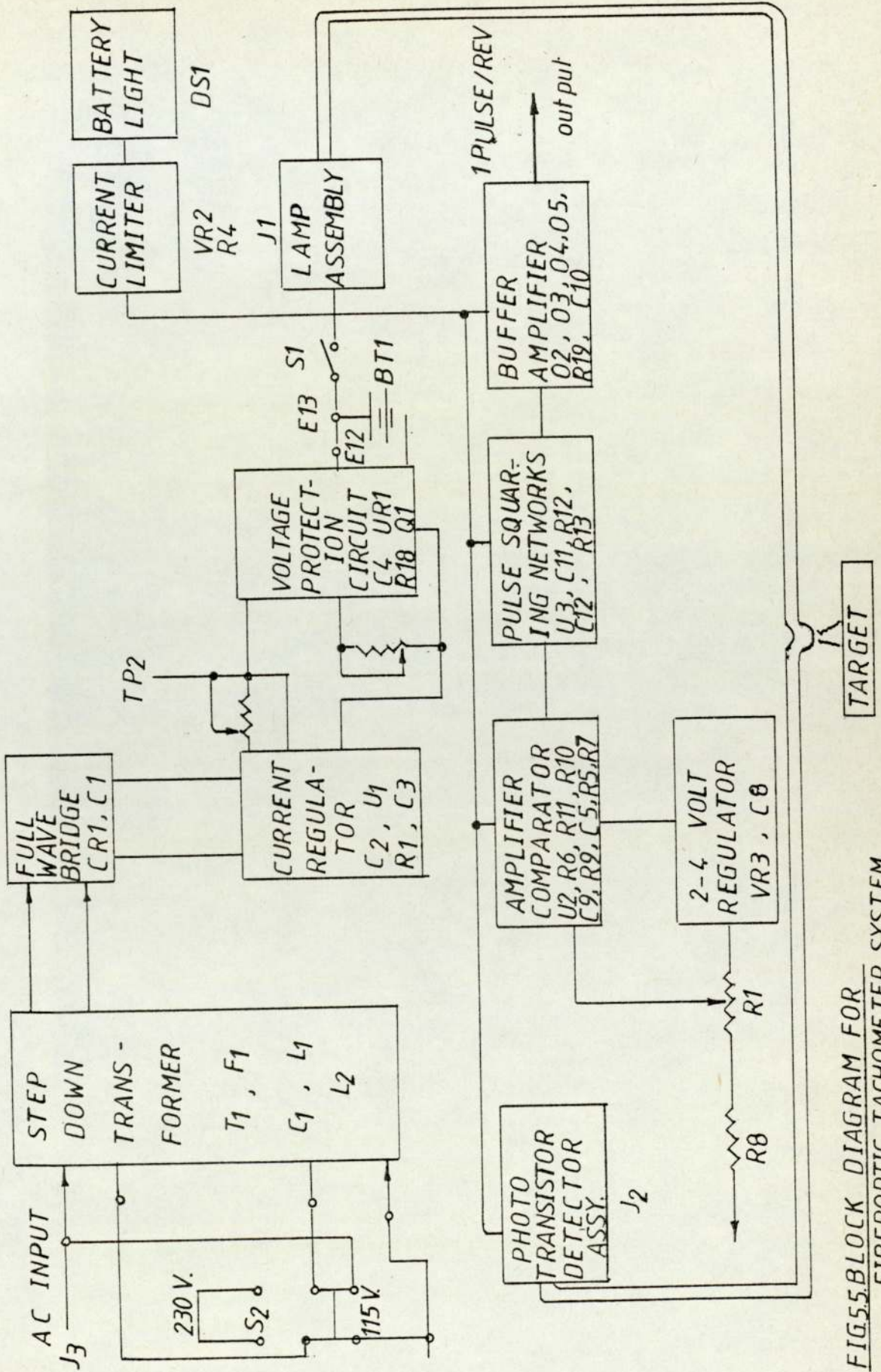


FIG. 5.5. BLOCK DIAGRAM FOR FIBEROPTIC TACHOMETER SYSTEM

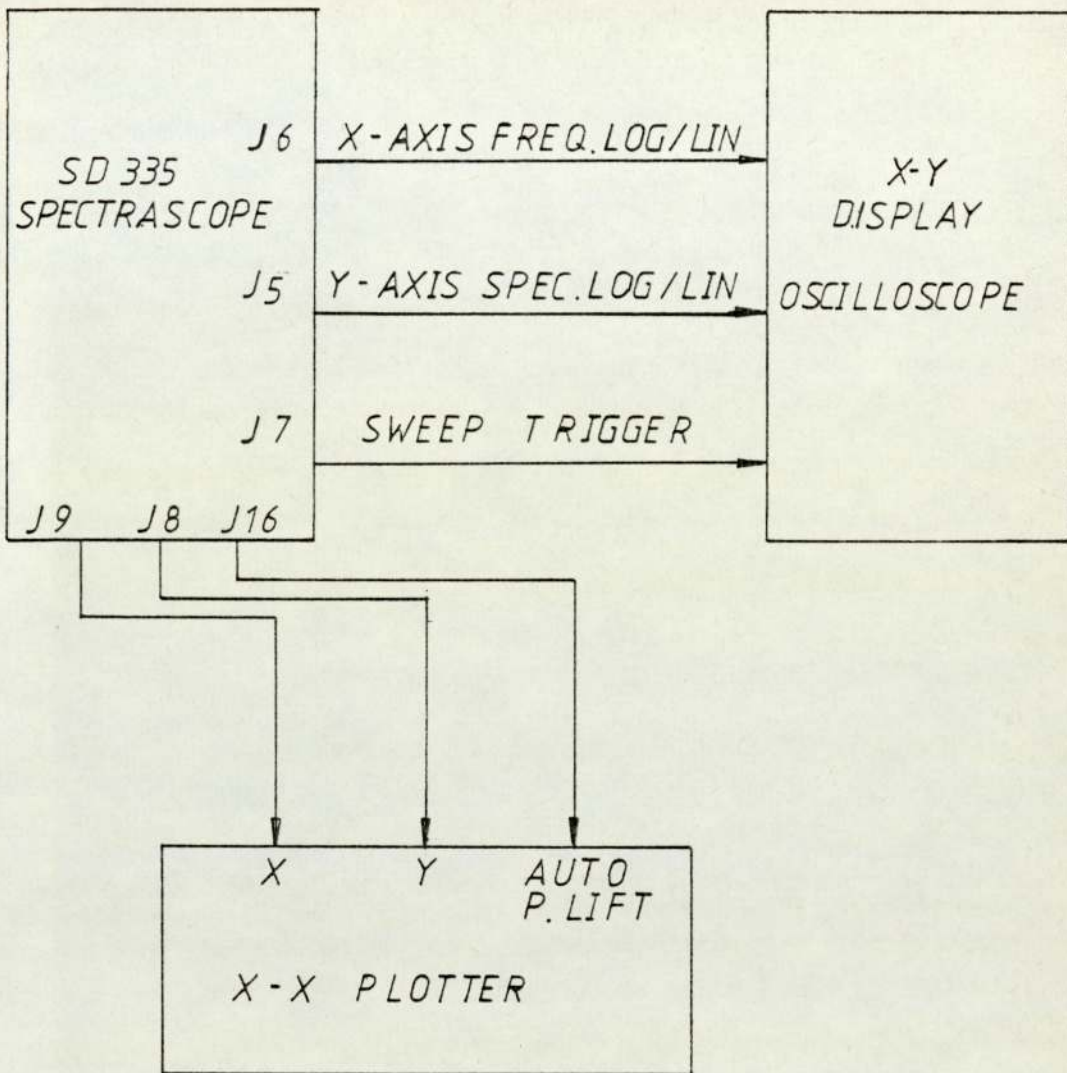


FIG. 5.6. SET UP FOR SPECTRASCOPE / OSCILLOSCOPE / PLOTTER

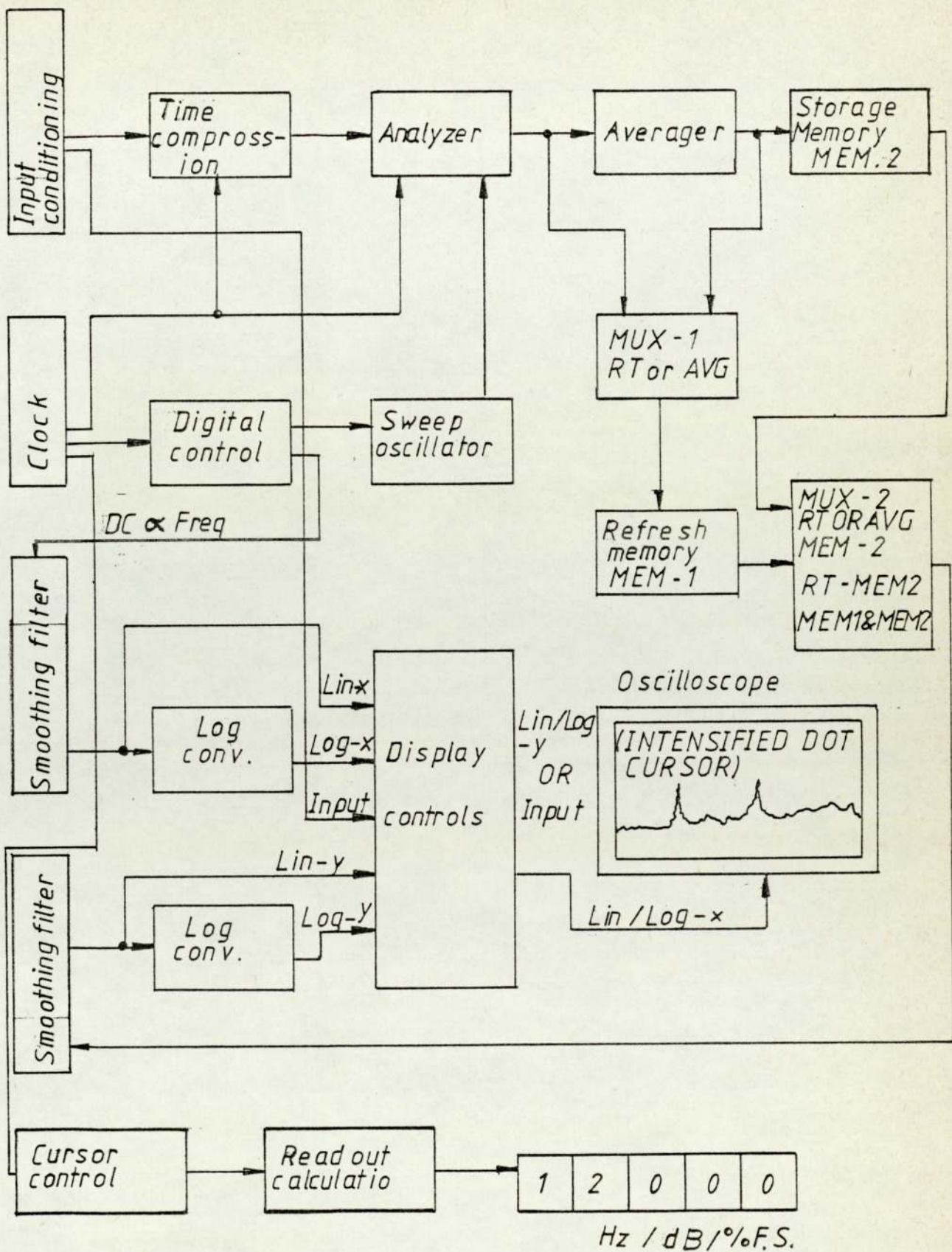


FIG.5.7. Simplified Block Diagram Spectroscope II

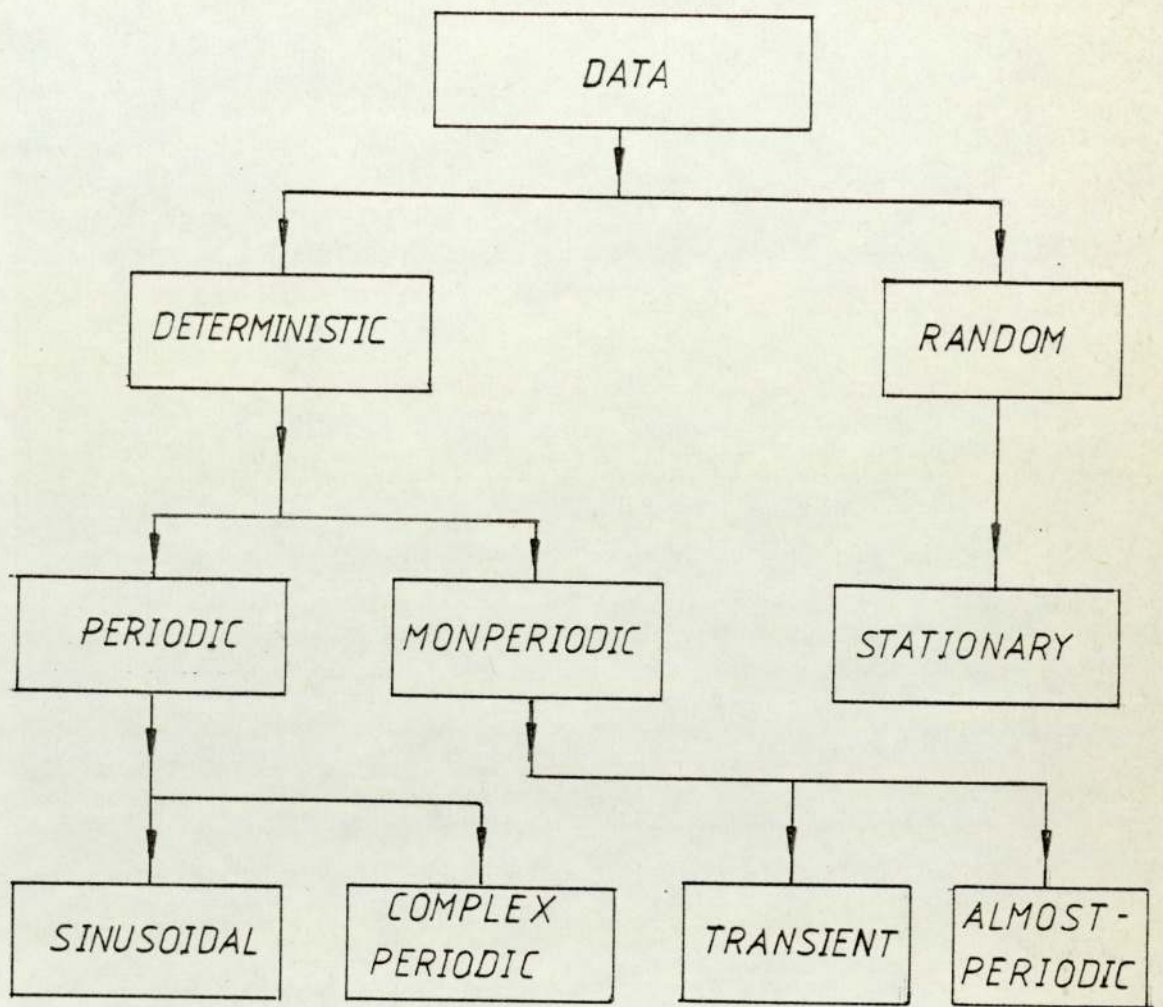


FIG. 5.8. DATA CLASSIFICATION

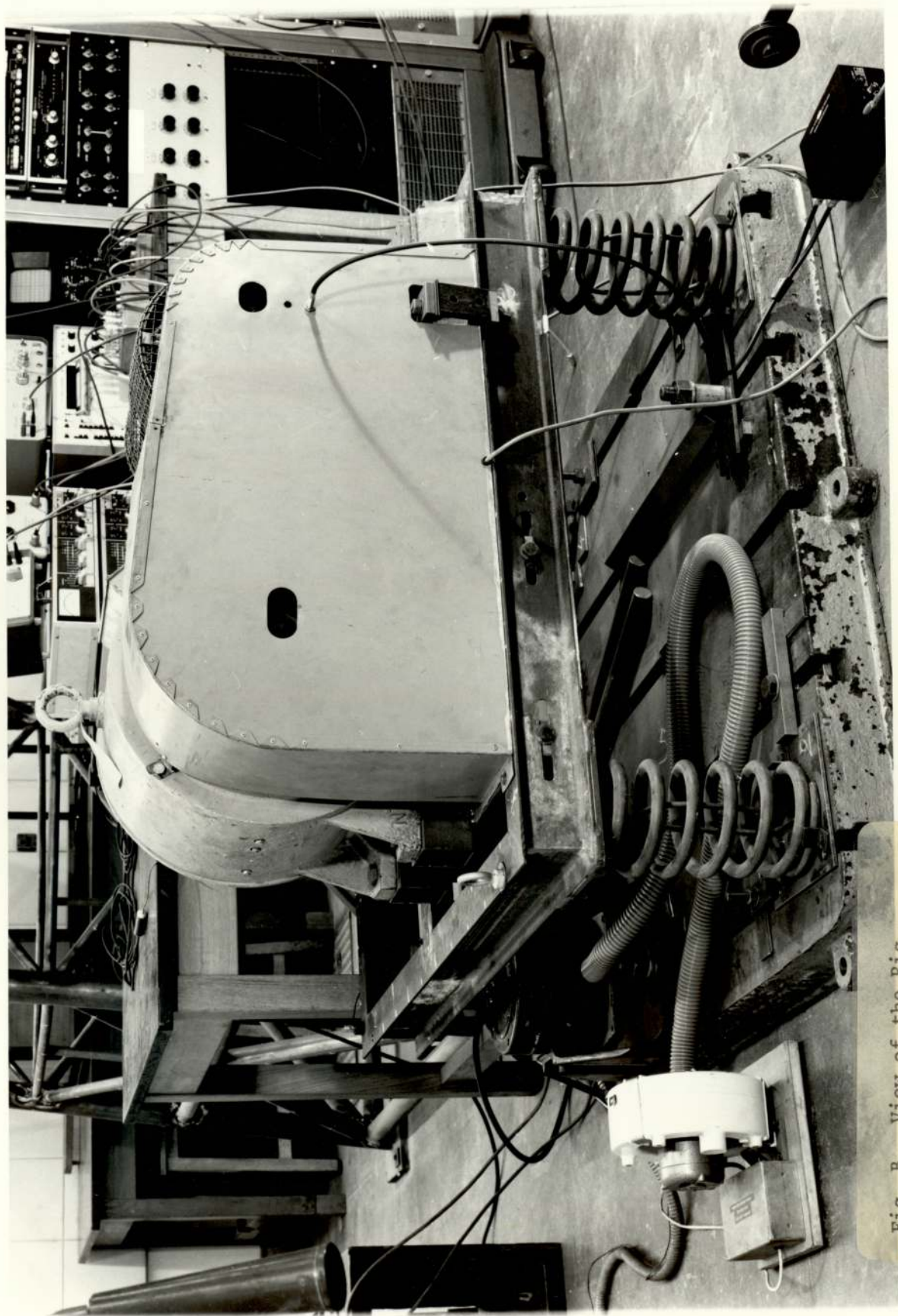


Fig. B View of the Rig
excited by the vibrator

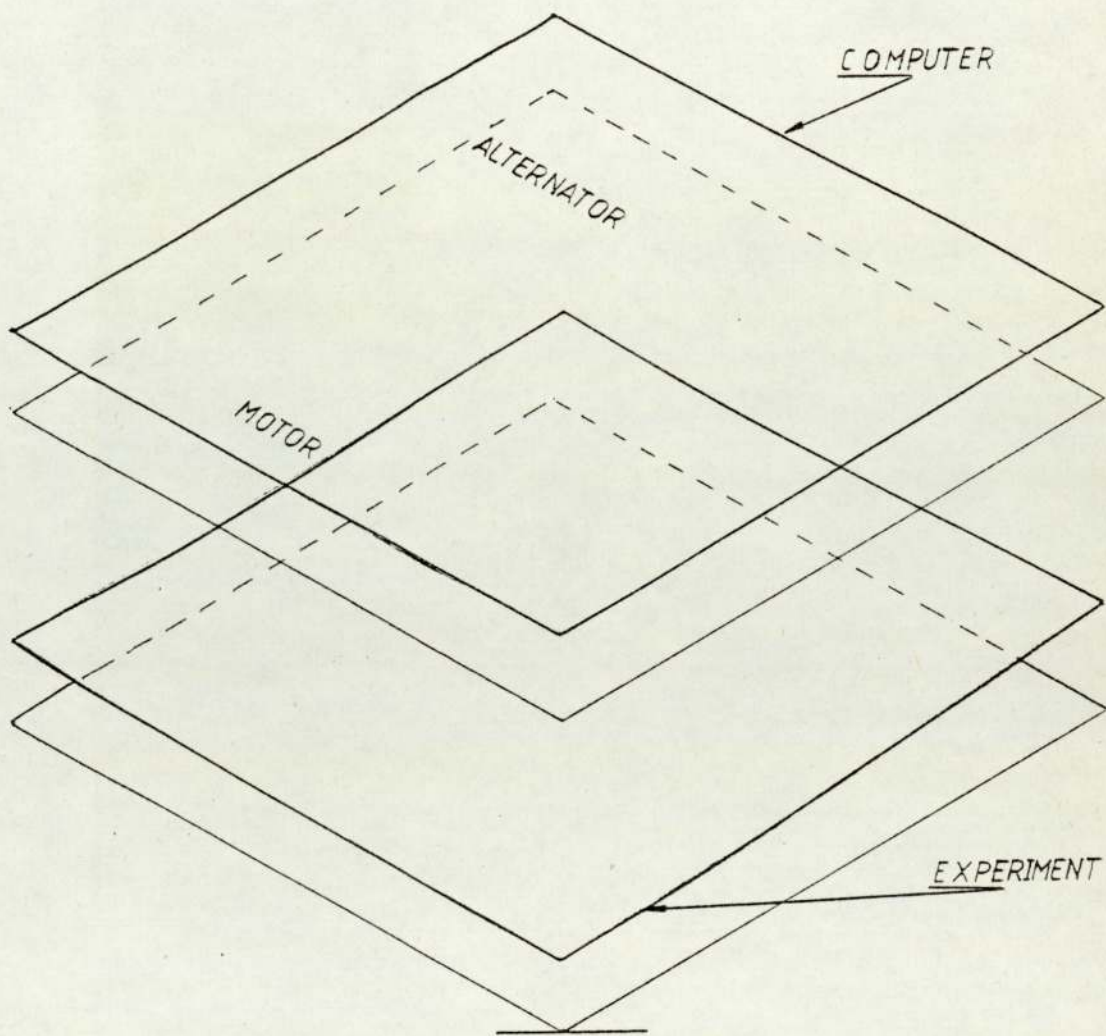


FIG. 5.9.

1 ST RIGID BODY MODE

EXP. = 4.3 c/s

COM. = 4.5 c/s

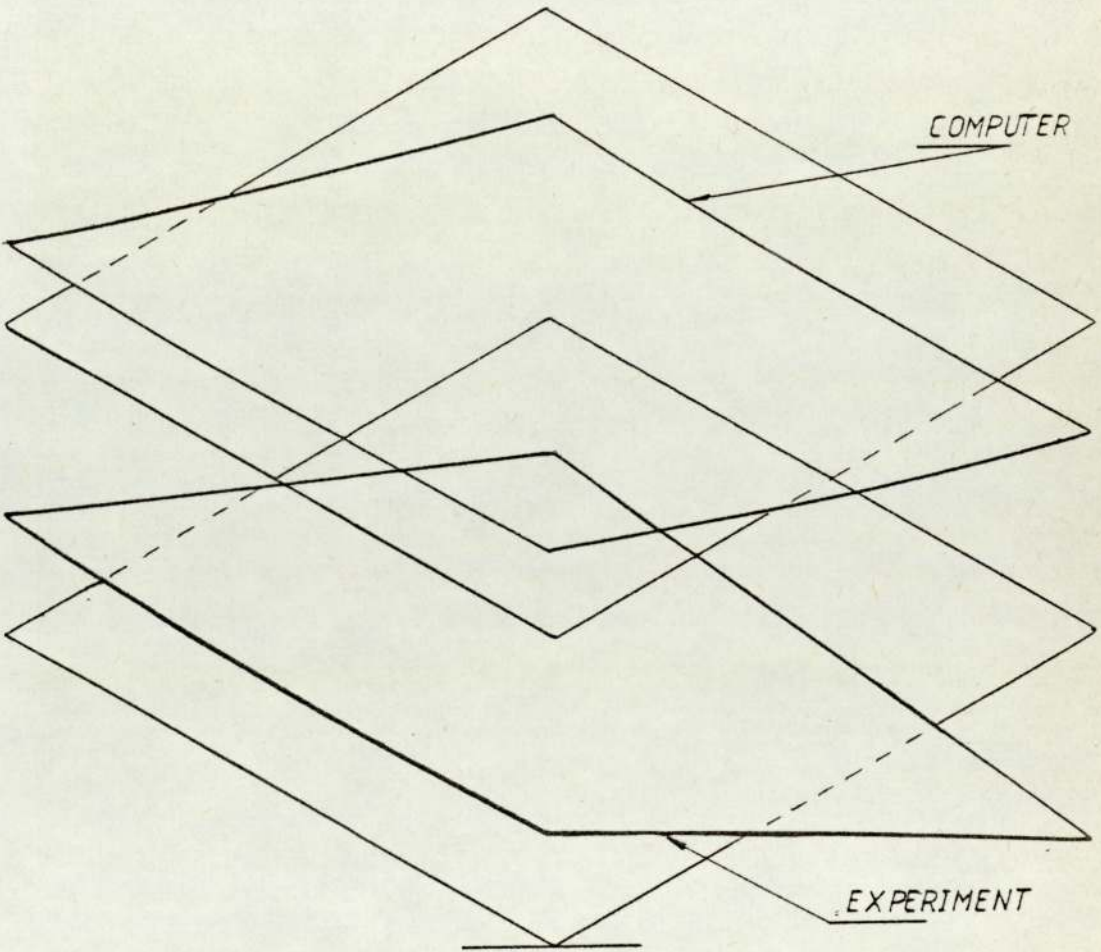


FIG. 5.10.
2ND RIGID BODY MODE

EXP. = 8.2 c/s

COM. = 7.1 c/s

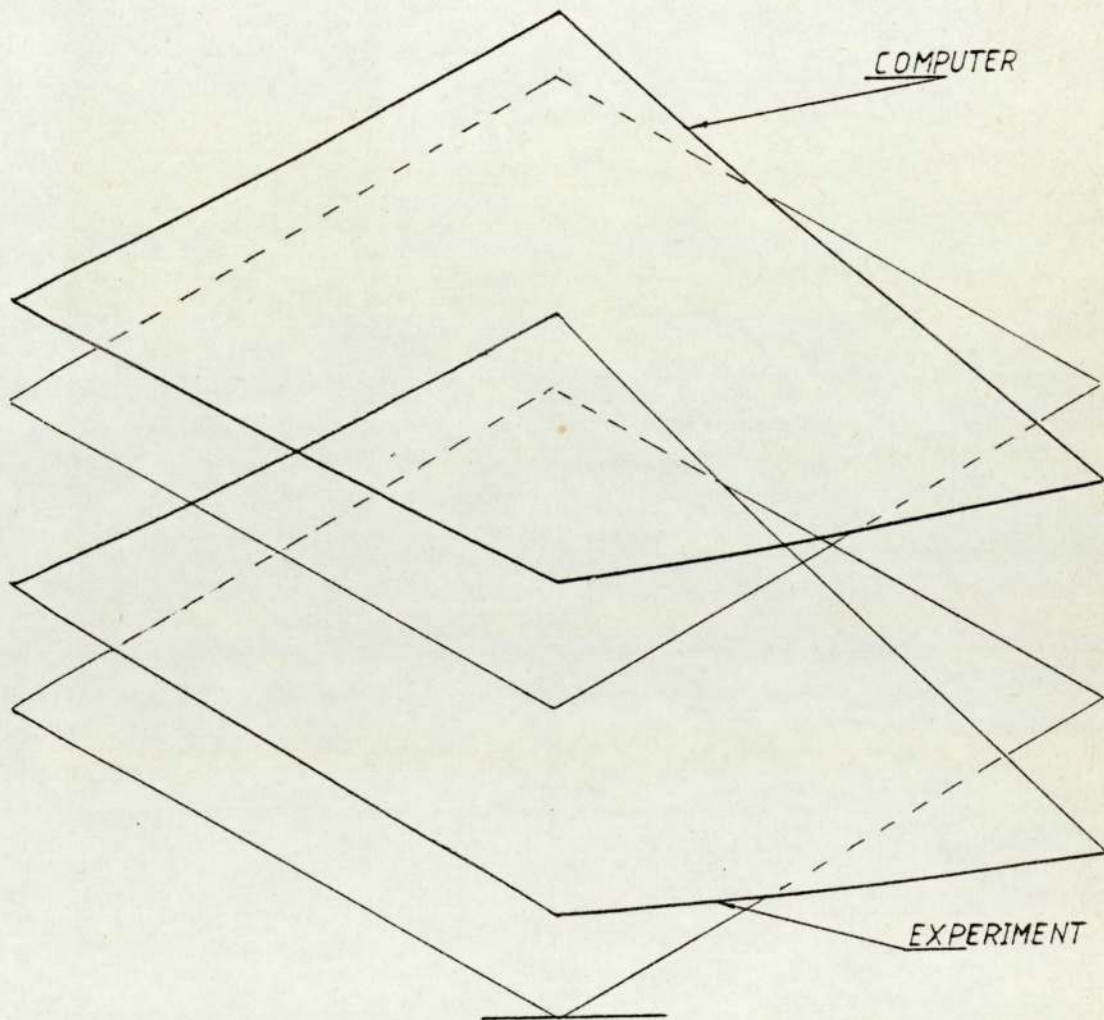


FIG. 5.11.
3 RD RIGID BODY MODE
EXP. = 9.1 c/s
COM. = 8.7 c/s

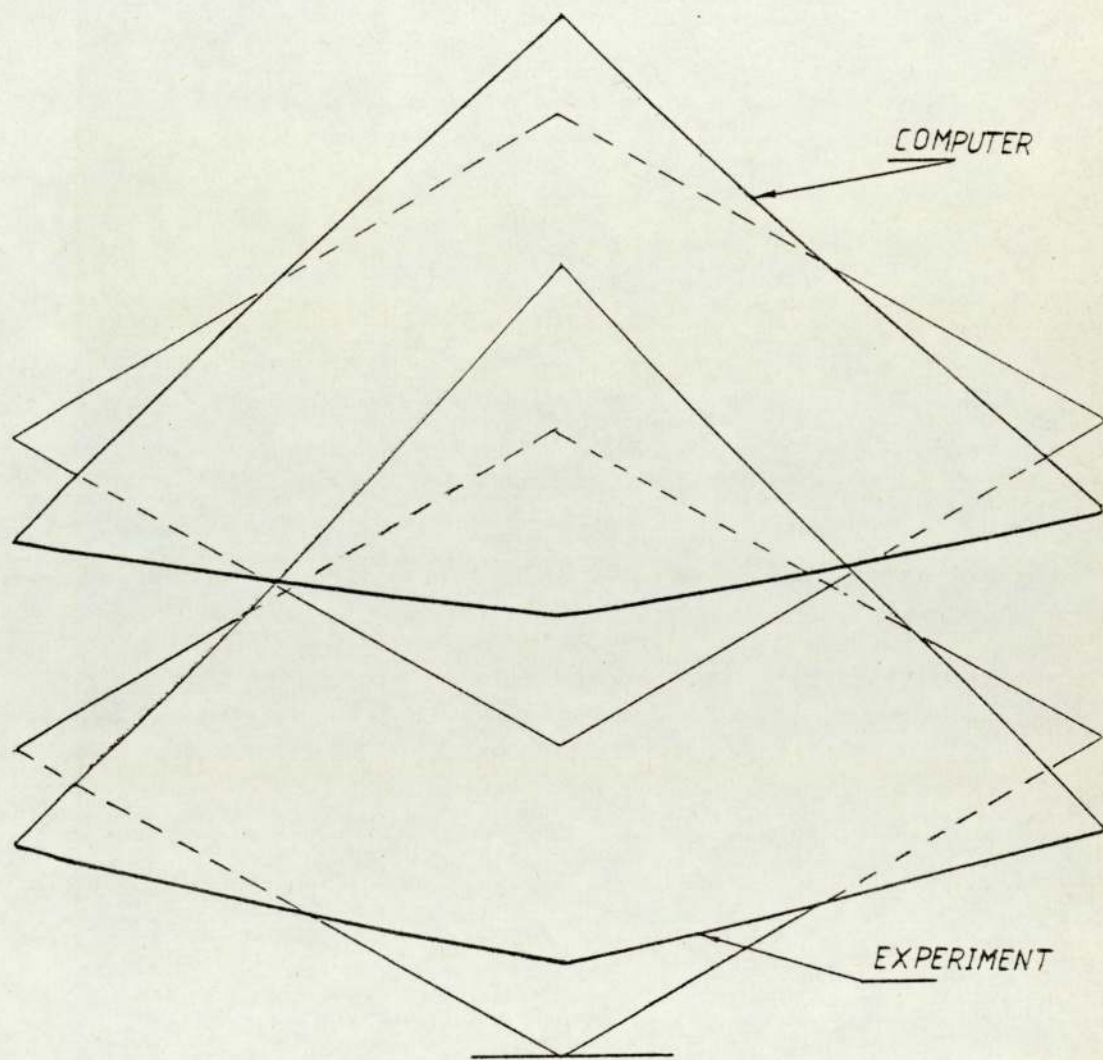


FIG. 5.12.
PLATE MODE

EXP. = 37.4

COM. = 43.34

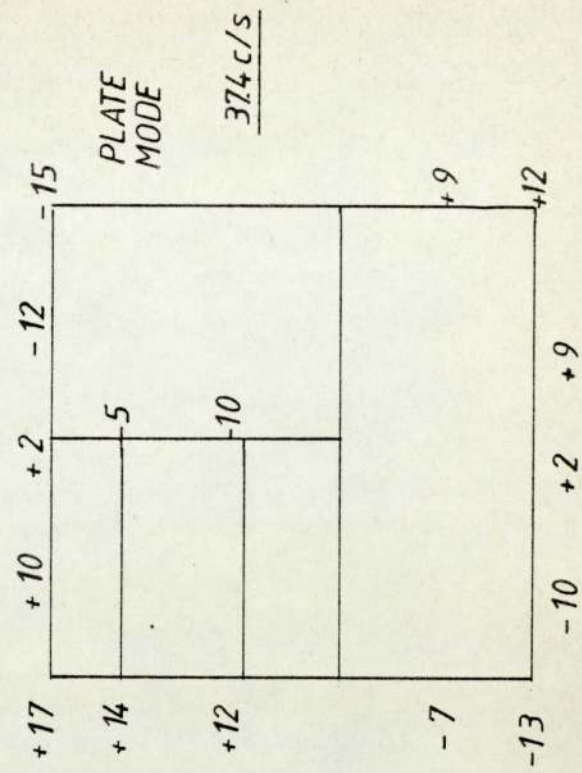
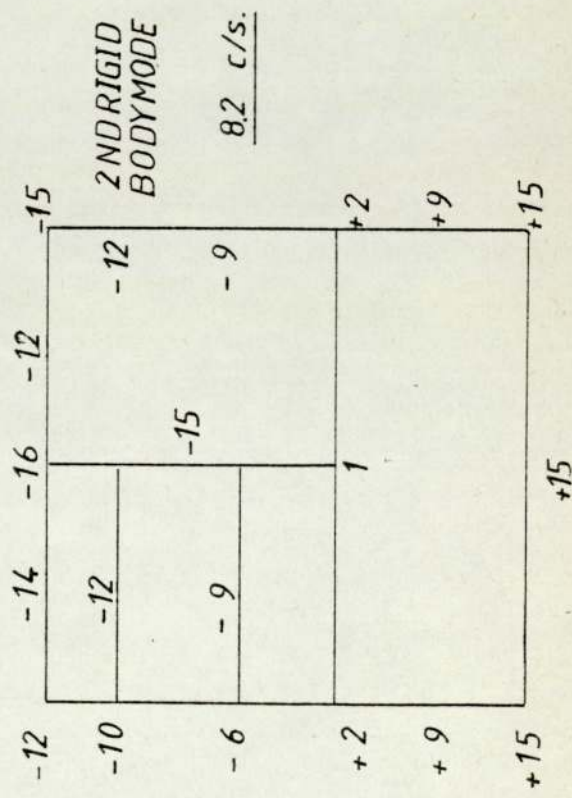
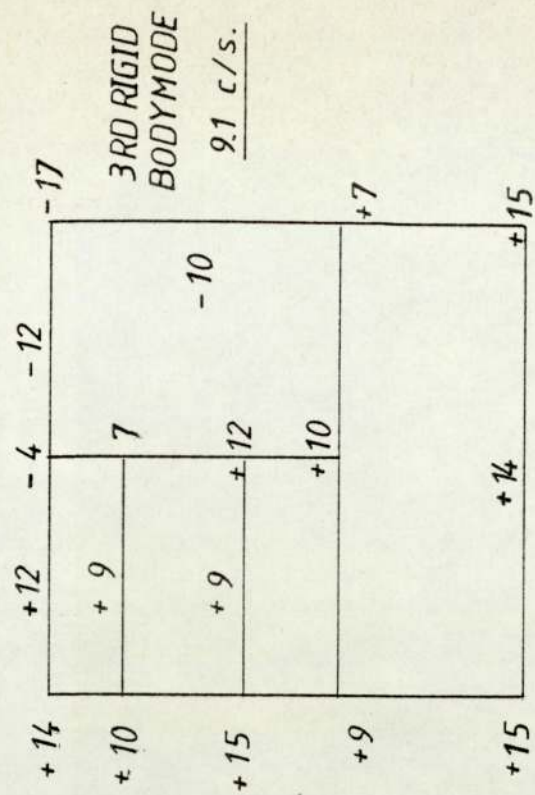
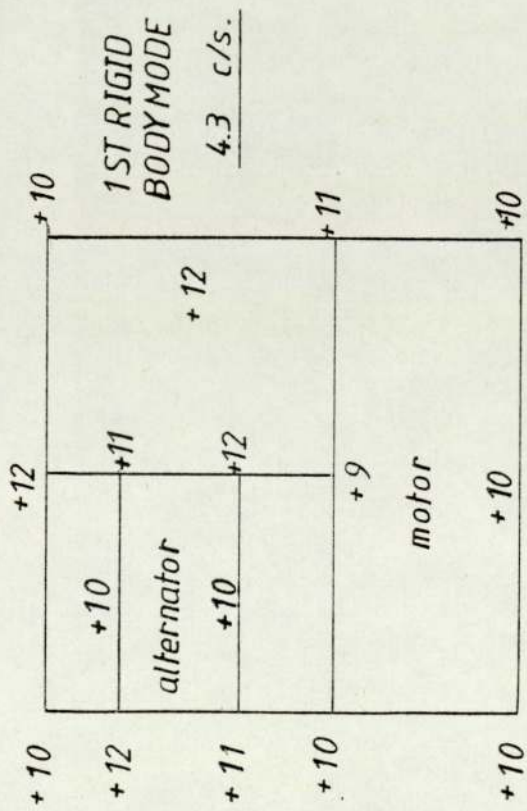


FIG.5.13 DIAGRAM SHOWING VALUES FOR THE FOUR MODES IN R.M.S.

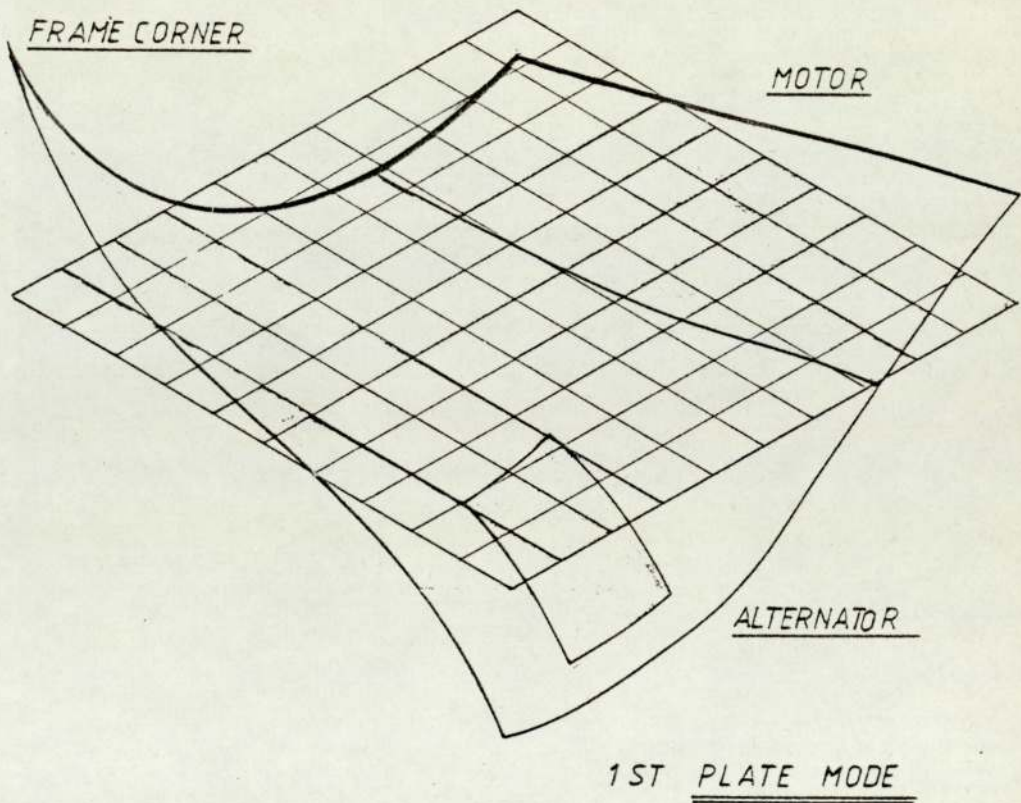


FIG. 5.14.
PICTORIAL REPRESENTATION SHOWING
PATCHES OF DISPLACED SURFACE COVERED BY
MOTOR AND ALTERNATOR BASES.

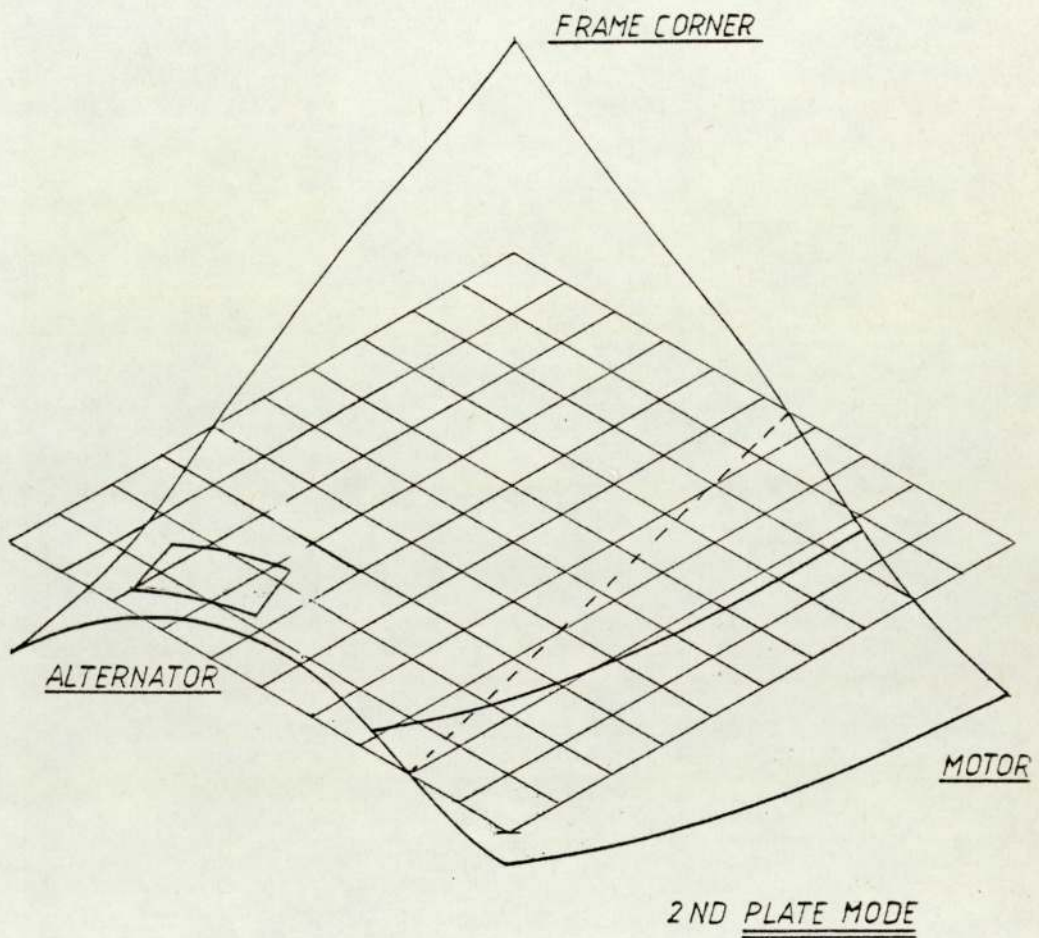


FIG. 5.15.
PICTORIAL REPRESENTATION SHOWING
PATCHES OF DISPLACED SURFACE COVERED BY
MOTOR AND ALTERNATOR BASES.

FIG. 5.16.
RESPONSE CURVE
FOR THE STATIC MODE
EXCITED BY VIBRATOR

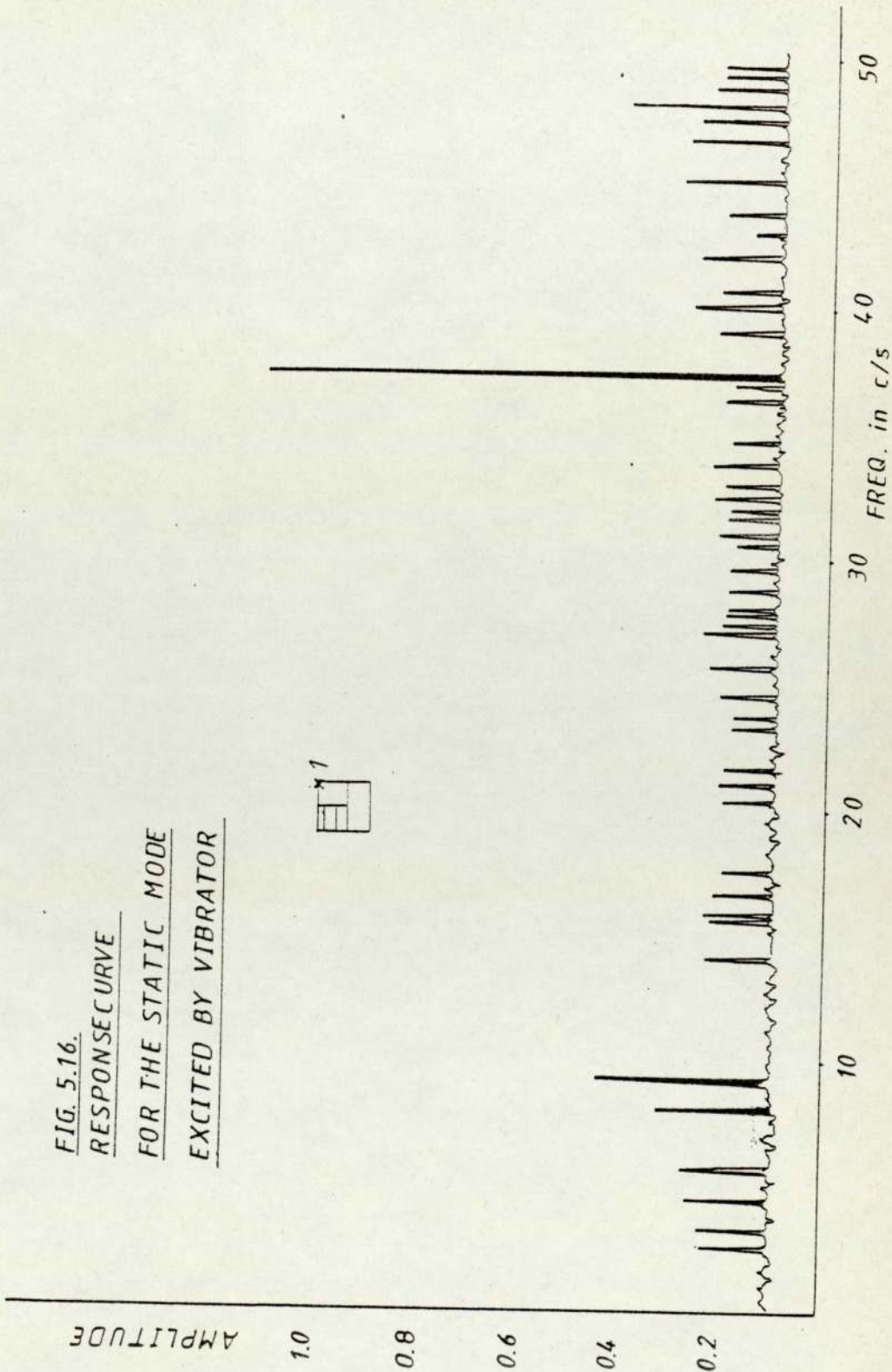


FIG 5.17 RESPONSE CURVE WITH FIXED FILTER FREQUENCY 4.3 HZ
Speed ratio 7:5 Picking signal position 1.

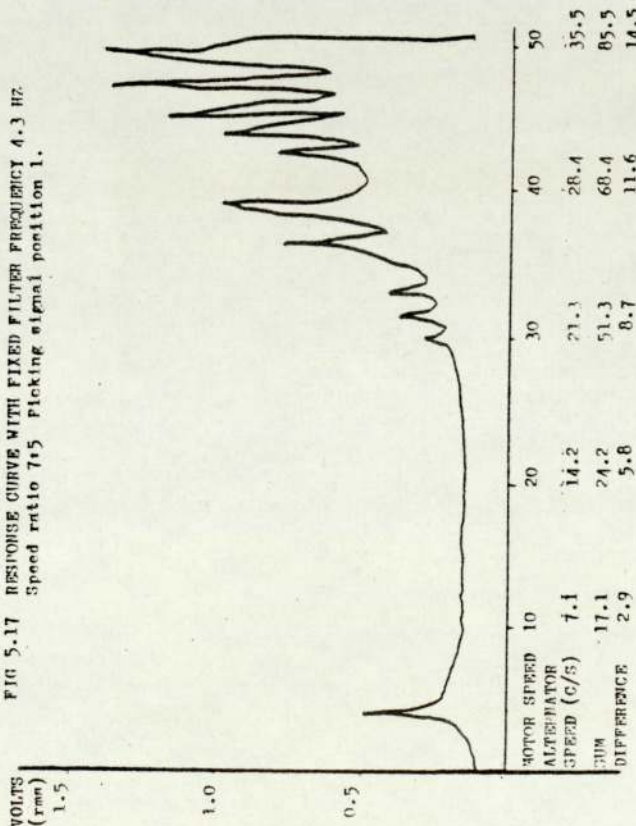


FIG 5.18 RESPONSE CURVE WITH FIXED FILTER FREQUENCY 6.2 HZ
Speed ratio 7:5 Picking signal position 1.

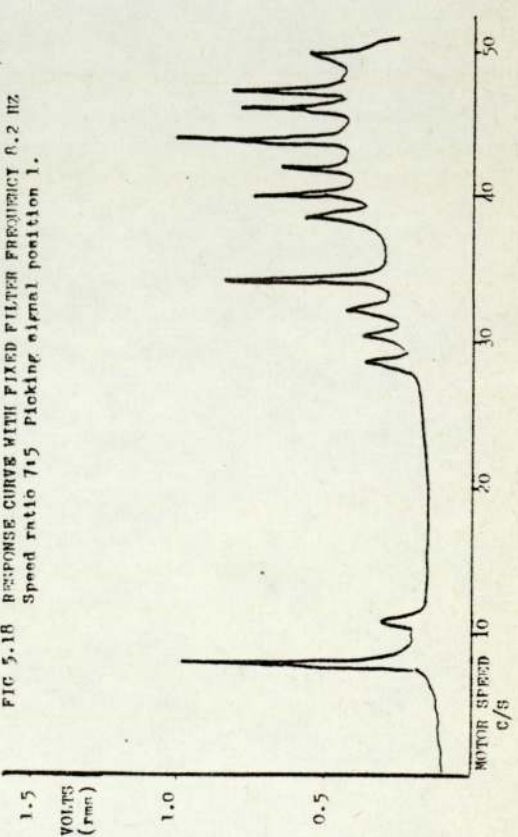


FIG 5.19 RESPONSE CURVE WITH FIXED FILTER FREQUENCY 9.1 HZ
Speed ratio 7:5 Picking signal position 1.

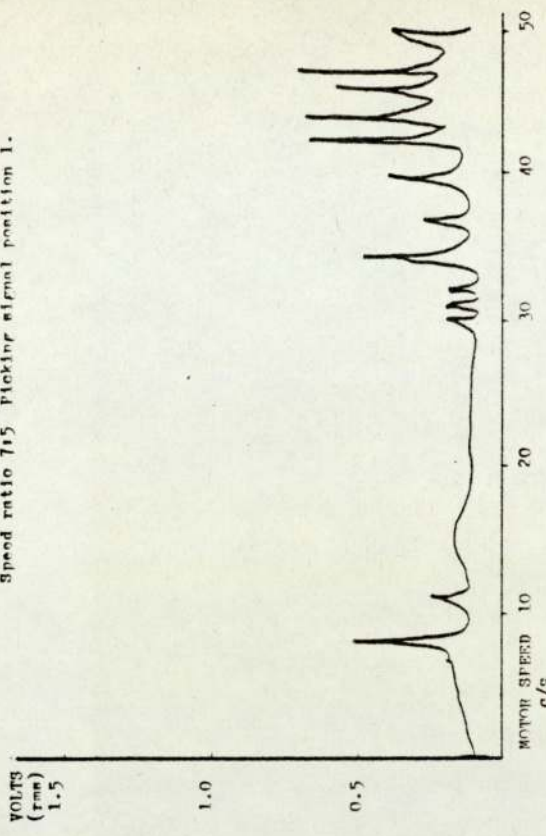


FIG 5.20 RESPONSE CURVE WITH FIXED FILTER FREQUENCY 37.4 Hz
Speed ratio 7:5 Picking signal position 1.

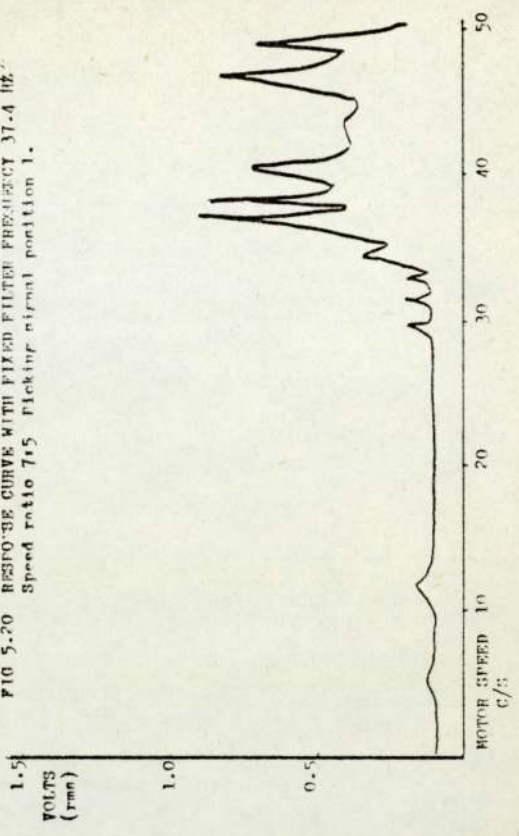


FIG 5.21 RESPONSE CURVE WITH FIXED FILTER FREQUENCY 4.3 HZ
Speed ratio 5/3 Flicking signal position 1.

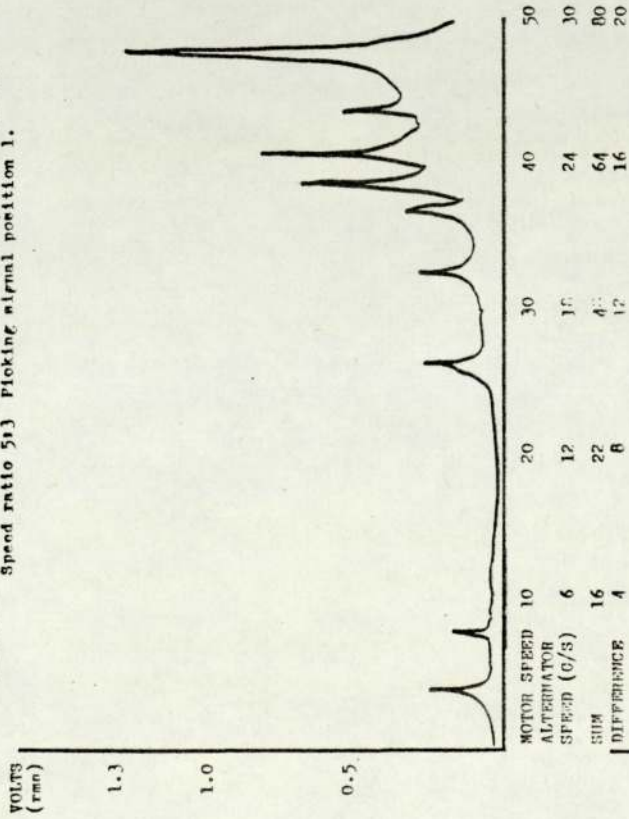


FIG 5.22 RESPONSE CURVE WITH FIXED FILTER FREQUENCY 8.2 HZ
Speed ratio 5/3 Flicking signal position 1.

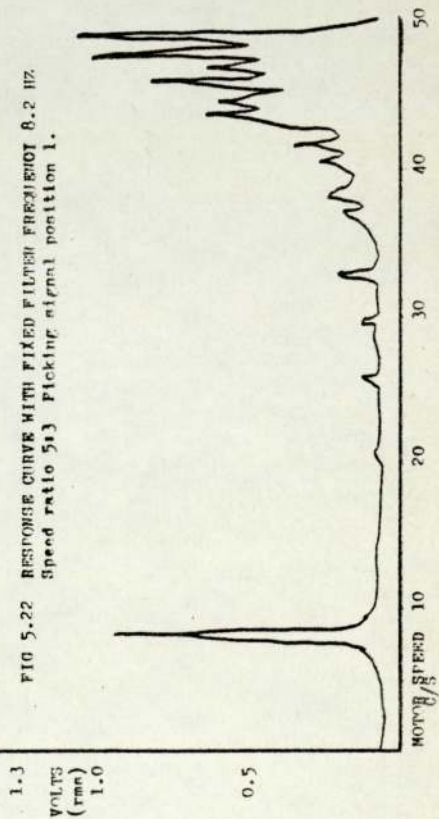


FIG 5.23 RESPONSE CURVE WITH FIXED FILTER FREQUENCY 9.1 HZ
Speed ratio 5/3 Flicking signal position 1.

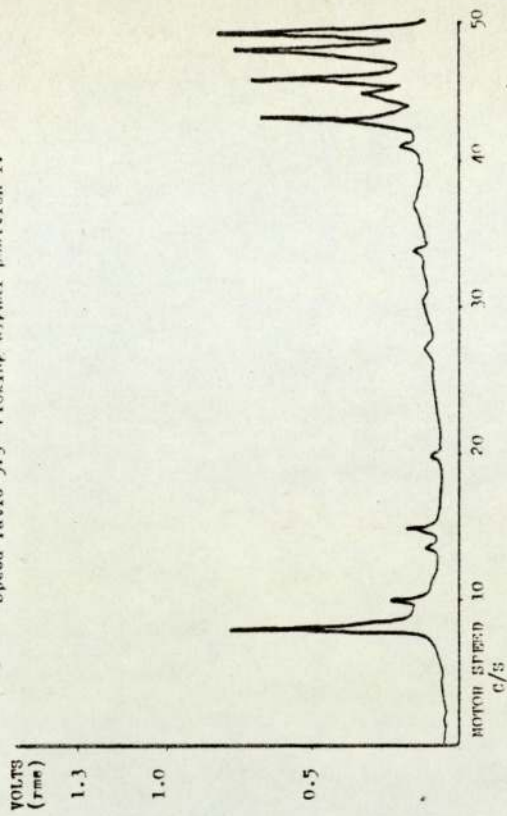


FIG 5.24 RESPONSE CURVE WITH FIXED FILTER FREQUENCY 37.4 HZ
Speed ratio 5/3 Flicking signal position 1.

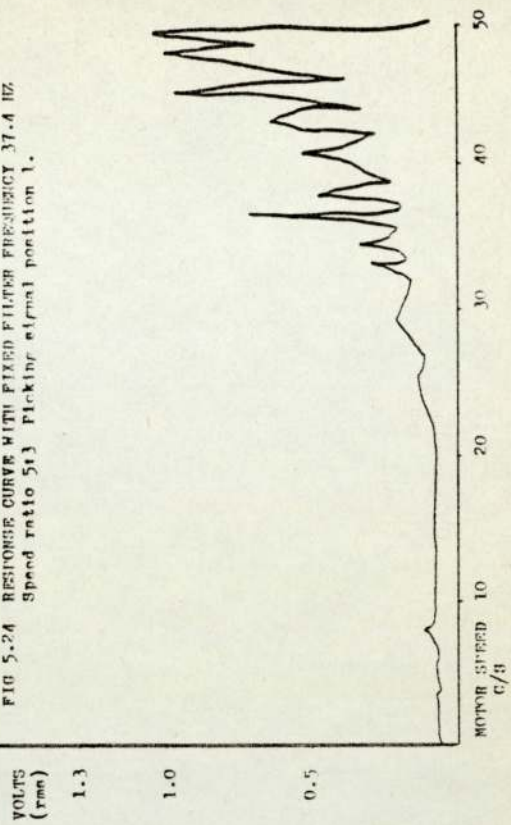


FIG 5.25 RESPONSE CURVE WITH FIXED FILTER FREQUENCY 4.3 HZ.
Speed ratio 3:1 Picking signal position 1.

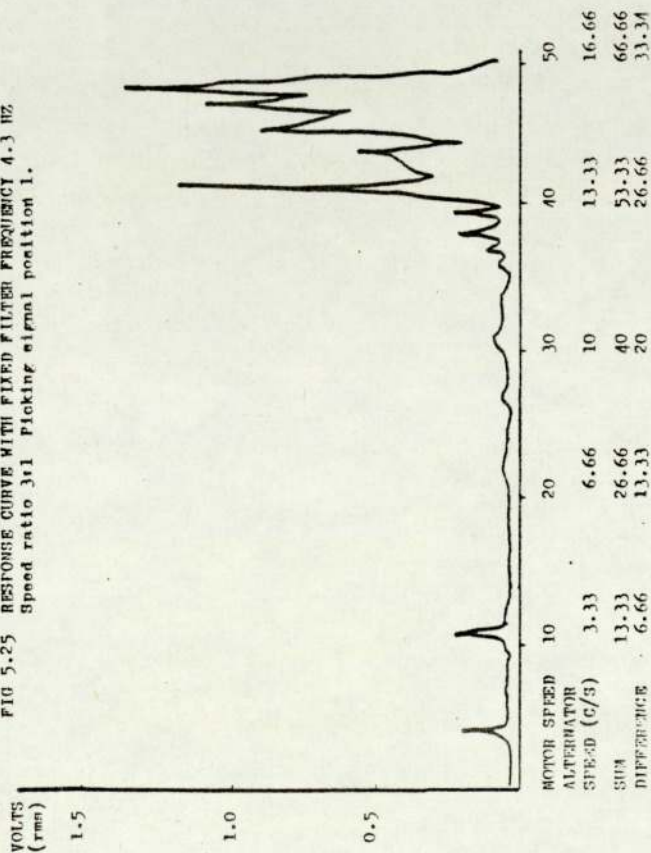


FIG 5.26 RESPONSE CURVE WITH FIXED FILTER FREQUENCY 8.1 HZ.
Speed ratio 3:1 Picking signal position 1.

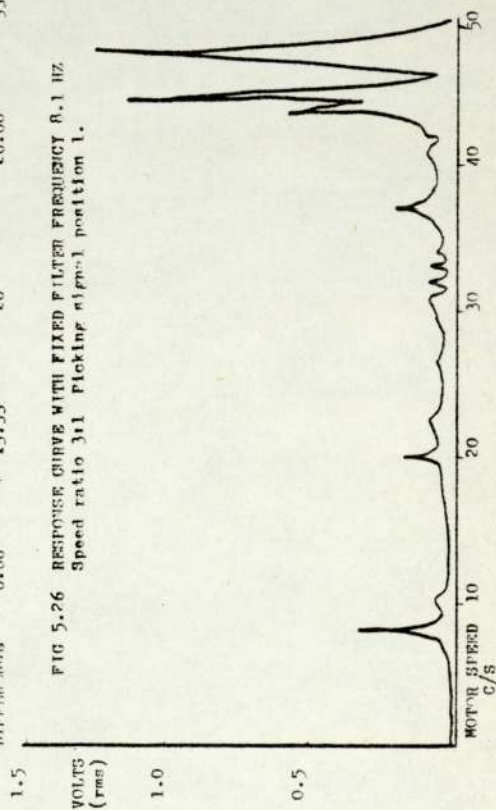


FIG 5.27 RESPONSE CURVE WITH FIXED FILTER FREQUENCY 9.1 HZ.
Speed ratio 3:1 Picking signal position 1.

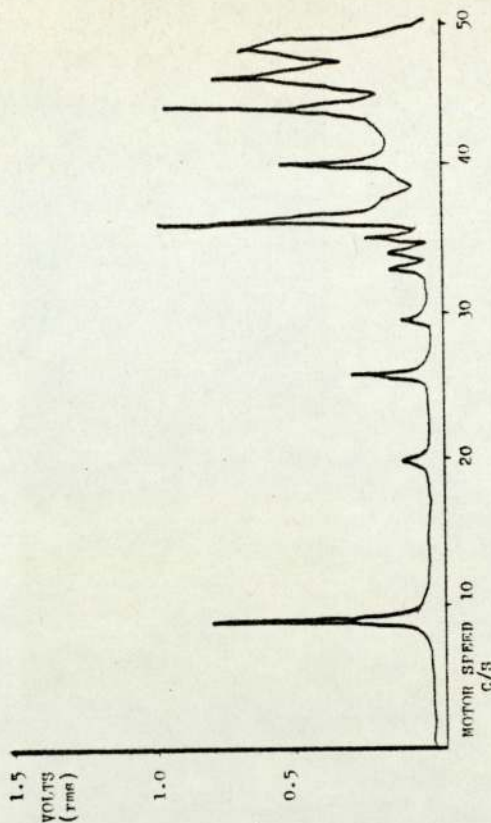


FIG 5.28 RESPONSE CURVE WITH FIXED FILTER FREQUENCY 31.4 HZ.
Speed ratio 3:1 Picking signal position 1.

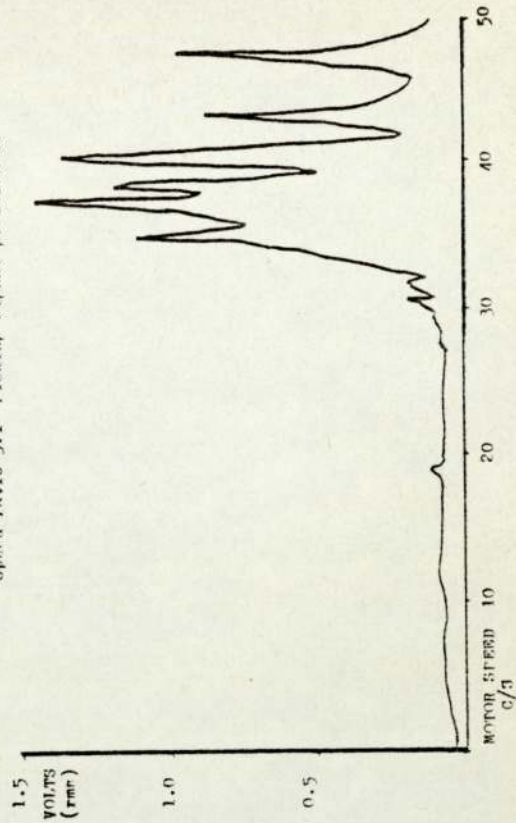


FIG 5.29 RESPONSE CURVE WITH FIXED FILTER FREQUENCY 4.3 HZ
Speed ratio 5:2 Picking signal position 1.

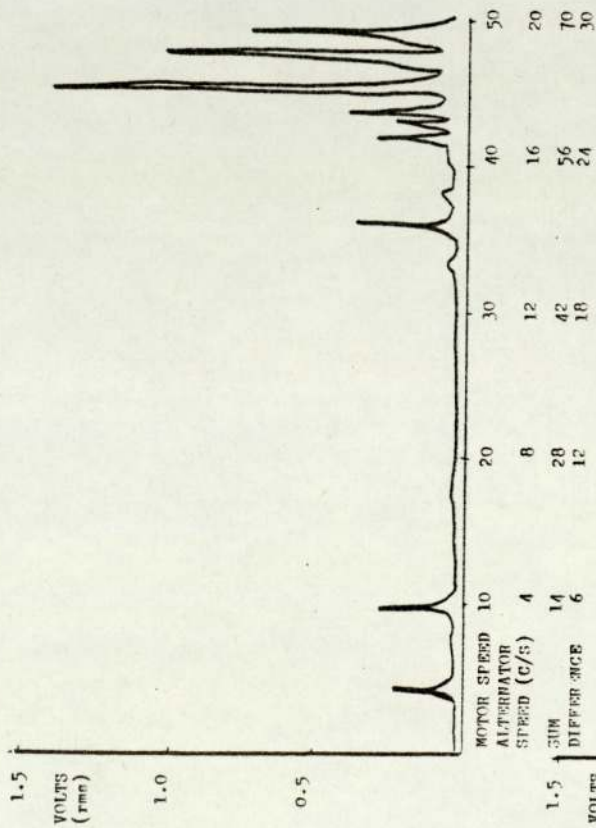


FIG 5.31 RESPONSE CURVE WITH FIXED FILTER FREQUENCY 9.1 HZ
Speed ratio 5:2 Picking signal position 1.

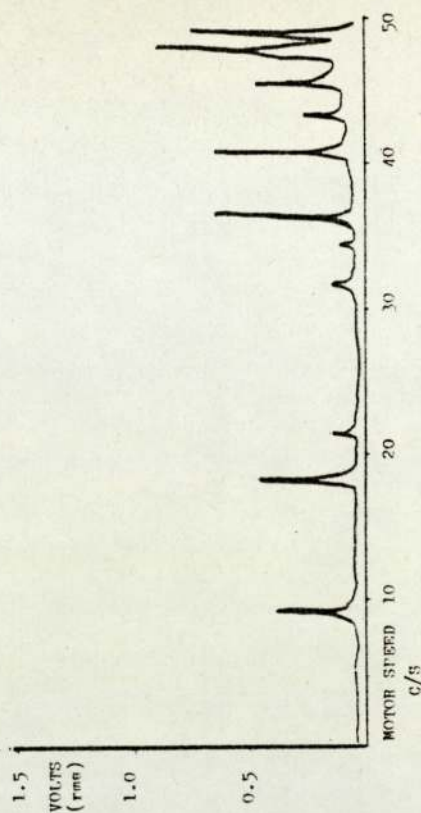


FIG 5.32 RESPONSE CURVE WITH FIXED FILTER FREQUENCY 37.4 HZ
Speed ratio 5:2 Picking signal position 1.

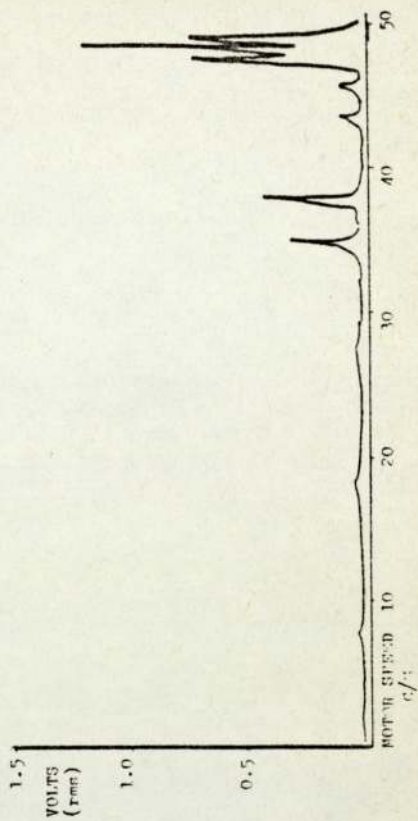


FIG 5.30 RESPONSE CURVE WITH FIXED FILTER FREQUENCY 8.2 HZ
Speed ratio 5:2 Picking signal position 1.

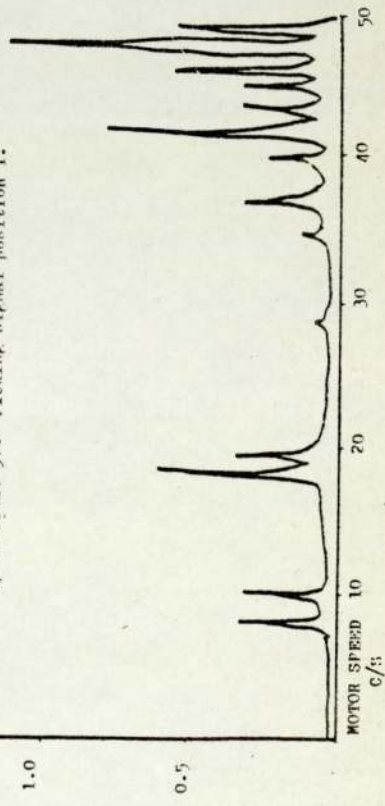


FIG 5.33 RESPONSE CURVE FOR THE MOTOR WITHOUT THE ALTERNATOR, WITH FIXED FILTER FREQUENCY 4.3 HZ Pickling signal position 1.

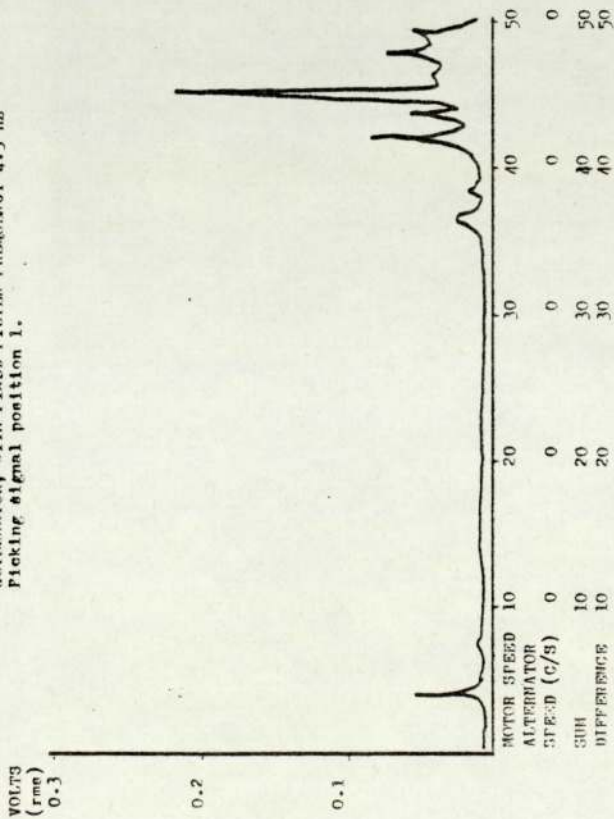


FIG 5.35 RESPONSE CURVE FOR THE MOTOR WITHOUT THE ALTERNATOR, WITH FIXED FILTER FREQUENCY 9.1 HZ Pickling signal position 1.

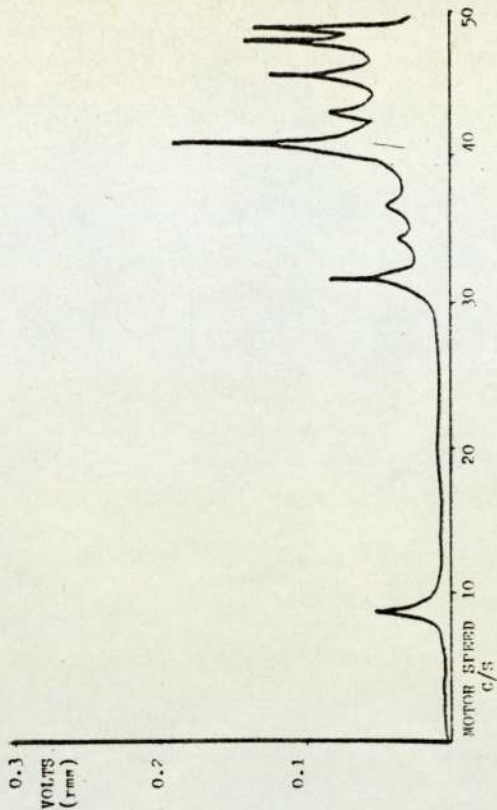


FIG 5.36 RESPONSE CURVE FOR THE MOTOR WITHOUT THE ALTERNATOR, WITH FIXED FILTER FREQUENCY 17.4 HZ Pickling signal position 1.

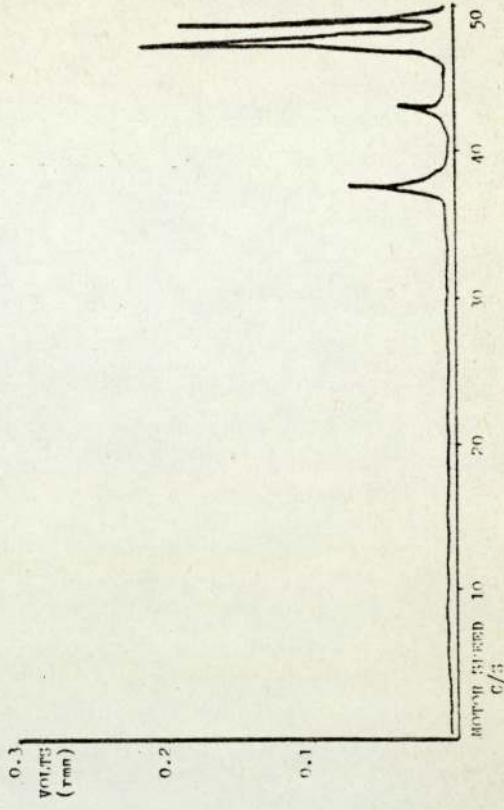


FIG 5.34 RESPONSE CURVE FOR THE MOTOR WITHOUT THE ALTERNATOR, WITH FIXED FILTER FREQUENCY 6.2 HZ Pickling signal position 1.

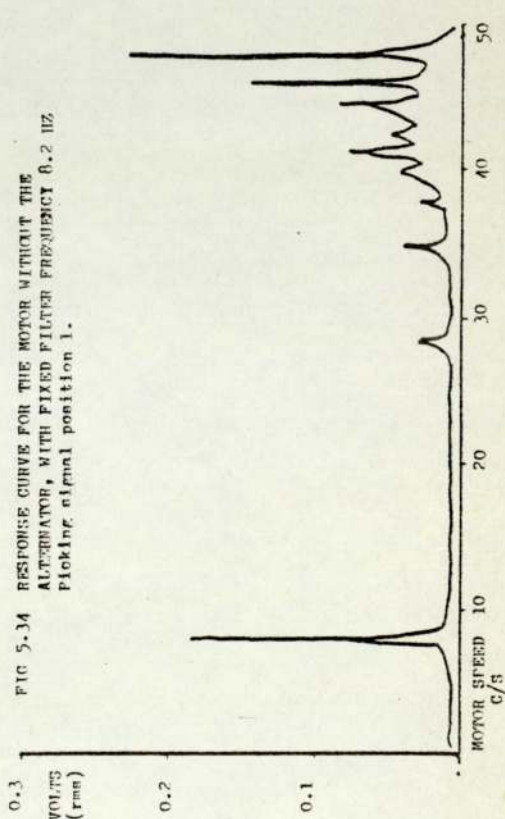


FIG 5.37 RESPONSE CURVE AND WAVE FORM
 Speed ratio 7:5 Starting the motor to
 maximum speed. Picking signal position 1.

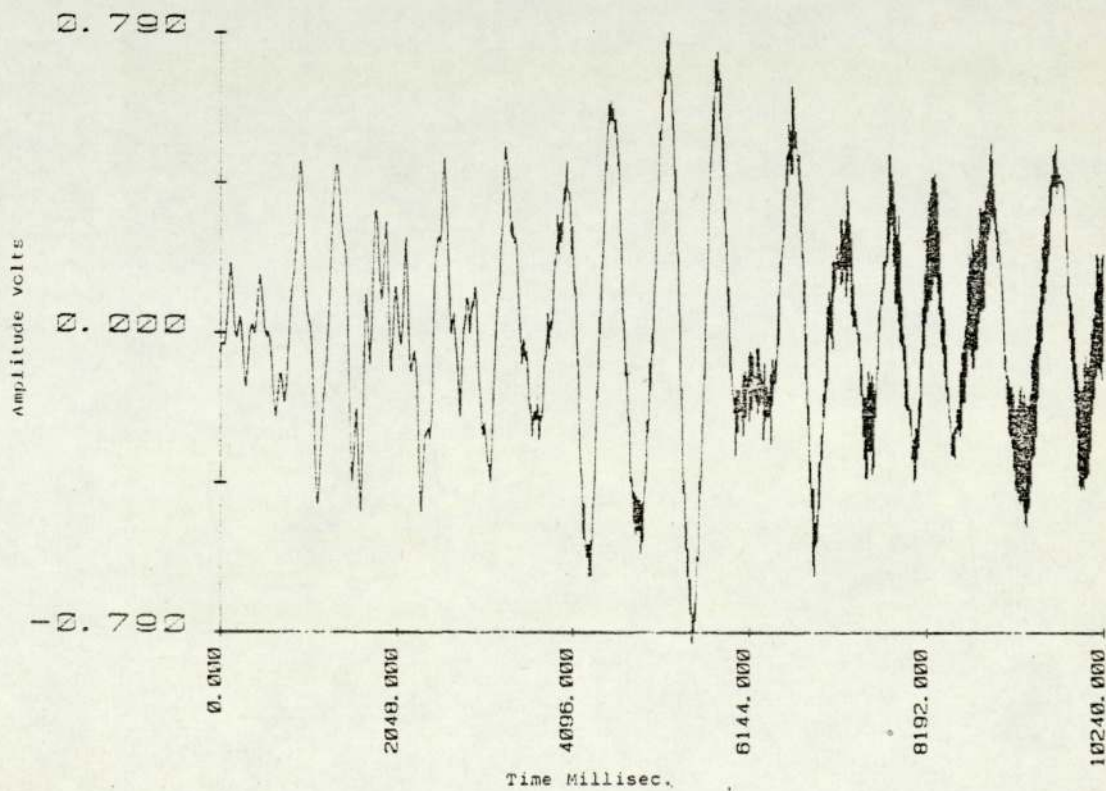
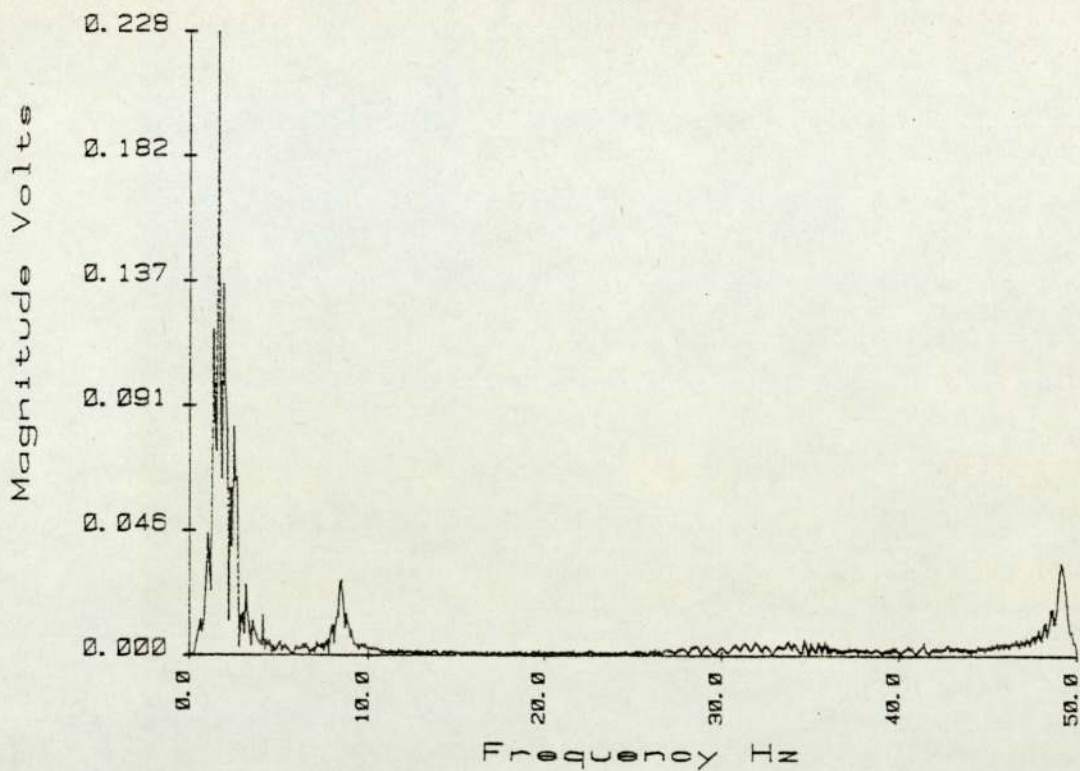
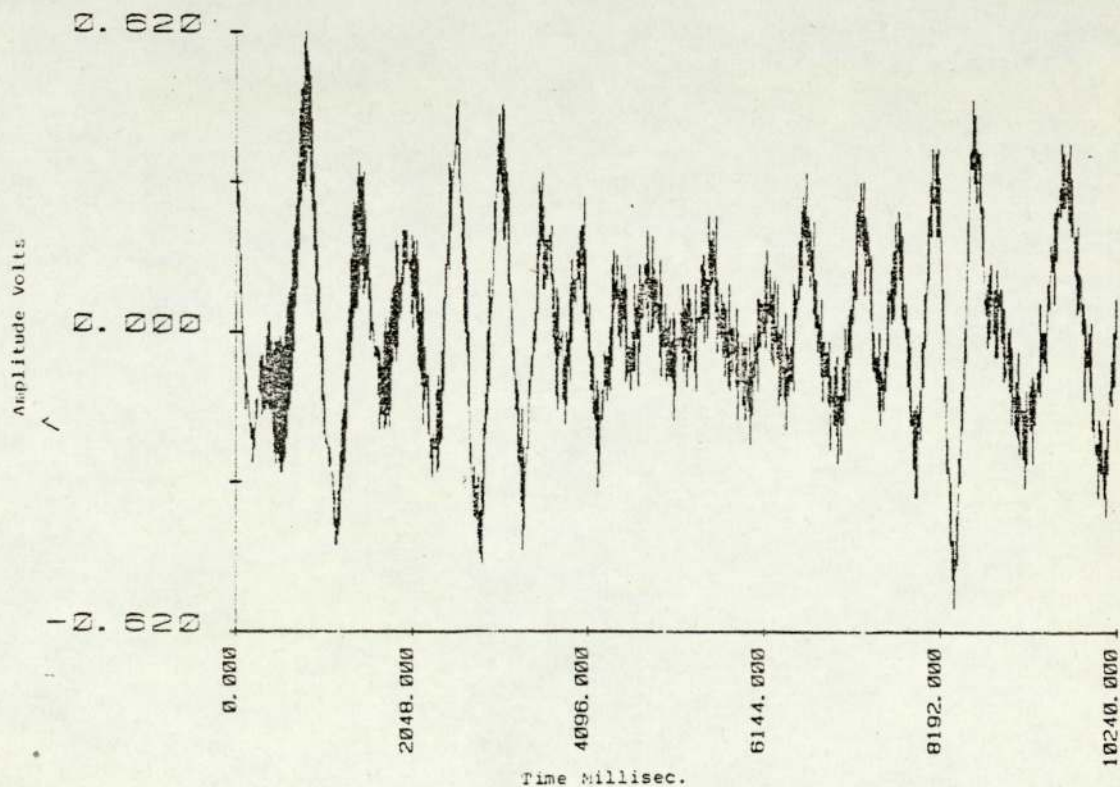
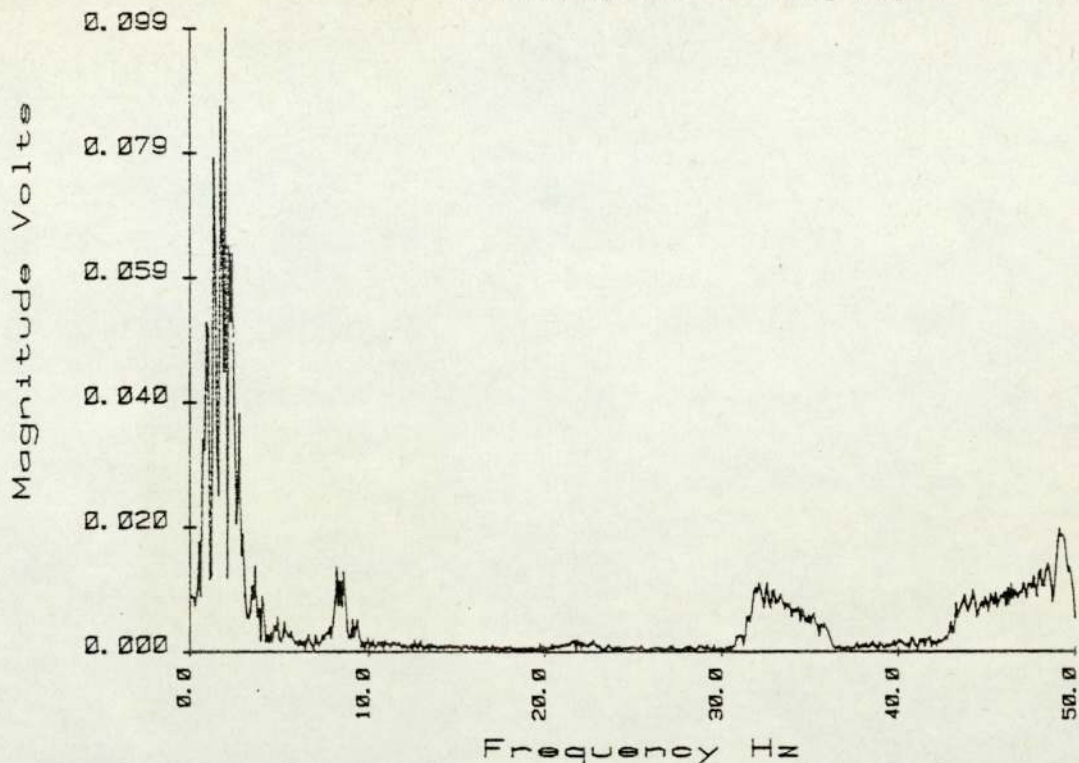


FIG 5.38 RESPONSE CURVE AND WAVE FORM
 Speed ratio 7:5. Shutting down the motor
 to zero speed. Picking signal position 1.



Magnitude Volts

FIG 5.39 Response curve and wave form.
speed ratio 7:5 . Motor running at
maximum speed. Picking up signal
position 1.

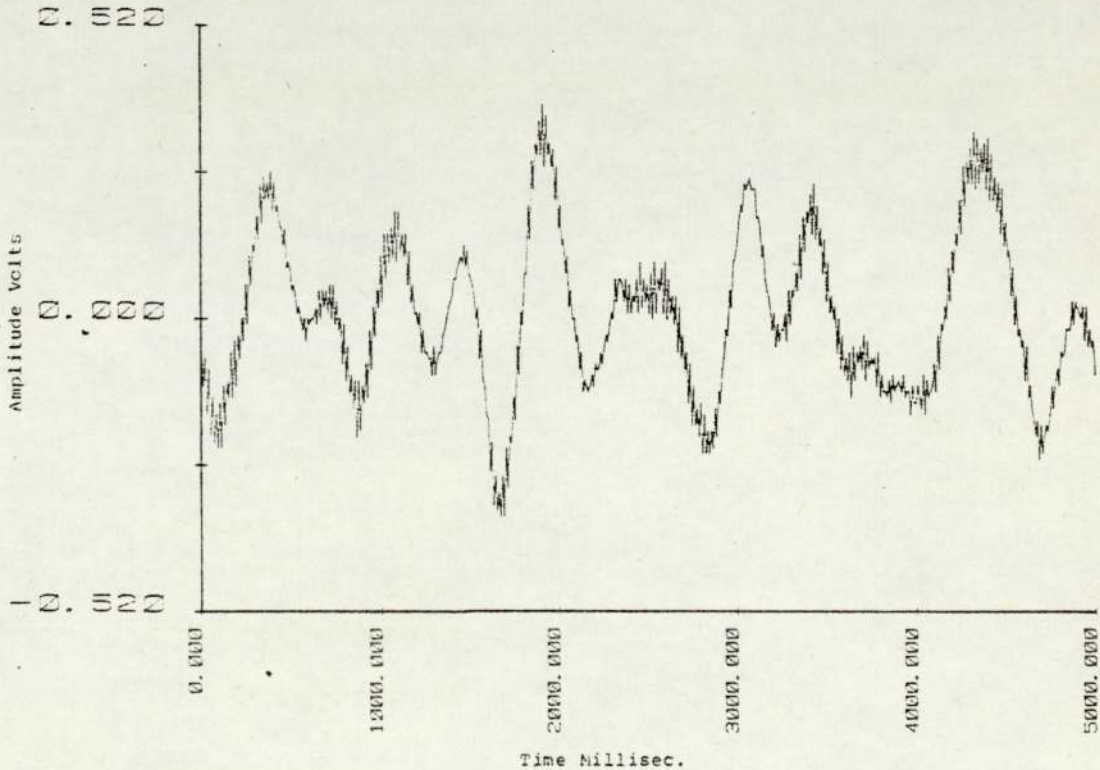
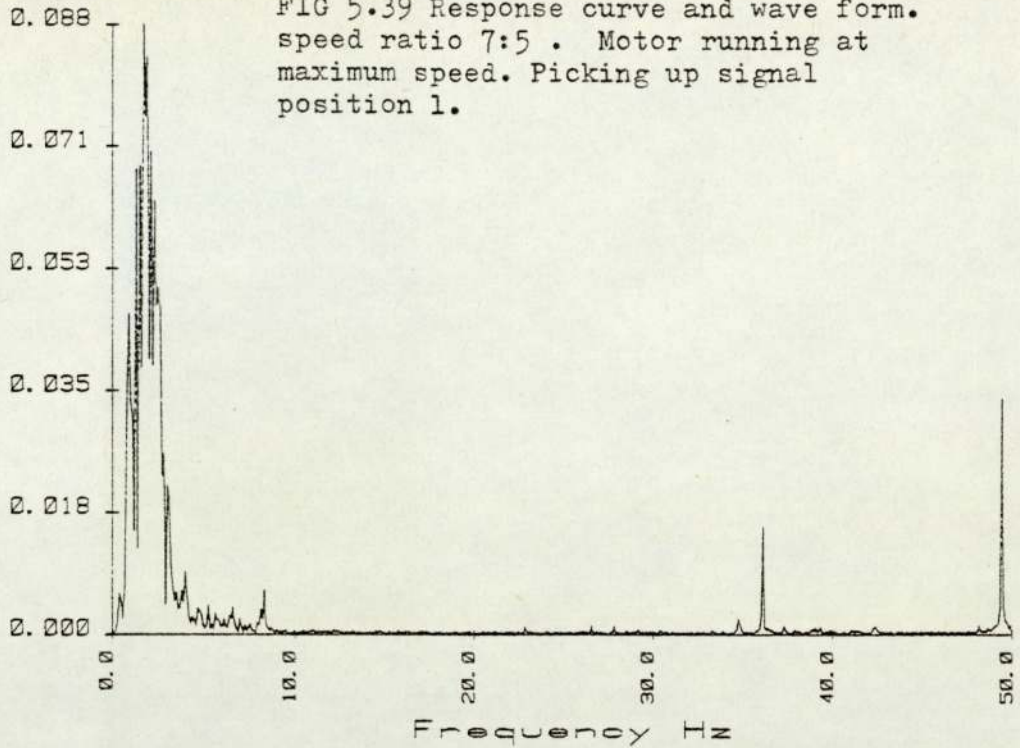


FIG 5.40 RESPONSE CURVE AND WAVE FORM
 Speed ratio 7:5. Motor running at 35 Hz.
 Picking signal position 1.

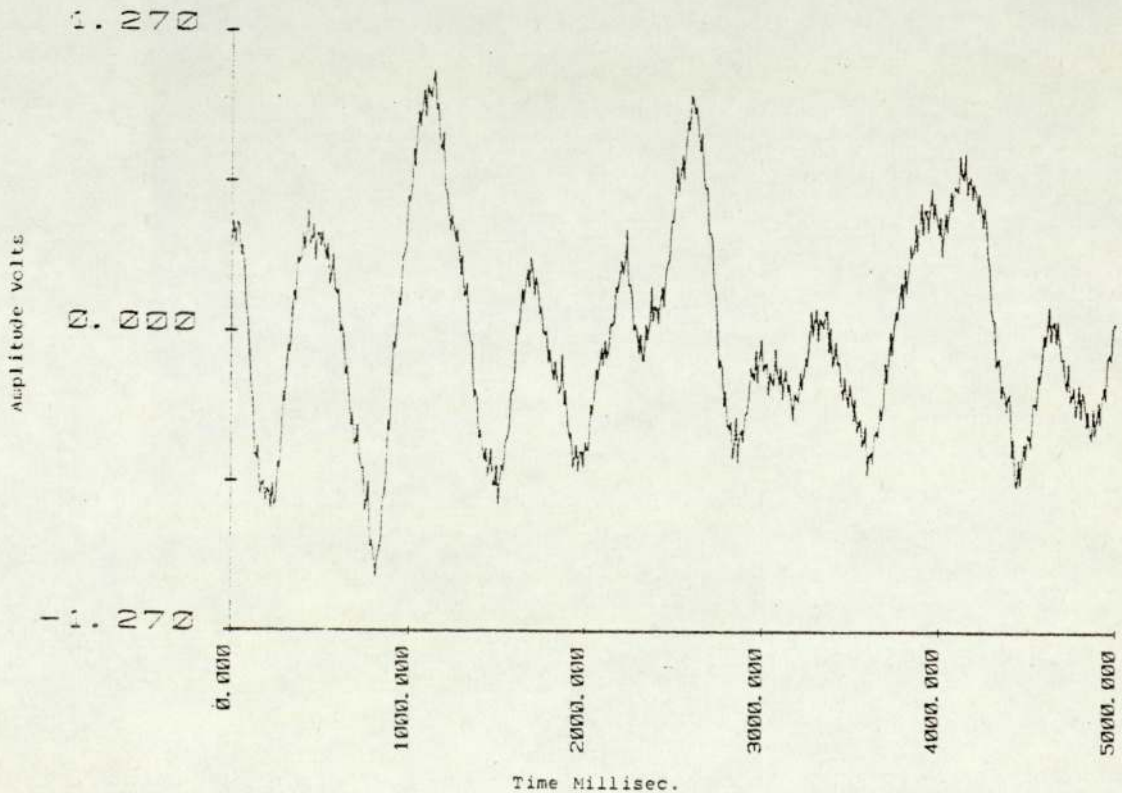
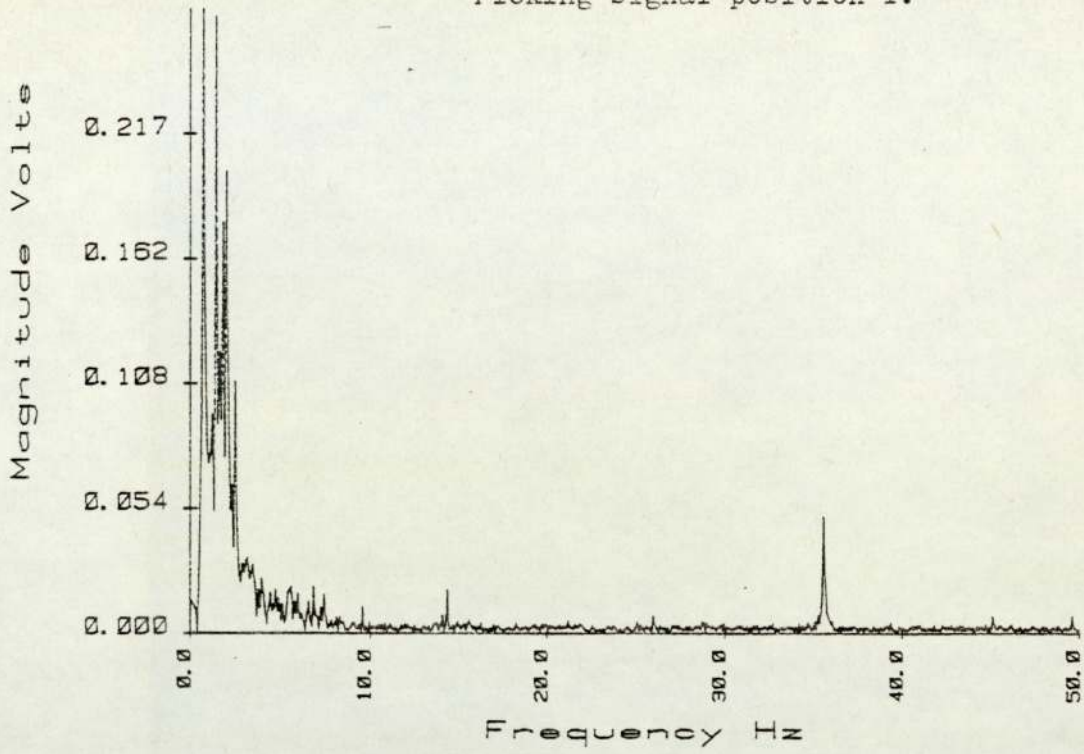
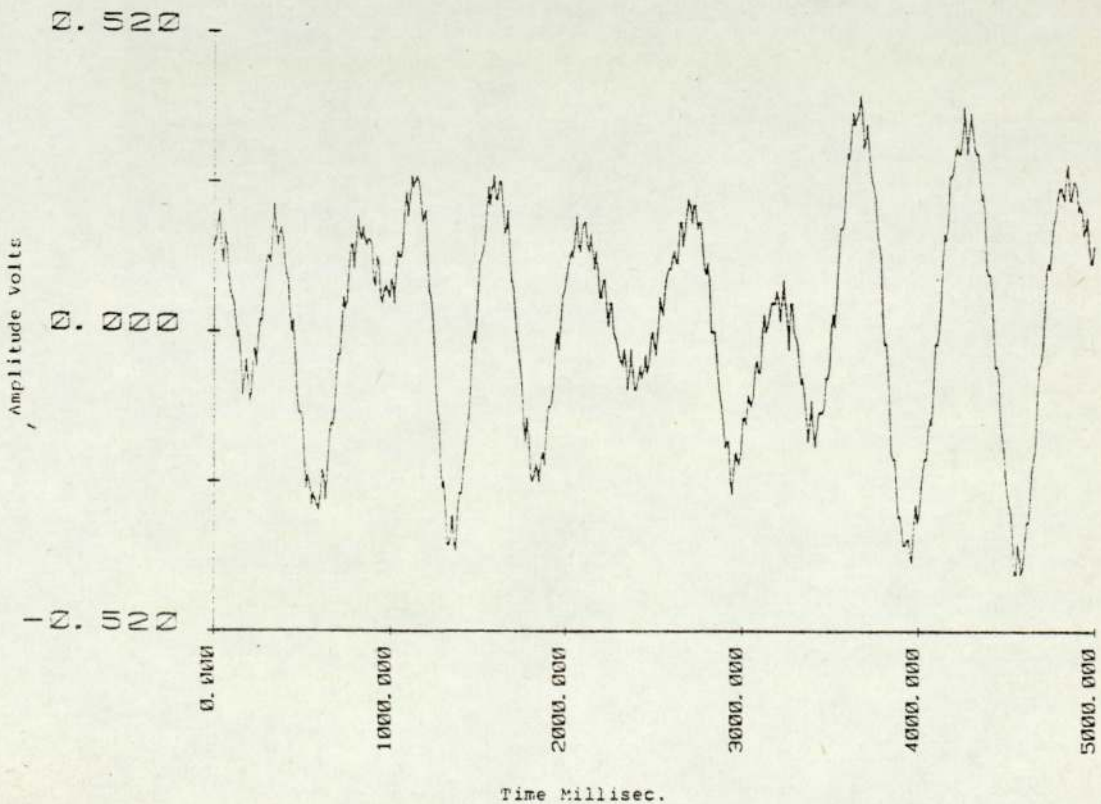
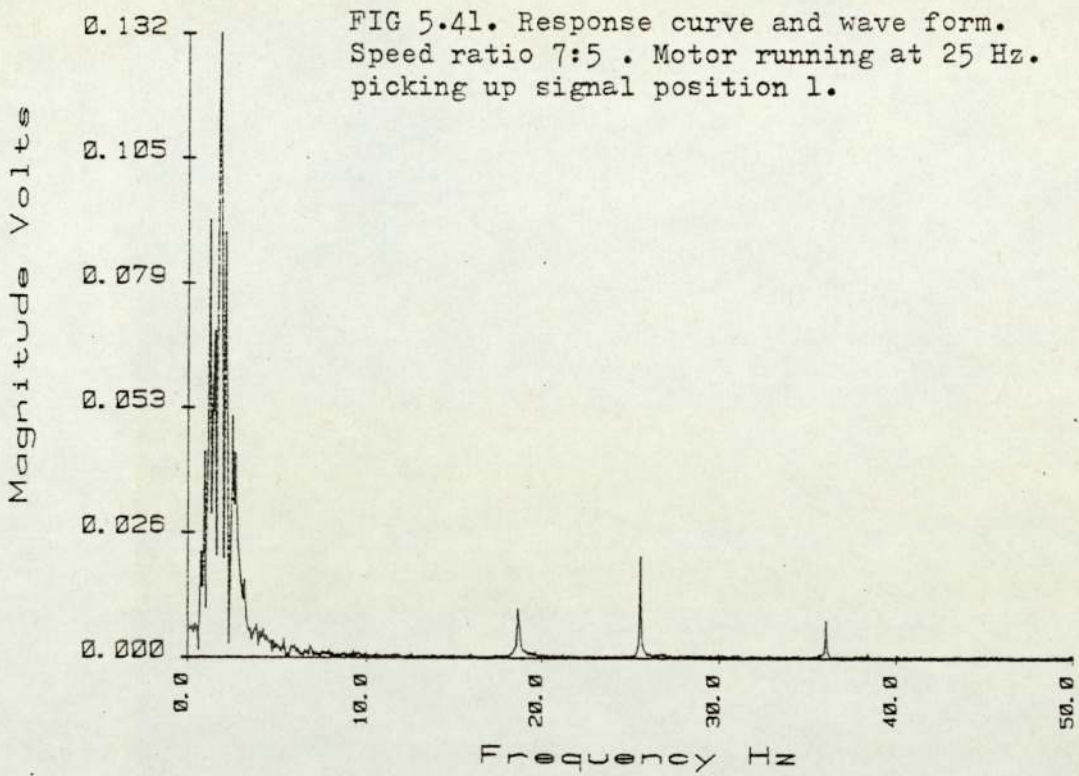


FIG 5.41. Response curve and wave form.
Speed ratio 7:5 . Motor running at 25 Hz.
picking up signal position 1.



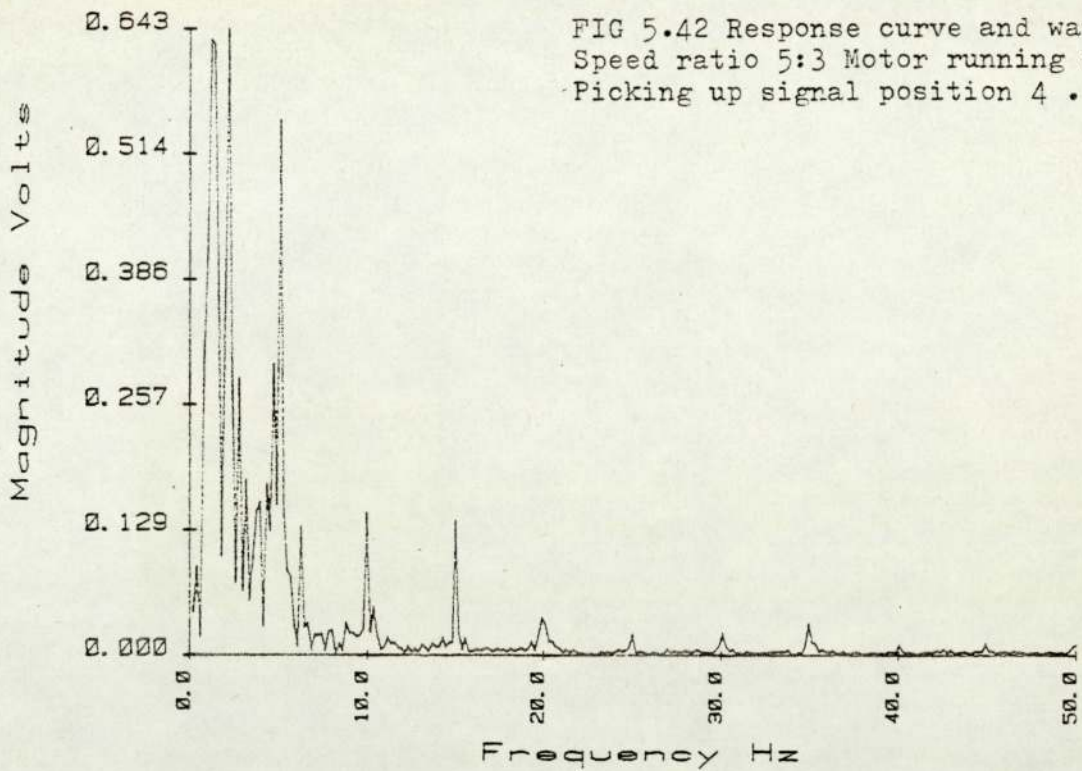
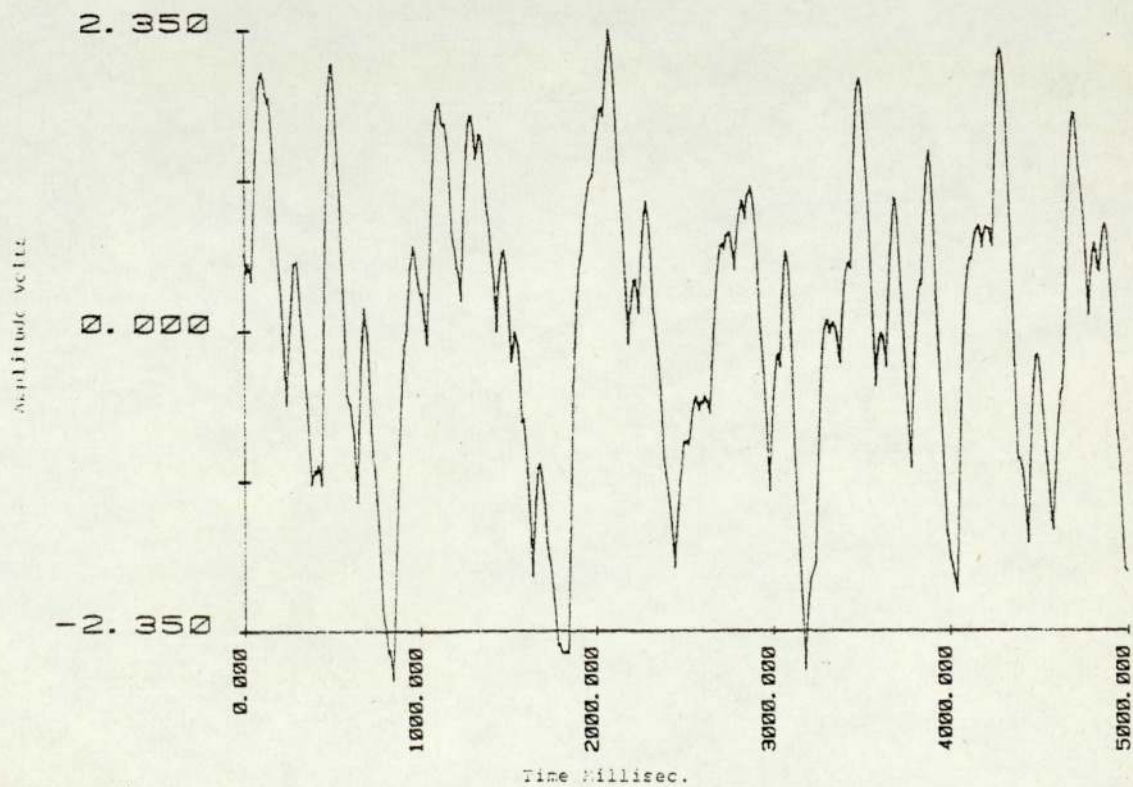


FIG 5.42 Response curve and wave form .
Speed ratio 5:3 Motor running at 35 Hz .
Picking up signal position 4 .



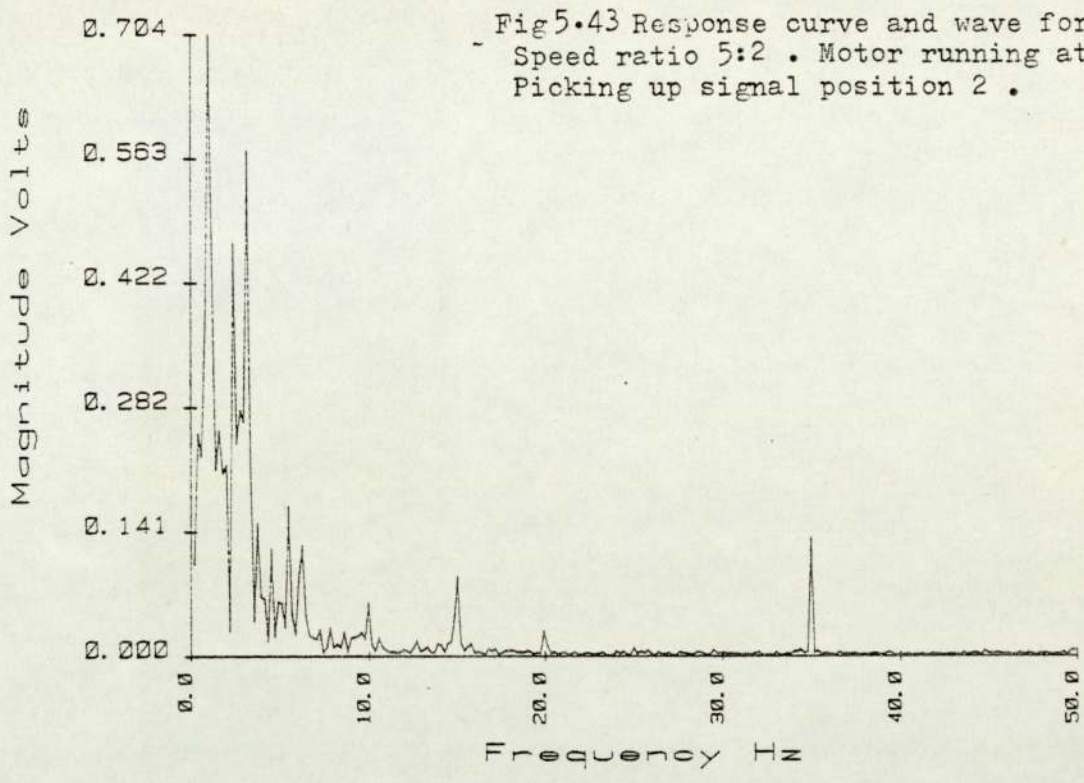
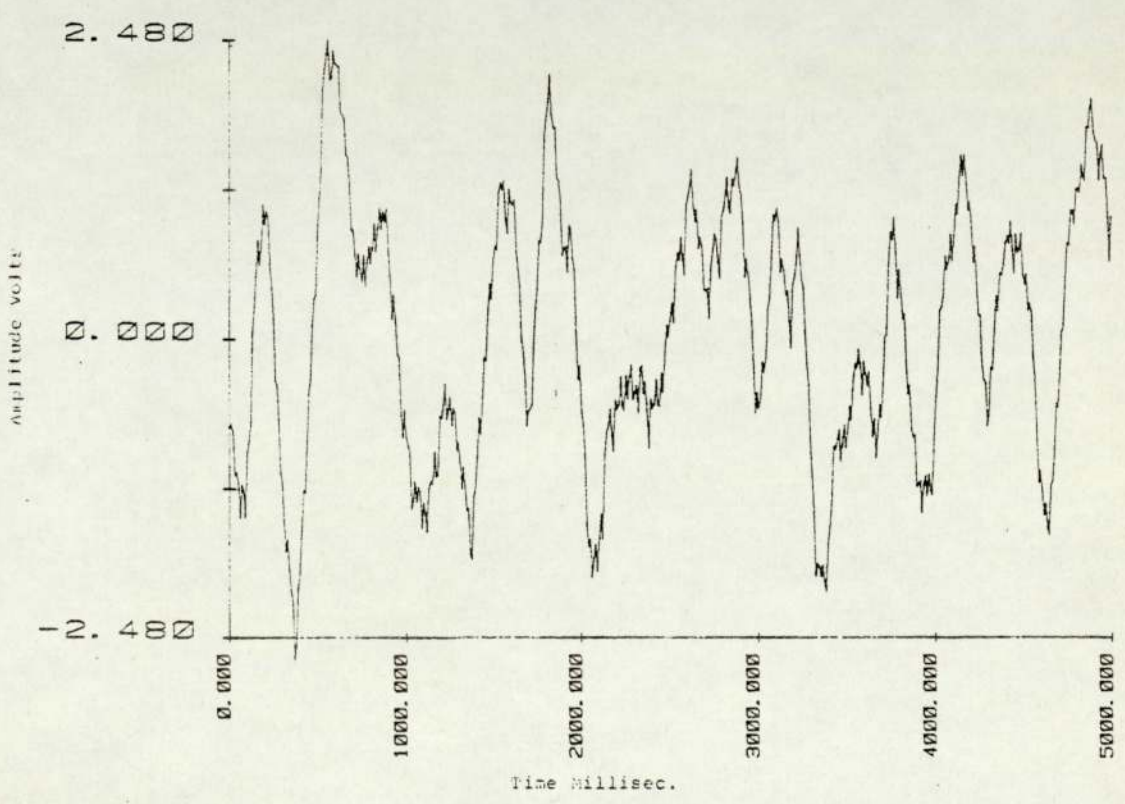
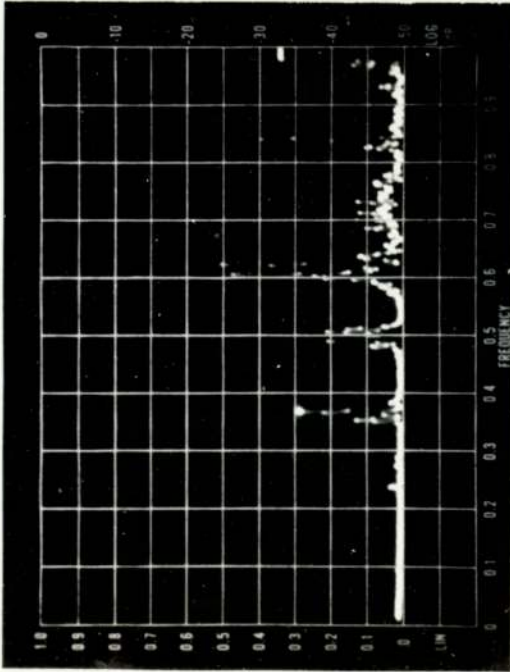


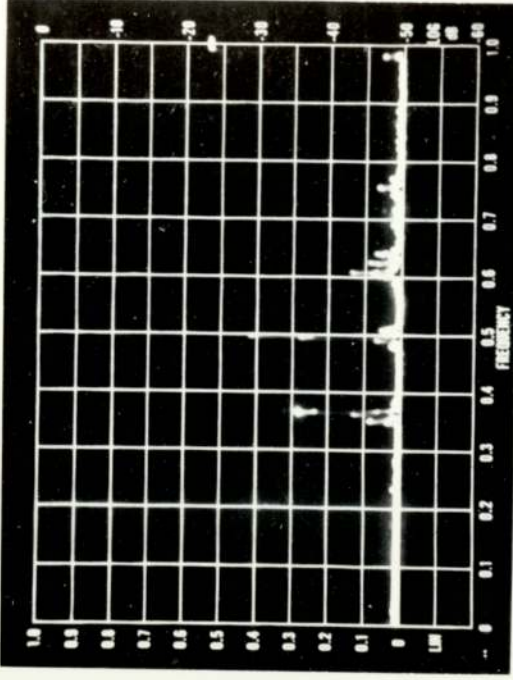
Fig 5.43 Response curve and wave form.
Speed ratio 5:2 . Motor running at 35Hz.
Picking up signal position 2 .



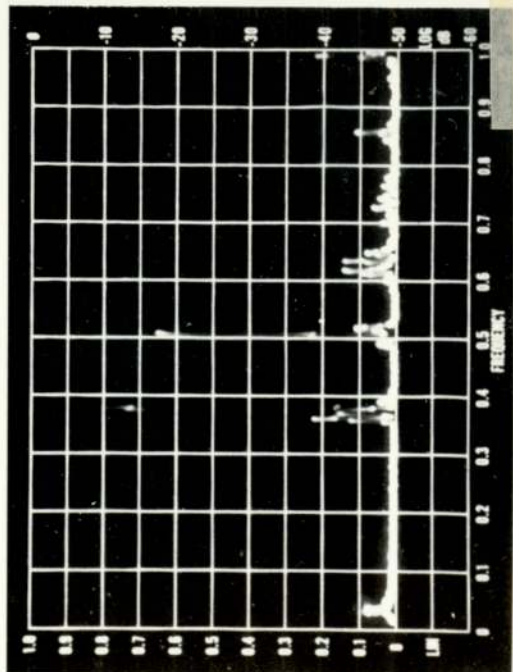
Case(1)



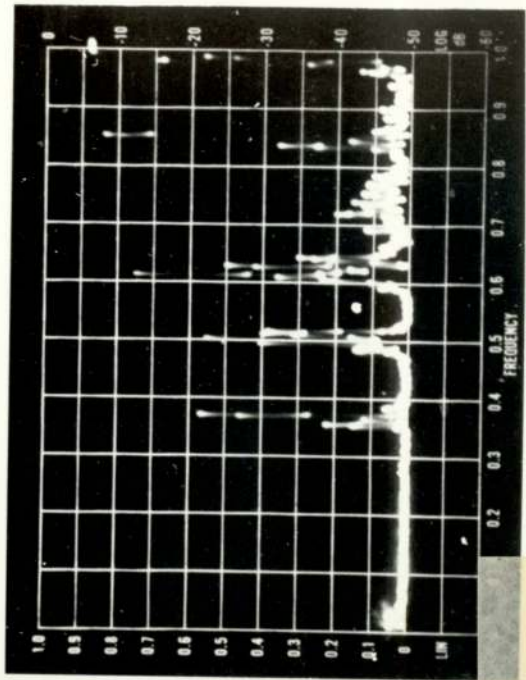
A



B



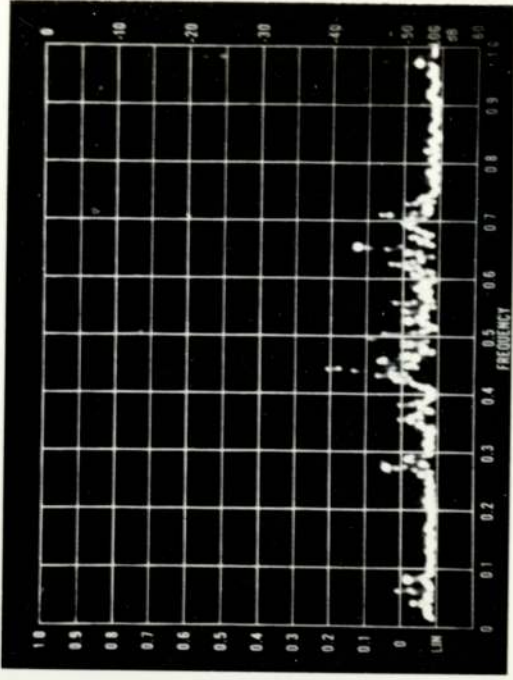
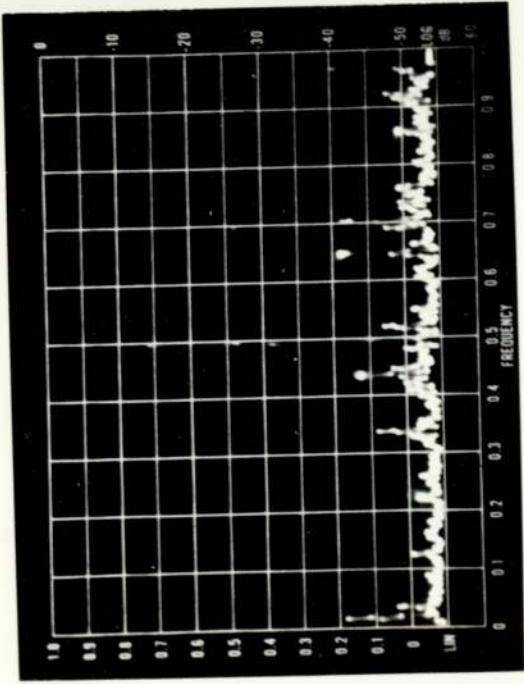
C



D

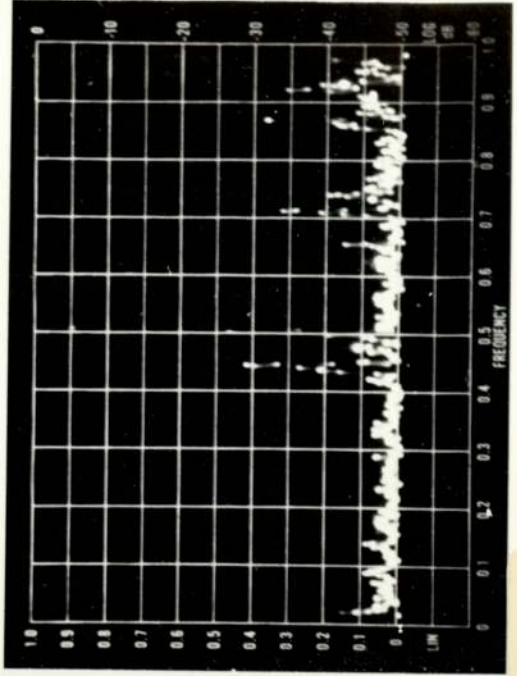
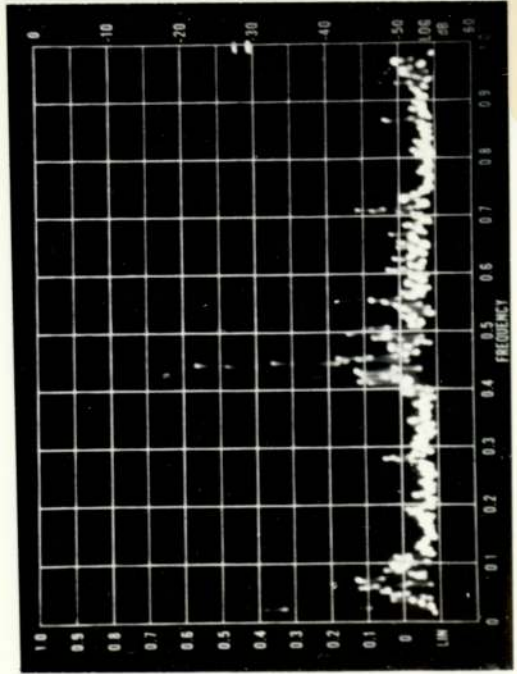
Fig. 5.44 The relationship between the modes and their spectral components. Speed ratio 7:5

Case (2)



A

B

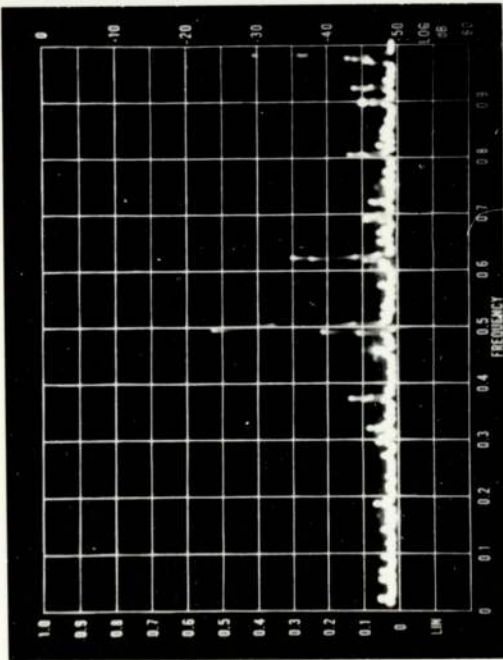


C

D

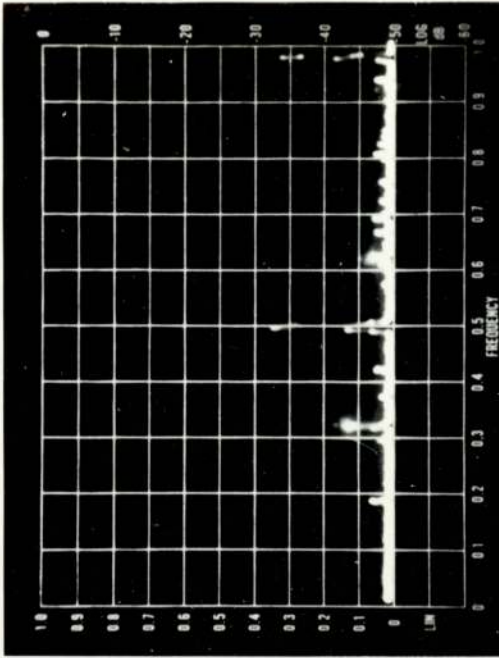
Fig. 5.45 The relationship between ghe modes and their spectral components. Speed ratio 5:3.

Case (3)

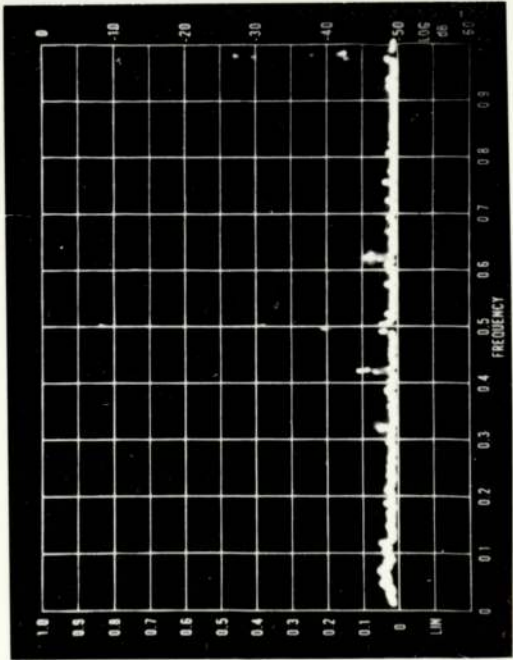


A

B



C



D

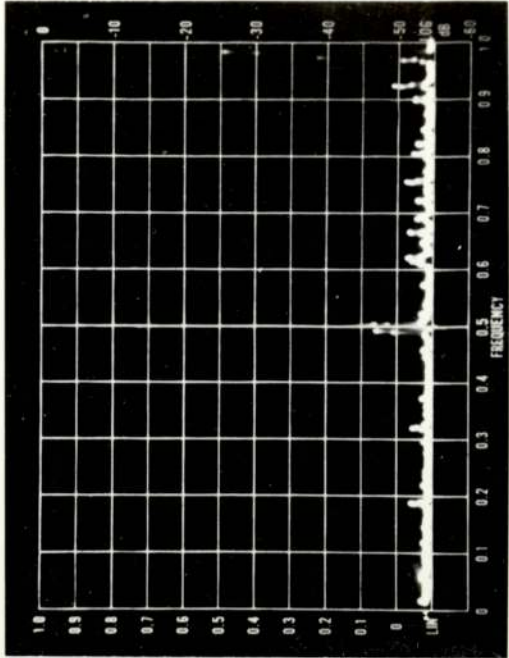
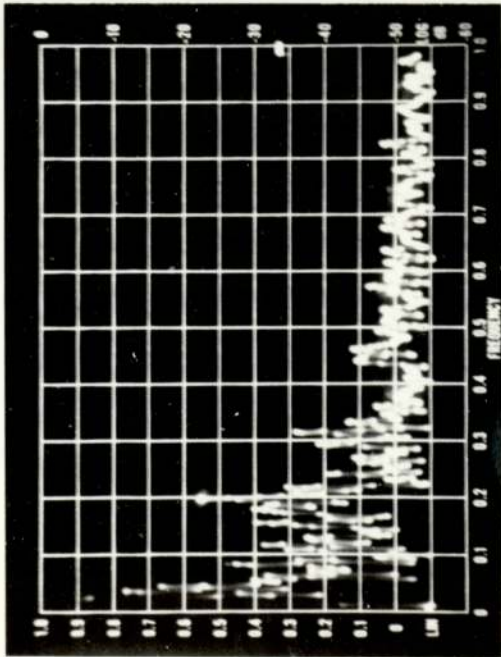
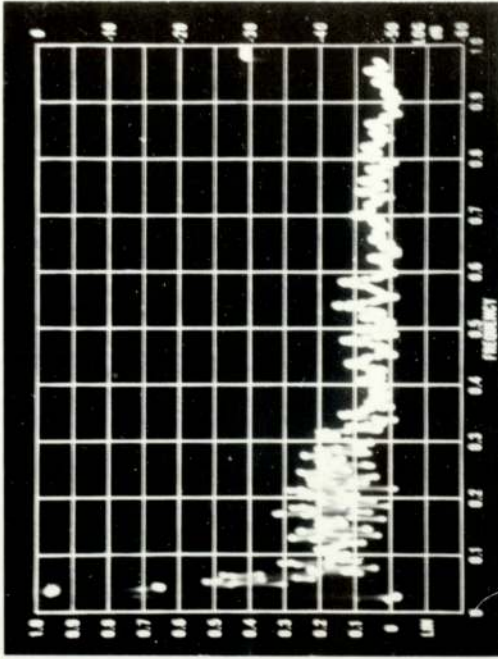


Fig. 5.46 The relationship between the modes and their spectral components. Speed ratio 3.7

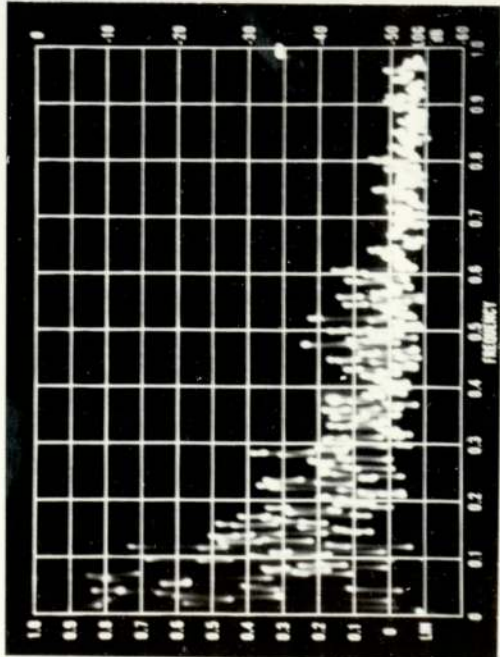
Case (4)



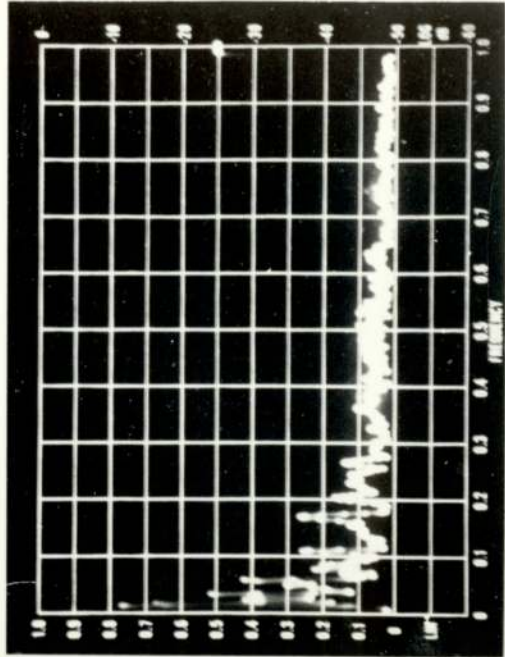
A



B



C

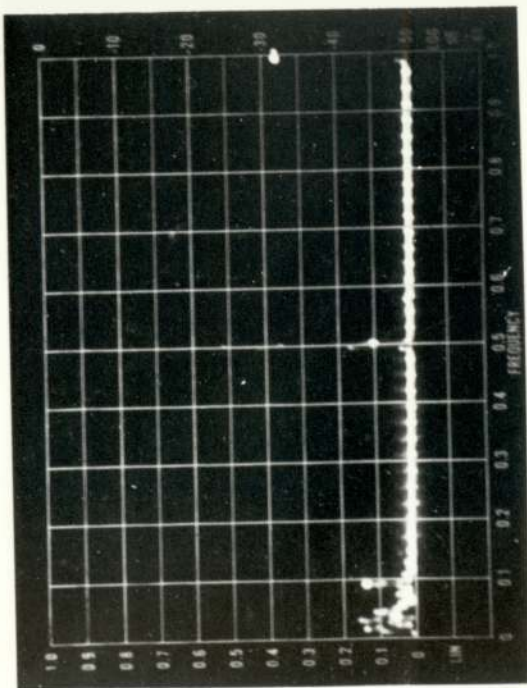


D

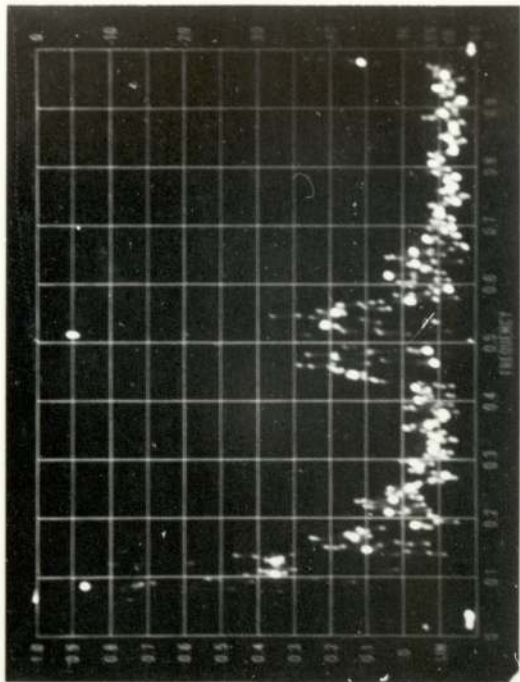
Fig. 5.47 The relationship between the modes and their spectral components. Speed

Case (5)

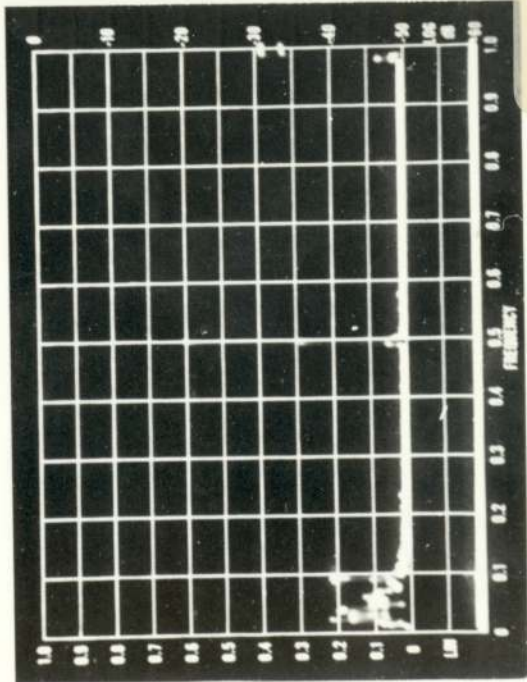
A



B



C



D

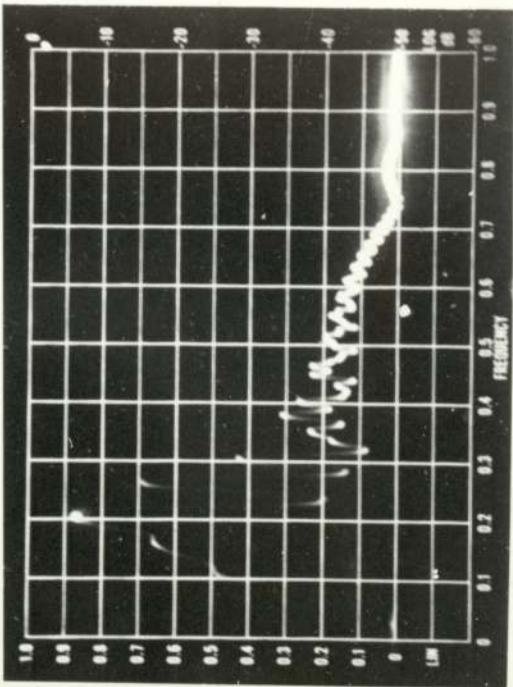


Fig. 5.48 The relationship between the modes and their spectral components. Just the motor running at maximum speed

applied load = 218.499 KGF
 deflection in mm.

1 = 0.132

2 = 0.022

3 = 0.013

4 = -0.0055

5 = 0.106

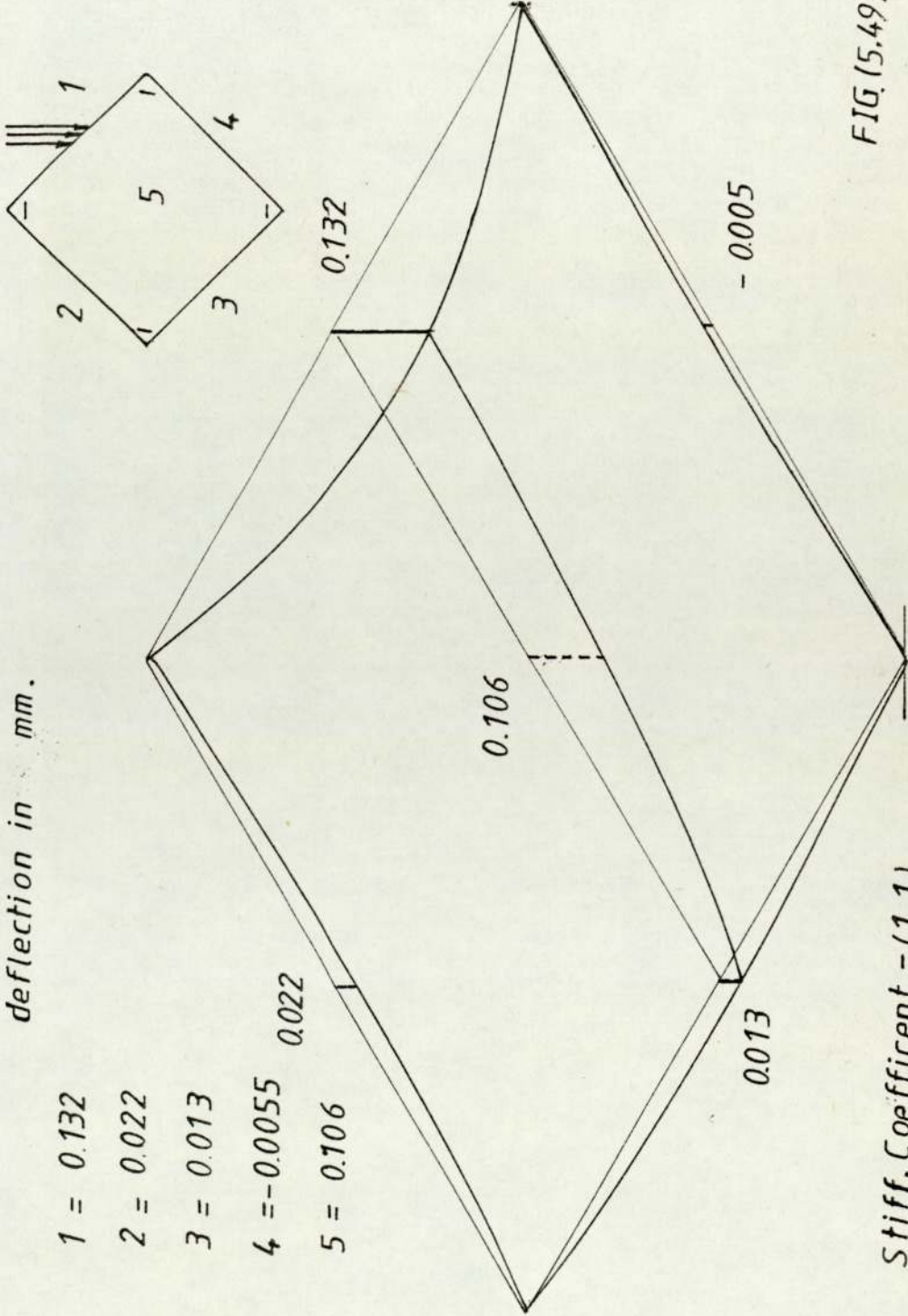


FIG (5.49)

Stiff. Coefficient = (1,1)
 = 218.499 / 0.132
 = 1655.2954 KGF/mm.

LOAD DEFLECTION CURVE
 FOR STRUCTURE SUPPORTED BY
 FOUR KNIFE EDGES.

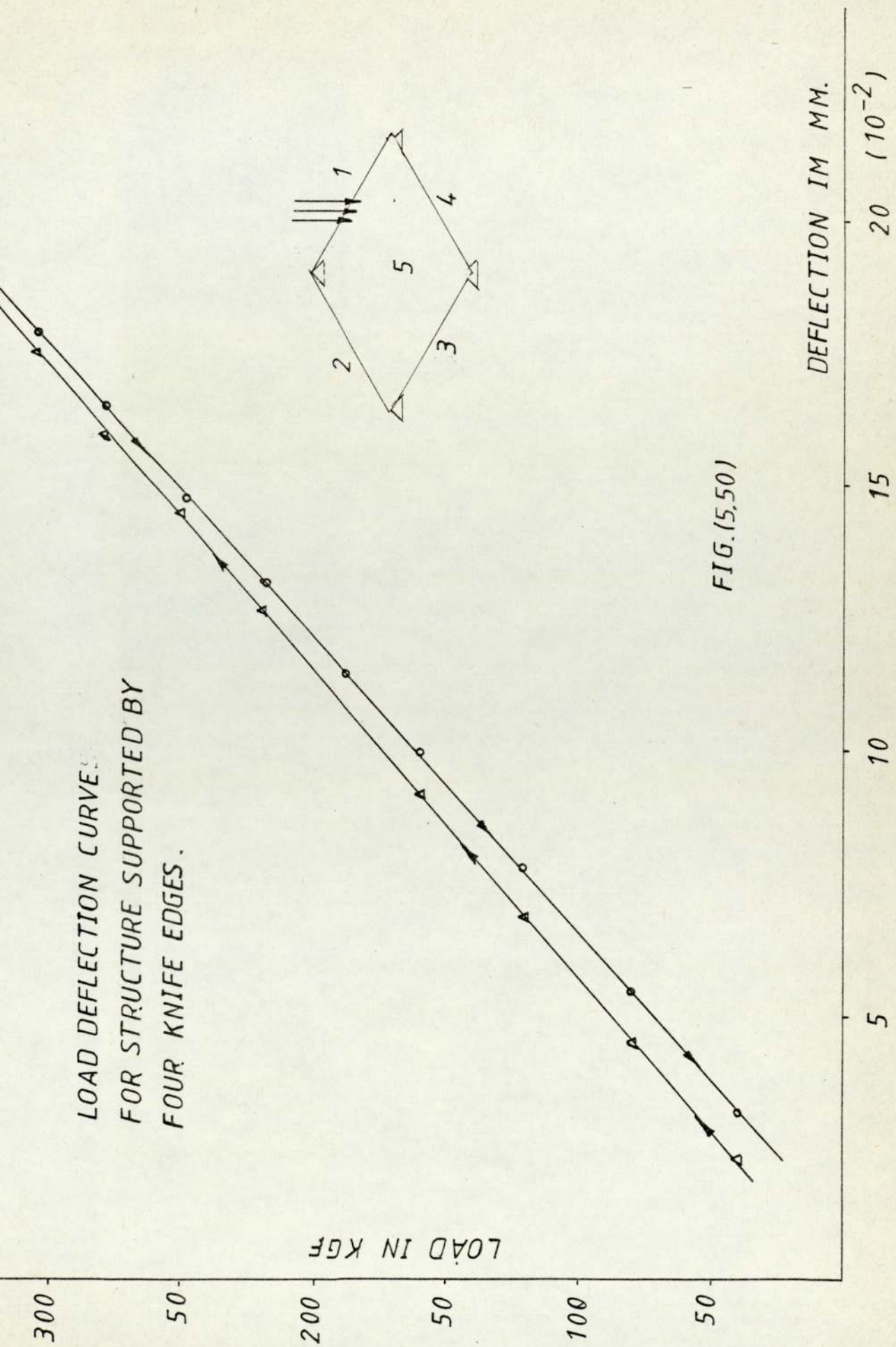
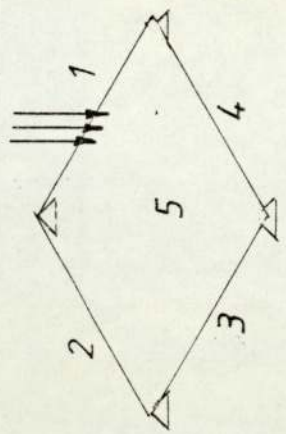
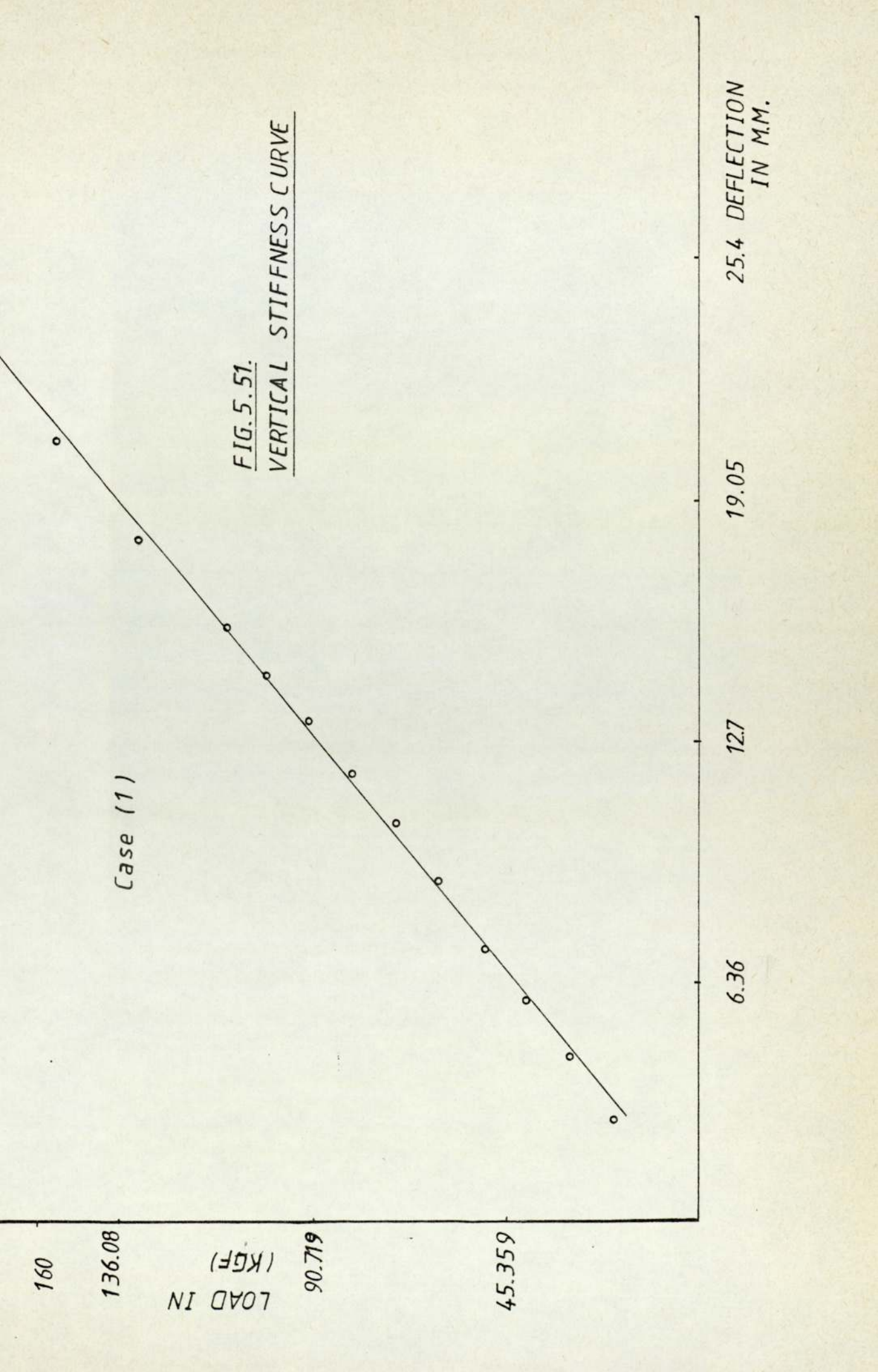
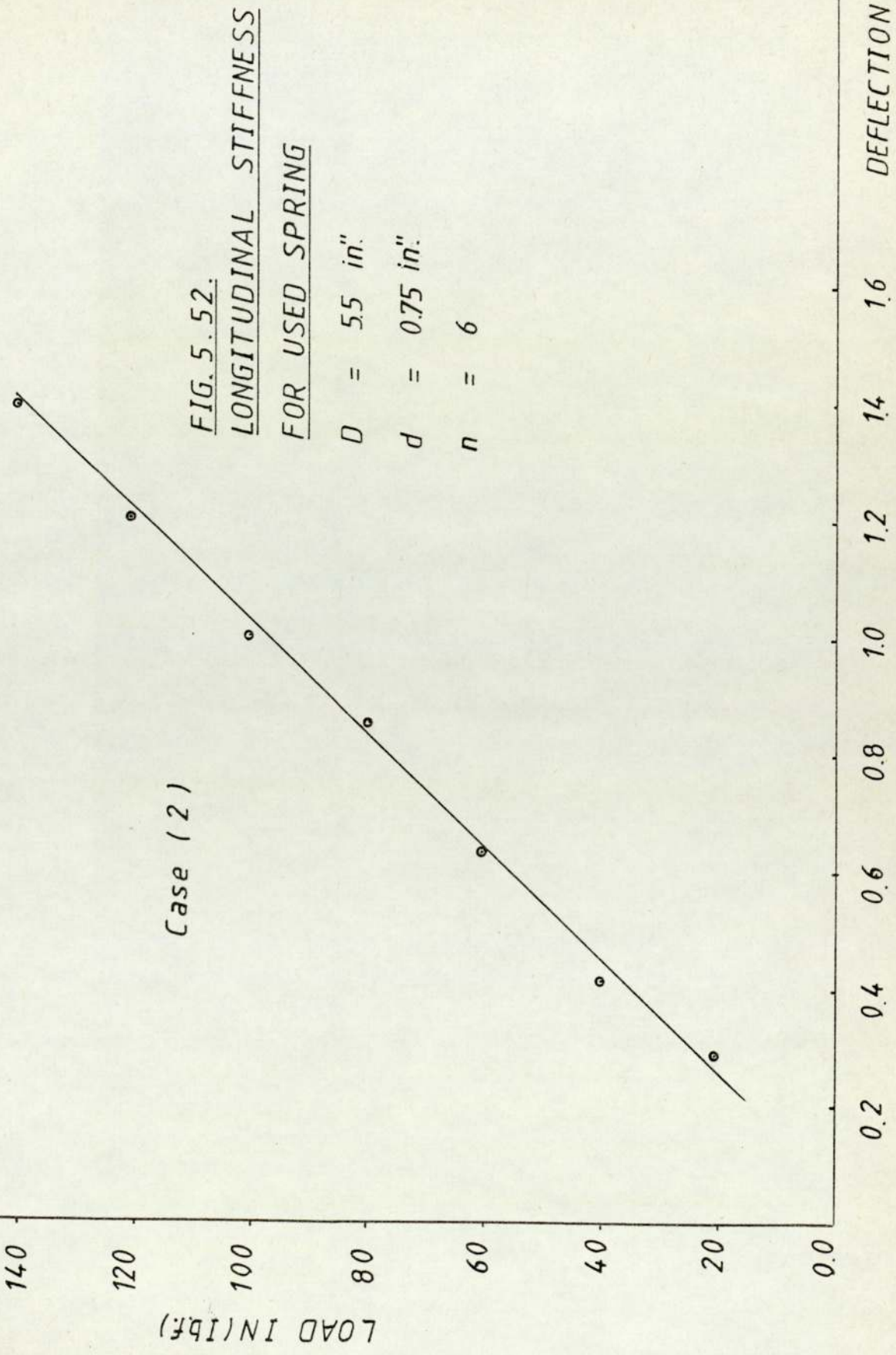


FIG. (5.50)







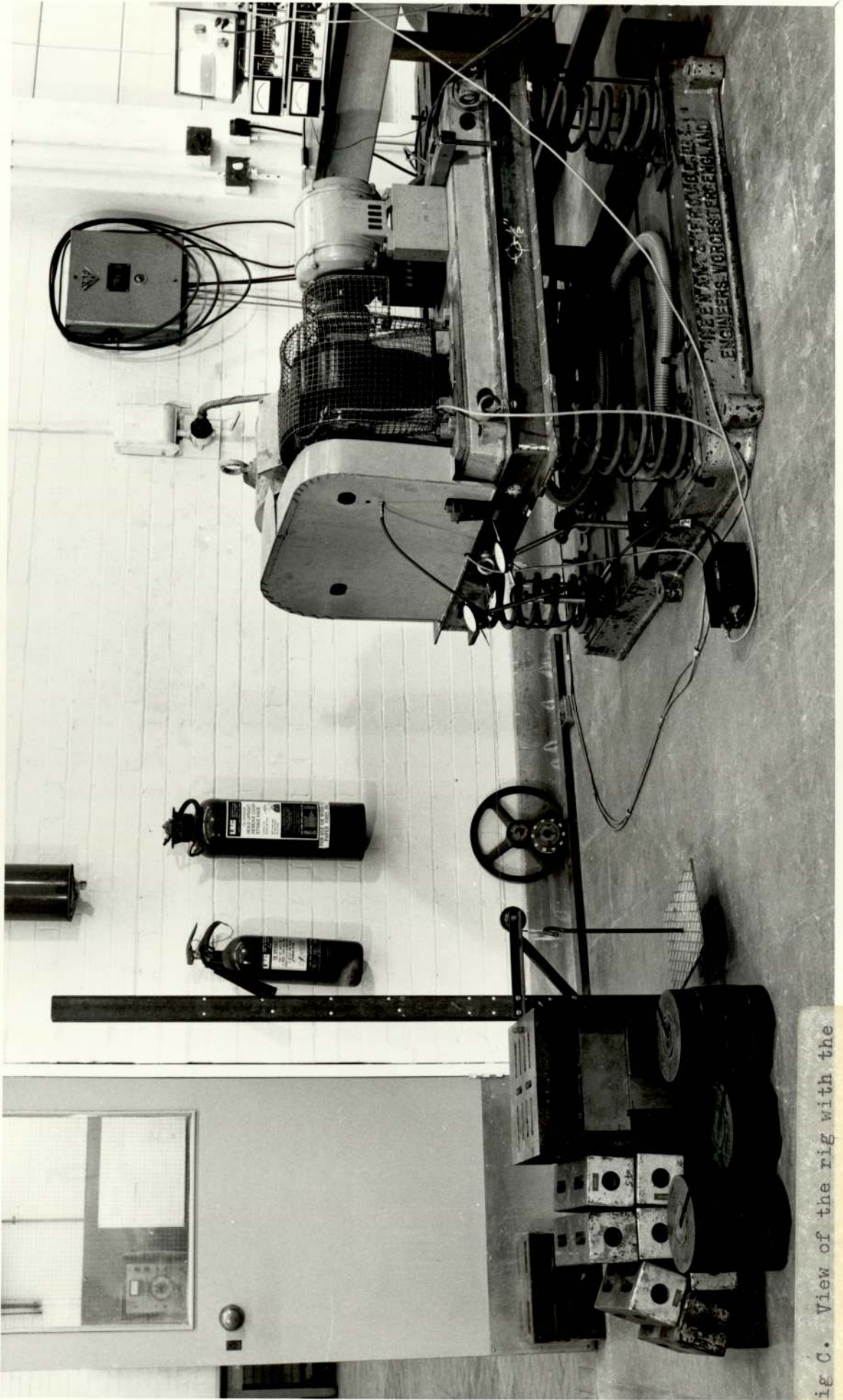


Fig C. View of the rig with the equipment to measure the sideways stiffness of the spring

Case (3)

200

LOAD IN KGf.

150

100

50

0.0

0.0 1 2 3 4 5 IN MM --- (A)

10 20 30 " " — (δ)

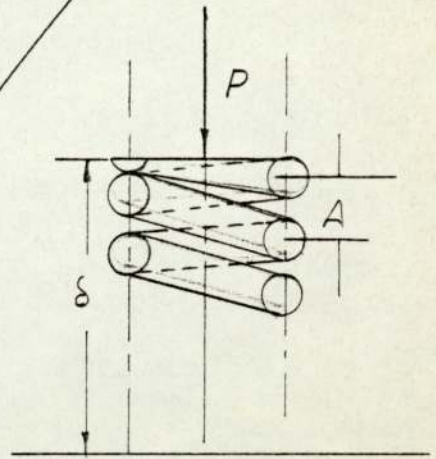


FIG. 5. 53. LOAD DEFLECTION CURVE ○—○

LOAD DEF. FOR FRIST AND SECOND COILS □—□

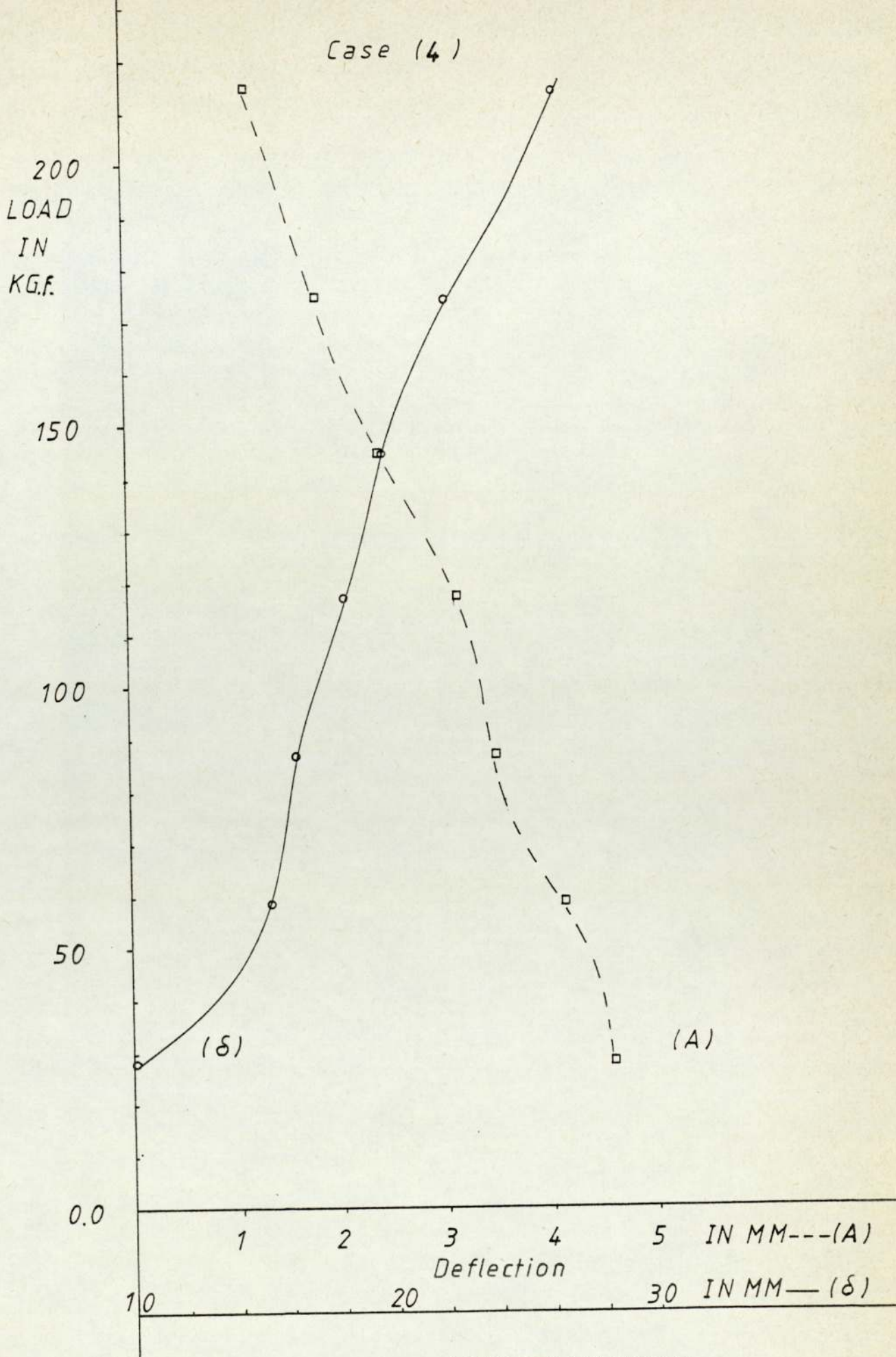


FIG. 5.54. LOAD-DEFLECTION CURVE ○—○
LOAD DEF. FOR FRIST AND SECOND COIL □---□

The Relation between the Modes and its
harmonics Tables 5.1 to 5.5

Table 5.1

<u>Case 1</u>		Modes, Hz	Range of higher harmonics Hz
Photograph	A	23	46.69
"	B	36.4	72.6
"	C	1.8	36, 61.2, 63
"	D	1.6	60.8

Table 5.2

<u>Case 2</u>		Modes, Hz	Range of higher harmonics Hz
Photograph	A	2.6	15.8, 33.8
		8.2	16.4, 24.4
		12.0	48
		17.6	52.8
"	B	2.4	26.4
		6.6	26.4, 66.0
"	C	1.8	9.2, 34.4, 41.4
		4.6	9.2, 41.4
		8.2	16.4, 74
"	D	15.8	47.4, 63.2

Table 5.3

<u>Case 3</u>		Modes, Hz	Range of higher harmonics Hz
Photograph	A	4.2	8.4
		5.4	10.8
		8.2	49.2
		9.2	36.8
		18.2	36.8
		22.8	45
"	B	10.0	20, 50
		12.4	24.8, 49.8
"	C	31.4	62.0
		8.8	17.8
"	D	31.4	62.8
		28.8	57.6
		31.4	62.8

Table 5.4

Case 4		Modes, Hz	Range of higher harmonics, Hz
Photograph	A	0.4	8.4
		4.0	8.0
"	B	1.2	6.4, 26.2
		1.4	11, 15.4
		3.0	9.0
		5.2	15.4
		7.4	29.4
"	C	5.2	15.6
		6.8	47.6
		8.6	17.2, 25.8, 34.4
		9.4	37.4
		16.4	33.0
"	D	2.4	26.2, 36
		5.0	15.0, 20.0, 30.0
		7.8	38.4
		8.0	24
		9.0	36
		12.0	24, 36

Table 5.5

Case 5		Modes, Hz	Range of higher harmonics, Hz
Photograph	A	8.2	50
"	B	2.2	9.2
"	C	2.8	8.4
"	D	1	6, 10.8
		1.8	9, 10.8
		2.2	9.2
		2.0	8.0

Table 5.6

Classification of possible resonances

Type of Resonance	Exciting Frequency ω is close to	Ratio of the Natural Frequencies Ω_1/Ω_2		Notation
		differs sufficiently from	is close to	
a) Pure main Resonance	Ω_j	m/k	-	$j=1,2$
b) Sub-harmonic Resonance	$N\Omega_j$			$m,k=1,2,3$
c) Ultra-harmonic Resonance	$\frac{1}{n}\Omega_j$			$m \neq k$
d) Sub-ultra-harmonic Resonance	$\frac{N}{n}\Omega_j$			$n, N=2,3$
e) Internal Resonance	Ω_j	-	m/k	for a) $\frac{N}{n}, \frac{n}{N} \neq 1, 2, \dots$
f) Non-periodic Combination Resonance	$\frac{N\Omega_1 + M\Omega_2}{n}$	m/k	-	$j=1,2$ $N, M = \pm 1, \pm 2, \dots$ $m, k = 1, 2, 3$
g) Periodic Combination Resonance	$\neq \Omega_j$	-	m/k	$m \neq k$

Table 5.7

The Vibrations displayed the following tendencies

Side band frequencies	Centre frequencies	Side band frequencies	Harmonic Zone No.
-	0	$(\omega_2 - \omega_1)$	0
$(2\omega_1 - \omega_2)$ ω_1		ω_2 $(2\omega_2 - \omega_1)$	1
$(3\omega_1 - \omega_2)$ $2\omega_1$	$(\omega_1 + \omega_2)$	$2\omega_2$ $(3\omega_2 - \omega_1)$	2
$(4\omega_1 - \omega_2)$ $3\omega_1$	$(2\omega_1 + \omega_2)$ $(\omega_1 + 2\omega_2)$	$3\omega_2$ $(4\omega_2 - \omega_1)$	3
	etc		

Tables 5.8 & 5.9 Measuring the stiffness coefficient of the structure

Table 5.8

Point	Applied Load	Deflection
	(Kgf)	mm
1	218.499	0.132
2	-	0.022
3	-	0.013
4	-	-0.0055
5	-	0.106

Table 5.9

Reading No.	Applied Load in Kgf	Reading Position in mm.					
		1	2	3	4	5	
0	0	0	0	0	0	0	
1	40.028	0.023	0.003	0.004	0.002	-0.021	
2	80.014	0.045	0.005	0.005	0.004	-0.070	
3	120.00	0.069	0.008	0.009	0.005	-0.075	
4	159.772	0.092	0.010	0.013	0.006	-0.072	
5	188.636	0.118	0.012	0.013	0.008	-0.105	
6	218.499	0.127	0.014	0.013	0.009	-0.102	
7	247.419	0.145	0.016	0.0135	0.005	-0.101	
8	277.092	0.160	0.185	0.0120	0.001	-0.095	
9	306.75	0.175	0.023	0.015	-0.001	-0.095	
10	336.41	0.193	0.0285	0.016	-0.002	-0.095	
Reversing the load from maximum to minimum							
11	9	306.751	0.179	0.0285	0.0160	-0.002	0.095
12	8	277.092	0.165	0.0250	0.0150	-0.004	0.100
13	7	247.419	0.148	0.0240	0.0150	-0.005	0.105
*14	6	218.499	0.132	0.0220	0.0130	-0.0055	0.106
15	5	188.636	0.115	0.0195	0.0170	+0.002	0.105
16	4	159.772	0.100	0.0180	0.0150	+0.001	0.110
17	3	120.000	0.079	0.0150	0.0170	+0.003	0.115
18	2	80.014	0.055	0.0120	0.0150	+0.006	0.116
19	1	40.028	0.32	0.010	0.0150	+0.008	0.119
20	0	0.00	0.008	0.008	0.0120	+0.010	0.121

TABLES 5.10 to 5.13

Table 5.10

MEASURING SPRING STIFFNESS

Loading No.	APPLIED LOAD	DEFLECTION	EFFECTED DEFLECTION IN EVERY STEP	TOTAL STIFFNESS	EFFECTED STIFFNESS IN EVERY STEP
1	22.4	0.060	0.060	373.333	373.333
2	44.8	0.110	0.050	407.272	448
3	67.2	0.174	0.064	386.206	350
4	89.6	0.234	0.060	382.905	373.333
5	112	0.286	0.052	391.608	430.769
6	134.4	0.352	0.066	381.818	339.393
7	156.8	0.412	0.060	380.582	373.333
8	179.2	0.465	0.053	385.376	422.641
9	201.5	0.5195	0.0545	387.872	411.009
10	224	0.5695	0.050	393.327	448.00
11	246.4	0.6195	0.050	397.740	448.00
12	268.8	0.6680	0.0485	402.395	461.855
13	291.2	0.7125	0.0445	408.701	503.370
14	313.6	0.7615	0.049	411.818	457.142
15	336.0	0.8166	0.0551	411.432	406.533
16	358.4	0.8749	0.0583	409.647	384.219
17	380.8	0.9249	0.050	411.720	448.00
18	403.2	0.9729	0.048	414.431	446.666
19	425.6	1.0239	0.051	415.666	439.215
20	448	1.0744	0.0505	416.977	443.564

Table 5.11

MEASURING LONGITUDINAL STIFFNESS (Case 2)

Read No	Applied Load (lb _f)	Deflection in
1	20	0.290
2	40	0.413
3	60	0.640
4	80	0.861
5	100	1.086
6	120	1.20
7	140	1.41

Table 5.12 INCREASING THE LOAD (Case 3)

No of Loading	Load in (Kg _f)	A in mm	δ in mm
1	28.920	4.60	10.00
2	58.480	4.18	13.49
3	87.340	3.57	15.16
4	116.970	3.45	15.55
5	145.830	2.56	21.70
6	174.690	2.00	25.50
7	214.718	1.13	31.80
8	245.580	0.38	36.10

Table 5.13 DECREASING THE LOAD (Case 4)

No of Loading	Load in (Kg _f)	A in mm	δ in mm
1	28.920	4.58	10.50
2	58.480	4.16	15.40
3	87.340	3.50	16.30
4	116.970	3.16	18.20
5	145.830	2.42	19.70
6	174.690	1.88	22.20
7	214.718	1.18	26.50
8	354.480	0.44	33.00

CHAPTER 6

DISCUSSION AND CONCLUSIONS

In this study, the results of both theoretical and experimental investigations carried out on a spring supported flexible platform carrying rotating machinery, indicate the vibration characteristics, dynamic response and elucidating conditions which favour the building up of excessive vibration when the unit is in operation with different speed ratios.

Many classical methods for determining the natural frequency exist but these do not give reliable or accurate results.

A new method of approach is needed to study the natural frequencies and the mode shapes. One of the main differences between the classical approach and the new one is that the new one takes into consideration the flexibility of the platform.

The structure studied was a platform belt driven unit of the frame type. The unit consisted of two machines, one of them with a very rigid base whilst the second machine had a more flexible base. Both were fixed on a frame.

The numerical techniques incorporated a computer programme developed for calculating the natural frequencies and the mode shapes.

A single programme for the solution of each parameter was developed initially and then combined into one programme. Using this programme, it is possible to study various vibration characteristics of the structure under consideration. Continuous structures have an infinite number of modes of vibration, but generally only the lowest of these are of importance in low frequency vibrations.

The techniques employed in this work were the Finite Element Method for the solution of the structural vibration problem, the derivation of consistent stiffness and mass matrices of structural elements.

Although our analytical capability has vastly improved, response time is still inadequate for design purposes, and there is a requirement for a simplified numerical technique. The present need would appear to be to develop an integrated design system based on these improved analytical capabilities. It is hoped that the experiences described here may be of some value to those who are involved in such design tasks.

The three rigid body modes and the plate mode are shown in Figs.(5.9), (5.10), (5.11) and (5.12) respectively to enable a comparison to be made between these and the theoretical results derived from the computer programme. These were found to be in good agreement. The values of these measurements are given in Fig.(5.13)

The first 'plate' modal shape Fig.(5.14) is built up of a bending motion between the motor and alternator, and a 'torsion' motion between the motor and alternator ends

of the frame. When the vibration in the first mode was viewed in the light of a stroboscope, the main apparent motion between the motor and the alternator was the 'bending' mentioned.

The second plate modal shape is mainly due to a torsion motion between the motor and the alternator Fig. (5.15). This was also apparent using the stroboscope. From the figure there is also evidence of a bending motion between the frame 'corner' shown and the opposite 'corner'.

This bending motion in the second mode then becomes the main motion in the third mode.

The phenomena listed below were caused by the presence of non-linearity in the system.

In this phenomenon a rigid body frequency was being excited when the forcing frequency was a harmonic of the Rigid Body Frequency.

With single forcing it was easy to show that the above was probably due to the fact that the transient of a non-linear system contained harmonics of its fundamental frequency, and that it was these harmonics which were being forced. The analogy would necessitate there being non-linearity in the flexible supports of the model, and in the static deflection test. This did indeed appear to be the case.

In this phenomenon a Rigid Body Frequency was being excited by the beat frequency of the forcing functions, and also by a harmonic of this beat.

With double forcing, it was shown that the combination frequencies occur naturally in a non-linear system, and to explain the first phenomenon above it was assumed that a resonance occurred when these frequencies coincided with the natural frequency.

The second phenomenon arose from the presence of harmonics of the natural frequency already present in the transient vibration of the plate mode which was being excited by the beat. Again, the analogy would necessitate there being non-linearity in the flexible supports, which was present.

In this phenomenon, the resonances due to the plate modes showed the characteristic jump effect, and there was also excitation of a plate mode by subharmonic forcing.

In the case of single forcing, Duffing's equations gave the jump effect as a common occurrence in systems with non-linear stiffness. It also stated that it was possible for subharmonics to occur in the transient of such a system.

This would explain the above phenomena by analogy, if the plate stiffness itself were non-linear and if the 'transient vibration of the plate' contained subharmonics of its natural frequencies which could be excited.

Non-linearity of the base of the alternator on the frame stiffness seems likely, and therefore it can be assumed that the base of the alternator is being affected by both its non-linearity and the stiffness of the supports. This would give a coupling effect between the frame and the supports which may show up in this case. In response curves, the

difference between the plate frequencies and Rigid Body Frequencies seems to suggest that coupling would take place.

From the curves in Fig. (5.51) it was evident that there was a minute amount of non-linearity in the spring behaviour. This was clearly shown in Figs. (5.53) and (5.54) especially when the load direction was changed. The coil ends used had plain ends without any sort of groundings, so special care was needed in determining the deflection.

The seating and decrease in the number of active coils with an increase in load agreed fairly well. In the case of decreasing the load to zero (Fig. 5.54) the curve looked more agreeable than in the case of increasing the load, (Fig. 5.53) in which the erratic effect was more clear.

Hence, it may be concluded that the seating was not uniformly progressive but proceeded erratically. This was mostly due to the irregularities in the helix.

The seating represented the accumulation of non-linearity at each end from the tip contact of the dead ends of the coils. The initial irregularities in the helix, the pitch angle, coil diameter, slope of the end seats etc. were not uniform and the actual seating necessarily hit only the high spots as it proceeded, thus contributing to this non-linearity.

Furthermore, there was probably some frictional resistance to the twist of the wire in the seated portion of the coil

and this may release itself suddenly when it acquires sufficient magnitude. Finally, the effect of non-linearity plays an important part in curving the load deflection graph.

Although there are many other modes in the response curve, the main reasons for these modes were the secondary unbalance effect and the non-linearity in the springs which gave rise to the coupling between the modes.

For the secondary unbalance effect, the resultant is either a vertical force tending to cause vertical vibration of the machinery on its mountings, or a couple tending to cause pitching vibrations about a transverse. If the vertical force does not act through the centre of gravity, it can produce pitching as well as vertical vibration, while if there is coupling between the modes, this excitation can also produce longitudinal vibration.⁽⁷⁰⁾ Another reason was the effect of non-linearity in the damping coefficients.

A practical method was used for checking the designs of flexible platforms by means of free vibration and response analysis programmes. If a particular mode of vibration gives unacceptable amplitudes, the free vibration analysis can be used to estimate the effect of a structural modification of the resonance. In this way, any proposed alteration can be checked.

The response analysis provides, at the design stage, an estimate of the level of vibration that can be expected from the rotating machinery.

It can be concluded that the modes of the structure have a variety of variables. This may look slightly ambiguous. It seems that the non-linearity in the spring supported structure gave rise to many sub-harmonic resonances, ultra-harmonic resonance, sub-ultra-harmonic resonance, or internal resonance. It also gave rise to non-periodic combination resonance, periodic combination resonance and the main resonance.

In the case of structural dynamic analysis, the main factor governing these analyses was the assumption of the orthogonality of the modes with respect to the mass, stiffness and damping terms. i.e. the identification parameter. In point of fact, no test responses are purely modal. By a suitable selection of the measuring points maximum response in the mode under investigation may be obtained with negligible interference from some of the other modes.

It must be borne in mind also, that the recorded motion may contain a rolling component of appreciable amplitude in addition to the twist component.

This indicates that sometimes in measuring the mode under investigation an interference from other modes may occur.

The type of resonances obtained from such a structure are classified in Table (5.6). The internal resonance, non-periodic combination resonance and the periodic combination

resonance, are the resonances which distinguish systems with several degrees of freedom from those having a single degree of freedom. Internal resonance becomes a special case, where the main resonance coincides with the sub-harmonic, ultra-harmonic or sub-ultra-harmonic resonance.

The periodic combination resonance is again a special case, where the combination resonance coincides with the aforesaid resonances (95). It can be concluded that the coulomb damping which was used was a non-linear damping phenomenon, since discontinuities existed in the damping force time history, when changes in direction of relative velocity occurred. This resulted in a non-linear equation of motion.

The results obtained during the work can be classified into two sections:

Section I

By the Finite Element Method the vibration characteristics of flexible platforms could be predicted at the design stage. The increasing size of modern rotating machinery was the main reason for bringing about a change from the traditional massive concrete foundation to a more flexible steel structure which is an assemblage of beams and plates. Because of its flexibility, it was important to be able to predict the dynamic behaviour of such a structure at the design stage by determining matrices corresponding to the mass and stiffness of the structure. The natural frequencies and corresponding mode shapes of the structure may be found by solving an eigen value problem. The response of the structure to sinusoidal

excitation was estimated by solving a set of simultaneous equations.

Although damping was not considered here, the structure damping may be represented by a matrix proportional to the stiffness matrix.

The results for the natural frequencies and the mode shape of the flexible platform theoretically and experimentally showed a high degree of correlation.

The stiffness coefficients measured compared favourably with the computer programme calculation.

The stiffnesses of the supports were found experimentally to be almost linear within the normal working range. However, elastic supports possess some non-linear characteristics in the working range, giving rise to a new phenomenon which may be completely different from the linear case.

There was an effect due to the end turns of the spring when the applied load was increased. There was always some progressive seating of the end turns, so that the number of completely free coils decreased with the load, and this increased the number of inactive turns. It was also noted that the total deflection of the dead or inactive coils on each end of the spring was greater than that which corresponded to the deflection of the free coils.

Any slight variation in spring wire or coil diameter had an effect on the load deflection characteristics of helical springs. A 1% change in the mean coil diameter meant a 3% change in the load deflection characteristic, while a 1%

change in the wire diameter resulted in a 4% change in the deflection characteristic (59).

It may be shown mathematically that the number of coils active at a given load is equal to the slope of the curve for one average coil at a given load over the slope of the curve for the whole spring coils at the same load.

If the system is excited by a single oscillator, the discrepancy between the experimental and theoretical results may be due to the miscalculation of all the input data.

Section II

Conclusions drawn from the linear and non-linear aspects:

In a linear system a resonance was produced when the forcing frequency was equal to the natural frequency.

In a non-linear system a resonance was produced when the forcing frequency was equal to the natural frequency or any of its harmonics.

The natural vibrations of a non-linear system contained harmonics of its fundamental frequency and this fundamental frequency differed from the linear case by only a small amount.

The force transmitted to the foundation was directly proportional to the spring deflection.

In forced vibration of an undamped single degree of freedom system, the motion response, the force transmissibility

and the motion transmissibility are all numerically equal.

The displacement response is defined by three frequency conditions, and the vibrating system is sometimes described as spring-controlled, damper-controlled or mass-controlled, depending on which element is primarily responsible for the system's behaviour.

The rigid body mode could be excited by the beat frequency of the forcing function, and also by harmonics of this beat.

With a double forcing function the combination frequencies occur naturally in a non-linear system. To explain the phenomenon that a rigid body mode was being excited when the forcing frequency was a harmonic of the rigid body mode, it must be assumed that a resonance occurs when these frequencies coincide with the natural frequency.

The effect of beating in a non-linear system is quite significant, especially if the system has more than one degree of freedom. With such systems, instability occurs, that is, the amplitude of vibration at each mode varies periodically.

Beating frequency may excite the system's natural frequency if the natural frequency is equal to $(n\omega)$, where n is a positive integer.

Marked ultra-harmonic behaviour cannot occur unless the frequency of the exciting force is slightly above $1/3$ of the natural frequency of the system.

Marked sub-harmonic behaviour was observed experimentally when the frequency of the forcing function was about 3 times

the natural frequency of the system.

For non-linear systems, other than with a cubic restoring force, it was shown that the stable ultra-harmonics of orders $(2r + 1)$, $r = 1, 2, 3 \dots$ exist and that sub-harmonics of order $1/(2r + 1)$ also exist.

If the system was excited by more than one force, then the solution would have been difficult to obtain. The difficulty in obtaining the experimental results was due to the fact that the system was unstable and varying in amplitude with time.

Points arising from the computer programme used:

The idealisation of the structure must go to great lengths to achieve a true and adequate theoretical model given an adequate maximum core size.

Since it was out of the question to represent the motor and its base in the computer programme, the tactic adopted was to increase the stiffness of the motor base.

Minor modification was necessary concerning the fixing of the motor base in the frame. A special arrangement was built to fix the motor base to the frame firmly.

It seems there is a need for obtaining more accurate assessment of the true joints condition in the vibration analysis of structures.

Suggestions for Further Work

In the model there were two separate areas of interest, i.e. the structure characteristics, and the non-linearity of the support. Further work can be carried out and studied in detail in the following aspects:

Idealisation of the structure with more degrees of freedom, especially the effect of the unknown journal bearings dynamic characteristics. Also the damping effect and the effect of coupling in it, and the solution for the isothermal form of Reynold's equation with variable viscosity.

More accurate representation of the rotating machinery with its components.

Study of the non-linearity of the damping coefficient. In the dynamics of structure every case has its own solution according to its characteristic behaviour, but there is still the need for more correct idealisation of such cases.

There is a continuing requirement for skilfully produced mathematical models.

Study of the gyroscopic effect for more rotating machinery coupled together with different speed ratios.

Study of the coupling between the modes with a non-linear spring system, treating the case as a multi-degree of freedom system (i.e. one with more than 6 degrees of freedom).

Optimum excitation analysis may be extended to the situation where transient vibration response of structures is a parameter for assessment of the structure condition.

REFERENCES

1. TAIG, I.C., and R.I. KERR
"Some Problems in the Discrete Element Representation of Aircraft Structures", in B. Fraeijs de Veubeke (ed.), Matrix Methods of Structural Analysis, AGAR Dograph, 72 : 267-315 (1964)
2. ARGYRIS, J.H.
"Continua and Discontinua",
Proc. Conf. Matrix Methods Struct. Mech.,
Wright. Patterson Air Force Base, Ohio,
Oct. 26. 28, 1965. AFFDL TR 66-80, 1966.
3. ARGYRIS, J.H. and S. KELSEY
"Modern Fuselage Analysis and the Elastic Aircraft"
Butterworth Scientific Publications, London, 1963.
4. KAMEL, H.
"Automatic Analysis of Fuselages and Problems of Conditioning"
Ph.D. Dissertation, University of London, London 1964.
5. PRZEMIENIECKI, J.S.
"Matrix analysis of shell structures with flexible frames"
Aeron. Quart. 9: 361-394 (1958)
6. ARGYRIS, J.H.
"The Matrix Analysis of Structure with Cut-outs and Modifications"
Proc. 9th Intern. Congr. Appl. Mech. Sect. II,
Mech. Solids, September 1956.
7. DENKE, P.H.
"A General Digital Computer Analysis of Statically Indeterminate Structures"
NASA Tech. Note D-1666 1962.
8. FOX, E.A.
"Mechanics"
Harper and Row, 1967.
9. WASHIZU, K.
"Variational Methods in Elasticity and Plasticity"
Pergamon Press 1968.
10. FORRAY, M.J.
"Variational Calculus in Science and Engineering"
McGaraw-Hill 1968.
11. PRZEMIENIECKI, J.S.
"Theory of Matrix Structural Analysis"
McGraw-Hill 1968.
12. BISHOP, R.E.D. and D.C. JOHNSON
"The Mechanics of Vibrations"
Cambridge Univ. Press 1960.

13. COURANT, R.
"Variational Methods for the Solution of Problems of Equilibrium and Vibration"
Bulletin of the American Mathematical Society,
Vol. 49, 1943, pp. 1-23.
14. LANGEFORS, B.
"Structural Analysis of Swept-back Wings by Matrix Transformation"
SAAN TN3, Linköping 1951.
15. ARGRIS, J.H. and S. KELSEY
"Energy Theorems and Structural Analysis"
Aircraft Engineering 1954-1955
16. TURNER, M.J., R.W. CLOUGH, H.C. MARTIN and L.C. TOPP
"Stiffness and Deflection Analysis of Complex Structures"
Journal Aeronautical Science, vol. 23, pp. 9, 1956.
17. ZIENKIEWICZ, O.C.
"The Finite Element Method in Engineering Science"
McGraw-Hill, London 1971.
18. VESSELOWESKY, S.
"Experimental and Theoretical Investigation of a Turbine Foundation"
Journal of Applied Mechanics, June 1940.
19. HULL, E.H. and SCHENECTADY, N.Y.
"The Effect of Foundation Stiffness on the Resonant Frequencies of Rotating Machines"
Determined by Non-rotating Models
Journal of Applied Mechanics, September 1941.
20. LÜRENBAUM, K.
"Beitrag zur Dynamik der gefederten Maschinen Gründung"
V.D.I.Z. 98 (1956) N. 18.21. June.
21. SHÄFFER, K.
"Schwingungserscheinungen an Turbo-Generatoren mit Stahlfundamenten"
V.D.I. Z. 100 (1958) Nr. 36 21 Dezem.
22. PÜST, L.
"Determining the Resonance Frequencies of Forced Vibrations of Turbo-generators with Foundation"
Experimental Mechanics, June 1967.
23. GROOTENHUIS, P.
"Vibration of Spring-Supported Body"
Journal Mech. Eng. Science, Vol. 7, No. 2, 1965.
24. RAMSDEN, J.N. and STOKER, J.R.
"Mass Condensation: A semi-automatic Method for Reducing the Size of Vibration Problems"
Int. Journal for Numerical Methods in Engineering
Vol. 1, pp. 333-349 (1969)

25. GUPTA, K.K.
"Vibration of Frames and other Structures with banded stiffness matrix"
Int. Journal for Numerical Methods in Engineering
Vol. 2, pp. 221-228 (1970).
26. WILSON, R.R.
"Dynamic Behaviour of Steel Foundations for Turbo-Alternators"
paper presented at the British Acoustical Society meeting on
'Finite Element Techniques in Structural Vibrations'
at Institute of Sound and Vibration Research,
Southampton, England, 24-25th March 1971.
27. DIETZ, H.
"Zum Tiefabgestimmren Stahltisch für Turbomachinen"
Der Stahlbau 16, 65-71, 1957.
28. KRAMER, E.
"The Effect of Foundations on the Smooth Running of Turbo-alternators"
Elektwirts 61, 1-9, 1962.
29. PESTEL, E.C. and LECKIE, F.A.
"Matrix Methods in Elastomechanics"
New York, McGraw-Hill, 1963.
30. WEBER, H.
"Über das Gemeinsame Schwingungswerkalten von Wellen und Fundament bei Turbinenanlagen"
VDI - Ber. 48, 55-62, 1961.
31. CROOK, A.W. and GRANTHAM, F.
"An approach to the prediction of the vibration of turbine generators on undertuned foundation".
ASME 67 - VIBR - 46.
32. PROHL, M.A.
"A general Method of Calculation critical speeds of Flexible Rotors"
Journal of Applied Mechanics 67, 142-148, 1945.
33. MYKELSTAD, N.O.
"A new Method of Calculating Natural Modes of Uncoupled beinding Vibrations of Airplane Wings and other types of Beams".
Journal of Aeronautical Science 11, 153-162 (1944).
34. RAMSDEN, J.N. STOKER, J.R.
"The solution of Vibration Problem on a Turbine Compressor set mounted on a Steel Foundation.
Proc. Instn. Mech. Engrs. Vol 191 15/77 (1977).
35. WIBERG, N.E.
"Matrix Structural Analysis with Mixed Variables"
Int. Jour. for Num. Met. in Eng.
Vol. 1. 225-245 (1969)

36. RAMSDEN, J.N.
"A Matrix for the solution of mixed rotating and non-rotating vibration systems"
Int. Journ. of Methods in Eng.
Vol. 1. 225-245 (1969)
37. RANEY, J.P.
"Identification of Complex Structures using Near-resonance Testing
NASA Langley Research Center.
Shock and Vibration Bulletin
Aug. No. 38 Part 2, pp- 23-32. (1968)
38. THOREN, A.R.
"Derivation of Mass and Stiffness Matrices from Dynamic Test Data"
Society of Automotive Engrs. SAE
AIAA paper No. 72-346, 1972.
39. YOUNG, J.P. and ON, F.J.
"Mathematical Modelling via Direct Use of Vibration data"
Soc. of Auto. Eng. Paper No. 690615.
40. ANDREWS, G.J.
"Vibration Isolation of a Rigid Body on Resilient Supports"
Journ. of Acoustical Society of America
Vol. 32 No. 8 Aug. 1960.
41. EFSTATHIADES, G.J. and WILLIAMS, C.J.H.
"Vibration Isolation using Non-linear Spring"
Int. J. Mech. Sci.
Vol. 9, pp. 27-44 (1967).
42. BAPAT, V.A. and SPINIVASAN
"Approximate Methods for Step Function Response of Undamped Non-linear Spring Mass Systems with Arbitrary Hardening Type Spring Characteristic"
Journ. of Sound & Vibration, 10 (3) pp.430-443, 1969.
43. MERCER, C.A. and REE, P.L.
"An Optimum Shock Isolator"
Journal of Sound and Vibration
18 (4) pp. 511-520 1971.
44. MAGNUS, K.
"Vibration"
Blackie & Sons Ltd. London, 1965.
45. JOHNSON, B.L., STEWART E.E.,
"Transfer Function for Helical Springs"
Journal of Engineering for Industry
pp. 1011-1016, Nov. 1969.

46. VOGET, R.F.
"A Number of Active Coil in Helical Spring"
Trans. ASME. pp. 467, Dec. 1932.
47. ANCKER, C.J., GOODIER, J.N.
"Pitch and Curvature Corrections for Helical Springs".
Trans. ASME. Dec. 1958.
48. WOOD, J.K.
Symposium on Formulation of Code Design of Helical Springs
Trans. ASME pp. 475-488 July 1942.
49. TOBIAS, S.A., HENRY, R.F.
"Modes at Rest and their Stability in Coupled Non-linear Systems"
Journal Mech. Eng. Sec. vol. 3, No. 2. 1961.
50. DOOREN, R.V.
"Numerical Computation of Forced Oscillations in Coupled Duffing Equation"
Numer. Math. 20, pp. 300-311, 1973.
51. BAPAT, V.A. and SPINIYASAN P.
"Effect of Static Deflection on Natural Frequency of Non-linear Spring Mass System by Direct Linearization Method".
J. Sound. Vibration 10 (3), pp. 444-454, 1969 .
52. STERN, M. and LENZI
"A Variational Treatment for the Response of Frame Structures to Oscillating Loads"
Journal of the Franklin Institute
Vol. 280, No. 3, Sept. 1965.
53. RUBINSTEIN, M.F.
"Analysis of Large Complex Frames on a Small Computer".
Journal of the Franklin Institute
Vol. 280, No. 2, August 1965.
54. LUND, J.W., and TONNESEN
"Analysis and Experiments on Multi-Plane Balance of a Flexible Rotor".
Journal of Eng. for Industry, Feb. 1972.
pp. 233-242.
55. EHRICH, F.F.
"Sum and Difference Frequencies in Vibration of High Speed Rotating Machinery".
Trans. ASME Journal of Eng. for Industry,
pp. 181-184

56. ALLAWAY, P.H.
"Vibration Amplitudes of Resiliently-Mounted
Machines".
Vibration Symposium Sec. 1. pp. 35-41 1966.
57. WARBURTON, G.B.
"Transmission of Vibrations"
Vibration Symposium, Sec. 2, pp. 43-59. 1966.
58. WALLER, R.A.
"Some Economic Aspects of Anti-Vibration
Devices"
Vibration Symposium Sec. 7, pp. 285-298. 1966.
59. WAHL, A.M.
"Mechanical Springs"
McGraw-Hill 1963.
60. ANSKER, C.J. and GOODIER, J.N.
"Pitch and Curvature Correction for Helical Springs".
Trans. ASME. 466 Dec. 1958.
61. GÖHNER, O.
"Schubspannung Verteilung im Querschnitt einer
Schrauben feder".
Ing. Archiv. vol. 1 1929-1930, pp. 619-633.
62. GÖHNER, O.
"Die Brechnung Zylindrischer Schraubenfedern"
Zeitschrift der V.D.I.
vol. 76, No. 11, pp. 269-272, 1932.
63. VOGET, R.E.,
"Number of Active Coils in Helical Springs".
Trans. ASME, vol. 56, p. 468, 1934.
64. PLETTA, D.H., SMITH, S.C. and HARRISON, N.W.
"The Effect of overstrain on closely coiled Helical
Springs and the variations of the number of active
coil with Load".
Virginia Polytech. Institute Eng. Expn. Sta. Bull.
24, June 1936.
65. KAYSOR, H.C.
"Calculation of the Elastic Curve of a Helical
Compression Spring".
Trans. ASME, vol. 62, p. 319 1940.
66. EDGERTON
"Machine Design"
ASME p. 53, 1939
Research Committee for Mechanical Springs.
67. MOLLOY, C.T. (ed.)
"Design of Vibration Isolations Systems"
S.A.E. Publication 1962.

68. CREDE, C.E.
"Vibration and Shock Isolation"
John Wiley and Sons, Inc., New York.
69. CREDE, C.E. and RUZICKA, J.E.
"Theory of Vibration Isolation"
Shock and Vibration handbook, Chapt. 30, 1976.
McGraw-Hill Book Co. , New York.
70. KER WILSON, W.
"Vibration Engineering" 1959.
C. Griffin & Co. Ltd., London.
71. SETHNA, P.R.
"Dynamic of a Four-wheeled Vehicle and
the Effects of Suspension Geometry".
Proc. Auto Div. Inst. Mech. Engrs.
1962-63. No. 6, p. 201.
72. MACDUFF, J.M.
"Isolation of Vibration in Spring-mounted Apparatus".
Product Eng. 1946. 17 (July), 106, 159 (Aug) 154.
73. VON KÁRMÁN, T. and BIOT, M.A.
"Mathematical Methods in Engineering, 1940.
McGraw-Hill Book Co., New York.
74. CRANDALL, S.H.
"Engineering Analysis" 1956.
McGraw-Hill Book Co., New York.
75. HUMMELL, A.
"Motorship Hansestadt Köln".
Schiffbau, 15th April 1939.
(see The Marine Engineer and Naval Architect, June 1939
p. 202). Describes steel spring mountings under main
engines. W.K. Wilson p. 128.
76. DEN HARTOG.
"Mechanical Vibration".
McGraw-Hill Book Co. 1956, pp. 375-376.
77. JACOBSEN, L.S.
"Steady Forced Vibration as Influenced by Damping".
Trans. ASME 52 (App. Mech. Sect. 169-178, 1930.
78. RUZICKA, J.E.
"Forced Vibration in System with Elastically Supported
Dampers",
Masters thesis, M.I.T. Cambridge, Mass., June 1957.
79. PAINTER, G.W.
"Dry Friction Damped Isolators",
Prod. Eng. 30 (31), pp. 48-51, Aug. 3, 1959.
80. VAN BOMMEL, P.
"Analysis of a Two-degree of freedom System with
Dry Friction Damping for Vehicles".
Arch. Eisenbahntech. 15, pp. 73-88, Dec. 1961 (in German)

81. LEVITAN, E.S.
"Forced Oscillation of a Spring-Mass System
having Combined Coulomb and Viscous Damping".
J. Acoust. Soc. Amer. 32(10, pp. 1265-1269, 1960.
82. STOKER, J.J.
"Non-linear Vibration in Mechanical and Electrical
Systems", vol. II, Waverley Press, Baltimore, 1950.
83. PANOVKO, Y.G.
"Applied Mechanics Proceedings, XI"
International Congress of Applied Mechanics,
Munich. A Review of the Method of Direct
Linearisation, 1964.
84. ATKINSON, C.P.
"Proceedings of the IV U.S. National Congress of
Applied Mechanics", pp. 57-62, on a Superposition
Method for Determining Frequencies of Non-linear Systems,
1964.
85. RIEF, Z.F.
"Effect of Static Deflection on the Natural Frequency
of a System with a Hardening Non-linear Spring".
J. Mech. Engrg. Sci. June 1967, p. 177.
86. GROBNER, W. and HOFREITER, N.
"Integraltafel, Erster Teil, Unbestimmte Integral".
Berlin, Springer Verlage.
87. TIMOSHENKO, S.
"Vibration Problems in Engineering", p. 309.
D. Van Nostrand Co. Inc. Princeton N.J. 1937.
88. WITTRICK, W.H. and WILLIAMS.
"Buckling and Vibration of Anisotropic or Isotropic
Plates Assemblies under Combined Loading".
Int. Journ. Mech. Science. pp. 209-239, vol. 16, 1974.
89. CHEUNG, Y.K.
"Finite Strip Method Analysis of Elastic Slabs".
Proc. ASCE Mech. Division pp. 1365-1378, Dec.1968.
EM.6.
90. DILL, E.H. and PISTER, K.S.
"Vibration of Rectangular Plates and Plates Systems".
Journ. App. Mechanics, pp. 101, 1969.
91. DAWE, D.J.
"On Assumed Displacement for the Rectangular Plate
Bending Element".
Journ. Royal Aeronautical Society, Vol. 71, p. 722, 1967.
92. MIKHLIN, S.G.
"The Numerical Performance of Variational Methods".
Wolters, Noordhoff Publishing, 1971.

93. STODOLA, A.
"Steam and Gas Turbines",
New York, pp. 1135-9, 1945.
94. WALLER, R.A.
"Some Economic Aspects of Antivibration Devices".
Vibration Symposium, 1965.
95. YAMAMOTO, T.
"Summed and Differential Harmonic Oscillations
in Non-linear Vibratory Systems".
Bulletin of J.S.M.E. 4, No. 16, p. 658, 1961.
96. YAMAMOTO, T. and HAYASHI, S.
"On the Response Curves and the Stability of
Summed and Differential Harmonic Oscillations",
Bulletin of J.S.M.E. 6, No. 23, p. 420, 1963.
97. BENZ, G.
"Schwingung nichtlinearer gedampfter systeme mit
pulsierenden Speicherwerten",
Thesis, Technische Hochschule Karlsruhe, 1962.
98. CHEN, Yu.
"Vibrations: Theoretical Methods."
Addison-Wesley Publishing Co., Inc. 1966.
99. ROCKEY, K.C.
"Recommended standard practices for structural
testing of steel Models"
TRRL Supplementary Report 254,
Crowthorne, Berks. I SSN pp. 0305-1315, 1977.
100. BROCH, J.T.
"Mechanical Vibration and Shock Measurements".
Bruel & Kjaer Measuring System, 1972.
101. DOWNHAM, E.
"Research Techniques in Non-Destructive Testing",
Vol. 2, Chapter 9, p. 295.
Atomic Energy Research Establishment, Harwell, Berks. England
Academic Press, 1973.

APPENDIX A

Response of Discrete Systems by Modal Analysis

It is always easy to adopt the following method referred to as modal analysis. The procedure is analogous to the Fourier analysis and can easily be applied to obtain the responses to initial conditions, harmonic excitations and periodic excitation.

The following is derived for the general expression covering all the cases just mentioned.

To start with the equation of motion

$$[m] \{\ddot{q}\} + [K] \{q\} = \{Q\} \quad (1)$$

where the excitation functions $Q_j(t)$ are arbitrary functions of time (periodic excitations are special cases). To use the modal analysis it is necessary first to solve the eigen value problem

$$[m] [u] [w^2] = [K] [u] \quad (2)$$

associated with the system described by (1). The solution of the eigen value problem (2) yields the modal matrix $[u]$ and the diagonal matrix of the eigen values $[w^2]$.

Using the expansion theorem the response may be described as a superposition of the normal modes in the form

$$\{q(t)\} = [u] \{\eta(t)\} \quad (3)$$

where $\{\eta(t)\}$ is a column matrix consisting of a set of time-dependent generalized co-ordinates. From equation (1)

it follows that

$$\{ \ddot{q} \} = [u] \{ \ddot{\eta} \} \quad (4)$$

so that introducing Equations (3) and (4) into Equation (1) we obtain

$$[m] [u] \{ \ddot{\eta} \} + [K] [u] \{ \eta \} = \{ Q \} \quad (5)$$

Premultiply both sides of Equation (5) by $[u]^T$ giving

$$[u]^T [m] [u] \{ \ddot{\eta} \} + [u]^T [K] [u] \{ \eta \} = [u]^T \{ Q \} \quad (6)$$

But the normal modes are such that

$$[u]^T [m] [u] = [I] \quad , \quad [u]^T [K] [u] = [w^2] \quad (7)$$

where $[I]$ is the identity matrix. In addition, we can introduce a column matrix of generalized force $N_r(t)$ which is associated with the generalized co-ordinates $\eta_r(t)$ and related to the forces $Q_j(t)$ by

$$\{ N \} = [u]^T \{ Q \} \quad (8)$$

In view of Equations (6) and (7), Equation (5) can be rewritten

$$\ddot{\eta} + [w^2] \{ \eta \} = \{ N \} \quad (9)$$

which represents a set of n uncoupled differential equations of the type

$$\ddot{\eta}_r(t) + w_r^2 \eta_r(t) = N_r(t) \quad r = 1, 2, \dots, n \quad (10)$$

This differential equation describes the motion of an undamped single-degree-of-freedom system. Hence the modal analysis consists of uncoupling the equations of motion by means of linear co-ordinate transformations; the transformation matrix is just the modal matrix $[u]$. Of course, the solution of the uncoupled equations of motion (Equation (10)) is considerably easier to obtain than the solution of the coupled equation (1).

The solution of Equation (10) may be obtained by means of the Laplace transform method. Transforming both sides of Equation (10) we obtain

$$s^2 \bar{\eta}_r(s) - s \eta_r(0) - \dot{\eta}_r(0) + w_r^2 \bar{\eta}_r(s) = \bar{N}_r(s) \quad (11)$$

where

$\bar{\eta}_r(s)$ and $\bar{N}_r(s)$ are the Laplace transforms of $\eta_r(t)$ and $N_r(t)$, respectively, and $\eta_r(0)$ and $\dot{\eta}_r(0)$ are the initial values associated with the generalized co-ordinate $\eta_r(t)$.

The subsidiary equation is:

$$\bar{\eta}_r(s) = \frac{\bar{N}_r(s)}{s^2 + w_r^2} + \frac{s}{s^2 + w_r^2} \eta_r(0) + \frac{1}{s^2 + w_r^2} \dot{\eta}_r(0) \quad (12)$$

By using Borel's theorem the r th generalized co-ordinate becomes

$$\eta_r(t) = \frac{1}{w_r} \int_0^t N_r(\tau) \sin w_r(t-\tau) d\tau + \eta_r(0) \cos w_r t + \dot{\eta}_r(0) \frac{\sin w_r t}{w_r}$$

$r = 1, 2 \dots n \quad (13)$

The integral in Equation (13) is known as the convolution integral.

The initial generalized displacement $\eta_r(0)$ and initial generalized velocity $\dot{\eta}_r(0)$ are obtained from the expressions

$$\{\eta(0)\} = [u]^T [m] \{q(0)\} , \quad \{\dot{\eta}(0)\} = [u]^T [m] \{\dot{q}(0)\}$$

(14)

where $\{q(0)\}$ and $\{\dot{q}(0)\}$ are column matrices of initial displacement and velocities, respectively.

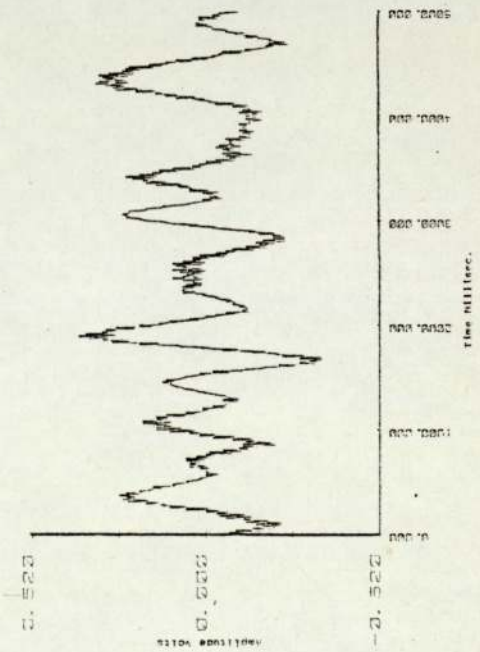
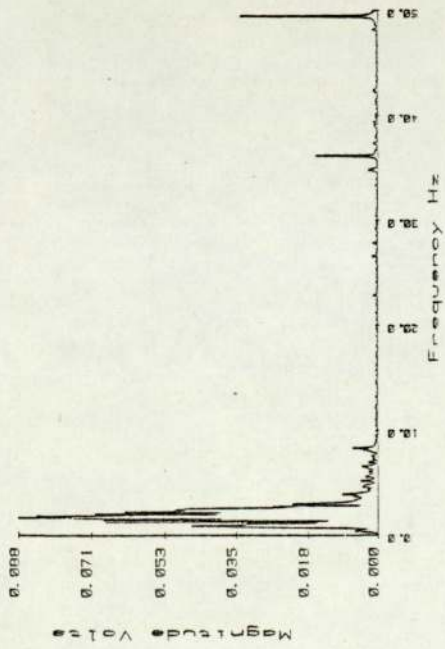
Introducing Equation (13) together with the initial conditions of Equation (14) into Equation (3), the response $\{q(t)\}$ may be obtained. The above formulation holds true regardless of whether the excitations $Q_j(t)$ are harmonic, periodic, or non-periodic.

APPENDIX B

From the analysis of vibrations measured at discrete points on the structure it can be concluded that the frequencies of the characteristic components of the vibration are related in some way to forces generated in defined ways within the rotating system. The system vibrates at frequencies equal to the exciting frequencies and also at frequencies which may be multiples of, sub-multiples of or differences between any two frequencies.

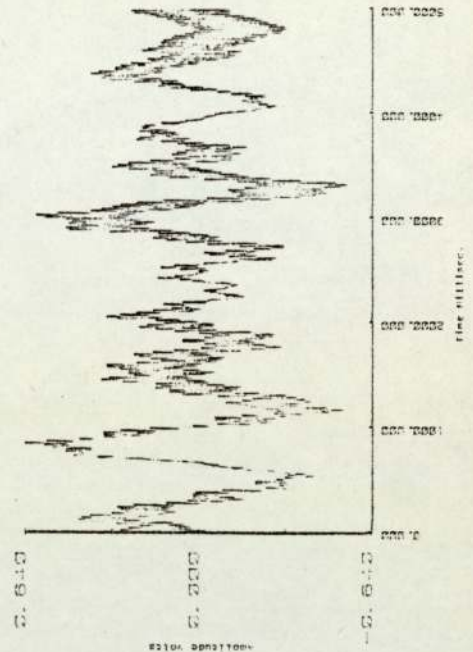
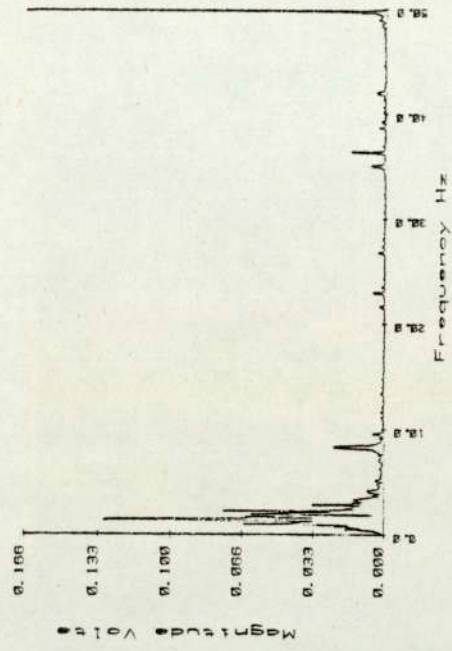
In other words, the system vibrates at frequencies equal to the exciting frequencies and also at frequencies which may be sum and difference frequencies according to the harmonic zone number.

Figs. (1A) to (30A) show some of the response curves and wave forms for the motor running at different speeds, with different speed ratios and different signal picking positions. In these response curves the x-axis indicates the frequency in Hz and the y-axis gives the amplitude in volts. In the wave forms the x-axis gives the time in milliseconds and the y-axis shows the amplitude in volts.



Response curve and wave form.
 Speed ratio 7:5, motor running
 at 50 Hz picking up signal
 position 2.

Fig. 1A



Response curve and wave form.
 Speed ratio 7:5, motor running
 at 50 Hz picking up signal
 position 1.

Fig. 2A

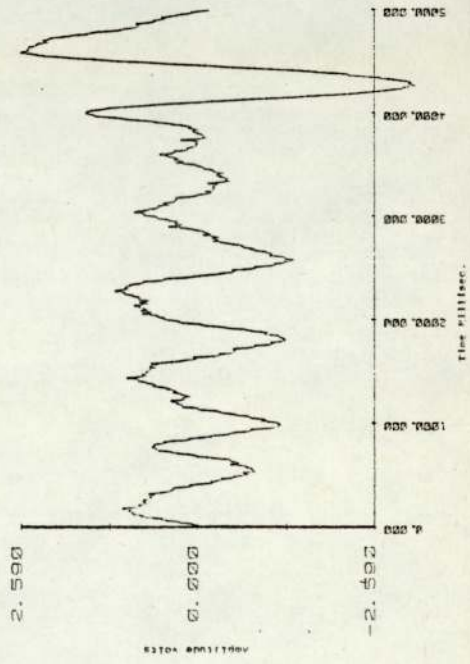
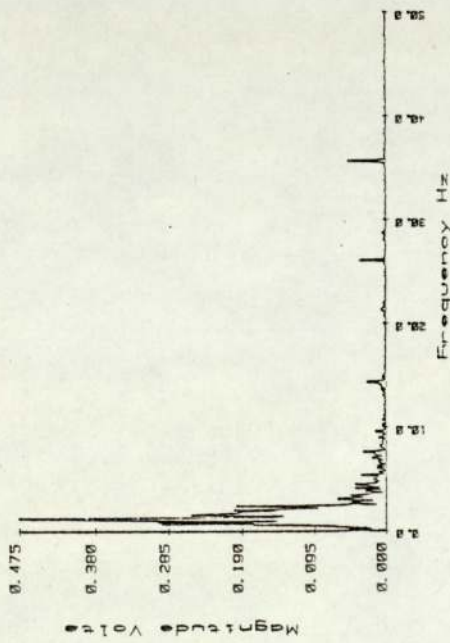


Fig. 3 A Response curve and wave form.
Speed ratio 7:5, motor running
at 35 Hz picking up signal
position 2.

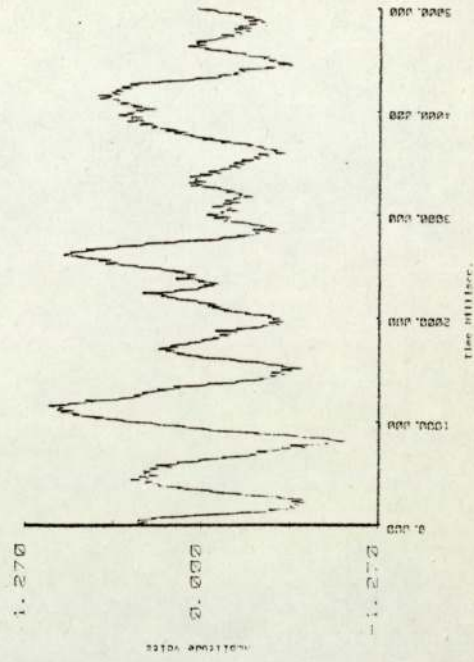
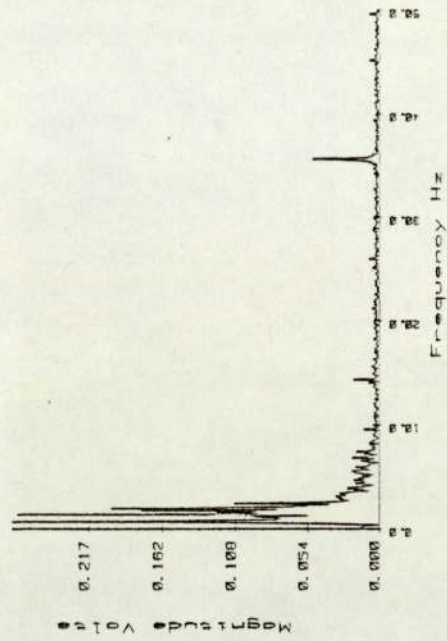


Fig. 4 A Response curve and wave form.
Speed ratio 7:5, motor running
at 35 Hz picking up signal
position 1.

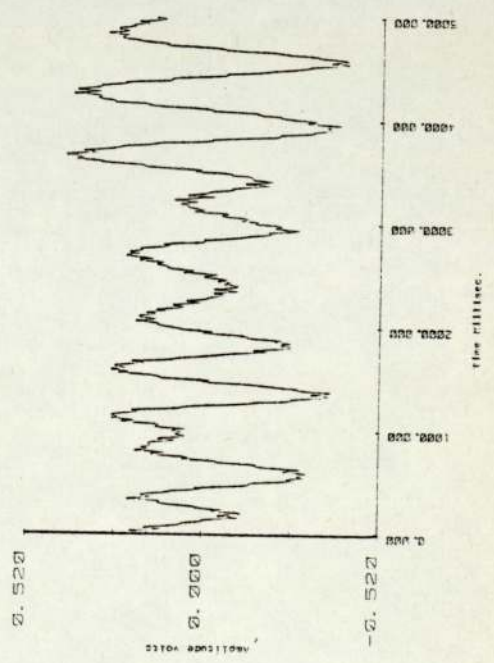
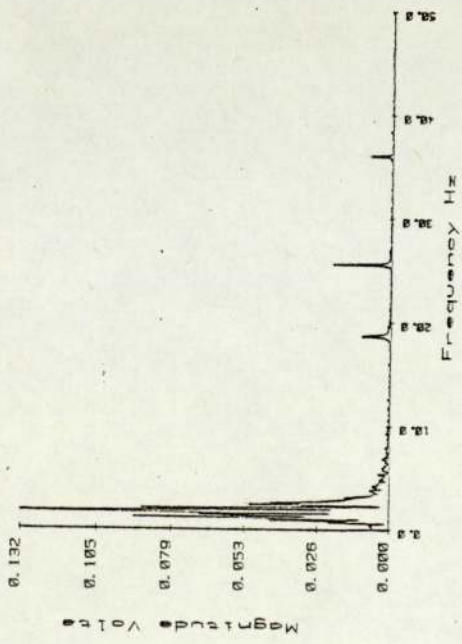


Fig. 5A
Response curve and wave form.
Speed ratio 7:5 motor running
at 25 Hz picking up signal
position 2.

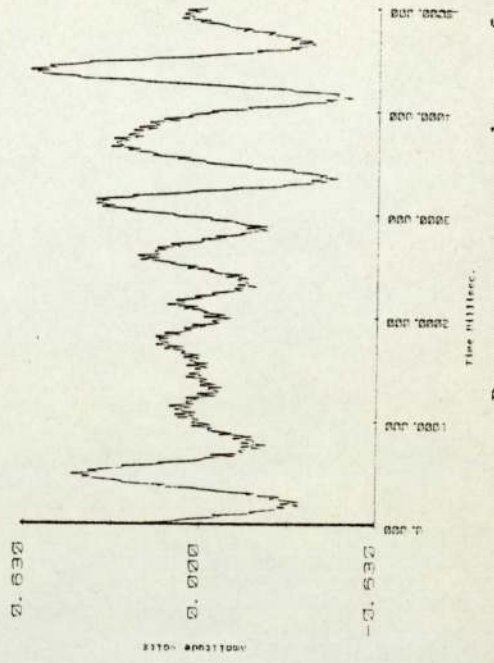
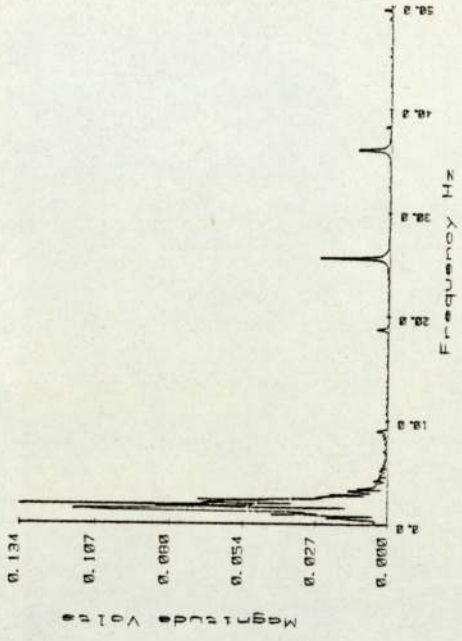


Fig. 6A
Response curve and wave form.
Speed ratio 7:5, motor running
at 25 Hz picking up signal
position 1.

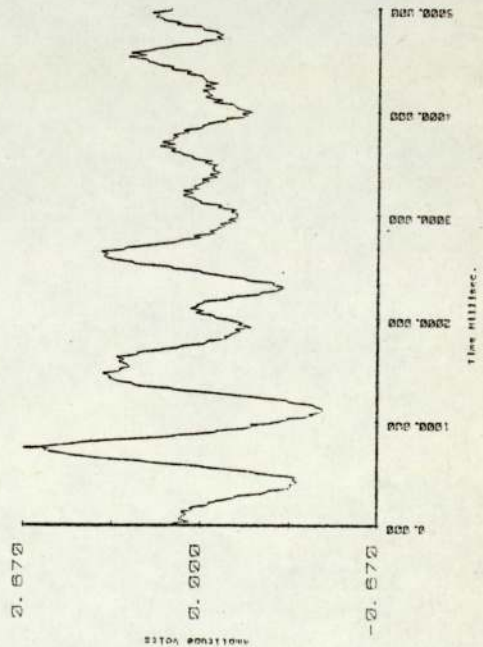
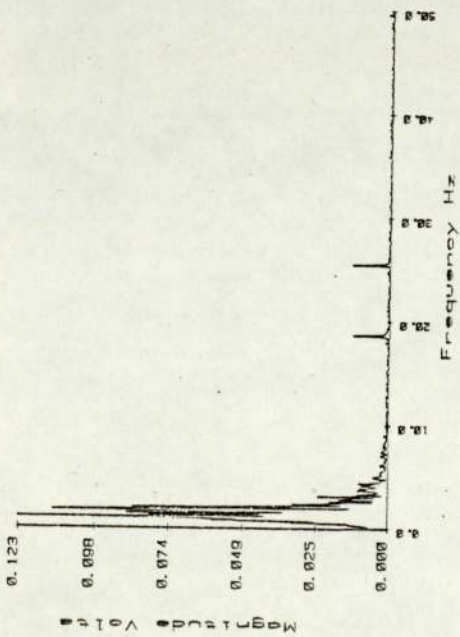


Fig. 7A
Response curve and wave form.
Speed ratio 7:5 motor running
at 25 Hz picking up signal
at position 4.

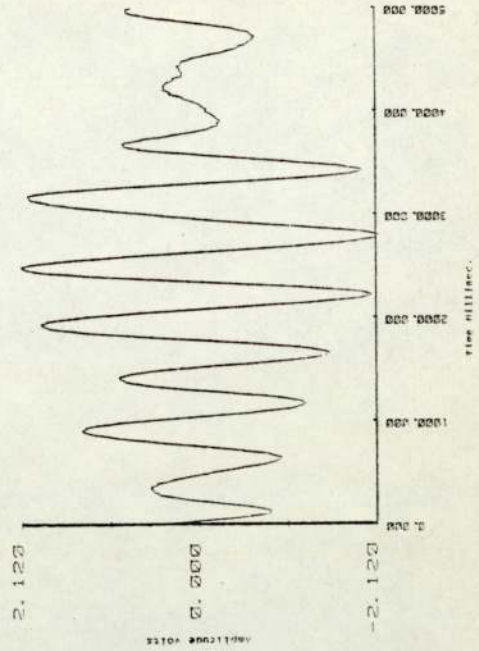
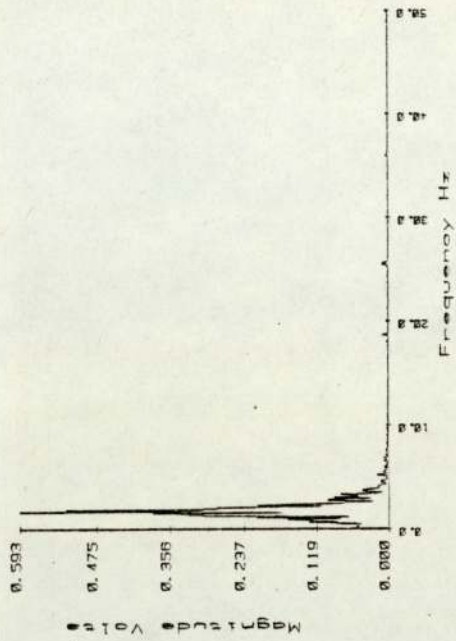
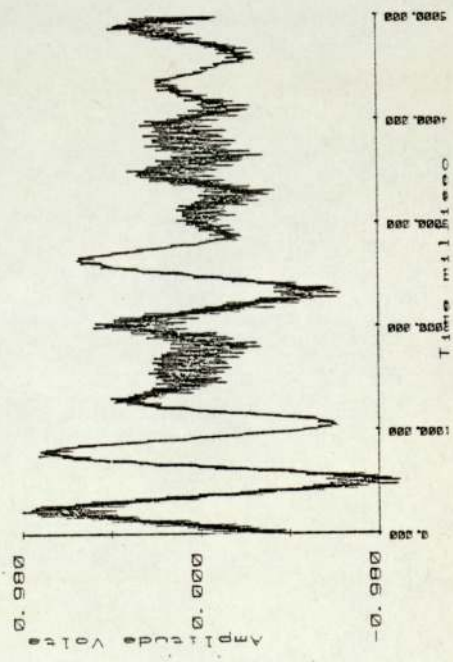
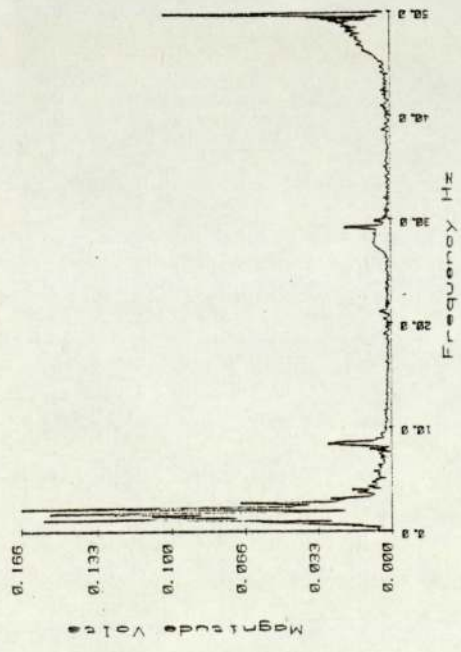
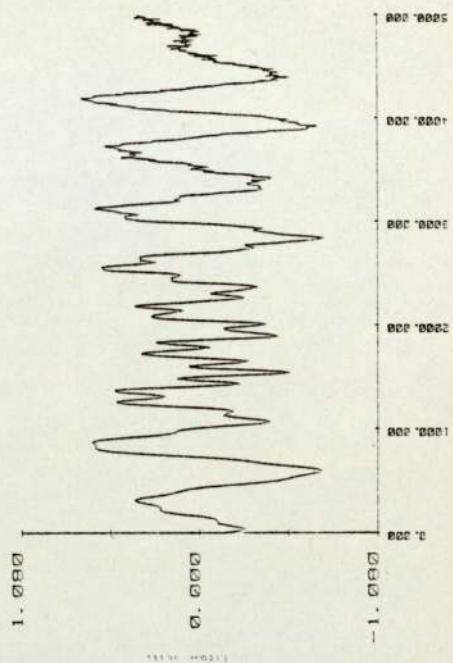
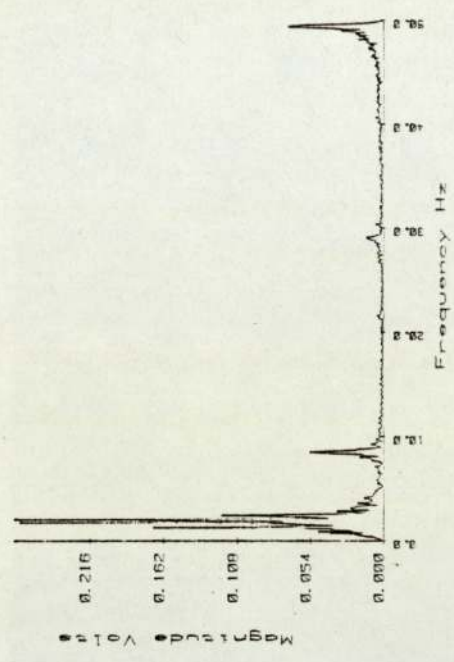


Fig. 8A
Response curve and wave form.
Speed ratio 7:5, motor running
at 25 Hz picking up signal
position 3.



Response curve and wave form.
 Speed ratio 5:3, shutting the
 motor to zero speed, picking up
 signal position 1.

Fig. 9A



Response curve and wave form.
 Speed ratio 5:3, starting the
 motor to maximum speed, picking
 up signal position 1.

Fig. 10A

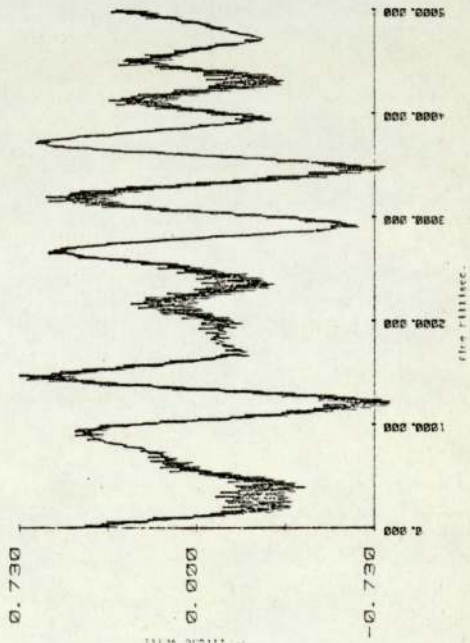
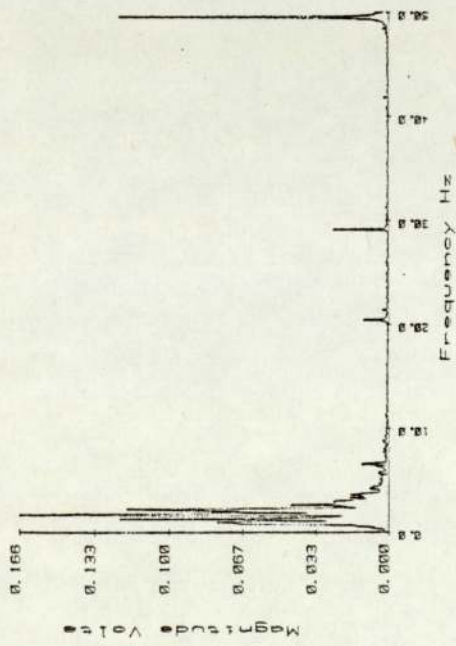


Fig. 11A
Response curve and wave form.
Speed ratio 5:3 motor running
at 50 Hz, picking up signal
position 2.

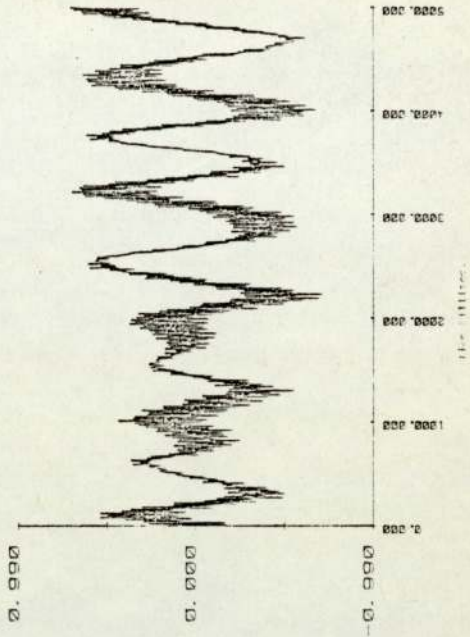
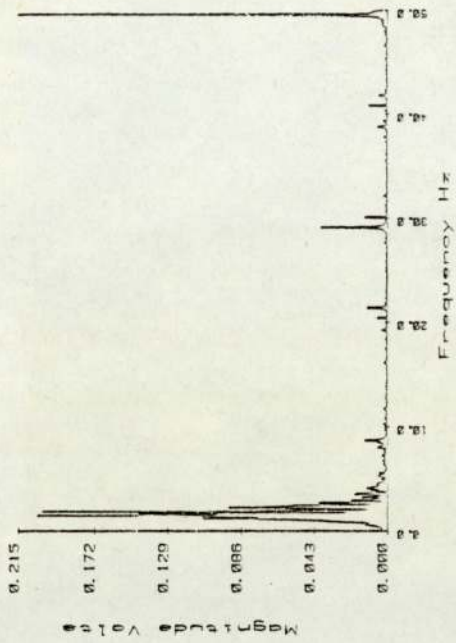


Fig. 12A
Response curve and wave form.
Speed ratio 5:3. Motor running
at 50 Hz, picking up signal
position 1.

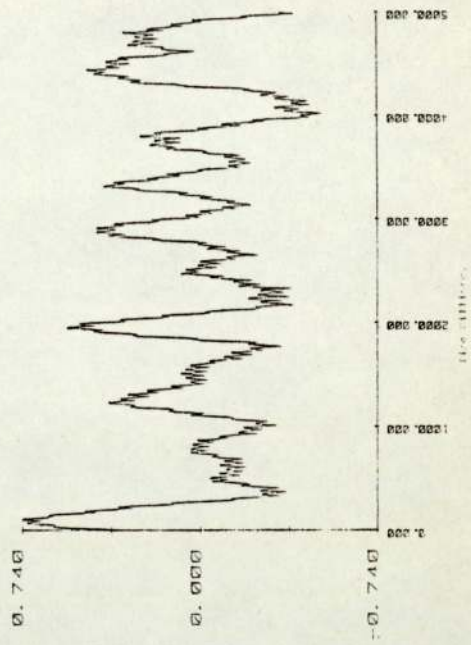
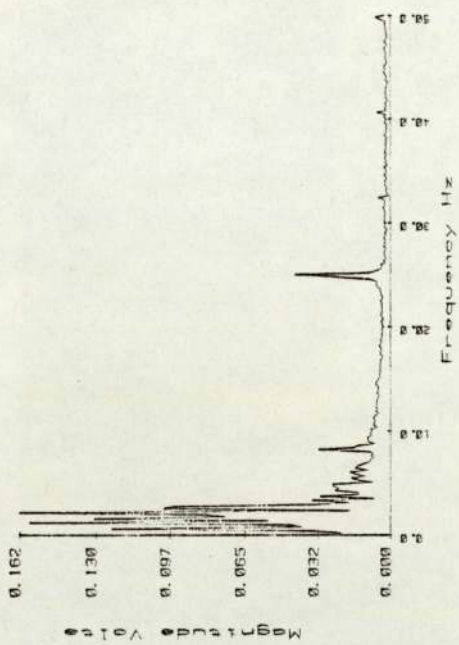


Fig. 16A

Response curve and wave form.
Speed ratio 5:3. Motor running
at 25 Hz, picking up signal
position 1.

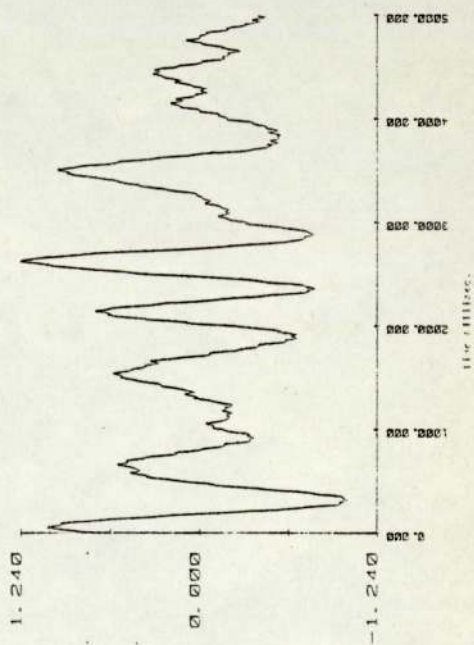
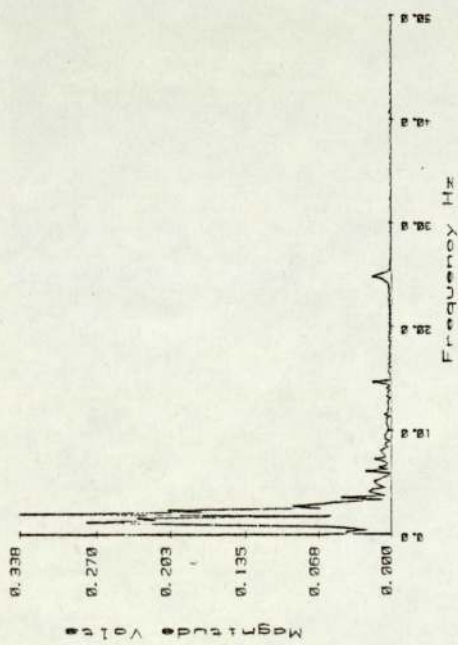


Fig. 15A

Response curve and wave form.
Speed ratio 5:3, motor running
at 25 Hz, picking up signal
position 2.

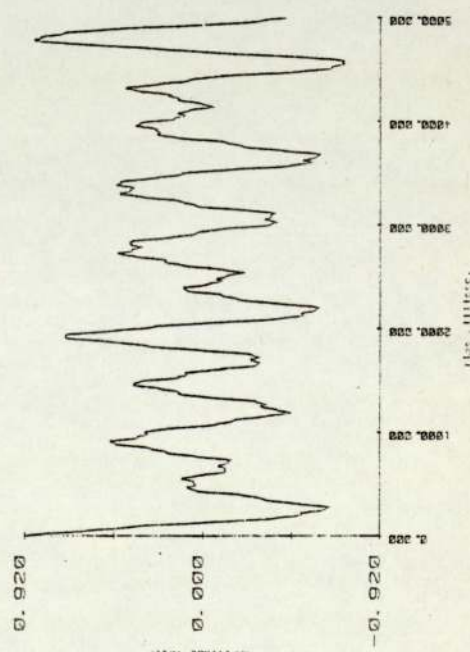
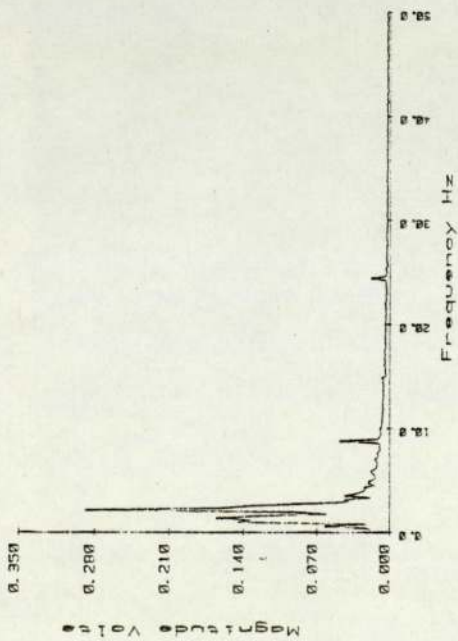


Fig. 17A Response curve and wave form.
Speed ratio 5:3. Motor running
at 15 Hz, picking up signal
position 2.

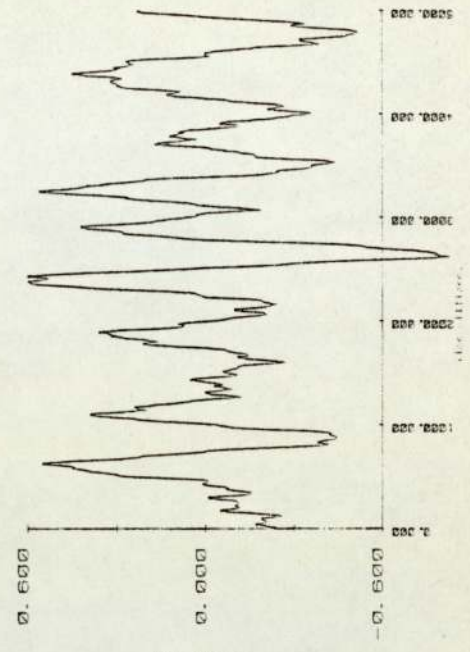
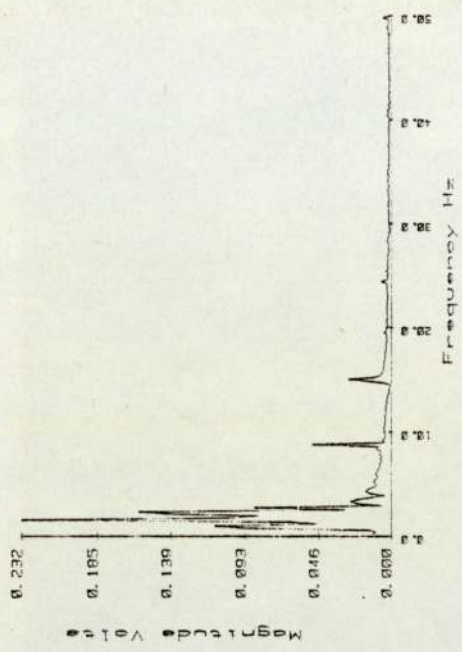
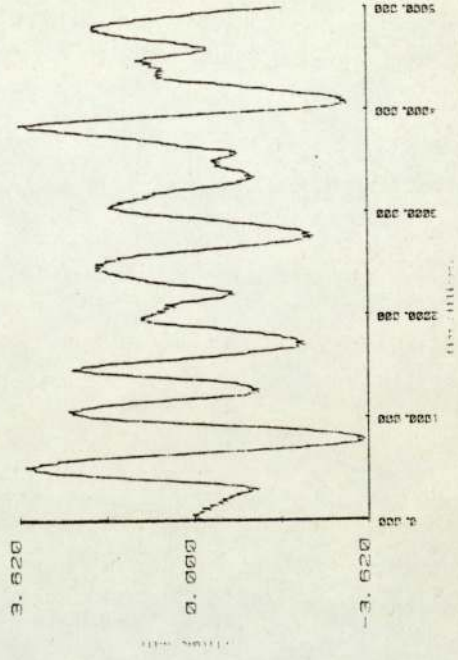
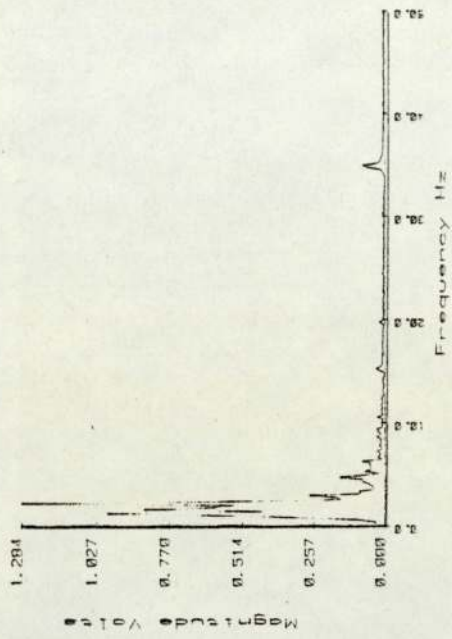
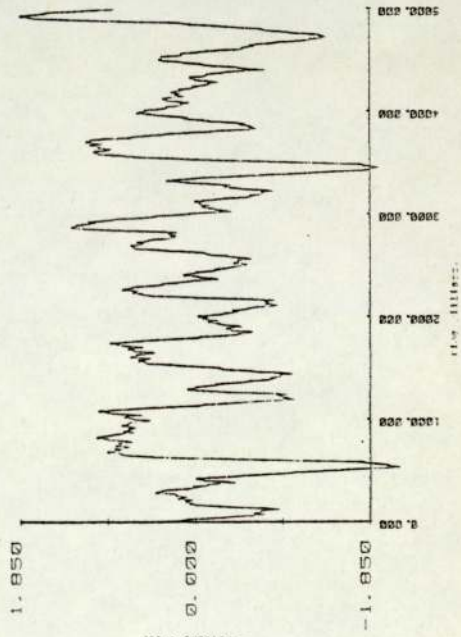
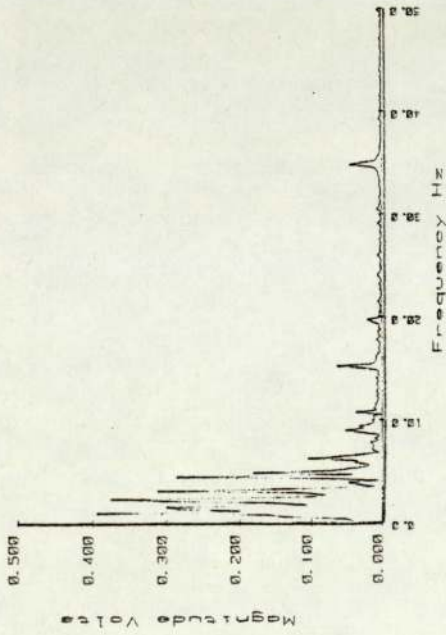


Fig. 18A Response curve and wave form.
Speed ratio 5:3, motor running
at 15 Hz, picking up signal
position 1.



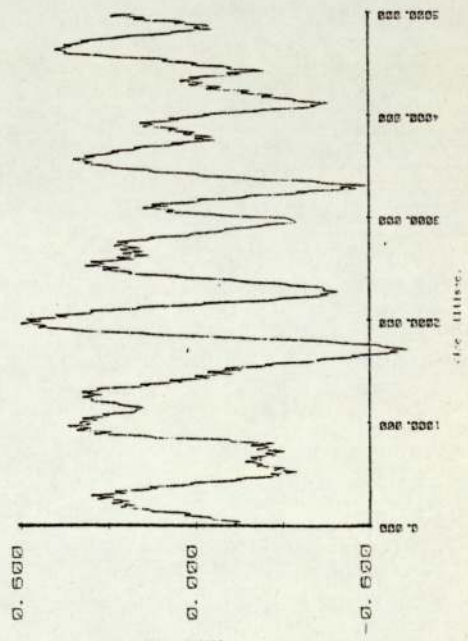
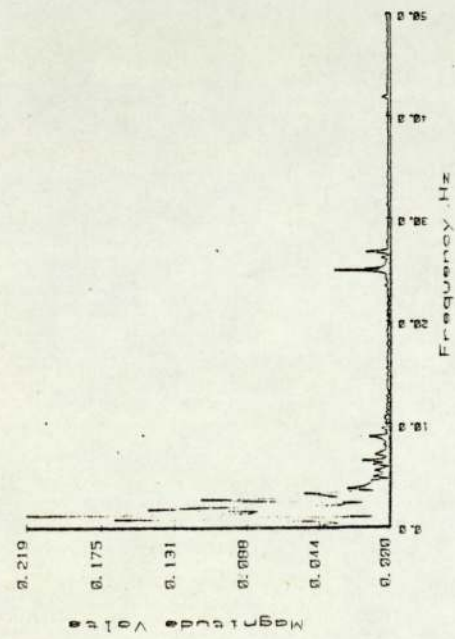
Response curve and wave form.
Speed ratio 3:1, motor running
at 35 Hz, picking up signal
position 3.

Fig. 20A

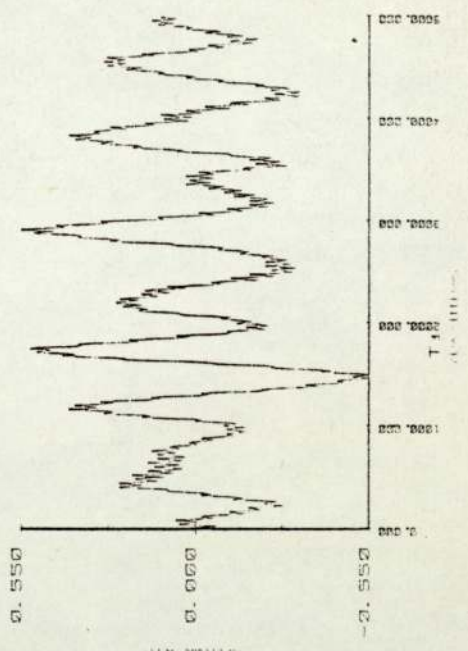
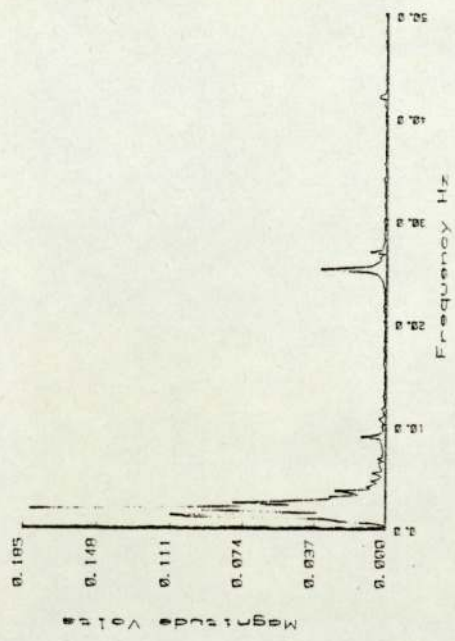


Response curve and wave form.
Speed ratio 3:1, motor running
at 35 Hz, picking up signal
position 4.

Fig. 19A



Response curve and wave form.
 Speed ratio 3:1, motor running
 at 25 Hz, picking up signal
 position 1.



Response curve and wave form.
 Speed ratio 3:1, motor running
 at 25 Hz, picking up signal
 position 2.

Fig. 22A

Fig. 21A

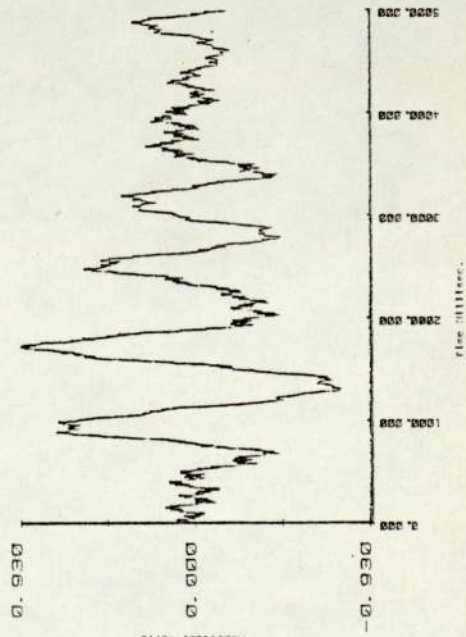
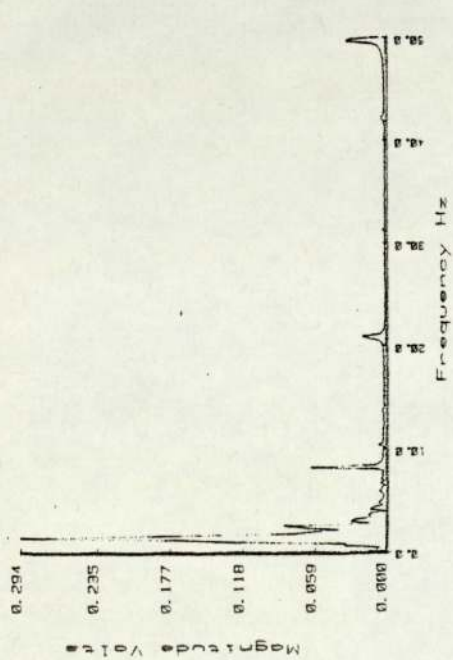


Fig. 23A
Response curve and wave form.
Speed ratio 5:2, motor running
at 50 Hz, picking up signal
position 2.

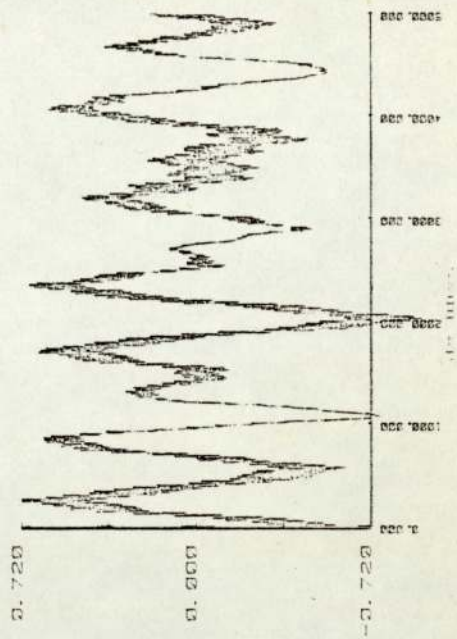
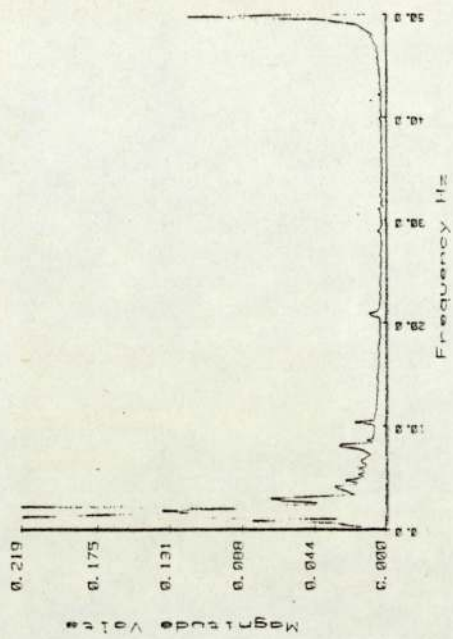


Fig. 24A
Response curve and wave form.
Speed ratio 5:2, motor running
at 50 Hz, picking up signal
position 1.

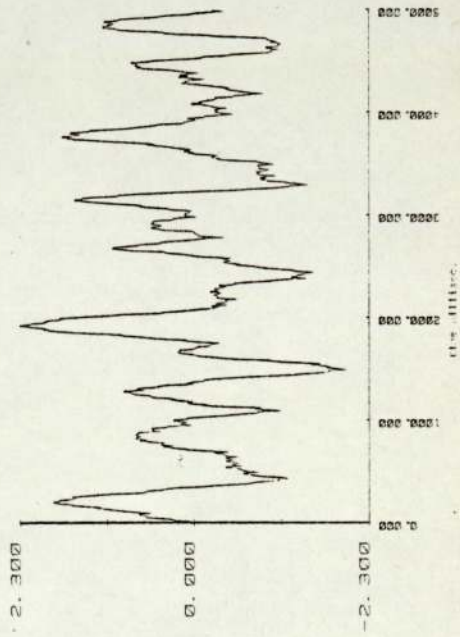
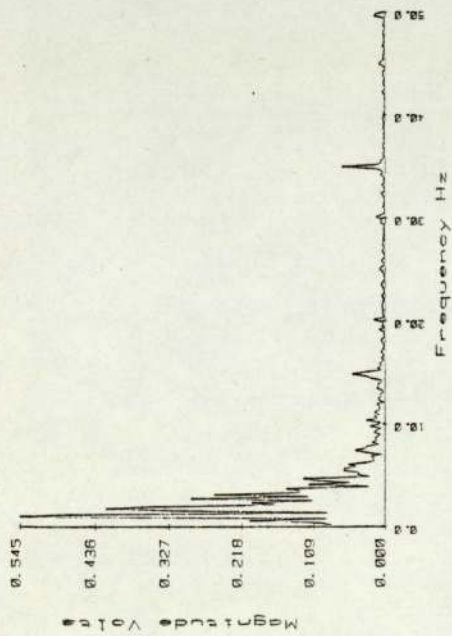


Fig. 25A
Response curve and wave form.
Speed ratio 5:2, motor running
at 35 Hz, picking up signal
position 1.

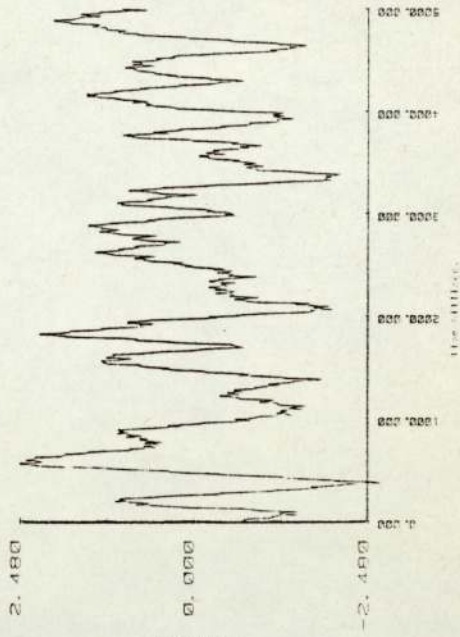
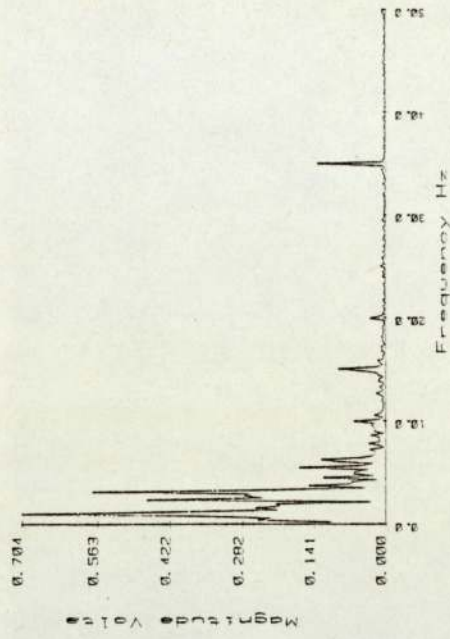


Fig. 26A
Response curve and wave form.
Speed ratio 5:2, motor running
at 35 Hz, picking up signal
position 2.

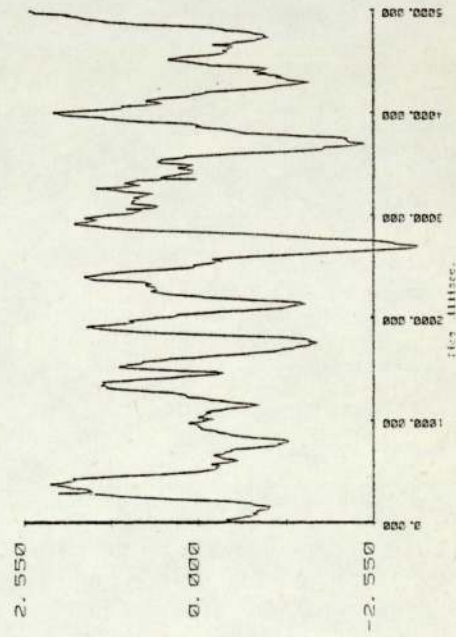
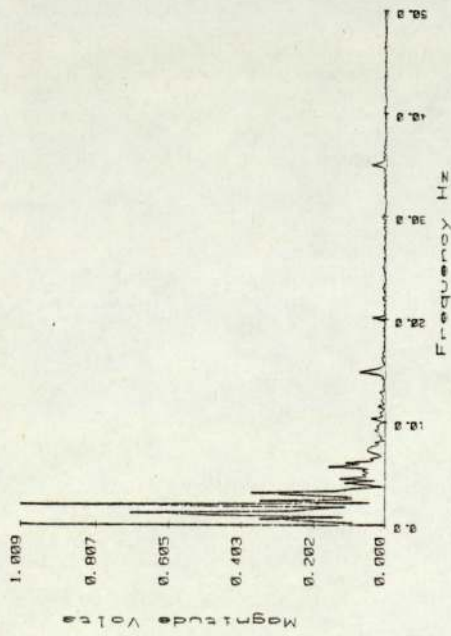


Fig. 27A Response curve and wave form.
Speed ratio 5:2, motor running
at 35 Hz, picking up signal
position 3.

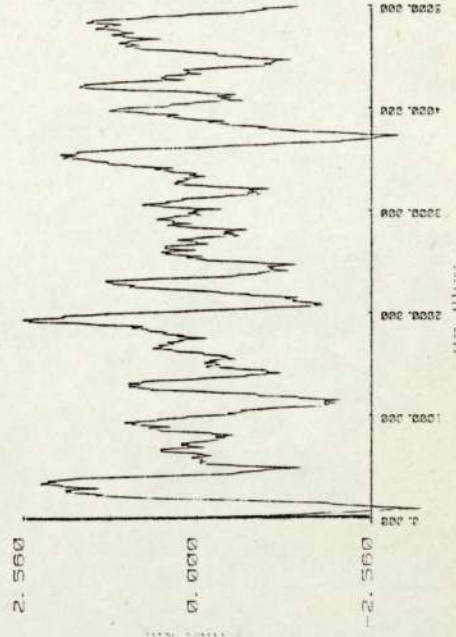
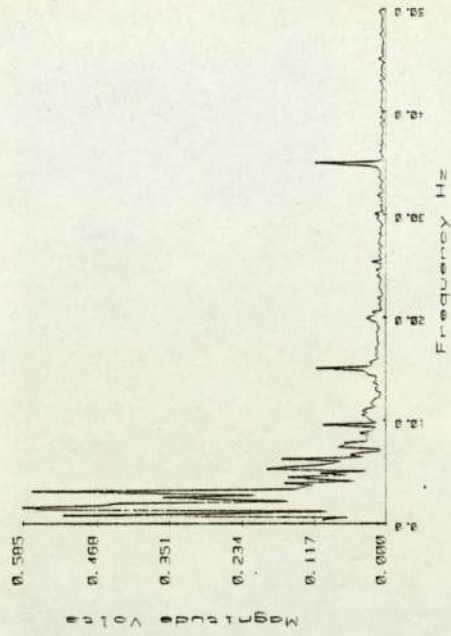
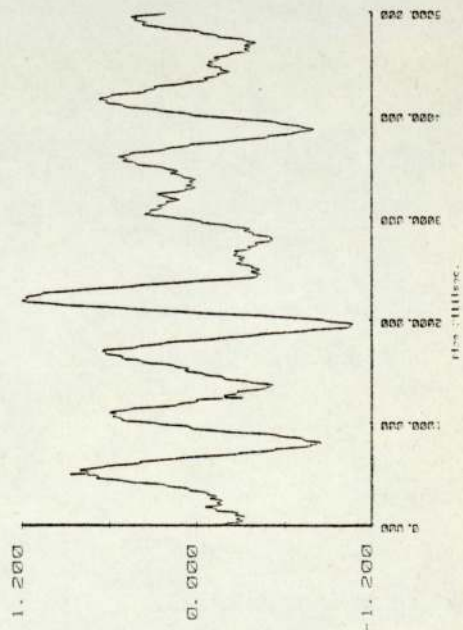
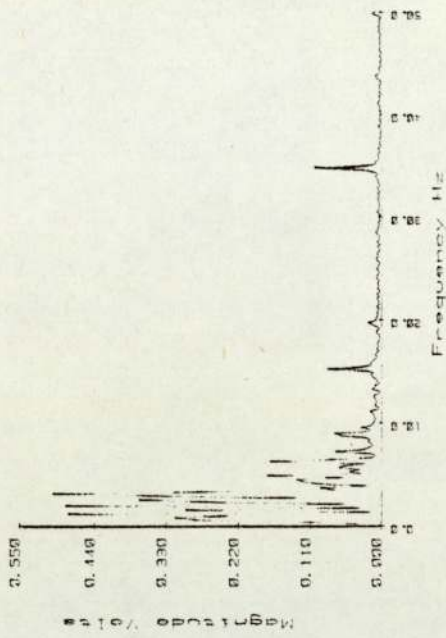
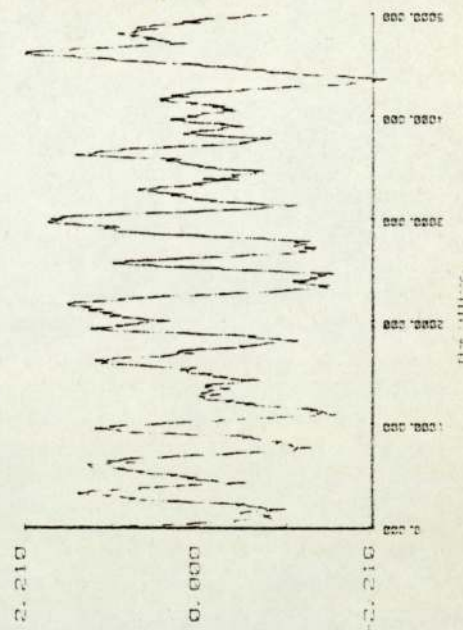
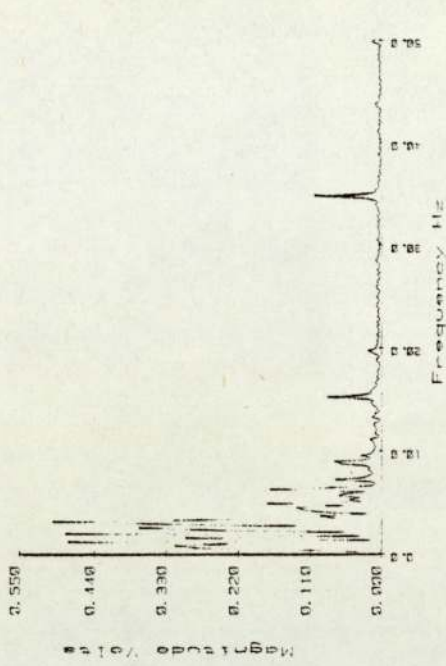


Fig. 28A Response curve and wave form.
Speed ratio 5:2, motor running
at 35 Hz, picking up signal
position 4.



Response curve and wave form.
 Speed ratio 5:2, motor running
 at 25 Hz, picking up signal
 position 2.

Fig. 29A



Response curve and wave form.
 Speed ratio 5:2, motor running
 at 25 Hz, picking up signal
 position 1.

Fig. 30A

APPENDIX C

Why Spring Steel acts admirably as an isolator

Steel springs have a damping coefficient of less than one-half of one per cent, a fact which contributes greatly to the excellent results obtainable using them as shock absorbers. Absorbing vibrations by means of damping implies a dissipation of energy in the form of heat. This is energy irretrievably lost to the machine.

This leads to a most important conclusion. When the operation of a machine sets up a vibratory motion in an adjoining structure, the energy used is spent for an entirely different purpose from that for which the machine was built. This energy is subtracted from the productive output of the machine. It is therefore profitable to regain as much as possible of this energy.

A correctly designed spring supporting the structure with a minimum of damping will save a considerable amount of this otherwise dissipated energy.

This effect, for example, can be demonstrated most strikingly on large motors, where it appears as an appreciable increase in speed when motors are correctly isolated. No definite figures about actual savings are available; some claim an increase in power of up to ten per cent.

Damping, to prevent excessive movements, is advantageous only when the machine is operated near resonance speed, but

better means than damping are available for this purpose to the designer of a spring-supported structure.

The benefits obtainable with a spring-supported structure are so great, physically and economically, that slight oscillation, hardly exceeding a few hundredths of an inch, is immaterial. A record taken from an actual rig shows the amplitudes vary from the time the set starts, passes through resonance, and attains operating speed. By making the springs very soft, main resonance will occur at a very low running speed and therefore be passed through so quickly that the small increase in movement due to resonance is hardly noticeable.

It is evident that a vibration isolation of 100 per cent with no oscillation of the operating system is impossible.

However, for a frequency ratio of 5:1 and with zero damping, the amplitude of motion will be within 4 per cent of the ideal machinery and vibration-absorbing efficiency of approximately 97 per cent. This means that the motion of the mass would be virtually imperceptible and the slight vibration transmission would be well beyond the human sensitivity range, detectable only by the finest instruments.

Actually, at low frequency ratios and with increased damping an increase of vibration transmission takes place; and for the low frequency ratio the phase angle is not 180 deg. but 0 deg. In other words, the stabilizing mass (the frame) is moving in the same direction as the disturbing

mass instead of against it and there is an increase in the vibration transmission. The phase angle is less than 90 deg. below resonance. It increases rapidly, a practically instantaneous change to 180 deg. with zero damping. That is why with a structure supported on springs, the amplitude of motion is reduced so quickly. The frame becomes an effective stabilizing mass as the phase angle suddenly changes from zero to 180 deg. The greater the damping factor, however, the slower the change in phase angle takes place, an added indication of the disadvantage of damping.

For the vertical vibratory motions the deflection of the spring controls the natural frequency of the isolator, and therefore must have a definite value regardless of the weight it has to support.

Hence it is important that the calculation of such a deflection in the isolator be made on a simple and reliable basis. The calculation of steel springs, based on modern practice employing the "Wahl" coefficient for the determination of deflection and stress, is very simple indeed.

The large deflections necessary for maximum isolating efficiency are easily obtainable through the choice of the proper physical characteristics, especially with a coil spring which has a higher loading capacity per pound of spring material than any other type of Isolator used for this purpose.

Therefore it is the writer's belief that this type of spring is the best choice for the most important and

difficult isolation problem.

Organic materials do not show the simplicity and advantages of the steel spring which does not depend upon its material, but rather, upon its wire diameter, outside diameter, etc. which may be chosen at will, while the former are restricted in their use as their elasticity depends upon the material itself and only to a minor degree upon shape.

This defect explains why organic materials cannot provide the necessary large deflections in the isolator for any reasonable thickness. So we can say that steel springs act admirably as isolators because of their shape, form, and heat-treatment possibilities.

APPENDIX D

The effect of an anti-vibration mounting on the Machinery

A crucial aspect of vibration effects is the use of an anti-vibration mounting on the machinery. Apart from the reduction of transmitted vibration, the provision of an anti-vibration mounting has a number of important effects which influence the decision.

- 1) The fundamental frequency of vibration of machinery and its mounting is low and must be run through when the machine is speeded up.
- 2) A critical frequency of the shaft is increased by the presence of an anti-vibration mounting⁽⁹³⁾.
- 3) The behaviour of a machine can be more easily and accurately monitored when it is on an anti-vibration mounting, as the amplitudes will be independent of the mounting stiffness.
- 4) Contrary to what is often expected, the forces on the bearing, due to the out-of-balance forces, are reduced under normal running conditions by the presence of an anti-vibration mounting.
- 5) When a machine is on a mounting, all equipment and the parts of the machinery other than those generating the out-of-balance forces must be able to withstand the movements.
- 6) All connections need to accommodate the movement of the mounting.

APPENDIX E

Why the change from traditional massive concrete to a
more flexible steel structure

Unwanted effects arise because of the transmission of vibration and structure failures. Considerable financial outlay and loss of production may result while substantial repairs or complete rebuilding are put in hand.

One of the main problems confronting the vibration engineer is the lack of positive and practical information on general anti-vibration products on the market. The average machinery installation design did not permit time, nor indeed the money, for research into the individual problem, and engineers were thus often forced to select a machine mounting device from a number of commercial products and relied entirely on the published literature for the necessary technical data and it was important to make sure that one did not follow too blindly, other people's experience.

Noble ⁽⁵⁸⁾ in his investigation of the foundations for large turbo block generators, came across some questions. He indicated that there appeared to be little English work (or foreign translations into English) dealing with large turbo block generators.

Whitman ⁽⁵⁸⁾ succeeded in producing results to 10 per cent within the theory but in the case of large blocks with

circulating water pipes and steam pipes, an error margin of 15 to 20 per cent would cause a very serious condition, with the sort of frequencies which should be avoided. Whitman evaluated the structural form of foundation blocks.

In the C.E.G.B. Research Establishment, theoretical calculations of a block, actual measurements were carried out while the block was in use. The results were found to have an error margin of up to 100 per cent. The fact that large variances were possible brought into question whether it was worth doing any calculations at all. A small-scale analysis block was also used. No correlation was found between the theoretical, the actual and the model. This confirmed the view that it is extremely difficult to predict characteristics of a turbo-block.

The author's opinion is that the increasing size of the modern rotating machinery gives the main reason for bringing about a change from the traditional massive concrete foundation to a more flexible steel structure which is an assemblage of beams and plates. Because of its flexibility, it is important to be able to predict the dynamic behaviour of such structures at the design stage.

The Finite Element displacement method may be used to determine matrices representing the mass and stiffness of the structure. The natural frequencies and corresponding mode shapes of the structure are found by solving an eigen value equation.

The response of the structure to sinusoidal excitation is estimated by solving a set of complex simultaneous equations. The structure damping may be represented by a matrix proportional to the stiffness matrix. Results for a typical theoretical case flexible platform are than compared with experimental measurements.

APPENDIX F

This Appendix gives two computer programmes. The first was a programme to calculate the mass and stiffness parameters.

The main programme then used the two matrices found by the first programme to calculate the natural frequencies and the mode shapes. This Appendix shows also the output of the main programme for the 4 main natural frequencies and the mode shapes.

360 $C(1,7) = C(3,8) = C(4,9) = C(6,10) = C(1,10) = C(3,12) = 1$
 370 $C(1,13) = C(3,14) = C(10,15) = C(12,16) = C(1,17) = C(3,18) = 1$
 380 $C(13,19) = C(15,20) = C(17,21) = C(18,22) = C(10,23) = C(11,24) = 1$
 390 $C(10,25) = C(11,26) = C(13,27) = C(14,28) = 1$
 400 $C(5,1) = -0.55$
 410 $C(6,1) = C(6,5) = C(6,9) = 0.2$
 420 $C(2,7) = C(2,13) = -0.275$
 430 $C(2,10) = C(2,17) = 0.275$
 440 $C(3,7) = C(3,11) = -0.15$
 450 $C(3,13) = C(3,17) = 0.15$
 460 $C(5,9) = 0.55$
 470 MAT PRINT C;
 480 MAT A = C * B
 490 MAT PRINT A;
 500 END

1 0 COM B (20,15)
 2 0 DIM A (20,20), C (20,15), L (7)
 3 0 MAT A = ZER
 4 0 MAT C = ZER
 5 0 $C(1,4) = C(2,6) = C(3,7) = C(4,9) = C(5,4) = C(6,6) = 1$
 6 0 $C(7,1) = C(8,3) = C(9,4) = C(10,6) = C(11,1) = C(12,3) = 1$
 7 0 $C(13,1) = C(14,3) = C(15,10) = C(16,12) = C(17,1) = C(18,3) = 1$
 8 0 $C(19,13) = C(20,15) = C(21,7) = C(22,8) = C(23,10) = C(24,11) = 1$
 9 0 $C(25,10) = C(26,11) = C(27,13) = C(28,14) = 1$
 100 $C(1,5) = -0.55$
 110 $C(1,6) = C(5,6) = C(9,6) = 0.2$
 120 $C(7,2) = C(13,2) = -0.275$
 130 $C(11,2) = C(17,2) = 0.275$
 140 $C(7,3) = C(11,3) = -0.15$
 150 $C(13,3) = C(17,3) = 0.15$
 160 $C(9,5) = 0.55$
 170 MAT PRINT C
 180 MAT READ L
 190 FOR I = 1 TO 7
 200 $J = 4 * (I - 1)$
 210 $A(J+1, J+2) = A(J+2, J+1) = 6 / (L(I)) \uparrow 2$
 220 $A(J+1, J+4) = A(J+4, J+1) = 6 / (L(I)) \uparrow 2$
 230 $A(J+2, J+3) = A(J+3, J+2) = -A(J+1, J+2)$
 240 $A(J+4, J+3) = A(J+3, J+4) = -A(J+1, J+2)$
 250 $A(J+1, J+1) = A(J+3, J+3) = 12 / (L(I)) \uparrow 3$
 260 $A(J+2, J+2) = A(J+4, J+4) = 4 / L(I)$
 270 $A(J+3, J+1) = A(J+1, J+3) = -A(J+1, J+1)$
 280 $A(J+2, J+4) = A(J+4, J+2) = 2 / L(I)$
 290 NEXT I
 300 MAT PRINT A
 310 MAT B = A * C
 320 MAT PRINT B
 330 REDIM A (15,15), C (15,28)
 340 MAT C = ZER
 350 $C(4,1) = C(6,2) = C(7,3) = C(9,4) = C(14,5) = C(16,6) = 1$

MAIN PROGRAM

```

10 DIM A(20,20),B(20,20),C(20,20),D(20,20),G(1,1)
20 DIM U(20),W(20),V(1,20)
30 DISP "NO OF DEGREES OF FREEDOM";
40 INPUT N
50 DISP "MAX ALLOWABLE ERROR IN VECTOR";
60 INPUT E1
70 REDIM A(N,N),B(N,N),C(N,N),D(N,N),W(N),V(1,N)
80 FOR I=1 TO N
90 FOR J=1 TO N
100 DISP "COFF A(I,J)";
110 INPUT A(I,J)
120 A(J,I)=A(I,J)
130 NEXT J
140 NEXT I
150 PRINT "MATRIX A"
160 PRINT
170 MAT PRINT A
180 FOR I=1 TO N
190 FOR J=1 TO N
200 DISP "COFF B(I,J)";
210 INPUT B(I,J)
220 B(J,I)=B(I,J)
230 NEXT J
240 NEXT I
250 PRINT "MATRIX B"
260 PRINT
270 MAT PRINT B
280 MAT B = INV(B)
290 MAT D = B * A
300 FOR I=1 TO N
310 MAT U = CON(N)
320 FOR J=1 TO 100
330 MAT W = D * U
340 E = W(N)
350 MAT W = (1/E) * W
360 FOR K=1 TO N

```

```

370 IF ABS (W(K)-U(K)) > E1 THEN 400
380 NEXT K
390 GO TO 430
400 MAT U = W
410 NEXT J
420 PRINT "ERROR IN VECTOR" > E1 " AFTER 100 ITERATION"
430 PRINT "1/LAMBDA = 1/E"
440 MAT V = TRN(U)
450 MAT W = A * U
460 MAT G = V * W
470 MAT U = (1 / SQRG (1,1)) * U
480 MAT V = (1 / SQRG (1,1)) * V
490 MAT PRINT U
500 IF I=N THEN 580
510 MAT B = U * V
520 MAT C = B * A
530 MAT C = (E) * C
540 MAT D = D - C
550 NEXT I
560 END
570 END

```

1/LAMBDA = 820:20965851

0.011798501
0.125295658
0.199656815
0.059302608
7.19231E-04
-0.422846729
0.082767134
-0.507857348
0.905721540
0.185998374
0.140819499
0.014055396
0.048410452
0.783289810
0.017549254

1/LAMBDA = 2011:201321

0.057538274
-0.283329698
-0.091189201
0.013885123
-0.046609238
0.199818138
-0.052480434
0.898762267
-0.254301103
-0.383649735
-0.277291080
0.019544636
-0.022265277
-1.106676448
0.015193655

1/LAMBDA = 2455:010063

0.054847736
-0.181005974
0.018774923
-0.040506876
-0.009992741
-0.034041284
-4.25177E-03
0.520808728
0.221018238
-0.194568474
-0.168351855
0.023458986
4.41849E-03
-0.564928304
0.021438207

1/LAMBDA = 2851:00021

0.000198851
-0.061746378
0.105037367
0.058097721
0.027137934
-0.263986751
-0.179297316
-0.096984298
0.421741904
-0.014701601
-0.060005611
0.026220794
0.053327118
0.207403111
0.035515989

The main natural frequencies & the values of the mode shapes .

APPENDIX G

Conversion Tables for Units

Length

1 ft	=	0.3048	m
1 in	=	25.4	mm
0.001 in	=	25.4	µm

Mass

1 ton	=	1016.05	Kg
1 lb	=	0.4536	Kg

Area

1 sq.in	=	6.4516×10^{-4}	sq.m
1 sq.ft	=	9.2903×10^{-2}	sq.m

Volume

1 cu.in	=	1.000×10^{-3}	cu.m
	=	16.387	cu.cm

Force

1 lbf	=	4.448 N = 0.453 Kp
-------	---	--------------------

(Mnemonic : 1 apple weight roughly 1 Newton)

Torque

1 lbf.in	=	0.11298	N.m
----------	---	---------	-----

Stress

1 lbf/in ²	=	6894.76 N/m ²	= 0.0703 Kp/cm ³
-----------------------	---	--------------------------	-----------------------------

Work

1 hph	=	2.684	MJ
1Kwh	=	3.6	MJ
1 ft lbf	=	1.3558J	

Stiffness

1 lbf/in	=	175.127	N/m = 17.858 Kp/m
----------	---	---------	-------------------